Engine Oil Contamination: Causes and Impact on Additive Efficiency

by

Alaaeddin Al Sheikh Omar

Submitted in accordance with the requirements for the degree of

Doctor of Philosophy

School of Mechanical Engineering

University of Leeds

Leeds, UK

March 2022

Declaration

The candidate confirms that the work submitted is his own, except where work which has formed part of jointly-authored publications has been included. The contribution of the candidate and the other authors to this work has been explicitly indicated below. The candidate confirms that appropriate credit has been given within the thesis where reference has been made to the work of others.

Papers contributing to this thesis:

In all papers listed below, the primary author performed all the experimental work, data analysis and preparation of publications. All other authors contributed to the proofreading of the articles prior to publication.

1. **Omar, A.A.S**., Salehi, F.M., Farooq, U., Morina, A. and Neville, A., 2021. Chemical and physical assessment of engine oils degradation and additive depletion by soot. **Tribology International, 160, p.107054**.
2. **Omar, A.A.S**., Salehi, F.M., Farooq, U., Neville, A. and Morina, A., 2022. Effect of Zinc Dialkyl Dithiophosphate Replenishment on Tribological Performance of Heavy-Duty Diesel Engine Oil. **Tribology Letters, 70(1), pp.1-14.**

Papers contributing to other works during the first year of PhD as a group project in the CDT program funded by EPSRC. In all papers listed below, the primary author and the next three authors performed all the experimental work, data analysis and preparation of publications. All other authors contributed to the proofreading of the articles prior to publication.

1. Wade, A., Copley, R., **Omar, A.A.,** Clarke, B., Liskiewicz, T. and Bryant, M., 2020. Novel numerical method for parameterising fretting contacts. **Tribology International, 149, p.105826.**
2. Wade, A., Copley, R., Clarke, B., **Omar, A.A.,** Beadling, A.R., Liskiewicz, T. and Bryant, M.G., 2020. Real-time fretting loop regime transition identification using acoustic emissions. **Tribology International, 145, p.106149.**

Acknowledgements

I would like to express my gratitude and appreciation to my supervisors Prof. Ardian Morina, Dr. Farnaz Motamen Salehi and Prof. Anne Neville who gave me the golden opportunity to work with them over the PhD period on challenging ideas, and for providing their invaluable guidance, suggestions, positive attitude and support throughout the PhD endeavour. Thank you. I would also like to thank all the members of IFS (Leeds), Leonardo (Sheffield) and the CDT team especially Kimberley Mathews who figured out lots of issues.

I would like to express my deepest thankfulness to my dear parents and my deceased for their love, prayers and support which help me in every step of my life. Warmest thanks to my little family my love (Shaza), daughters (Layan and Lara) and my son (Wissam). Without their support and love over this period, none of these would have been possible.

Aladdin Al Sheikh Omar.

Abstract

In recent years, there has been an increasing demand in the commercial market to prolong the service life of engine oil. Oil contamination is one of the most important factors that influence friction, wear and which continuously accelerates oil degradation. The main contaminants in diesel engine oil are soot and water. The engine oil with a high level of soot causes an increase in oil drain interval to minimise the effect of hard soot particles on contact surfaces. Water is also a destructive contaminant that affects engine oil's physical and chemical stability. Many studies have been conducted on the effects of oil contaminants on oil performance, however the effects of oil contamination on additives and oil degradation are not fully understood yet. Engine oil additives have been widely used to enhance oil performance, reduce the effect of oil contamination and extend the lifespan of engine oil. Thus, the main focus of this study is to investigate the impact of soot and water on additives and the bulk oil and then replenish the influenced additives to regain the tribological performance of engine oil.

To achieve this, the effects of soot or/and water in different engine oils and ageing conditions have been studied in the boundary lubrication regime. Chemical analysis of engine oil was conducted using Fourier Transform InfraRed Spectroscopy (FTIR) and Inductively Coupled Plasma (ICP). Different surface analysis techniques to measure wear, chemical analysis of surface and particles size distribution were employed in this research, such as X-ray Diffraction (XRD), Atomic Force Microscopy (AFM), Transmission Microscopy (TEM) and Scanning Electron Microscopy (SEM)/Energy- Dispersive X-ray (EDX). Depth filtration technique and centrifugation were used to reclaim the contaminated oil. ZDDP antiwear additive at varied levels was used to replenish the consumed additives in heavy-duty used oils.

The results indicate that carbon black (CB) contamination, commonly used as a surrogate for soot, affects the tribological performance of the oil. CB contamination at ageing conditions

influences engine oil's chemical and physical properties. The results confirm that reclaiming the aged oil performance can not be achieved by just removing the CB particles. Other mechanisms such as oil degradation and additive adsorption on CB adversely affect the aged oil performance during the removal of CB. Likewise, water contamination in engine oil reveals an increase in wear. The performance of the reclaimed oil from water contamination is also influenced by additive depletion and dissolved water remaining in the oil.

This study shows that additive replenishment before and after reclaiming the heavy-duty used oil from either soot or/and water can be applied. The results show a reduction in the additive concentration in the reclaimed oils due to additive adsorption on soot and additive depletion by water. The results reveal that the amount of added Zinc Dialkyldithiophosphate (ZDDP) to regain the oil performance can be determined. It is found that the existence of soot or/and water requires a large amount of ZDDP to perform similar to fresh oil. However, reclaiming the used oil reduces the amount of added ZDDP that is needed to gain oil properties. The results show a higher level of ZDDP is used to replenish the additives when both soot and water are removed from used oils compared to the removal of just soot. Additive adsorption on soot, additive depletion by water and remaining water are considered the main mechanisms that influence the ZDDP replenishment process in the presence of both soot and water contamination.

Table of Contents

List of Figures

List of Tables

Nomenclature

Parameters	Definition	Units
μ	Friction coefficient	-
F	Friction force	N
W	Load	N
λ	Lambda ratio	-
h_{min}	Minimum film thickness	nm
R_q	Root mean square surface roughness	nm
$E^{\sim}$	Effective Young's modulus	Pa
$R^{\sim}$	Reduced radius of curvature	m
α	Pressure viscosity coefficient	Pa^{-1}
l	Contact length	μm
η_0	Dynamic viscosity	$Pa.s$
U	Entrainment speed	m/s
a, b	Contact zone dimensions	μm
$E1, E2$	Young's Modulus of body 1 and 2	Pa
$R1, R2$	Radius of body 1 and 2	m
$v1, v2$	Poisson ratio of body 1 and 2	-
P_{max}	Maximum Hertzian contact pressure	Pa
d_p	Diameter of spherical solid particle	nm
ρ_p	Density of spherical solid particle	kg/m^3
r	Centrifuge radius of solid particle	m
$\mu_\circ$	Centrifuged liquid dynamic viscosity	$Pa.s$
$\rho_\circ$	Centrifuged liquid density	kg/m^3
ω	Angular velocity of the centrifuge	rad/s
τ	Time for the particle to travel for a distance	s

η	Filtration efficiency of centrifuge	-
V_p	Velocity of solid particles	m/s
V	Kinematic viscosity of the centrifuged liquid	$Pa.s$
g_c	Centrifugal acceleration	m/s^2
$\mathcal{E}$	Media filter efficiency	-
$C1, C2$	Soot concentration before/after filtration	%
Q	Flow rate	m^3/s

Abbreviations

CBP	Carbon Black Particles
FFO	Fully Formulated Oil
VI	Viscosity Improver
KF	Coulometric Karl Fischer Titration
ICP	Inductively Coupled Plasma
FTIR	Fourier Transform InfraRed Spectroscopy
SEM	Scanning Elector Microscope
ZDDP	Zinc Dialkyldithiophosphates
PPM	Parts Per Million
XRD	X-ray Diffraction
AFM	Atomic Force Microscope
XPS	X-ray Photoelectron Spectroscopy

1 Chapter (1) Introduction

1.1 Motivation

In the U.S, it has been reported that over 1 billion gallons of lubricants annually are replaced in light trucks/passenger cars every year. Additionally, more than 250 million gallons of lubricants are consumed in the large truck market segment [1]. Therefore, engine manufacturers are facing greater demands to increase the oil change period and consequently reduce the total costs on customers on the one hand, and the impact of waste oil on the environment on the other hand.

The major factors that adversely affect the performance of engine oil and accelerate oil degradation are oxidation, nitration, contamination and additive depletion [2]–[4]. Used engine oils are replaced regularly in machinery and vehicles to reduce the effect of various contaminants including dirt, salt, water, incomplete products of combustion and other materials. The contaminants accelerate the chemical breakdown of lubricating oil and subsequent chemical interactions producing corrosive acids and other harmful substances [5]. Fundamentally, every engine oil has its specific chemical structure, and consequently, the function of the lubrication liquid depends on the chemical structure that controls its properties over time.

Engine oil maintenance is required to provide the following functions for a finite period: surface protection, cleaning out the metal wear debris, cooling the sliding surfaces and related components, dispersing the sludge in lubricants and protecting the engine internals from corrosion and rust. Many pure lubricants such as petroleum-based hydrocarbon blends or other lubricants based on synthetic hydrocarbon-type compounds do not meet all modern engine or other industrial applications requirements. A widely accepted solution to enhance lubricant performance is adding a relatively small weight percentage of additive materials to the base stock to improve the tribological performance and decelerate oil degradation [6]. One of the biggest concerns is the efficiency of additives after they are used in the engine and

subsequent materials as the result of chemical interactions with oils and oil contaminants. The change in the chemical structure or depletion of the additives could influence the tribological performance and accelerate the oil degradation [7]–[13]. As a result, the automotive industry aims to monitor and improve the additive performance to extend the oil drain interval and reduce the fuel consumption that is resulted from an increase in friction and wear [14]–[16].

In recent years, automotive manufacturers are increasingly using their resources towards producing self-driving cars with a higher degree of efficiency and minimal environmental impact. However, despite all of the advanced features in self-driving cars made so far, there are still concerns about using durable materials and effective lubricants, material and energy losses due to wear and friction. The effect of the implementation of intensive advanced tribology on potential annual savings in energy, cost and CO_2 emission in different sectors is represented in Figure 1.1. The data show that potential savings can be achieved by adopting innovative design solutions (including Electric Vehicles (EVs)), new lubrication technologies and advanced materials. One of the most critical factors that affect wear and friction is controlling the lubricant performance over the use. This can lead to investigating the effect of extending the service life of lubricating oil using different methods such as the additives replenishment method [17].

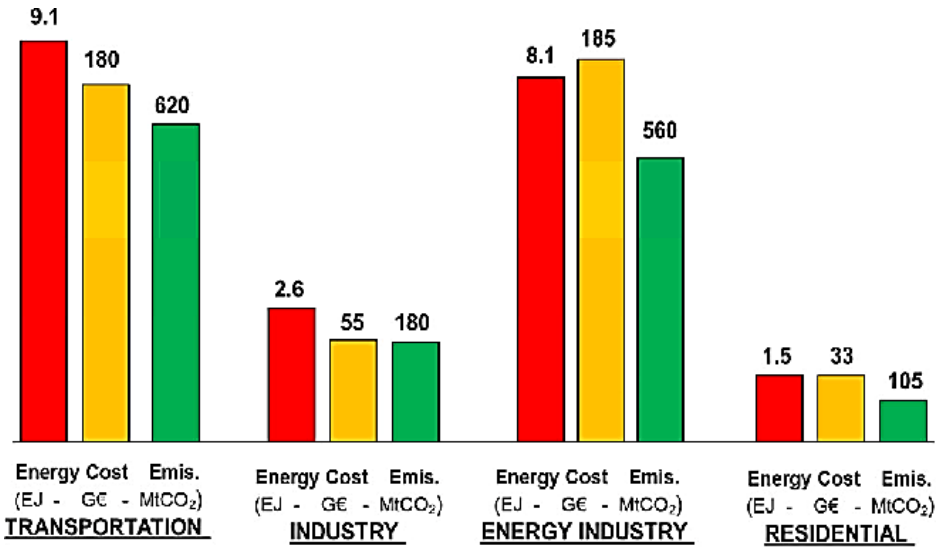

Figure 1.1: The effect of the implementation of intensive advanced tribology globally on potential annual savings in energy, cost and CO_2 emission over the next 8 years in different sectors [17].

Oil contamination is one of the main mechanisms that influence the tribological performance of engine oil and causes higher energy losses. There are different types of contaminants such as the contaminants that come from internal or external sources. Soot and water contamination are considered the most destructive contaminants in engine oil causing a host of problems. The level of soot and water increases with engine working hours until it reaches the level where the lubricating oil is no longer fit to continue service.

Soot in engine oil is one of the most common reasons for changing the engine oil [18]. Soot causes an increase in wear, influences friction and continuously accelerates oil degradation [19]. The longer the engine working hours are, the higher levels of soot are produced. Consequently, engine oil with a high level of soot causes a decrease in oil drain interval to minimise the effects of hard soot particles on contact surfaces [20]. Abrasive wear is the most common surface damage in the presence of soot contamination. This leads to a decrease in the engine oil performance and hence engine failure [21]–[23]. The effect of abrasive wear varies depending on the tribofilm thickness and soot particles diameter [24]. There is a lack of understanding of the effects of soot on additives especially additives adsorption on soot, oil degradation, oil performance and oil drain interval. Some studies [10]–[13] have reported that additives were adsorbed on soot, but none of these studies investigated the effect of the increase in soot surface area (soot level) on the additive adsorption and the effect of additives adsorption on wear. This study explores the relationship between soot level and additive adsorption. The effect of additive adsorption on soot and additive depletion on wear is also investigated in this project. In addition, soot effects on oil degradation and tribological performance at ageing conditions are presented. The effect of ageing oil on physical and mechanical properties of soot partciles are discussed in detail. Soot size distrabution in heavy-duty engine oil and the possiblity to be removed using medial filter is explored.

Water is known as the second harmful contaminant in engine oil after soot because it affects the physical and chemical stability of lubricants [25]. Water can promote a host of chemical reactions (hydrolysis) between the base stock, suspended contaminants and oil additive

resulting in the formation of free peroxide and radical compounds [26]. Water affects wear performance and tribofilm formation on the rubbing surfaces [27]–[29]. It is widely observed that the effect of water on additive depletion and the effect of additive depletion on wear are not understood in most tribological studies. In this project, the existence of water in engine oil, water effects on wear, additive depletion by water and the effect of additives depletion on the chemical composition of tribofilm are investigated.

This project not only studies the effect of removing the oil contaminants on additive concentration and engine oil performance but also investigates the effect of the additive replenishment process on oil performance. Filtration techniques can potentially remove contaminants from the engine oils however, there is still unknown whether engine oil can perform as a fresh oil after reclamation or not. This is because other contaminants such as degradation products and dissolved water are difficult to remove by filtration and can also influence the oil functionality. It is possible to determine the amount of depleted additives and the effects on wear, which allows the possibility to consider potential means of replenishing these additives to bring the oil performance back to the original and thereby extend the oil change intervals.

1.2 Aims and objectives

This project aims to improve the understanding of the effects of soot and water contamination on the service life of lubricants in heavy-duty diesel engines. The work encompasses the effects of soot and water contamination on tribological performance, oil degradation and additives depletion under diesel engine conditions.

In order to achieve this goal, the main objectives of this project are summarised as follows:

1. Investigate the effects of soot contamination at ageing conditions on rheological properties of engine oil, tribological performance, additives adsorption on soot and oil

degradation, This will help to understand the reclamation process of used oils in heavy-duty diesel engines.

2. Study the existence of water at different phases (dissolved or free) in engine oils and its effects on wear, additives depletion and oil degradation. This will enable us to understand the reclamation process of used oil when both water and soot contaminants exist in heavy-duty engine oils.
3. Investigate the ZDDP replenishment process in heavy-duty engines in the existence of soot and water contamination. This will help us to explore the ability to extend the service life of used oil in heavy-duty engines.

1.3 Novelty statement regarding previous research gaps

The key novelty and contribution from this research based on aim and objectives are described below:

- Additives adsorption on soot particles has been detected in previous studies, however, the effects of an increase in soot surface area on additives adsorption and oil degradation and how these influence wear will be investigated for the first time.
- Filter manufacturers are exploring the efficiency of depth filters to reclaim used oil and these data have not been published yet. In this study, a depth filter to remove the soot will be explored.
- Developing a new method to determine the water saturation in engine oils. This will lead to investigating for the first time the effects of water separation above the saturation level on additive depletion and hence wear.
- Many patents have published different designs to replenish the depleted additives, but the effects of additive replenishment on used oil performance have not been explored before.

1.4 Thesis Outline

The thesis is divided into ten chapters. The outline of this thesis are presented as follows:

- **Chapter (1):** This chapter introduces the project topic and discusses the motivation and objectives of this project. It also discusses the gaps in the research due to the lack of understanding of the effect of oil contamination on oil degradation, additive depletion and tribological behaviour of contact surfaces.

- **Chapter (2):** This chapter provides an overview of the fundamentals of tribology science. This chapter discusses different types of engine oils, lubrication regimes and chemical formulation of additives.

- **Chapter (3):** This chapter discusses in-depth the effects of oil contaminants, including soot and water, on engine oil and its additives. It also discusses the effect of the additives replenishment process on extending the service life of engine oil.

- **Chapter (4):** This chapter presents the details about the experimental procedures and techniques applied in this study.

4. **Chapter (5):** The effect of carbon black contamination on the tribological performance of oils, oil degradation and additives is investigated in this chapter.

5. **Chapter (6)** The effect of soot in heavy-duty used oil on the oil reclamation is studied In this chapter.

- **Chapter (7)** The effect of water contamination on the performance of oils, oil degradation and additives is investigated in this chapter.

6. **Chapter (8)** The effect of ZDDP replenishment on the performance of heavy-duty used oil containing soot or/and water is investigated in this chapter.

- **Chapter (9)** This chapter provides an overall discussion on the effect of carbon black/soot and water on oil degradation and additives depletion at ageing conditions. This chapter discusses the oil reclamation after removing soot or water from oils. The improvements in the performance of used oil or reclaimed oil after applying the additive replenishment process are also discussed in this chapter.

- **Chapter (10):** This chapter highlights the main conclusions of this research and outlines recommendations for future research work related to this study.

- **Chapter (11):** This chapter provides all the references used in this study.

2 Chapter (2) Basics of tribology

In this chapter, the basics of the tribology topics that will be used to understand the tribological experimental data have been summarised. The chapter is divided into two main sections. The first section introduces the basic information of tribology, for example, friction and wear types. The second section discusses the lubrication system including different types of engine oils, lubrication regimes and chemical formulation of additives that are used in different applications.

2.1 Tribology

Tribology is defined as the branch of science and technology which focuses on the interaction between surfaces that are moving relative to each other. Tribology term is derived from the Greek word “Tribos” which means rubbing between contact surfaces. Tribology is an important scientific discipline that requires different skills of materials scientists, engineers, chemists, physicists, designers, metallurgists and computer scientists. Tribology combines three known subjects; friction, wear and lubrication [30].

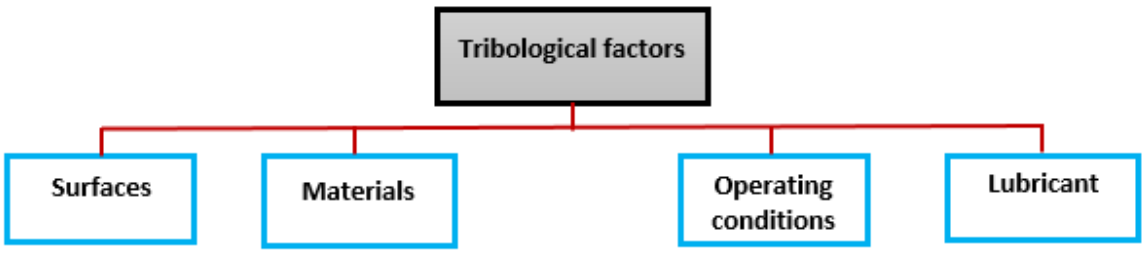

Figure 2.1: Main tribological factors [31].

When analysing any tribological problem, several major tribological factors must be taken into an account (Figure 2.1) to break down any particular situation into simpler problems. Understanding the tribological factors and their effects on the whole tribological phenomena can reduce the cost of maintenance and improve the performance of machine elements. Some of these factors will be discussed in the following sections in more detail.

2.1.1 Friction

Friction is the resistance to slide or motion when one solid body moves tangentially along or over another [32]. In some applications, high friction is desirable such as car tires on the road surface (friction coefficient of which ranges from 0.5 to 1.2), clutches and sport boots. However, low friction is also desirable between sliding mechanisms for instance, engine parts, hard disc systems and indoor latches [33]. Friction between the components in the engine depends on many factors such as normal load, contact area, surface roughness, oil properties, velocities of the sliding surfaces, component geometry and other operational variables. Reducing the friction level between engine parts can reduce the waste in engine power. The magnitude of friction is often described in terms of the coefficient of friction(μ), which is the ratio of friction force $(F)[N]$, to the applied load $(W)[N]$, as seen in Equation 2.1 [34].

$$\mu = \frac{F}{W} \qquad \text{Equation 2.1}$$

2.1.2 Wear

Wear is progressive damage on the rubbing surfaces, which involves material loss due to moving the surface of the body over another under load [35]. Wear is the main cause of material loss which influences the performance of engineering components and leads to mechanical parts failure. Fundamentally, lubricants are applied to reduce wear and friction in most engineering applications hence increasing the lifespan of mechanisms [36]. Figure 2.2 describes the relationship between the most commonly used wear terminologies.

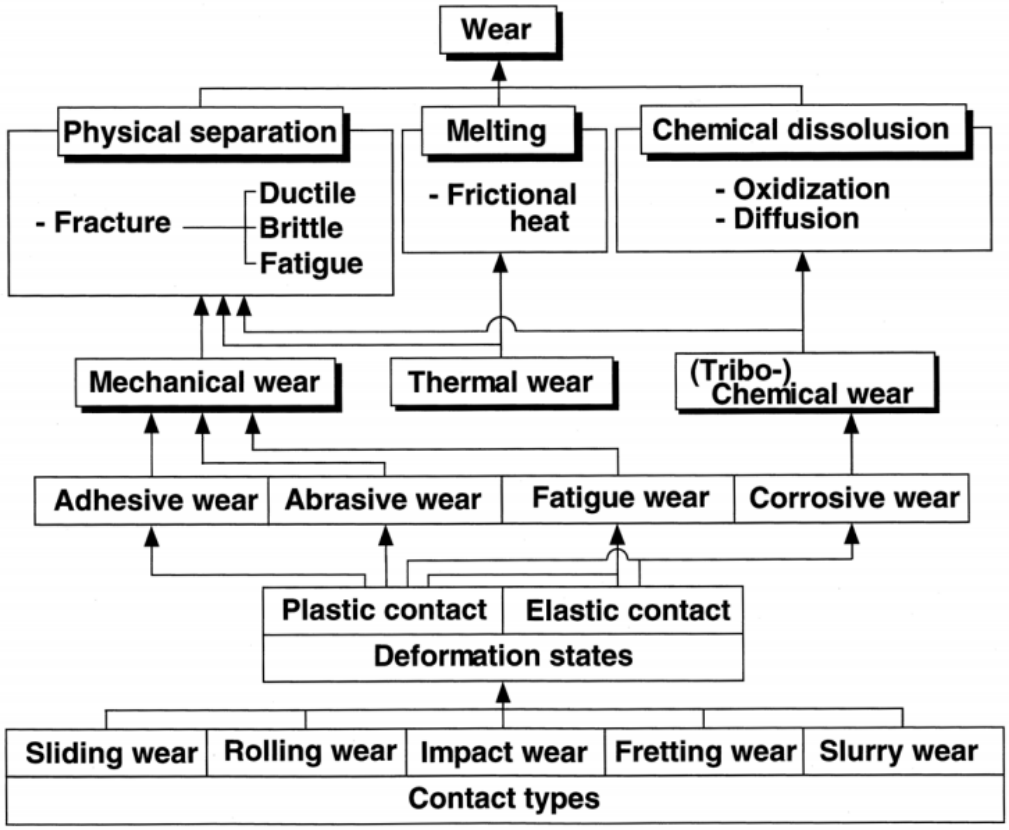

Figure 2.2: Wear types and the interrelations between each other [37].

According to ISO 15243:2004, four wear mechanisms are:

Abrasive wear:

Abrasive wear occurs by ploughing out the material of soft surfaces by a hard surface that is penetrated into a soft counterface in relative motion. There are two main types of abrasive wear. Firstly, two-body abrasive wear is caused by hard asperities of the contact surface penetrating into the other surface, which is softer. The asperities plough the material out of the soft surface as shown in Figure 2.3. Secondly, three-body abrasive wear occurs when a third body, such as products of corrosion, wear debris, dirt, and adhesive wear debris ingress into the rubbed surfaces and wear the softer surfaces as illustrated in Figure 2.4 [18,19].

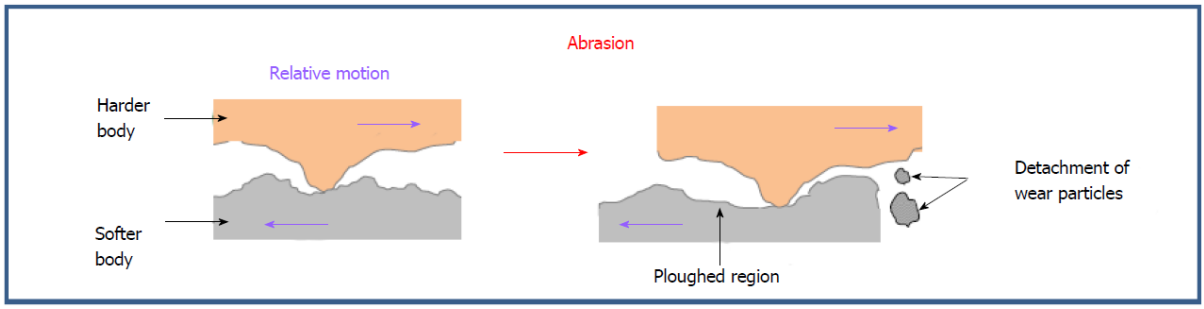

Figure 2.3: Schematic of two-body abrasive wear [40].

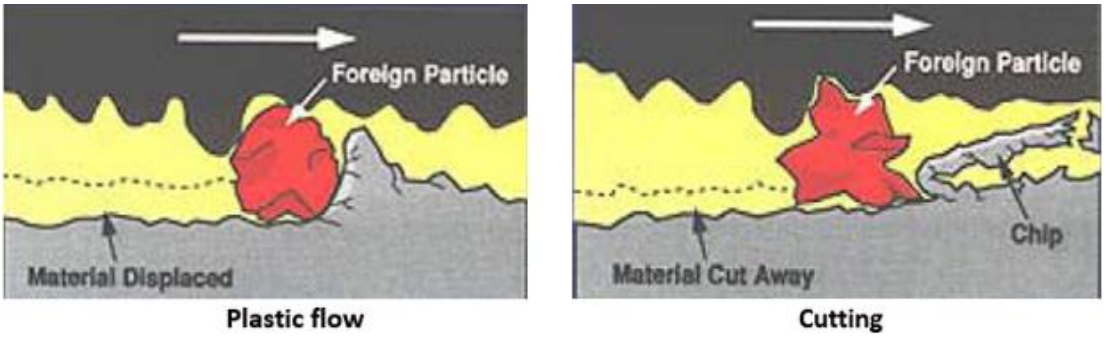

Figure 2.4: Schematic of three-body abrasive wear [41].

The effect of abrasive wear can be minimised by the modifications of material properties and operating conditions such as [42]:

i. Increase the hardness of contact surfaces.
ii. Remove the abrasive particles by filtering.
iii. Increase the thickness of the lubricating protective film; hence the contact surfaces can be separated effectively.
iv. Reduce the roughness of contact surfaces.

Adhesive wear

Adhesive wear occurs when the asperities in interfacing surfaces of the sliding contact bond resist the relative sliding at asperity junctions. Plastic deformation under compression and shearing at asperity junctions causes the transference of a fragment from one surface and getting attached to another surface as shown in Figure 2.5. As the sliding between the surfaces continues, the separated fragments which come off from the surface and transfer away, may come back and attach themselves again to the original surface. Adhesion is most

likely to happen when direct contact between overlapping surfaces occurs in both mixed and boundary lubrication regimes [43].

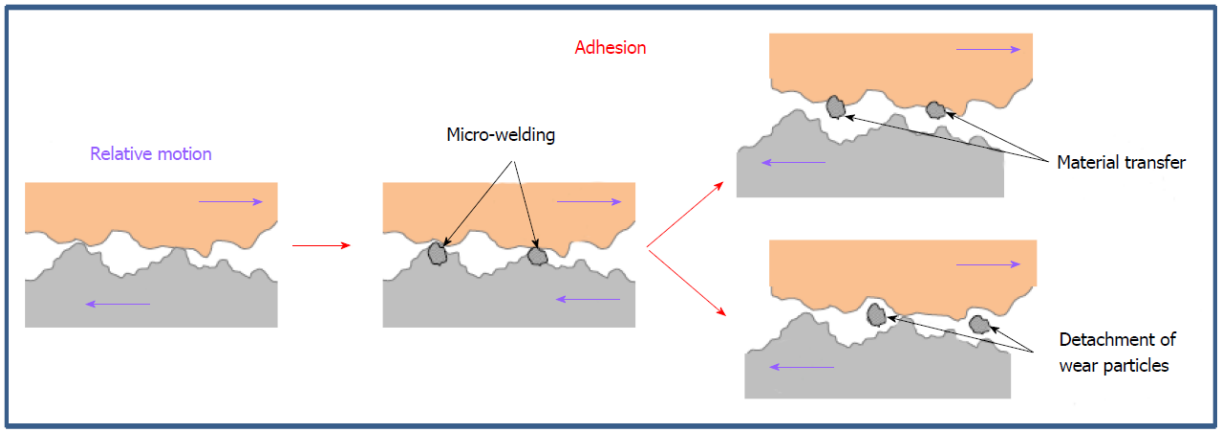

Figure 2.5: Schematic of adhesive wear [40].

Corrosive wear

A complicating matter results from the combination of chemical reactions and rubbing between the surfaces. The chemical reaction builds a thin layer poorly adhered to the surface, and with continuous rubbing of surfaces, the layer will be removed and built faster again at a higher rate. Building oxide layers on metal surfaces under humid conditions is the most common example of corrosive wear [44].

Fatigue wear

Fatigue wear can occur in the surfaces during the cyclic loading or stress variation over time especially if the applied load is greater than the fatigue strength of the material. Fatigue cracks start at the contact surfaces and spread to the subsurface locations [45].

Erosive wear

Erosive wear is surface damage that is caused by solid particles that move at high velocity in a fluid. Erosive wear commonly happens in the elastohydrodynamic lubrication regime such as rolling bearing [46].

2.1.3 Lubrication system

Lubricants are substances that are used between two moving surfaces to reduce any negative effects on contact surfaces. Lubricants play a major role to reduce friction and wear, cool the contact, and clean the surface from wear particles and external dust. Lubricants in engineering applications can appear as liquid, semi-solid (greases), or solid (coating and particles) [47]. There are a wide range of materials that are used as lubricants to reduce friction and wear including grease, (mineral, synthetic or vegetable) oil, water, process fluid and air. Basically, mineral oils are used in the most ubiquitous in many tribological interfaces. Lubrication regime formation in tribology applications is correlated with the function of the oil properties, interacting surface properties (materials, texture and conformity), and working conditions (temperature, pressure, load and speed). The best scenario that minimises friction and wear between the contact surfaces is to have two fully separated surfaces or form a protective film on the rubbed surfaces. Determining the lubrication mode is depended on the film thickness and surface roughness. The Lambda ratio (λ) is used to determine the lubrication regime as written in Equation 2.2, which is represented by the ratio of minimum film thickness (h_{min}) to the composite surface roughness. R_{q1} and R_{q2} in Equation 2.2 represent the root mean square surface roughness of interacting surfaces [48], [49].

$$\lambda = \frac{h_{min}}{[(R_{q1})^2 + (R_{q2})^2]^{\frac{1}{2}}} \qquad \text{Equation 2.2}$$

Dowson and Higginson [50] developed the minimum film thickness in the following equations. In this study, the experimental section is based on the point-line contact (pin on the plate). The minimum film thickness is determined for point contact in Equation 2.3 and line contact in Equation 2.4.

$$\frac{h_{min}}{R^{\sim}} = 3.63\left(\frac{U\eta_0}{E^{\sim}R^{\sim}}\right)^{0.68} (\alpha E^{\sim})^{0.49} \left(\frac{W}{E^{\sim}R^{\sim}}\right)^{-0.073} (1 - e^{-0.68k}) \qquad \text{Equation 2.3}$$

$$\frac{h_{min}}{R^{\sim}} = 2.65\left(\frac{U\eta_0}{2E^{\sim}R^{\sim}}\right)^{0.7}(2\alpha E^{\sim})^{0.54}\left(\frac{W}{E^{\sim}R^{\sim}2l}\right)^{-0.13} \quad \text{Equation 2.4}$$

Where, $E^{\sim}$ the effective Young's modulus $[Pa]$ calculated from Equation 2.6, $R^{\sim}$ the reduced of curvature calculated from Equation 2.5, W is the normal load $[\mathrm{N}]$, α is the pressure viscosity coefficient $[\mathrm{Pa}^{-1}]$, $2l$ $[\mu m]$ is the contact length and k=1, η_0 is the dynamic viscosity of the oil at room temperature $[Pa.s]$, $U = \frac{U_1+U_2}{2}$ is the entrainment speed of the two contact surfaces $[m/s]$.

$$\frac{1}{R^{\sim}} = \frac{1}{R_1} + \frac{1}{R_2} \quad \text{Equation 2.5}$$

$$E^{\sim} = \frac{2E_1E_2}{(1-\nu_1)^2E_2 + (1-\nu_2)^2E_1} \quad \text{Equation 2.6}$$

Where, E_1, E_2 and ν_1, ν_2 are Young's modulus and Poisson's ratio respectively of two contact surfaces.

The maximum contact pressure is calculated according to Stachowiak [51] as illustrated in Equation 2.7:

$$P_{max} = \frac{3W}{2\pi ab} \quad \text{Equation 2.7}$$

Where, a, b contact zone dimensions (μm) are determined according to Hertz equations.

Four main lubrication regimes can affect the wear and friction of contact surfaces depending on the Lambda ratio (specific film thickness)(λ):

Hydrodynamic lubrication regime (HL): in this regime, the lubrication film thickness is much thicker compared to the composite of surfaces roughness. The specific film thickness $\lambda > 10$ and both contact surfaces are completely separated from each other by lubrication film with no asperities contact from interacting surfaces. The minimum film thickness is larger than one micron and depends on the working conditions [29, 31].

ElastoHydrodyanmic lubrication regime (EHD): specific film thickness in this lubrication regime occurs at $4<\lambda<10$, similar to the HL regime both surfaces are fully separated by lubrication film, but the film thickness ranges between 0.1 to 1 µm. If the load is high enough on the surfaces at high speed can cause elastic deformation in the asperity contact of surfaces. This mode of lubrication occurs in rolling/sliding contacts such as gears, follower contacts and rolling element bearing [29, 32].

Mixed lubrication regime: the specific film thickness of this regime occurs at $1<\lambda<4$, some asperities of rubbed surfaces come into direct contact in some regions, where others asperities are separated. Film thickness is in the range of 0.05 to 1 µm. The friction coefficient increases with the increase in contact asperities of rubbed surfaces [29, 33].

Boundary lubrication regime: the specific film thickness of this regime occurs at $\lambda< 1$, the roughness of rubbed surfaces is much larger than the thickness of the oil which is separating the contact surfaces. Most regions of surfaces come in direct contact with each other causing an increase in the friction coefficient. Boundary lubrication regime occurs at high load conditions, low-speed vibration or continuous stopping /starting. The film thickness varies from 0.005 to 0.01 µm [29, 34].

The transition between different lubrication regimes is presented graphically in the Stribeck curve as shown in Figure 2.6.

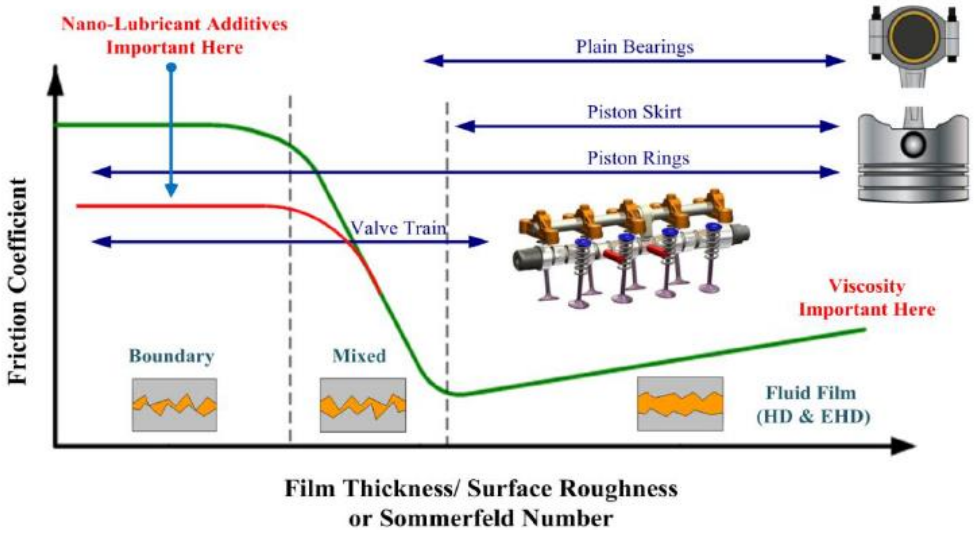

Figure 2.6: Stribeck curve of the lubrication system in an internal combustion engine [56].

2.1.3.1 Liquid lubricants

Lubricants formulation is a process of blending two main substances to prepare the lubricant that meets the requirements of working conditions [57]. These substances are categorized into two groups: base oils and additives. Base oils form most of engine oils content. A small amount of different additives (5-20 wt%) are mixed with lubricating fluids to improve lubrication performance. Base oil categories are classified according to the American Petroleum Institute (API) in Figure 2.7. Oil groups (I–III) are manufactured from crude oil through many distillation and refinery processes [58]. Basically, they are so-called mineral oils that are manufactured from crude oil, mineral oil constitutes the majority source of base oil. In brief, mineral oil is composed of various hydrocarbons (cycloalkanes, aromatics, heterocyclic compounds, normal and branched alkanes, etc. It seems difficult to find the chemical content of mineral oil as it varies with refinery processes and production area. For this reason, kinematic viscosity is used to represent the base oil properties at 40 °C and 100 °C.

Group (I) oil is produced by extracting organic sulphides and unsaturated hydrocarbons using solvents. Catalytic hydrogenation is used to decompose organic sulphides and unsaturated hydrocarbons to produce Group (II). On the other hand, Group (III) oil is produced by catalysing the isomerization of hydrocarbons molecules. The difference between Groups I-II

and Group III base oils are their rheological properties [47]. Group (IV) is a chemical synthetics oil that consists of poly-alpha-olefins (PAOs). Group (VI) is made by using mixtures of different alpha-olefins with a viscosity index as high as 140. These oils are limited by the availability of feedstocks and cost. Finally, group (V) contains all other remaining base oils such as chemical synthetics such as diester oil and some mineral oil such as naphthenic oil [59], [60].

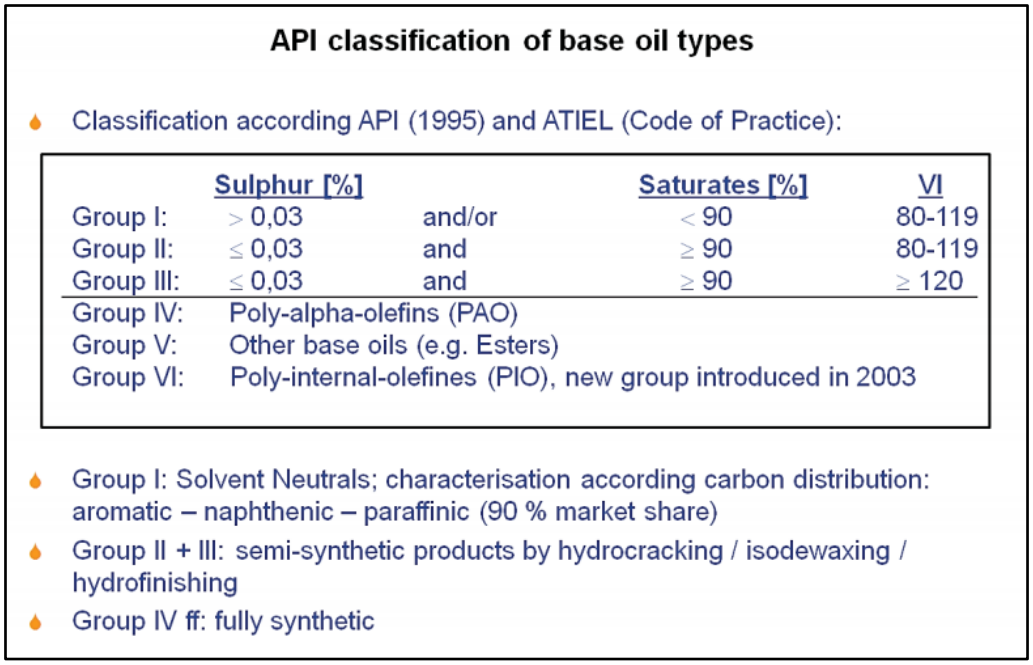

Figure 2.7: API classification of base oils, VI column refers to the Viscosity Index [61].

Based on different types of base oils and combinations of additives that are used to achieve a high level of working performance. Manufacturing engine oils, so-called “formulation”, requires a high level of engineering experience to choose the right base oil and additives that are suitable for the specific application. The following section will highlight the principles of additive manufacturing and its effect on working performance [47].

2.1.3.2 Additives

Almost all commercial oils including fully formulated oil contain several additives to improve their performance. Additives in engine oil play a major role in resisting oxidation, protecting metal surfaces, preventing wear and corrosion, minimising deposit formation, improving characteristics, extending the applicability of lubricant, enhancing the engine oil stability, and

extending the lubricant's service life [62]. The ZDDP as an example chemically reacts with metal surfaces to form tribofilm on the surface of piston, cylinder and rings reducing wear [63]–[65]. While MoDTC (Molybdenum Dithiocarbamate) attracts usually due to the high polarity to metal surfaces forming planner layers of graphite which reduce friction in piston rings and exhaust valves in the engine [66]–[68]. However, the concentration of these additives (ZDDP or MoDTC) in lubricating oils has taken into account the environmental and toxicological considerations [69], [70].

Additives can be classified into two main groups; chemically active and chemically inert substances. Chemical active additive interacts with the contaminants for instance soot and water to reduce their effects on oil performance. It also interacts with metal surfaces in the presence of temperature to form a protective film. Chemical active additives include rust and corrosion inhibitors, extreme pressure and anti-wear agents, oxidation inhibitors, detergents and dispersants. In contrast, inert chemical additives enhance the physical properties of lubricants including viscosity modifiers, foam inhibitors, emulsifiers, pour point depressants, etc. [71].

Table 2.1: Main additive elements originated from the additive compounds [37], [39].

Additive elements	Additive function	Additive compounds
Mg	Detergent/dispersant	magnesium sulfonates, phenates and salicylates
Ca	Detergent/dispersant	calcium sulfonates, phenates and salicylates
S	Detergent/dispersant [a], Friction modifier [b] Anti-wear [c], anti-oxidants [d]	Sulfonates [a], MoS_2 [b], ZnS [c], ZDDP [c], sulphurised terpenes, dibenzyl disulphide, Alkyl sulphides and aromatic sulphides [d]
P	Anti-wear [a], detergent [b]	Zinc dithiophosphate (ZDP) [a], phosphonates [b]
Zn	Anti-wear [a], antioxidant [b]	ZDDPs [a], ZnS [b]
Mo	Friction modifier	organomolybdenum compounds
Si	Anti-foaming	polydimethylsiloxanes

Commercial engine oils contain different multifunctional additives in the form of either purchased as formulated oil for the desired function or as a package. However, Fully Formaluted Oil (FFO) contains different types of additives. The properties and actions of each of these additives are prepared to be used as a single or dual additive compound due to mutual and competing interactions between additive systems. Most common additive elements in formulated engine oil are correlated to functionality [62] as illustrated in Table 2.1.

2.2 Summary

The chapter reviewed the basic topics correlated to tribology for instance, friction, wear and lubrication system. The chapter reviewed the friction principle and the main factors that cause an increase or decrease in friction coefficient. It also discussed different types of wear that can be seen in different conditions and contact mechanics. This chapter reviewed in detail the lubrication system in engine oil including relevant equations to determine tribofilm thickness and lubrication regimes. The chemical formulation and classifications of engine oils were discussed. The reviewed essential topics will provide a better mechanistic understanding of the experimental results obtained in this study.

In the following chapter, the state-of-the-art review is focused on the effect of the main oil contaminants on the performance and degradation of engine oils. Both soot and water are presented in terms of their influence on the tribology performance and oil change intervals as well as filtration techniques and replenishment process of depleted additives.

3 Chapter (3) Literature review

This chapter reviews the state-of-the-art knowledge about the effect of the main oils contaminants on the performance and degradation of engine oils. Both contaminants soot and water are presented in terms of their influence on the tribology performance and oil change intervals as well as filtration techniques and the replenishment of depleted additives. This chapter is divided into four main sections. The first section introduces the soot in engine oil including soot formation in diesel engines, soot effects on the tribological performance, the size distribution of soot in used oil, mechanical properties of soot nanoparticles and the efficiency of soot removal techniques. Section two discusses the water contamination phases in engine oil, the expected level of water in the oil, the damages that can be caused by water and the effects of water on the tribological performance. Section three presents the effect of soot and water on additives. Section four reviews engine oil change interval and the engine oil quality as well as the additive replenishment system. Finally, section five summarises and draws conclusions on the most important aspects and knowledge gaps discussed throughout this chapter. **Error! Reference source not found.***Figure 3.1* aims to summarise the research approach on engine oil contamination and the planned works to extend the oil change interval.

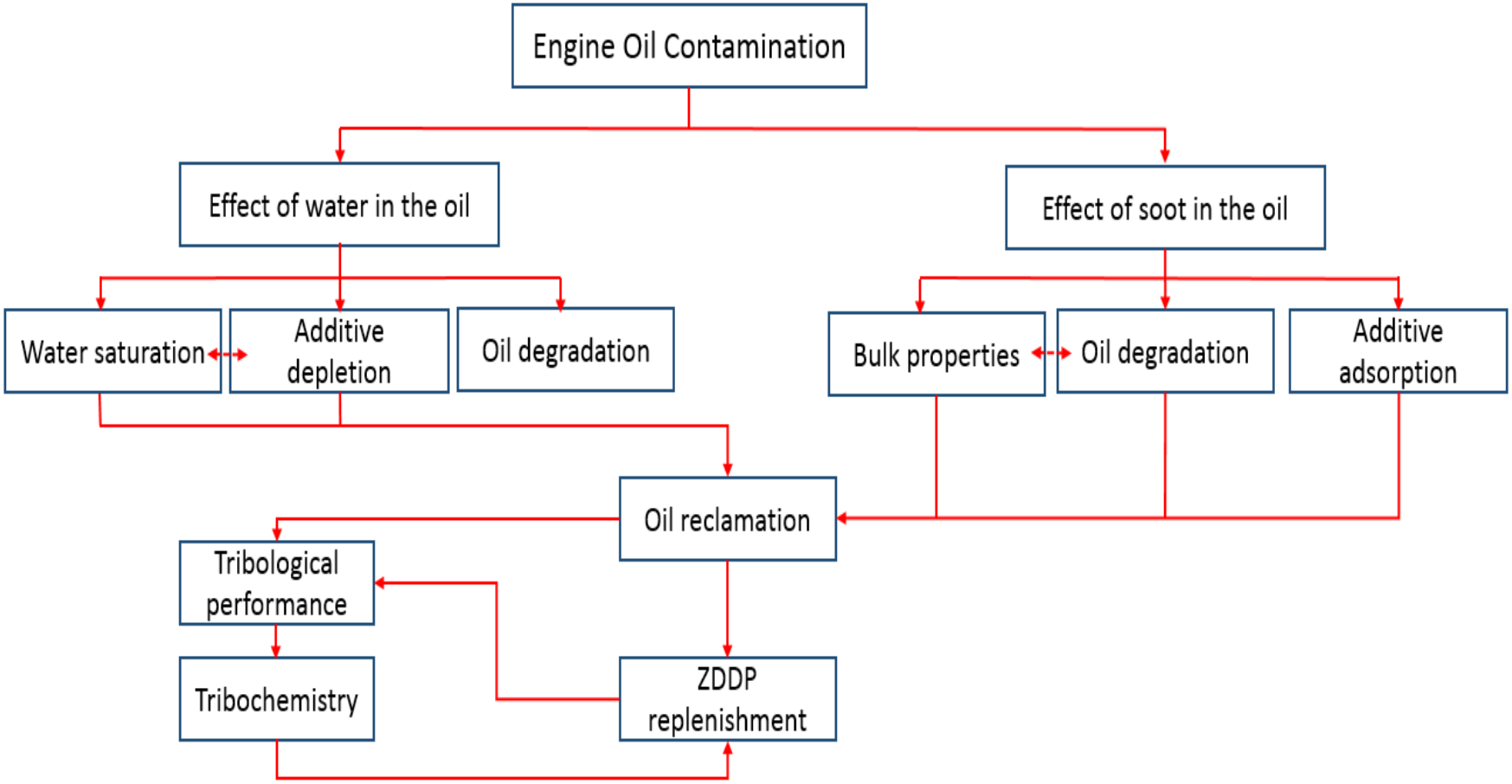

Figure 3.1: Schematic of the effect of engine oil contamination on the lubrication system and the planned works to extend the oil change interval.

3.1 Soot in engine oil

3.1.1 Soot generation in diesel engine

Soot describes microscopic carbonaceous particles of different sizes and shapes that are formed due to the incomplete combustion of hydrocarbons. It contains ash, unburned hydrocarbons and carbon. The unsaturated hydrocarbons are polycyclic aromatic hydrocarbons (PAHs) and acetylene. Chemical analysis of soot proved that it contains 90 % carbon, 4 % oxygen, 3 % hydrogen and a small amount of sulphur, nitrogen and traces of metals. Soot particle size in a diesel combustion engine is in size up to 40 nm and the particles conglomerate with a mean size of 200 nm and up to a maximum of approximately 500 nm. Soot formation stages and the growth of soot particles are demonstrated in Figure 3.2.

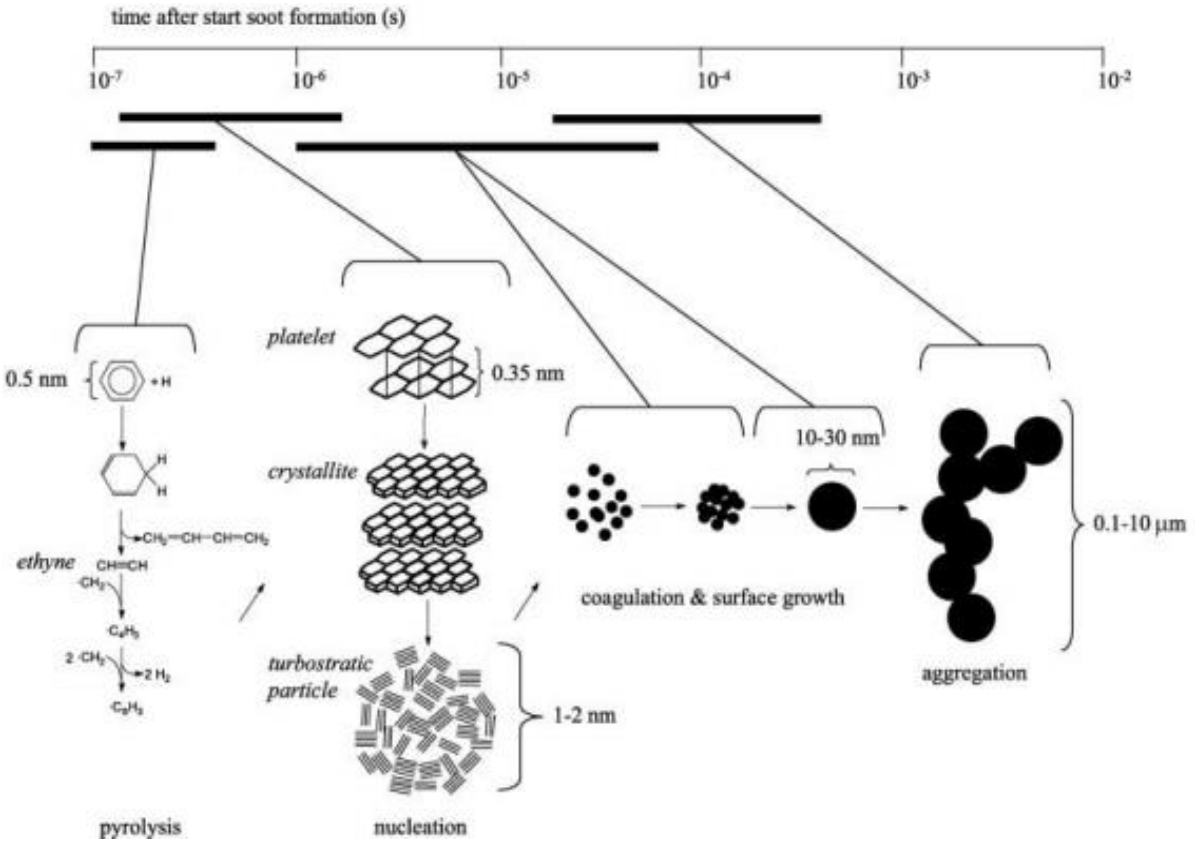

Figure 3.2: Formation stages of soot particles in diesel engine oil [18].

In severe burning conditions, soot particles aggregate and grow over time up to microns. However, hydrocarbons that are trapped inside the soot are the main effect of the reduction

in the size of particles when are burned out due to contact with each other. Soot is formed and disintegrated throughout the combustion oxidation processes. Basically, when soot particles that are formed in the initial burning stage come into contact with the air higher than the fuel, most of these particles will be oxidised. The majority of soot particles are absorbed by the lubricating oil and the rest of the particles will be exhausted. The agglomeration of soot particles in engine oil has a soft behaviour when it scratches the surfaces, while individual soot particle has an extremely hard effect on the sliding surfaces [7, 44].

3.1.2 The effect of soot particles on engine oil performance

Designing lubricants that are able to maintain their chemical and physical properties in the existence of soot particles for a long time has been a subject of interest. Many approaches addressed the problem, by means of how engine mechanisms and their interfaces are actually influenced by soot particles. This requires inspecting what concentration of soot particles can be tolerated in engine lubricant and the effect on tribological performance. However, many different theories investigated the formation of soot, soot particle properties and their effect on the performance of engine oil as will be investigated in the next sections. In order to simulate the effect of soot on lubricating oil, there are three different options to choose test samples; used engine oil, carbon black mixed with new oil or extracted engine soot mixed with the new oil. Basically, carbon black mixed with fresh oil is a well-known method of producing the test samples as it is easy to prepare, inexpensive and constant contaminated with the same particles at each time [73].

3.1.2.1 Effect on Friction

Soot in engine oil has an extreme effect on the tribological performance and more specifically the friction between the sliding surfaces. Penchaliah et al. [75] stated the oil that contained contaminants (moisture, sulphuric acid, soot, and oxidation) at varying levels produced a lower friction coefficient compared to uncontaminated oil. They suggested that the reduction of friction values is due to CB in engine oil. Liu et al. [76] studied the friction using cylinder-on-

disc reciprocation to measure the variation of friction coefficient with a variety of diesel lubricating oils with different levels of soot contamination. The soot used in tests was produced in a fired engine. The friction coefficient decreased with the existence of soot in engine oil. The results showed that soot particles in oil acted as a friction modifier. In contrast, Pin-on-disc measurements were carried out by Ramkumar et al. [77], the results for diesel lubricants that contained diesel soot particles at different contamination levels revealed that the friction coefficient and wear increased. Chinas-Castillo and Spikes [78] indicated that soot particles in oil influenced EHD oil film thickness, and therefore affected the characteristics of friction on the contact surfaces especially when the initiation soot diameter was larger than the protection film thickness. In this case, the level of soot and the agglomeration of the particles in oils were considered the main reasons for the increase in the friction coefficient.

3.1.2.2 Effect on wear

There are four major wear types in diesel engines: fatigue, adhesion, abrasion and corrosion. Corrosion involves several chemical reactions that lead to adhesion, fatigue and abrasion hence mechanical damage on contact surfaces. For all of these wear mechanisms mentioned above, the oil contaminated by soot particles is a predominant driver of wear failure [71]. Joly-Pottuz et al. [14] found that adding carbon black particles to base oil showed defects sites on steel surfaces related to the highly abrasive process with an increase in friction and wear. Colacicco and Mazuyer [80] studied the wear behaviour of soot particles in diesel engines and the aggregation of soot particles, especially in the inlet of the contact surfaces which caused starvation, and consequently transferred materials between the contact surfaces due to the adhesive between the asperities of contact surfaces. Berbezier et al. [81] inspected the role of soot particles in mild lubricated wear and they found that wear increased due to the reduction in tribofilm coverage on sliding surfaces.

Corso and Adamo [82] examined the lubricant additives' reactivity with diesel soot and they found that the existence of soot particles induced a transition from anti-wear Fe_3O_4 to pro-wear

FeO. They explained this phenomenon, in specific conditions such as high soot concentration and high temperatures with limited oxygen that reaches contact surfaces, the metal surfaces form oxide FeO instead of Fe_3O_4. While abrasive wear as a result of soot particles was widely investigated, Ratoi et al. [23] found that dispersed carbon black in formulated oils can remove ZDDP tribofilms by abrasion. Similarly, Kuo et al. [21] showed that soot abrasive action, in rocker arms and crosshead wear tests, was responsible for removing the whole tribofilm from the contact surfaces. Consequent to the hardness of soot particles, the graphite and carbide surfaces were also abraded by soot. Many studies discussed the effect of soot percentage on wear. The results clearly showed an increase in wear with the increase soot particles level in oil as demonstrated in Figure 3.3 [56, 57].

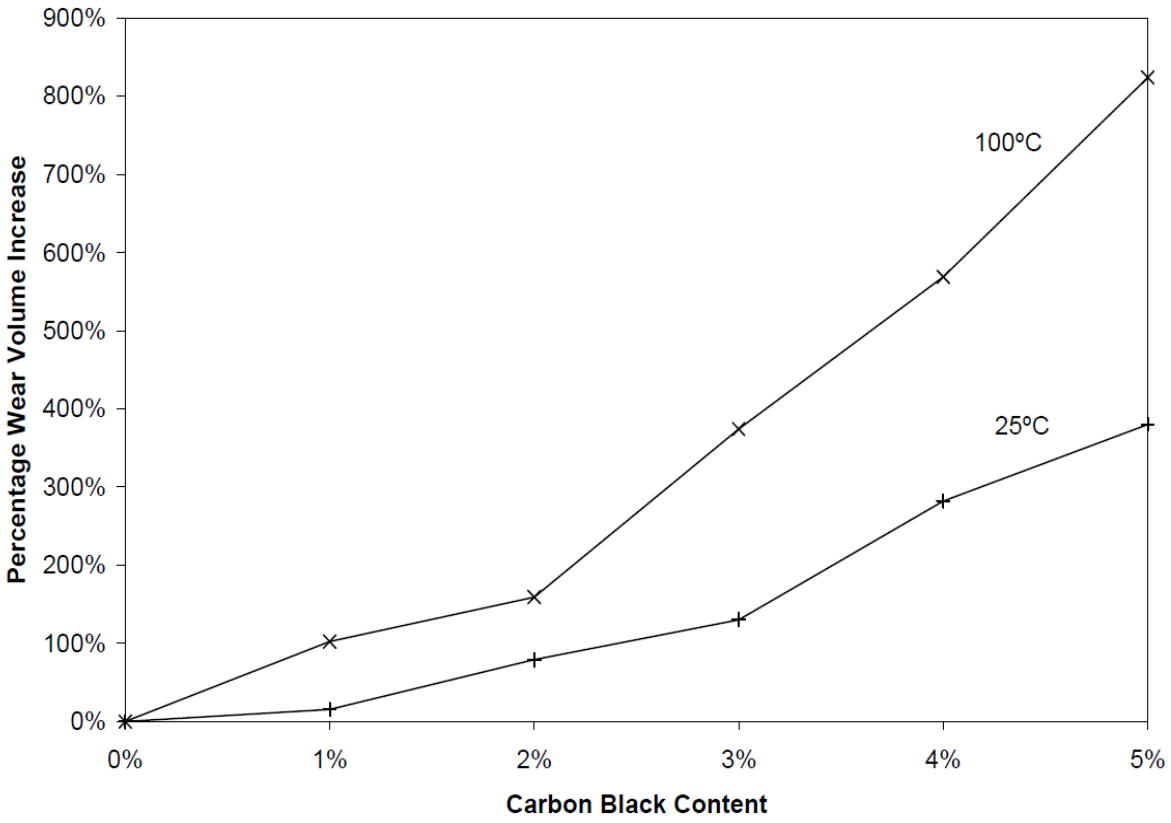

Figure 3.3: The effect of soot level in base oil on the wear of ball-on-flat testing at 25°C and 100°C [84].

Figure 3.4 demonstrates the wear scars characteristics change in response to varied testing temperatures and CB content in oil. Abrasion and plastic deformation on surfaces were observed due to possible starvation of oil between rubbed surfaces [84].

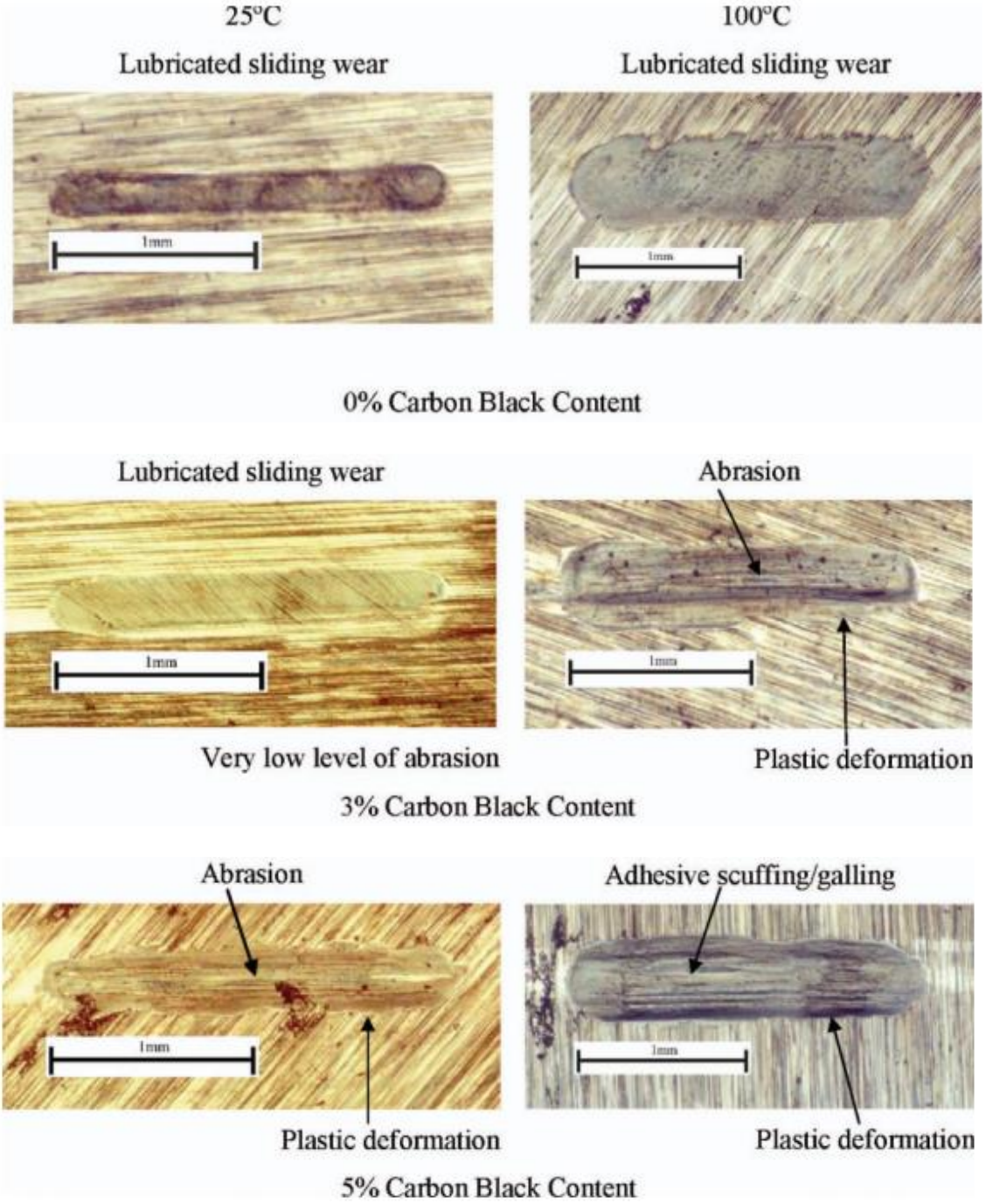

Figure 3.4: Wear scars images of oil containing 0, 3 and 5 wt%CB at 25 and 100 °C [84].

The effect of soot on rubbed surfaces is represented in Figure 3.5 for two different oils, base oil contained a little amount of additives (15W40) and formulated oil CD SAE 15 W-40. The abrasive wear effect varies depending on the film thickness and soot particle diameters. In this case, the formation of tribofilm correlated with oil type. For example, the formulated oil film thickness was two times thicker compared to the tribofilm of base oil 15W40 which contained

a small amount of additives. The agglomeration of soot particles and hard abrasive occurred when the base oil was used. This caused starvation preventing the oil to access the contact surfaces which led to an increase in wear [22].

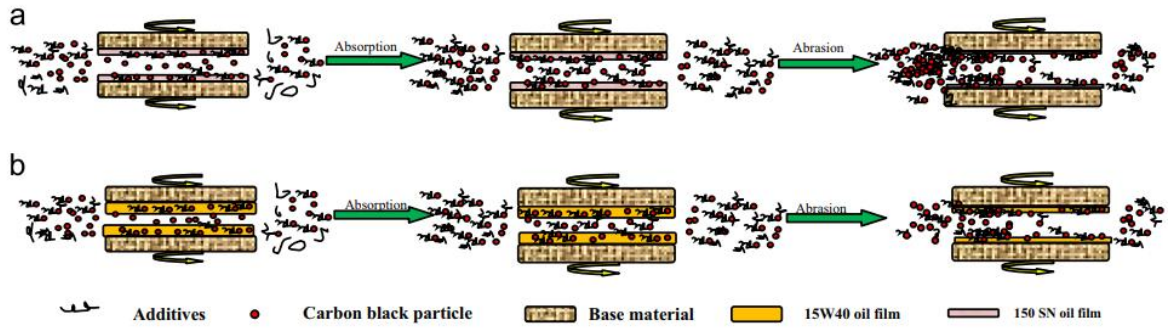

Figure 3.5: Schematic of engine soot and its effect on the tribological mechanism for two different oils a) 150 SN (base oil) and b) CD SAE 15 W-40 (formulated oil) [22].

A high concentration of soot contamination in the engine oil causes oil starvation due to a blockage of soot particles in the inlet of contact surfaces [24], [85]. Sato et al.[24] revealed that starvation occurred due to the agglomeration of soot particles with a diameter larger than the oil film thickness leading to high wear as illustrated in Figure 3.6b. To minimise the starvation problem, more dispersant is added to reduce the soot agglomeration and its effect on the wear. It is worth mentioning that using too much dispersant can also promote corrosion in rubbing surfaces [86], [87]. Abrasive wear is the most common surface damage in the presence of soot contamination. This leads to a decrease in the engine oil performance and hence engine failure [21]–[23]. The effect of abrasive wear varies depending on the film thickness and soot particle diameter [24]. With the low level of soot and high film thickness, abrasive wear is the most common effect on the surface as represented in Figure 3.6a.

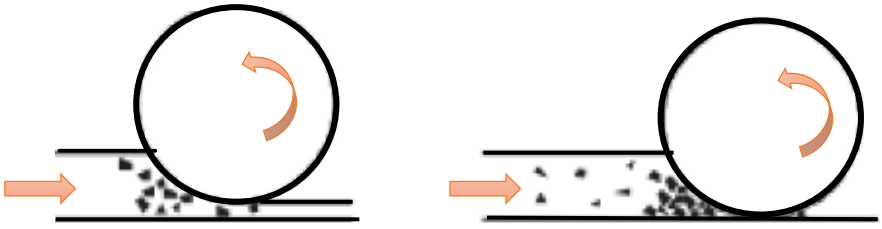

a) Abrasion wear b) Starvation wear

Figure 3.6: Simulation of abrasion wear and starvation phenomenon in the presence of soot particles [73].

3.1.2.3 Effect on viscosity

Several studies were carried out to understand the lubricant viscosity behaviour with soot contamination. George et al. [25] tested three oil samples containing soot with different types of base oil, different amounts of dispersant and ZDP. They investigated the effect of the various soot level on viscosity at different temperatures. The results indicated that the viscosity of oil increased with the increase of soot level in samples at both 40 and 90 °C. In addition, the study showed that viscosity behaved nonlinearly at 40 °C, compared to a linear variation at 90 °C with the same amount of soot. The statistical analysis of the system focused on the interactions between the variables that control oil thickness. The results showed that the effect of ZDP levels and base stock were negligible at 40 °C, whereas the high level of soot and dispersant caused an increase in the viscosity of the oil samples at 40° C and 90 °C. Ryason and Hansen [88] clearly showed that increasing the soot level in oil leads to an increase in viscosity which can influence oil performance, especially at low temperatures. They proved that the viscosity had a linear increase with the increase in soot level until less than 1 wt%. Whereas the viscosity increased rapidly with the increase in soot level above 1 wt%. Figure 3.7 shows the reason behind viscosity changes in engine oil under different working conditions in the presence of oil contaminants [89].

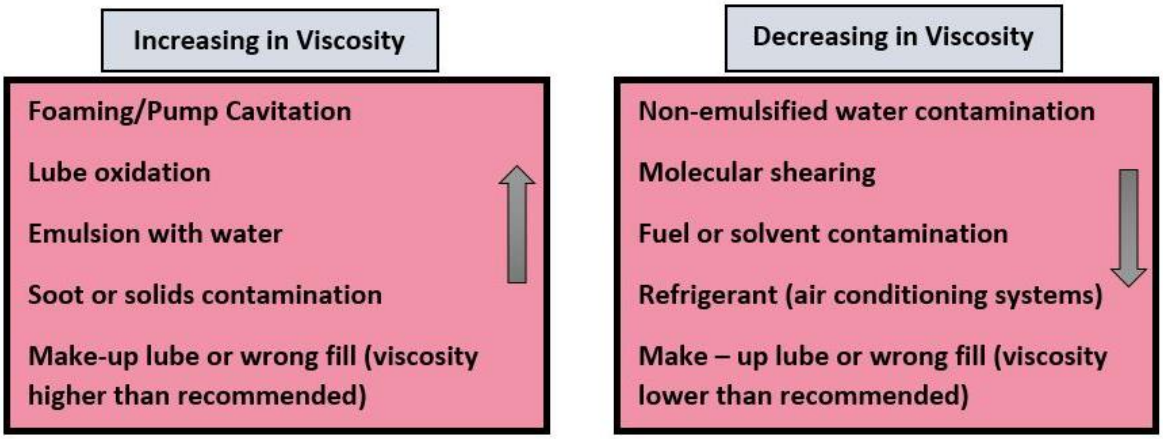

Figure 3.7: Factors that affect the oil viscosity [89].

3.1.2.4 Effect on degradation

The degradation of engine oil is defined as an irreversible chemical deterioration that can lead to a significant reduction of its Total Base Number (TBN). (TBN) is used to measure an alkaline content in the oil and hence its ability to neutralise acids that are generated during the combustion process. When the oil degrades over the lifespan, the oil will no longer able to neutralise acids. This causes an increase in oil contaminants, failures of protection films and an increasing probability of corrosion. The existence of soot in engine oil tends to degrade the oil and decrease TBN due to the high acidity of the oil. Kawamura et al. [90] summarized lubricant degradation mechanisms that cause wear in the engine components. There are many by-products of the diesel combustion process including unburnt hydrocarbons, carbon monoxide, oxides of nitrogen, and carbon dioxide. Combustion by-products are highly acidic which influence TBN and degrade the lubricant. Additives in the oil are used to face these acidic materials, but over time the additives will be depleted due to the interaction with degradation products. For instance, dispersant additive retains wear debris and soot particles within the oil to assist in the reduction of engine wear. Increasing soot particles in oil depletes the dispersant and decreases the ability to retain any more soot or debris. Other additives are degraded due to the interaction with acid combustion products. All of these factors cause oil degradation and losing the oil ability to perform its functions [91]. Figure 3.8 illustrates the oil degradation cycle over the service life of engine oil.

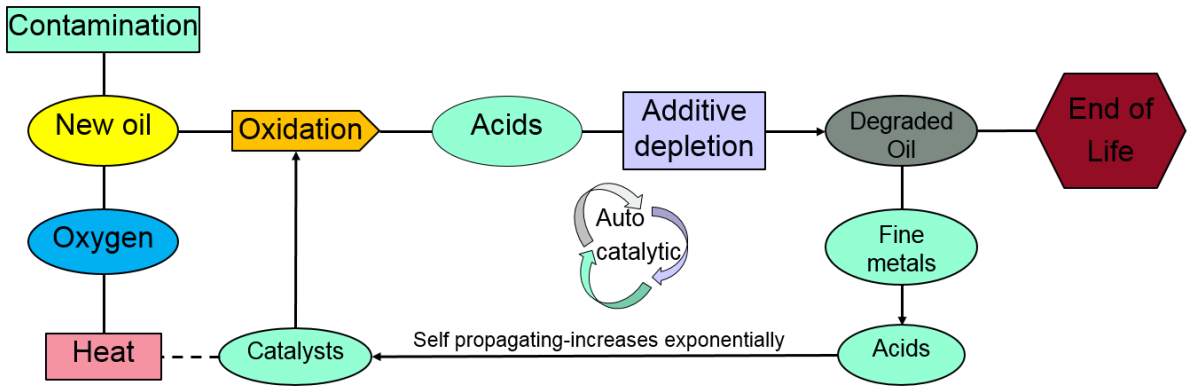

Figure 3.8: Oil degradation cycle [92].

3.1.2.5 Oxidation and sulfation

Oxidation is a series of chemical reactions of the engine oil that leads to the breakdown of the engine oil. Three key stages have been indicated during the oil oxidation as shown in Figure 3.9. In the initiation stage, the hydrocarbons from the base oil chemically react with atmospheric oxygen to produce a hydrocarbon free radical. In the propagation stage, the chemical reactions between hydrocarbons free radical, oxygen and catalysts form peroxide radicals. In the final oxidation process, the hydroperoxides produce organic acids and other oxygenated compounds [93].

Antioxidants depletion in this stage accelerates the oxidation process. The presence of temperature influences the oxidation mechanism, higher temperature involves a higher oxidation rate in engine oil. The chemical composition of engine oil, additives, contaminants, reactive metals and time (vehicle millage) affect the oil stability and accelerate the oxidation rate. Fourier-Transform Infrared Spectroscopy (FTIR) technique is used to monitor the contaminants including soot, water, fuels, sulfonation, oxidation and nitration of base stocks of oils [94], [95]. Oil oxidation is accelerated in the presence of soot. Motamen Salehi et al.[10] demonstrated that ageing oil containing CBP increased the oil oxidation compared to oil aged with no CBP. The study on the effect of soot levels on oil oxidation has shown that higher levels of soot in the engine oil cause a higher oil oxidation rate [13]. Also, combustion by-products formed during the combustion process such as unburnt hydrocarbons, carbon monoxide, oxides of nitrogen and carbon dioxide can be detected in a used oil [90]. The presence of these by-products in the used oils results in increasing the rate of oxidation, nitration and sulfation due to their interactions between oil, soot and additives [73].

Sulphate by-products are produced as a result of the oxidation of sulphur-containing compounds in engine oils. Post chemical interactions between sulphate by-products and water can form sulphuric acids (H_2SO_4) [94]. Sulfation accelerates the production of varnish and sludge leading to an increase in oil degradation [94], [96]. The presence of sulphur in soot

particles may induce sulfation in engine oil. The $S-O$ and $S=O$ bands are referred to the formation of sulphate by-products as an increase in FTIR intensity. FTIR technique is used to identify the sulfation at the $S-O$ and $S=O$ bands in FTIR spectra in regions around 1150 and 1250 cm^{-1} respectively [94]–[96].

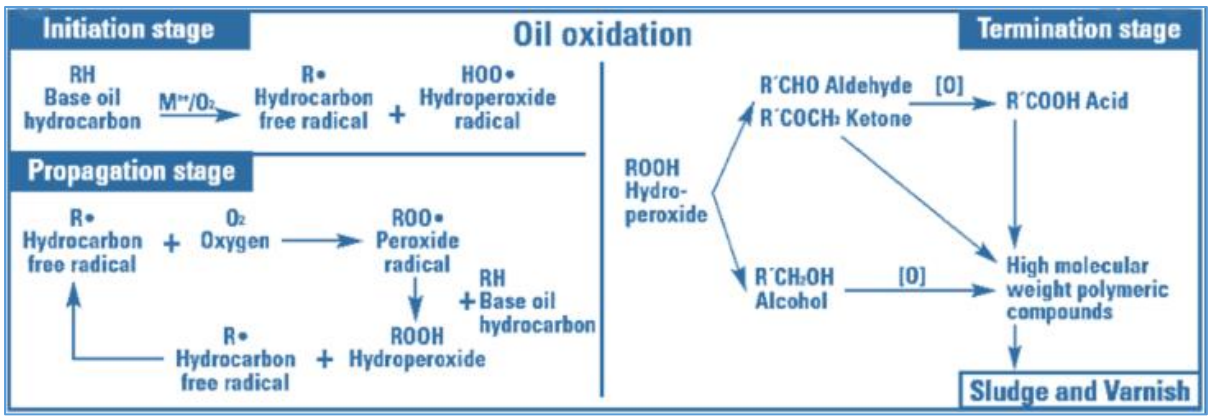

Figure 3.9: Schematic of the oxidation process stages of engine oils [93].

3.1.3 Mechanical properties of soot

Soot particles are identified as carbonaceous material (>90 % carbon) which is produced during the combustion process in the diesel engine. Several investigations have revealed that soot has a topically spherical shape with varied sizes starting from a few tens of nanometers of primary particle, while soot primary particles can easily aggregate and reach up a few hundred nanometers [97], [98]. The soot crystal structure consists of the core and the outer shell which can vary from mostly amorphous or random to perfectly ordered crystalline structure of graphite [99]. Based on several studies [21], [85], [100] revealed that wear of contact surfaces is correlated to abrasion of soft surfaces by hard soot particles as shown in Figure 3.10. Soot particles are hard enough to abrade the contact surfaces of engine components. Uy et al. [97] showed that different types of soot had a difference in the morphology of particles which could affect the hardness of particles and hence the wear.

Consequently, soot nature and its wear effect on the surfaces are an interesting area in the lubricant industry. However, understanding soot particles in terms of structure, morphology

and mechanical properties under sliding or compression is a major issue to reduce the wear effects [99]. Motamen Salehi et al. [10] studied the absorption of ZDDP additive on soot particles. The results showed a significant reduction in zinc and phosphorous concentration due to additive adsorption on soot particles. The authors proposed that additive adsorption on soot particles due to the high reactive surface of soot causes a change in the hardness of particles. The interaction between calcium phosphates, which is a detergent compound and considered a hard material in nature, and soot particles could change the abrasive characteristics of these particles [101]. Therefore, the interaction between the additives, oil and soot surfaces can contribute to ambiguous analytical results and need more understanding of how that influence the mechanical properties of soot particles.

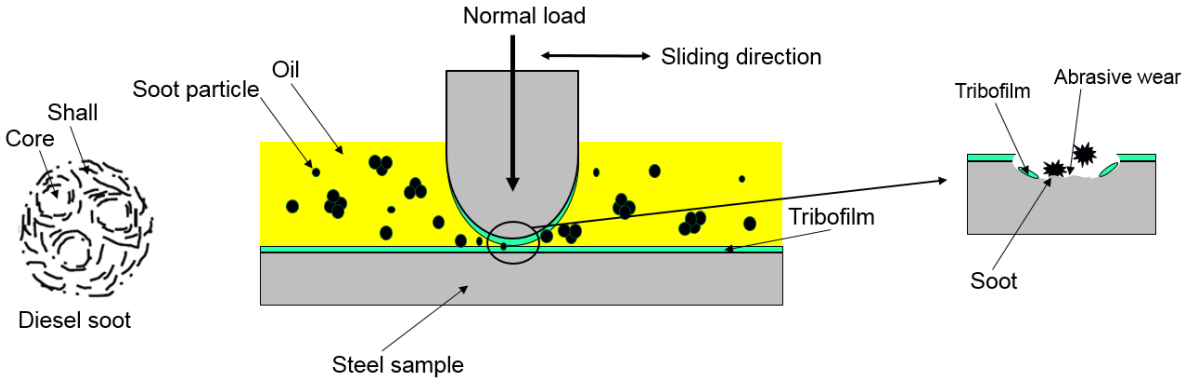

Figure 3.10: Schematic of abrasive wear caused by soot particles (created by author).

The in-situ TEM nanoindenter technique has been used in several works to identify the nanoscale mechanical properties of various types of nanosize materials such as silicon nanowires [102], silicon nanospheres [103], MoS2 nanoparticle [104], ZnO nanowires [105] and carbon nanotubes [106]. Lahouij et al. [107] studied the mechanical properties of signal and agglomerates of soot particles. Sliding and compression tests were performed to investigate soot particles' behaviour using the In-situ TEM nanoindenter technique. The results showed that soot in either signal or agglomeration states resisted the applied deformation load. The signal particle of soot under compression was exhibited elastic-plastic behaviour without any damage of soot after compression until 7 GPa contact pressure. However, the elastic behaviour of the single soot was reflected in the behaviour of soot aggregation.

Sliding tests of soot showed at both signal and agglomerate soot particles could roll between rubbing surfaces with occasional sliding occurring under shear conditions. Jenei et al. [108] performed In-situ compression tests of soot to measure the mechanical properties of soot particles extracted from the diesel engine. During the compression, the soot particles exhibited an elastic-plastic behaviour and suffered from permanent changes in the size and shape of their structure. The results showed an increase in calculated hardness and Young's modulus of the soot particles after consecutive compressions. The contact pressure was subjected to up 16 GPa and no noticeable break-up was observed after compression while the structure of soot was changed. The hardness of soot particles was registered in the range of 3-16 GPa. The hardness of soot is in the range of 3-16 GPa which is harder than ZDDP tribofilm 2-5 GPs [108]. While Bhowmick et al. [109] performed soot nano-indentation using AFM as shown in Figure 3.11a, the results demonstrated that a maximum load of 100 µN was recorded to resist the indentation movement into the soot particles/agglomerates as illustrated in Figure 3.11b.

In order to better understand the factors underlying the wear caused by soot particles, it is important to understand the behaviour of soot particles and to characterise potential changes in their mechanical properties, for example, changes in hardness due to the mechanical stress or additives adsorption.

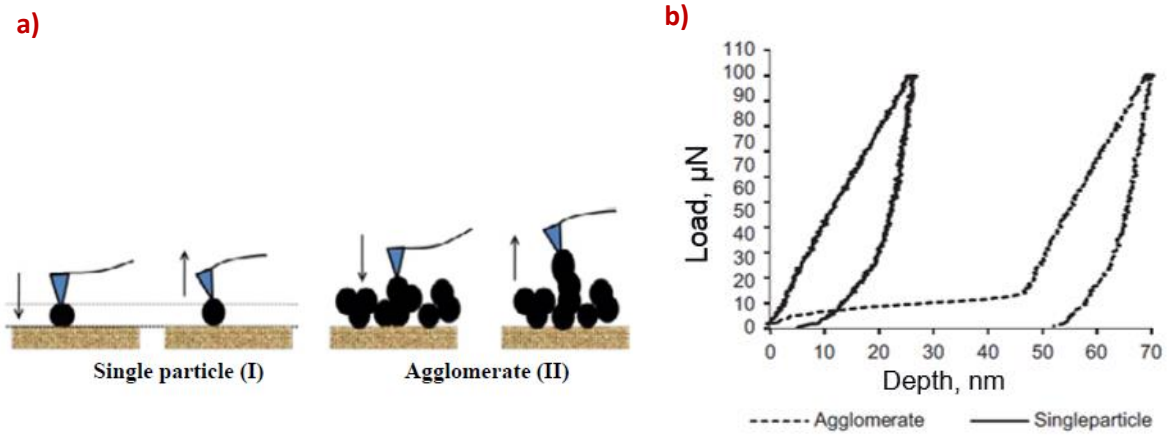

Figure 3.11: a) Schematic of AFM tip indenting and retracting from soot particle/agglomerates and b) deformation behaviours of diesel soot particle/agglomerates [109].

3.1.4 Soot size distribution

Most of the soot exists in oils as carbon nanosized agglomerates, mostly in a cluster or chainlike-shaped structure with a characteristic length of up to 200 nm [110]. Figure 3.12 shows soot size distribution with different single injection runs, the images show an increase in the intensity of soot with increased runs number in the engine. The number of soot aggregates per image and diameters of the primary soot particles for different runs are increased as shown in Figure 3.13a and b respectively [111].

Gautam et al. [71] showed that wear increases with an increase in the soot concentration in oil. Soot reduced the efficiency of the antiwear additive to protect the surface from soot causing an increase in wear. The effect on wear is correlated to the soot characteristic in either particles or agglomerates. According to Li [112] study, the results reported that abrasive wear happens and the wear scar width is matched to the size distribution of soot particles. As suggested by Yue et al. [113], soot size distribution and aggregate morphology can increase the severity of oil rheology.

Soot size distribution is of interesting factor that affects the oil properties and for insight, it provides details for the formation and growth of soot. The understanding of soot size distribution and its influence on the oil properties and tribological performance is impeded by the reliable characterisation technique. FTIR technique is widely used to determine the soot concentration in oil, but this technique does not give enough details about the number of particles and size distribution of soot particles [114]. Analysing of TEM images has been used by several investigators [110], [112], [115], [116] to assess the shape and size of soot agglomerates and their distribution in oil. In this project, the TEM technique will be used to determine the shape and size of particles in real engine oil.

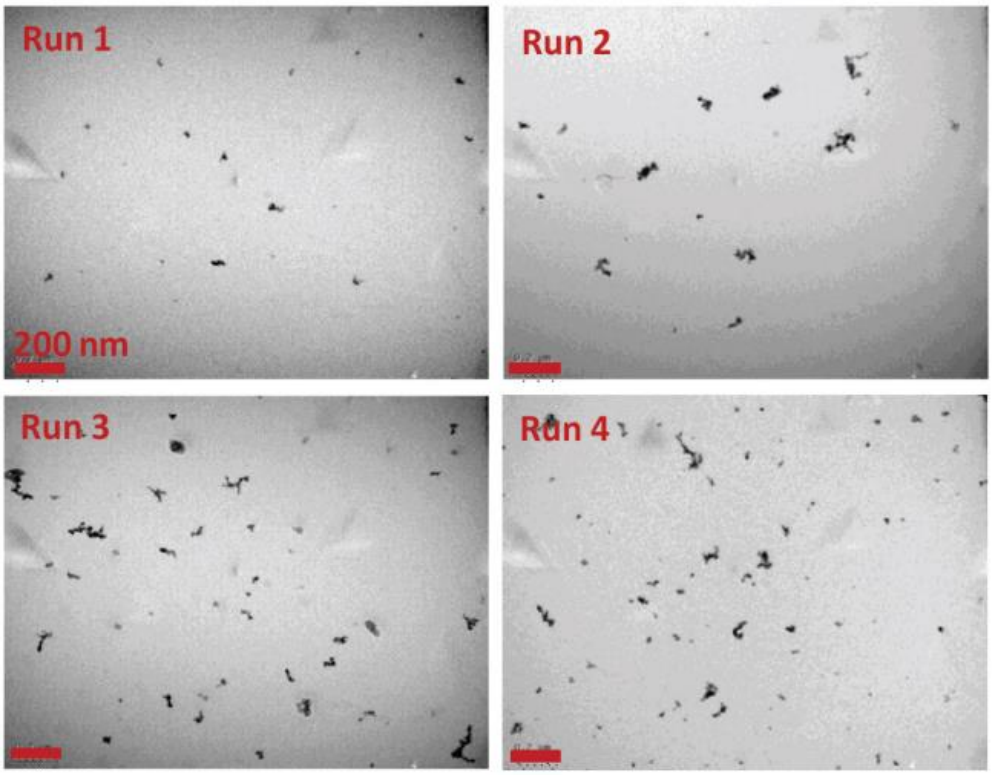

Figure 3.12: TEM images of soot of different single injection runs [111].

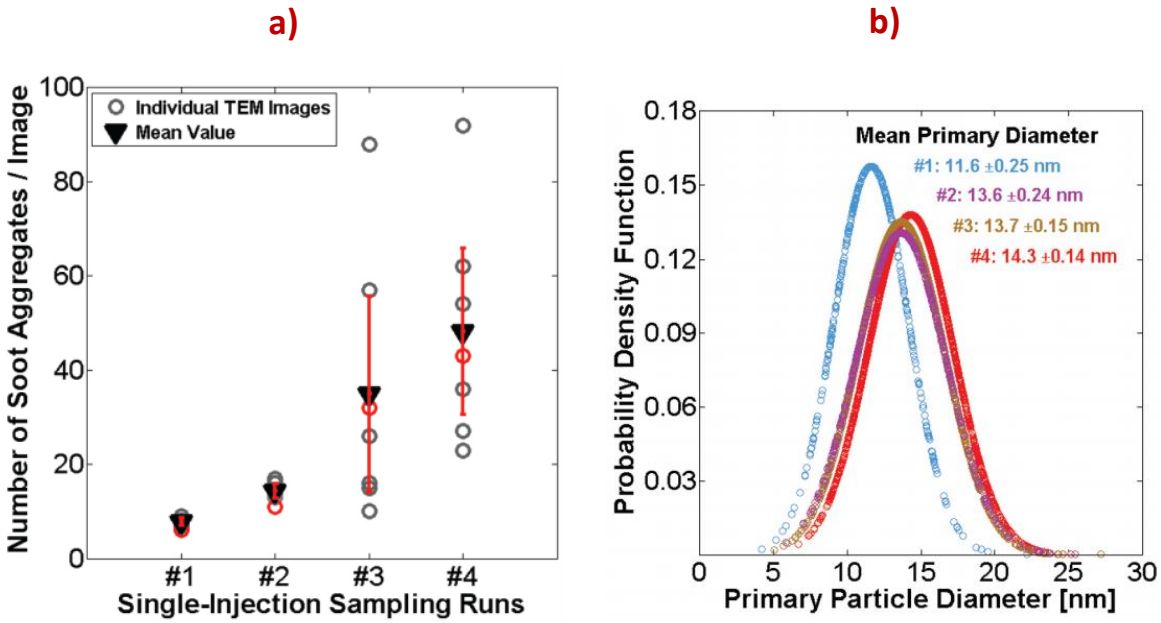

Figure 3.13: a) The number of soot aggregates per image, b) the diameter of the primary soot particles for different runs [111].

Soot size distribution is influenced by dispersant levels in engine oil. Much dispersant concentration exists in the oil, the small size of soot particles will disperse in the oil causing

much less wear [117]. Sato et al. [24] showed that soot particles with size distribution less than tribofilm thickness produce less wear compared to particles size larger than tribofilm thickness.

3.1.5 Soot removal techniques

Vehicle manufacturers have been facing a commercial challenge to extend oil change intervals using different filtration techniques. There are two main full-flow filtration systems fitted in most heavy-duty vehicles such as media filters and centrifugal filters. The efficiency and the ability of these filters to remove the soot particles are presented in this study as follows:

3.1.5.1 Media filter

Diesel engines produce the soot and combustion by-products that end on the surface of engine components. Therefore, a good filtration system is required to protect the engine from these contaminants. The diesel filtration system of heavy-duty trucks typically uses two oil filters: a full-flow filter and the bypass filter. In the new filter design, both filters combine into a single filter as shown in Figure 3.14. A full flow of oil into the filter maintains the easy engine oil transfer throughout the lubricating system during normal engine operation. While, in bypass filter, the oil is transferred throughout the tight media with high-pressure oil is needed to force the oil to go through low porosity media. Nearly 10 % of engine oil can be filtered in the bypass filter without effect the lubricating operation circuit in the engine [118]. Both filters have been designed to provide good filtration for engine oil under severe operating conditions. The flow filter is designed to trap the contaminants with a size of 30 µm and larger. While bypass filter has the ability to capture the smaller size of particles down to 5 µm. Approximately 75 % of the trapped contaminants in the filter consist of soot and sludge. The oil filter should be replaced every time that used oil is changed to reduce the risks of clogging the filter [119], [120]. A bypass filter has a significant improvement in oil performance after using a bypass filter compared to a full-flow filter as shown in Figure 3.15.

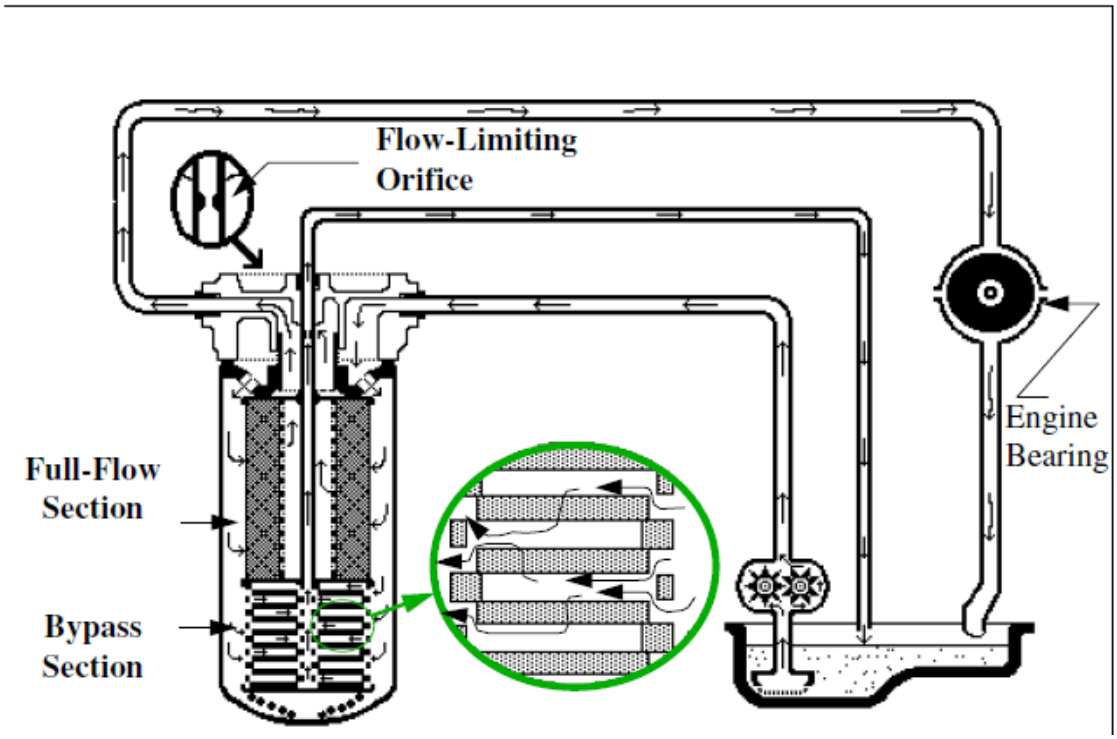

Figure 3.14 Lubricating filter circuit for combination filter consists of full flow and bypass filters [118].

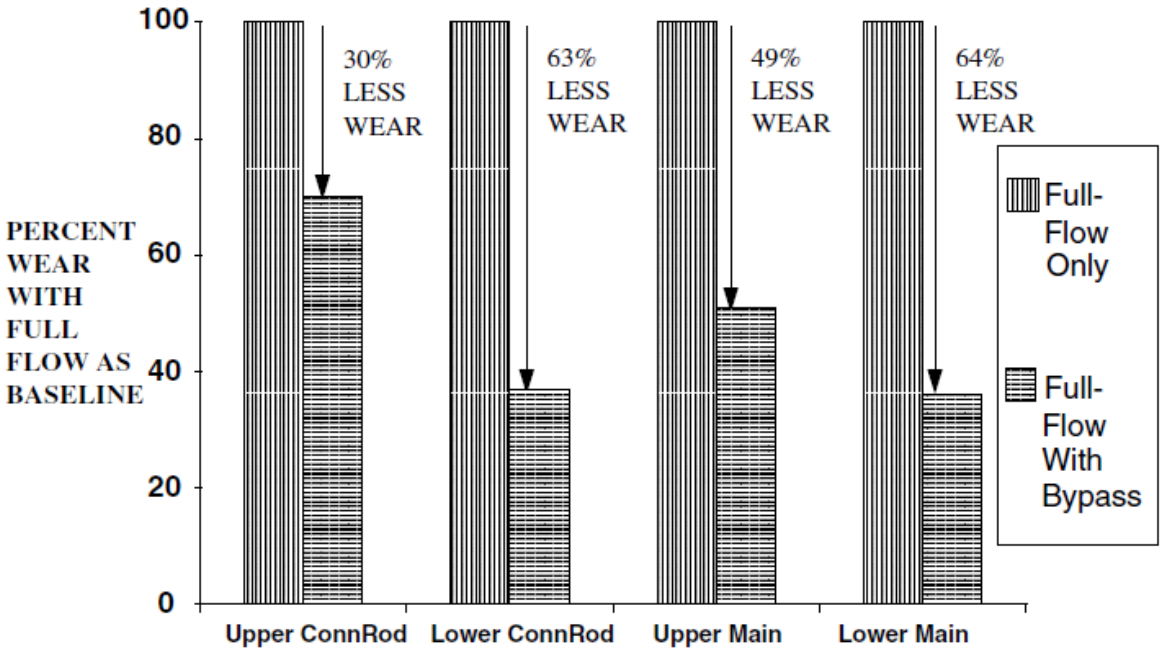

Figure 3.15: Comparison between the wear after using bypass filter compare to full flow filter in different engine components [118].

Based on the material constriction and structure, the particles removal offers a new design of filter called depth filter. The common disposable filter is used the surface filter consists of one

layer of woven or brown fibrous or polymeric materials of construction such as cellulose, glass fibres, polyester and nylon as shown in Figure 3.16b. The surface filter can retain only coarse suspended particles in oils. Once the filter surface is blocked by these particles, the filter will no longer provide further filtration action. Adding depth to the filtration media in greater degrees can prolong the filter service life and increase the effectivity to capture the heterogeneous range of particles sizes. The depth filter consists of multi-layers with tortuous paths through the filter section as shown in Figure 3.17 to allow the contaminants to travel within the filter resulting in a high holding capacity of contaminants [121].

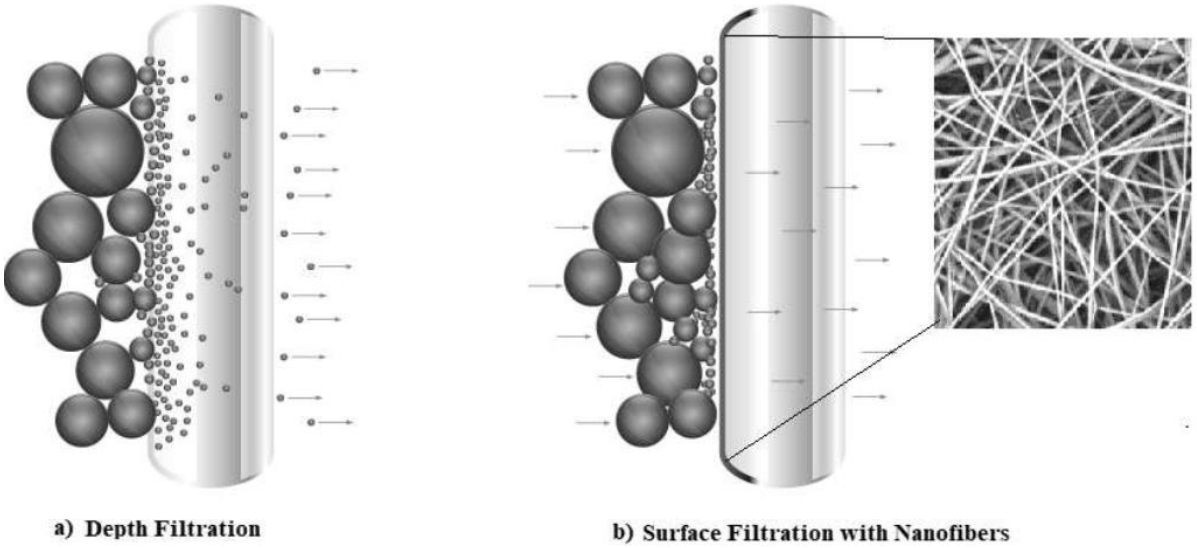

Figure 3.16: a) Depth filtration b) Surface filtration of nanofibers (one layer) [122].

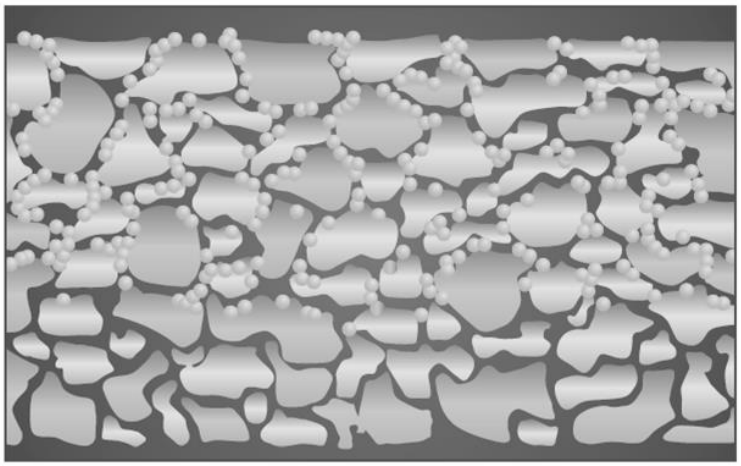

Figure 3.17: Tortuous path in the depth filter [121].

Figure 3.18 shows full-flow with depth bypass filter shows a decrease in wear of rod bearing in engine compare to other types of filtration [118].

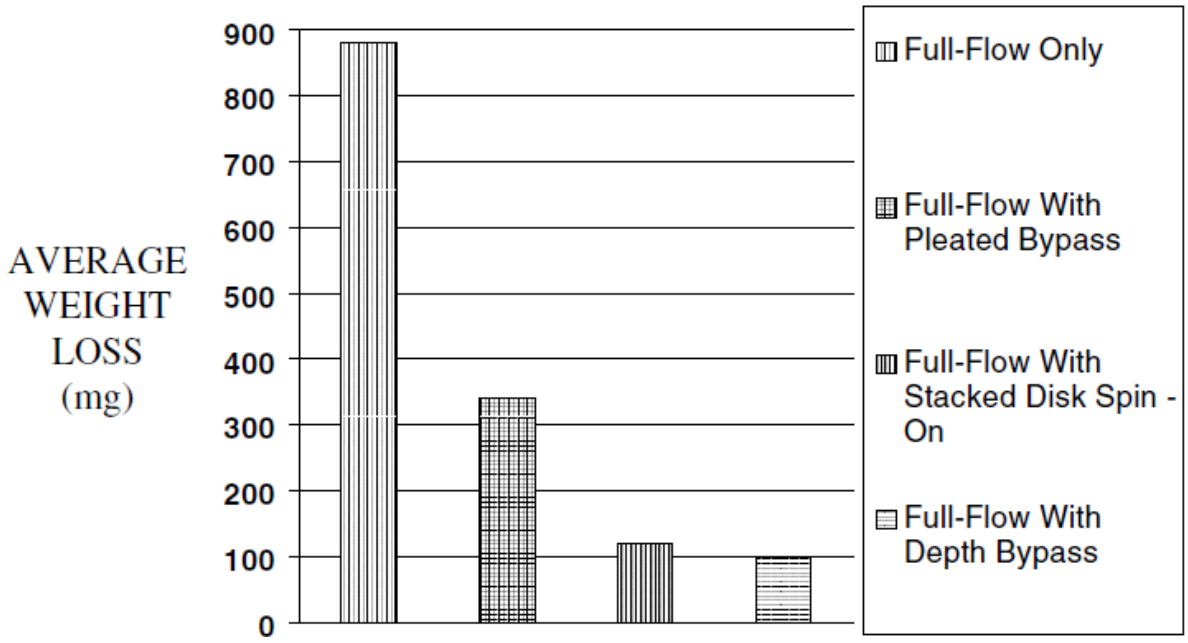

Figure 3.18: Rod bearing wear with different filtration types compare to depth filter [118].

3.1.5.2 Centrifugal filter

The principle of centrifugation separation has been used in oil filter design. The oil is directed into the centrifugal filter and the rotor spinning inside the filter uses the centrifugal force to accelerate and deposit on the internal wall of the filter as shown in Figure 3.19a. The contaminant particles are stuck in the wall and built a layer above the layer of solid particles. The centrifugal force depends on the density of the particles to remove them from oils, thus there is no restriction on the contaminant particles' size. The centrifugal filter has two main advantages compared to the media filter. Firstly the filtration process remains constant during the service interval. Secondly, there is no limitation in particles sizes that can be removed by centrifugation filter compared to other filters design. In practice, the lower particles' size can reach less than 1 µm. The basic principle of centrifugal sedimentation theory can be explained as a spherical solid particle with a diameter d_p and density ρ_p suspended in the oil at radius r with oil dynamic viscosity μ_o and density ρ_o. The whole system is rotating at a constant angular

velocity $\boldsymbol{\omega}$ about vertical axis as shown in Figure 3.19b. Strokes law calculates the time τ is needed for the contaminant particle to travel for a distance Δr from initial point in oil to internal filter wall, the law is given in Equation 3.1 [120]:

$$\tau = \frac{18\mu_{\circ}\, Ln((r+\Delta r)/r)}{{d_p}^2 \Delta\rho\, \omega^2} \qquad \text{Equation 3.1}$$

Where $\Delta\rho = \rho_p - \rho_{\circ}$ is the difference in density between the solid particle and the oil.

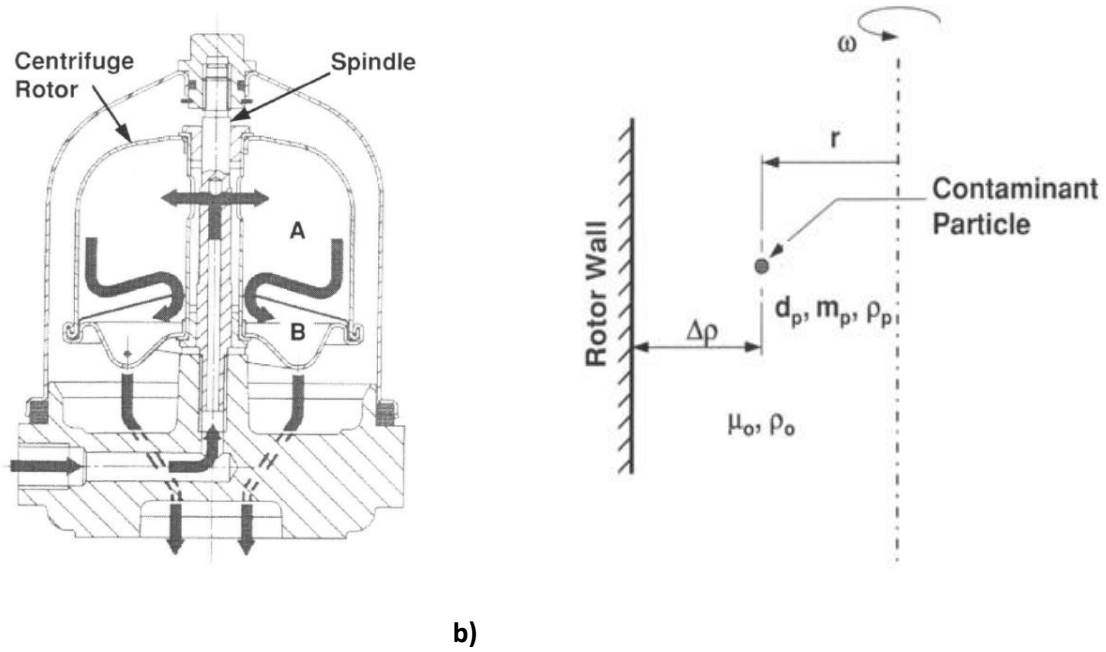

Figure 3.19: a) Centrifugal oil filter b) centrifugal sedimentation [120].

Equation 3.1 shows that in engine oil with lower viscosity, the particles move easily through the oil and hence easier to be removed from the oil. Therefore, engine oils tend to be at low viscosity which is good for solid particles separation. The shorter travel distance Δr of the particle has to travel into oil and stick on the filter's wall also affects the centrifugation process. The equation demonstrates that the dominant parameters are the two squared parameters $\boldsymbol{\omega}$ and d_p. The speed $\boldsymbol{\omega}$ is controlled by the centrifugal filter design, while the particle diameter d_p is correlated with the function of the contaminant. Thus the importance of maximising rotation speed $\boldsymbol{\omega}$ is clear. The oil conditions consecrations that influence the filtering efficiency (η) of centrifugal oil filter in a particle/oil system is shown in Figure 3.20. The filtering efficiency (η) against the particle size curve as shown in Figure 3.20 is correlated with $\tau, \mathrm{r}, \omega, \Delta r$ and $\mu_{\circ}$

parameters. The resulting curve will assume to have the form given in Figure 3.20. Increasing the rotation speed ω, radius of rotation r and residence time τ moves the curve to the left hence smaller contaminant particles can be removed. While decreasing the viscosity of oil μ_o and the distance of particle Δr to travel to internal wall of filter also moves the curve toward Y axis [120].

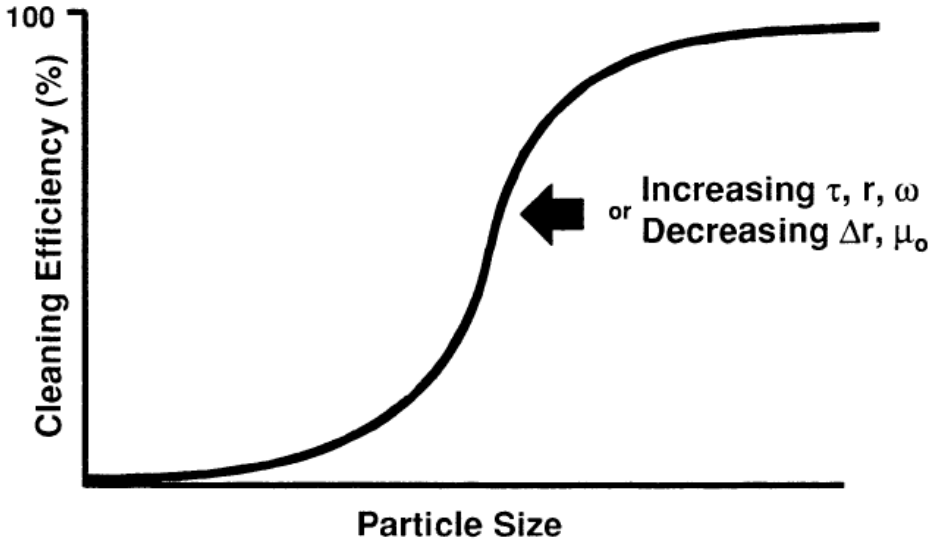

Figure 3.20: Oil conditioning consideration that effect centrifuge cleaning efficiency [120].

Oil temperature during the centrifugal process is of the utmost important factor that increases the filtration efficiency. The velocity of contaminant particles and water droplets in oil during the filtration follows Stoke's Law as shown in Equation 3.2:

$$V_p = \frac{D^2.(\rho_p - \rho_o)}{18.V.\rho_o}.g_c \qquad \text{Equation 3.2}$$

Where V_p the velocity of particles, D particle diameter, ρ_p particle density, V kinematic viscosity of the oil, ρ_o oil density and g_c centrifugal acceleration.

The higher temperature of the oil is, the more filtration efficiency is produced. As both viscosity and density of oil decrease when the temperature increases. Therefore, increasing the velocity of the particles to be removed from the oil and stuck in the filter's wall [123].

Table 3.1 demonstrates different filtration systems that are used in engines to remove different particles sizes.

Table 3.1: Filtration systems that are used in engines [118]–[120], [123].

Types of filter	Oil flow type	contaminant type	Particle size
Full flow filter	Full flow	soot	≥30 µm
Bypass filter	Partial flow	soot	≤5 µm
Depth filter	Full flow	soot	No data
Centrifugal filter	Full flow	soot and water	Nano-sized particles

3.2 Water in engine oil

Water is one of the most common and destructive contaminants in the lubricants after soot [66]. Water contamination in engine oil causes a host of problems including; accelerating fatigue of metal surface, increasing wear, producing corrosion, and breaking down of the oils [69, 70]. The following sections will cover the water content in lubricants and how water can access engine oil, how much water is expected in a real engine, what kind of damage can be caused by water, the effect of water on the tribological system, and the water effect on additives.

3.2.1 Water types in the oil

Water in engine oil is found in three different phases as illustrated in Figure 3.21a:

- Dissolved water: the first phase of water in oil is called dissolved water which is under saturation level. Water molecules disperse in engine oil in very small sizes and are invisible. Water in this state is very similar to moisture molecules in the air on a humid day. However, dissolved water is the least dangerous or with little effect on the oil.
- Emulsified water: when the amount of water exceeds the saturation level or the level that water can be dissolved, the oil loses its ability to absorb any more water results

an emulsified state. In this water state, water molecules suspend in the oil as microscopic droplets. Engine oil can be characterised a hazy or cloudy appearance.

- Free water: as water content increases in oil, the extra amount of water over the emulsified water level in oil leads to separate and form free water. This state of water is usually found in the bottom of sumps or tanks. However, emulsified and free water are the most dangerous states that influence the lubricating system and cause further problems [127].

The point that lubricants can not hold any more dissolved water is known as the saturation point. The amount of dissolved water increases with increasing temperature as seen in Figure 3.21b [29]. However, the amount of water that can dissolve in oil depends on many factors that will be discussed in more detail later on.

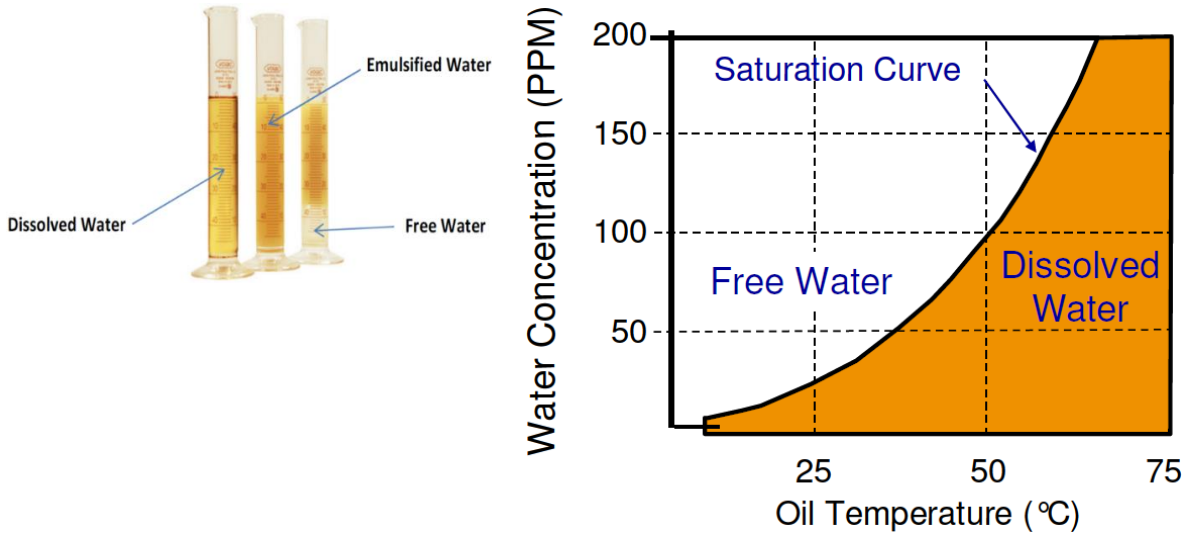

a) **b)**

Figure 3.21: a) Water states in oil; free water, emulsified water and dissolved water [127] b) the effect of temperature on the level of dissolved water in engine oil [29].

3.2.2 Sources of water in the oil

Water enters the oil engine in different ways and moves in the lubrication system in several physical and chemical states. The most common ways that water gets into the engine are:

- Absorption: engine oil is a hygroscopic material to a certain extent which means the oils can absorb moisture directly from the air. The amount of water that can be absorbed by the engine oil, is affected by the air's relative humidity and water solubility in the oil (saturation point). Depending on the pressure and temperature, water solubility in oil varies from 100 ppm of the oil that contains a low level of additive to several thousand (ppm) of oil that contains a high level of additive and synthetic oils. Absorbed water by engine oils under a humid environment is always dissolved in the beginning. Then, pressure and temperature modifications condense more water to produce free and emulsified phases.
- Oxidation, combustion or neutralization: fuel combustion in engines creates water in the exhaust gases as a by-product. These problems are associated with the worn improper scavenging and liners/rings that cause water to access the engine oil system. Water can also be formed in engine oil as a result of the chemical reactions through certain types of oxidation and corrosion processes. In a lubricating system, water is also produced when an alkalinity improver neutralises acids that are created during the combustion process.
- Heat exchangers: leaky or corroded heat exchanger is the most common source of water contamination in the lubricating system. A rupture in the heat exchanger surface causes a high amount of water to enter the engine compartment.
- Condensation: humid air enters oil compartments leading to moisture condensation on the ceilings and walls above the oil level. The rate of condensation increases extremely with the temperature change. Eventually, the water condensation will coalesce and get down to form a layer of free water or puddle.
- Free water entry: water enters the oil compartment during oil changes. Water condensation in storage containers is the most common source of this category [128].

3.2.3 Water expected in the oil

Water, once in engine oil, continuously searches for a stable state of existence. Unlike lubricating oil, water is a polar molecule that significantly influences or limits its ability to dissolve. Many additive compounds that have polar extremities can markedly increase water's ability to dissolve in the oil. In the absence of dissolved polar compounds (additives) in the oil, water molecules become unable to attach to additive molecules resulting in an increase in the amount of water without attachment. Therefore, any additional water molecules resulting from a supersaturated environment will cause the formation of free water. This free water suspends in the oil or settles in puddles at the bottom of the sump. This supersaturated solution can also occur as a result of lower oil temperature. When free water is suspended in oil, an emulsion state or colloidal suspension is likely to exist. This causes a haze in the oil [128].

Engine oils and industrial lubricants always tend to emulsify the water rather than demulsify it. Many additives work in humid conditions to disperse the water in the engine oil and prevent the formation of droplets of free water. These additives influence the character of mineral oils in terms of emulation and solubility of water in oils. For example, transformer oils reach the saturation level with 3 to 10 ppm of water, oil-based hydraulic fluids typically reach the saturation state in a range between 100 ppm (0.01 %) to 1000 ppm (0.1 %), automotive oils are typically saturated with a percentage between 1 to 5 % of water, and Stern tube lubricants, which is used in aft bearing on a ship population shaft contains 16 % of water without any evidence to reach the saturation level [129].

Water concentration in lubricating oils could be influenced by several factors such as relative humidity, pressure, oil additives and temperature. The relationship between water concentration in oil and the amount of water in the air are linearly proportional according to Henry’s law [130]. Figure 3.22 illustrates the linear relationship between humidity in the air and water concentration in oils that contain different additives. For all oils, it is quite clear that the water amount in oils increases with the increase of air humidity [131].

Table 3.2 shows the expected level of dissolved, emulsified and free water in different lubricating oil. The water level is related to the oil type, operating temperature, additive type and pressure [127].

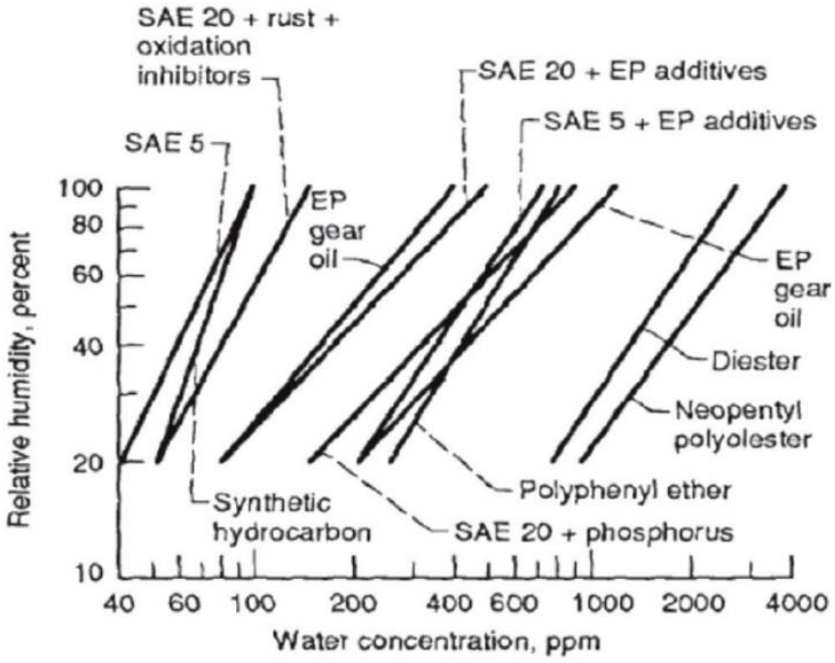

Figure 3.22: Water adsorption for different oils blend with different additives under humidity conditions [130].

Table 3.2: The level of dissolved, emulsified and free water in different types of lubricating oils [127].

Oil	Dissolved (ppm)	Emulsified (ppm)	Free (ppm)
New hydraulic fluid	0-200	200-1000	>1000
Aged hydraulic fluid	0-600	600-5000	>5000
New R&O Oil	0-150	600-500	>500
Aged R&O Oil	0-500	500-1000	>1000
New crankcase oil	0-2000	2000-5000	>5000

In service warning limits, water contamination level as mentioned above depends on the operating conditions of equipment being lubricated and types of lubricating oils. Table 3.3 shows the warning limits for different applications containing water in-service lubricating oil.

This summary of information is based on the manufacturer's requirements and general experience [132].

Table 3.3: Warning limits of water contamination into oils for several types of equipment [132].

Equipment	Attention (%)	Urgent (%)
Medium speed diesel engines	0.2	0.5
Slow- speed engine system oil	0.2	0.5
Turbo chargers	0.05	0.5
Turbo generators	0.05	0.5
Steam turbines	0.05	0.5
Gear boxes	0.05	0.5
Hydraulic systems	0.05	0.5
Air compressors	0.05	0.5
Refrigeration	0.05	0.5
Compressors	0.01	0.05
Stern tubes	1.0	3.0

The water level in engine oils has to be as low as possible to avoid any damage to the engine bearing. This results from a displacement of tribofilm in the presence of free water droplets which eventually causes cavitation inside the engine bearing. It is commonly agreed that water concentration does not have to exceed 0.2 % (2000 ppm). Also, a high level of water leads to a corrosive attack on the bearing [78, 79]. The water concentration in the drain oil due to the adsorption from ambient air or leaking was found typically below 10000 ppm (1%) and although variations are widely seen in several studies [78, 8].

3.2.4 What type of damage can water cause?

Excessive water in the engine oil influences its physically and chemically properties, leading to a series of different failures such as:

Hydrogen-induced fractures: this failure is sometimes called blistering or embrittlement. Water molecules are attracted to microscopic cracks by capillary action. Hydrogen atoms resulting from the breakdown of water molecules cause an increase in the propagation and fatigue fractures. Cracks are formed by both free water and soluble water (dissolved and emulsified water) as demonstrated in Figure 3.23 [81, 82].

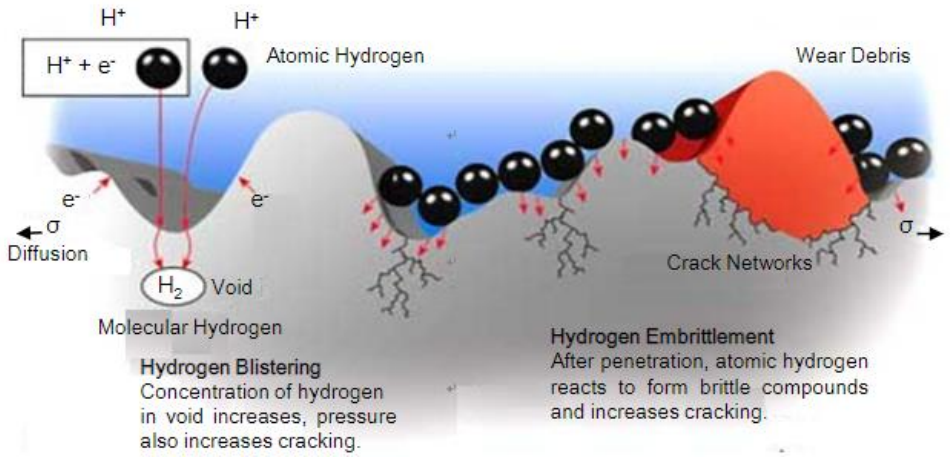

Figure 3.23: Schematic of hydrogen embrittlement fractures formation [139].

Corrosion: both dissolved water and free water have a great effect on corrosion failure. Consequently, metal surfaces will be pitted and etched. In the worst case, water in oils causes iron oxides that lead to the hard abrasive on metal surfaces and accelerates the wear [81, 84, 85]. Figure 3.24 shows an example of wear due to corrosion reactions between the DLC coating surface and stainless steel.

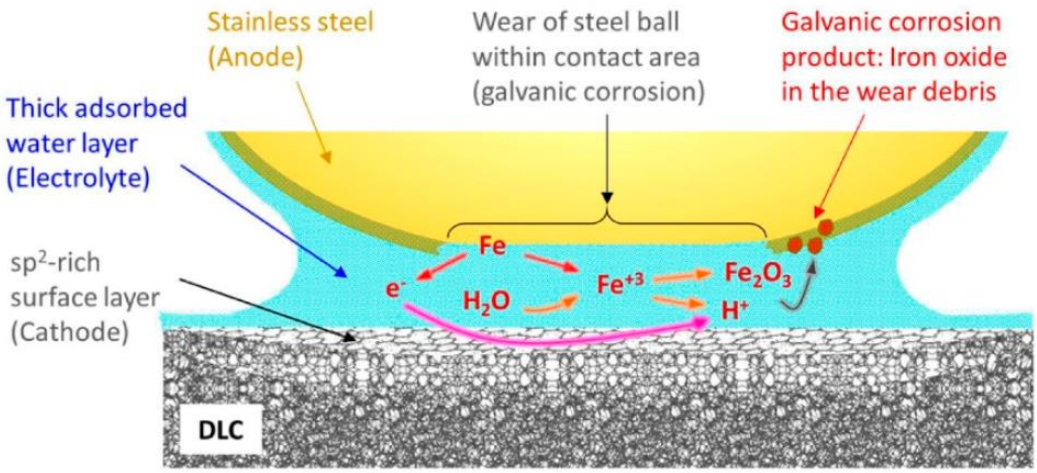

Figure 3.24: Schematic of the reaction among steel surfaces, DLC surface and water involved in the rubbing process [142].

Additive depletion: water in oils diminishes or depletes the performance of oil additives such as detergents, dispersants, anti-wear, rust inhibitors, antioxidants, extreme pressure and demulsifying agents. Water will hydrolyse, agglomerate, transform or wash the additives out of engine oils. Water in oils induces the formation of sludge or acids on the bottom of the sump [136]. In this project, the research will focus on additives depletion by water and more details will be covered in a later section.

Oil flow restrictions: water molecules are of very high polarity and have the ability to attract or attach the lubricant impurities that are also polar such as carbon fines, resin, spent additives, oxides and other particles, to form emulsions or sludge droplets. When sludge droplets accumulate in feed lines, orifices, or filters, it restricts or impedes the oil flow, causing oil starvation and an eventual failure [136].

Aeration and foam: water molecules reduces the interfacial tension of oil, which leads crippling the ability to air-handling, causing aeration or foam. Air weakens the oil tribofilm and induces oxidation, cavitation, and overlaps with oil flow [81, 87].

Impaired film strength: water droplets in oils are pulled into the rubbing of opposing surfaces under a load. Consequently, water globules may explode or flash into superheated steam at the loading zone. This causes sharp damage in the tribofilm and potentially a surface fracture [136].

Microbial contamination: water promotes microorganisms in oils as bacteria and fungi. The growth of microbes over time produces waste by-products or thick biomass suspensions that cause a filter plug and influence the oil flow [136].

Water washing: pressurized water has a direct effect on oil additives. As known, water has a density higher than lubricating oil. Therefore, if free water is too much, the additives may be washed out of the lubricant zone [144].

Oxidation: lubricants consisting of hydrocarbons include a large number of isomers. The primary degradation mechanism due to hydrocarbon's chemical structure of lubricants is oxidation. The oxidation promotes the formation of alcohols and carboxylic acids, especially in the presence of water [89, 90]. Basically, when engine oil is subjected to elevated temperatures in the presence of oxygen. The oil reacts and forms peroxides compounds to form another compound called free radicals. Both compounds (peroxides and free radicals) are highly reactive products that cause an increase in the formation of varnish, sludge and impair oil flow [81, 91].

3.2.5 Water effect on the oil

Wear and friction: engine oil during the internal combustion process is required to manage the high by-product contamination such as combustion by-products, soot, deposits, etc. Water is one of the by-products of the combustion process, and it is difficult to drain the settled water every day from the bottom of the oil crankcase [88, 92]. Water has been identified as the main contaminant after soot which influences the wear and friction of contact surfaces. Several studies [142], [149] reported that friction coefficient was less affected compared to wear. Friction slightly increased in the presence of water in both its vapour and liquid phases [142]. In this PhD project, the metal-metal contact will be studied, therefore, the review will focus on the metals contact. Fundamentally, water can affect wear in three different ways; Firstly, water can modify the adsorption property of organic compounds by reducing its capability of long-chain molecules to adhere to metal surfaces. It affects the formation and removal of tribofilm

in boundary regime. Secondly, water can also influence the interfacial chemistry of tribofilm formation. Eventually, water causes pitting failures especially on rolling surfaces [142].

The polarity of water molecules also has an effect on the tribofilm due to the high polarity of water molecules compared to the additives, so water molecules can attach to metal surfaces and prevent the additives from forming tribofilm to protect the surfaces [75]. Parsaeian et al. [150] studied the effect of humidity conditions on wear depth at 80 and 98 °C using MTM-SLIM with different relative humidity levels. The results showed an increase in the average wear depth with a higher level of humidity at both temperatures, and the higher water concentration was a significant effect at a lower temperature. This is explained as mentioned above in Henry's law which states that increasing the relative humidity leads to an increase in the water absorption level. In another paper, Parsaeian et al. [151] investigated three different 0.5, 1.5 and 3 % of water levels in oil at 80 and 100 °C. The results reported an increase in wear depth and decrease in tribofilm thickness with higher water concentration at both temperatures as illustrated in Figure 3.25.

Cen et al. [149] reported that adding water or adsorbing more water from humid air before the tribology tests increases the wear. The results agreed with the theory of hydrolysis effect of ZDDP triboflim that water can decay the stability of tribofilm by reducing the adherence of tribofilm to metal surfaces [152]. Cen et al. [149] studied the effect of free water on base oil with ZDDP in sliding boundary conditions, They found that adding 1 % of dissolved water did not affect the physical properties of the oil (viscosity, TAN and oxidation level). At the same time, wear increased with adding free water or absorbing water from the humid air of the test without a significant friction change. The PAO lubricant contained 1 % ZDDP was investigated in the existence of 1 % water, and the results demonstrated an increase in wear by 24 % [75]. Glabbeek et al. [153] studied the effect of dissolved water on the tribological performance of different oils with parentage from 70 to 1600 ppm of Polyester (PE) oil and 200 to 1700 ppm of Polyalkylene Glycol (PAG) oil. The findings showed a decrease in wear on cast iron plates with an increase in water concentration.

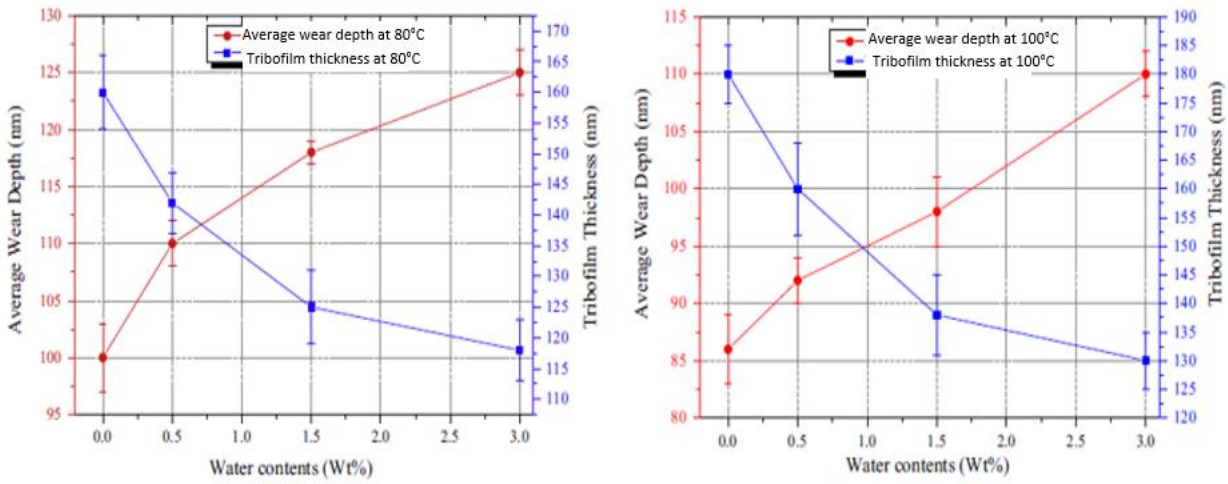

Figure 3.25: Effect of water content in engine oil on both wear and tribofilm thickness at 80 and 100°C [151].

3.3 Oil contamination effects on additives

3.3.1 Additive depletion

Additive depletion is a harmful chemical process in which the additives lose their efficiency by decomposing or reducing in concentration. Oil contaminants accelerate additives depletion such as; soot particles, fine metals, water and acids. Monitoring additive levels and replacing the oil's additives when necessary help to maintain oil performance and its chemistry and extend the oil lifespan. When the additive level in oil decreases, the oil oxidation and acid levels will increase. Consequently, it will reduce the oil's ability to protect the contact surfaces [154].

Basically, additive elements in oil are consumed or depleted in different ways;

- Adsorption by different oil contaminants such as soot particles [10] and interacted or washed out by water [136] [26].
- Ultra-filtration techniques lead to removing some additives with contaminants [155].
- Formation of the protective film on contact surfaces [156].
- Decomposition or degradation of additives under severe conditions during the use in real conditions [157] or ageing oil in labs [7].

3.3.2 Soot effects on additives

The interaction between additives and soot particles in engine oil has been investigated by several studies. Hosonuma et al. [158] found that the decomposition of ZnDTP in engine test occurred quickly, and the adsorption of these decomposition products by diesel soot was investigated. The results showed that soot particles adsorbed zinc-containing compounds and a little adsorbing of phosphorous-containing compounds. Gautam et al.[71] reported that soot particles did not adsorb phosphorous compounds significantly as a result of the reaction between the soot and oil additives. Many researchers have explored soot/CB behaviour with traditional additives in the lab, Olomolehin et al. [159] studied the effect of ZDDP additive on oil contained carbon black, the results showed ZDDP additive in the presence of carbon black produced severe wear and the lube oil when ZDDP left out had less wear effect. They reported that the combination of carbon black and ZDDP was strongly antagonistic in terms of wear.

Antusch et al. [160] stated that wear was not just influenced by the soot percentage in oil, but also the surface chemistry, reactivity and morphology of the soot particulate being more important mechanisms. ZDDP absorption by carbon black particles at (1 and 5 %CB) percentages was investigated by chemical analysis of CB particles using EDX and oil analysis using ICP and FTIR. Results showed a significant depletion of zinc and phosphorous antiwear additives due to additives adsorption by carbon black [10]. The extracted CB particles from SAE 15 W-140 indicated that additives adsorption in the existence of CB occurred. The EDS analysis for extracted CB particles detected some elements belonging to the additives such as Zn, P, Mg and Ca [22]. While Berbezier and co-workers [81] suggested that ZDDP adsorption by CB was not the main factor in increasing the abrasion wear. In particular, two other factors had important effects; firstly, the modification of mechanical and physical properties of the reaction film in the presence of carbon black in their composition secondly, the reduction in the surface coverage rate of ZDDP molecules on contact surfaces.

Besides, the interaction between the soot and reactive compounds could be responsible for additive depletion by the soot. These will also change the crystalline structure of soot particles or modify their turbostratic structure. The hardness of particles increases due to the soot being trapped between the rubbing surfaces in the presence of extremes locally pressure and temperature, which might induce the change in the amorphous and crystalline nature of carbonaceous soot. The higher hardness of soot compared to engine components was considered the main factor in the increase in wear [161]. Sharma and co-workers [162] found the presence of constituents of an anti-wear additive such as (Zn, P and S) on soot particles due to adsorption of these elements by soot particles. The study illustrated that there were interactions between the soot and detergent. These interactions promoted the formation of nanocomposite particles of turbostratic carbon with embedded calcium sulfates and calcium phosphates. The formation of calcium phosphates which are hard in nature on the soot particles led to an increase in the abrasive characteristics of these particles. Patel and Aswath [163] studied the chemical composition of soot extracted from the Mack-T12 dynamometer engine test. The soot from both cylinder and crankcase showed the presence of calcium, sulphides of zinc and iron, phosphates of calcium and zinc, sulfates of zinc, and zinc and iron that came from oil additives. Dairene et al. [97] investigated the soot chemically using XRF, they reported that extracted soot particles from diesel engines contained organic elements that originated from the oil additive such as P, S, Ca, Zn, Mg, Mo; and some elements came from the wear metals such as Fe, Cr, Al, Cu . Chemical analysis of diesel soot, that were extracted from crankcase oil using XRD, showed the presence of additive compounds such as $CaZn_2(PO_4)_2, CaSO_4,\ Zn_3(PO_4)_2,\ ZnO$ and $Ca_3(PO_4)_2$. These compounds came from degradation products of crankcase oil, anti-wear inhibitor and detergent compounds [164].

Finally, Green and Lewis [91] identified that lubricant can hold and control soot particles within the oil and disperse it using a dispersant. The results concluded that dispersant amount was limited due to corrosion problems in the engine as adding too much dispersant could cause free amines to be correlated with dispersant. The function of the dispersant is to interact with

organic contaminants such as soot and disperse them in the lubricants, as seen in Figure 3.26. The main function of dispersants is surfactants, which is similar to detergent. However, dispersant has more polar groups to capture the organic contaminants sufficiently and to keep them dispersed in the oil. Removal of the organic contaminants such as soot from oil during the filtration process also results in the removal of attached additive molecules on these particles, in either dispersant or detergent, causing additives depletion [47].

Additive adsorption on soot in FFO has not been fully understood in terms of the interaction between the additives and soot, and the effect of the increase in soot levels on additives adsorption. Finally, if the additives are adsorbed on soot, it is important to understand whether this process influences the tribofilm formation and tribological performance.

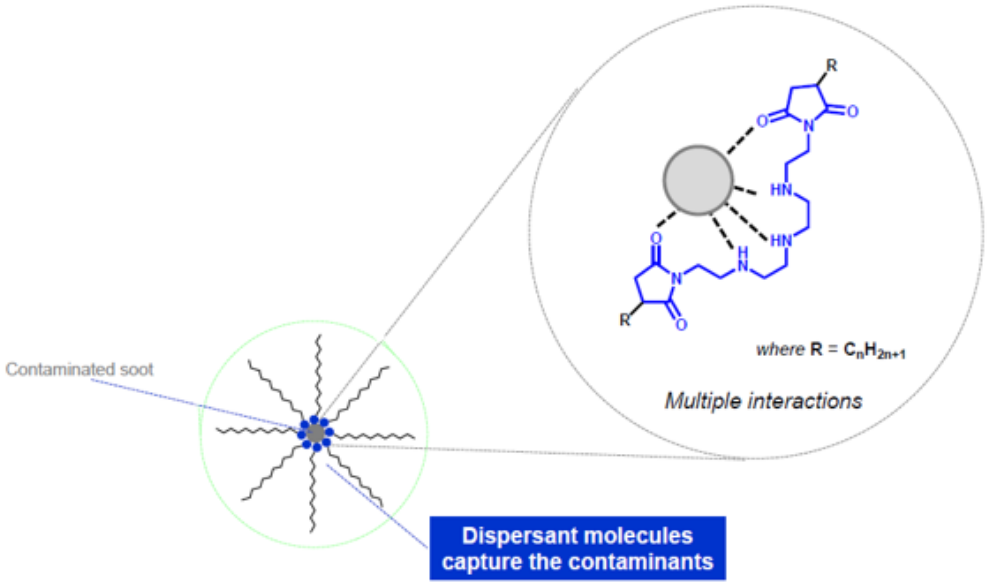

Figure 3.26: Working principle of dispersant molecules in the presence of soot particles in engine oil [47].

3.3.3 Water effects on additive

The hydrolysis effect on lubricants has been considered the main factor that contributes to the chemical breakdown of engine oil in the presence of water. Water can remove additives and this phenomenon is called “washing additives”. Almost all additive agents are formulated to

have the ability to dissolve in the oil's base stock, while oil additives have less or limited solubility in water. However, some additives still have a solubility in water; which means some additives can be removed from the engine oil during the water filtration process [136].

With few exceptions, the physical and chemical stability of engine oil is threatened by even a small amount of suspended water. Chemical reactions (hydrolysis) with compounds and atomic species, including base stock, oil additives and suspended contamination can be promoted by water molecules in oil. In combination with metal catalysts, heat and oxygen; water promotes the formation of free radicals, oxidations and peroxide compounds. Oxidation inhibitors play a major role to neutralize peroxides and break the oxidation chain reactions to form stable compounds. Moreover, oxidation inhibitors react with water to form sulfonic acids and hydrogen sulphide. Experiments have shown that common antiwear additives such as ZDDP which forms antiwear tribofilms, can be destroyed even by a slight amount of water in oil at high temperatures [26]. Moreover, water also interacts with viscosity improvers and rust inhibitors. Consequently, undesirable by-products, such as inorganic and organic acids, sludge and varnish, are formed [26].

Water effect on anti-wear additives: ZDDP decomposition in the presence of water in oil accelerates the formation of zinc polyphosphates and alkyl sulphides, and the formation of acid by-products [165]. Rounds [166] suggested that ZDDP decomposition occurred not only by the thermal decomposition but also due to the hydrolysis process. Fuller and co-workers showed that long-chain phosphates, which result from decomposing of adsorbed ZDDP on rubbing surfaces, hydrolyse these long chains in the presence of water causing the formation of short-chain polyphosphates and phosphoric acid as described in Equation 3.3 and Equation 3.4 [93, 113].

$$7Zn(PO_3)_2 + 6H_2O \rightarrow Zn_7(P_5O_{16})_2\ (short\ chain\ polyphosphate) + 4H_3PO_4$$

Equation 3.3

$$2Zn(PO_3)_2 + 3H_2O \rightarrow Zn_2P_2O_7\ (short\ chain\ polyphosphate) + 2H_3PO_4$$

Equation 3.4

Dissolved moisture in the lubricants reduces additive performance and promotes corrosion. The reaction products increase the wear due to the destruction of ZDTP additive when it reacts with water at temperatures of 60 °C and above. Other acidic compounds are formed as a second reaction with metal protective film causing a negative effect on the rubbing surfaces [114, 115]. Phosphate esters are usually used as antiwear or extreme pressure additives. Phosphate esters interact with metal surfaces to produce a polymeric coating on surfaces to protect bearing surfaces [170]. Hydrolysis of phosphate esters due to the reaction between the triester with water molecules to produce a diester and aromatic alcohol. Further chemical reactions, under the same conditions, produce the monoester and finally lead to the formation of phosphoric acid products [11, 89].

Water effect on Detergent/Dispersant: dispersant and detergent additives in lubricants are used as the first barrier to protect the oil from water contamination. Water is known as a polar molecule which is similar to the additives that have polar heads. The heads of additives latch onto water molecules and surround them, and the non-polar tails of additives allow the additives to dissolve easily into oil as explained in Figure 3.27.

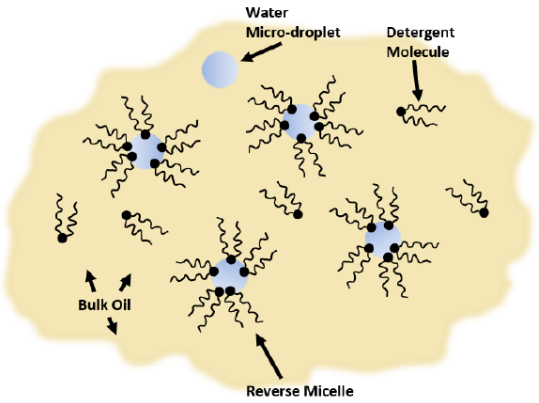

Figure 3.27: Reverse micelles interaction with detergent and dispersant additives [171].

When the water content in oil increases, more reverse micelles are generated until they reach a level where the water amount overwhelms these additives and free water will form [171].

Removing water molecules during the filtration, which are surrounded by detergent and dispersant additives, will also remove these additives.

Besides, several additives contain sulfur, phosphorus, or nitrogen atoms in its molecule. The oxidation of these additives promotes the formation of mineral acids and their derivatives. These acidic products attack the contact surfaces and decrease the service life of the lubricants [47]. Sulfonates as an example in the base stock of engine oil are present as a detergent additive. Sulfate oxidation occurs either as a sulfonation and/or sulfation process. Sulfonation implies a chemical reaction where sulfonic acid is formed, while sulfation is a reaction by which salts or esters of sulfuric acid. A detergent additive is degraded, as the car runs, by chemical reactions as shown in Equation 3.5 with the formation of sulfuric acid as a side product as described in

Equation *3.6*. However, the IR spectrum is used to detect the formation of oxidized materials (sulfur oxide) in the region around 1150 cm^{-1} [43, 118].

$$R - CH_3 + R^1 - OH \xrightarrow[O_2]{SO_2} R - SO_3H\ (Alkysuphonic\ acid) + R^1 - O - SO_3H(Alcohol\ sulfuric\ acid) \quad \text{Equation 3.5}$$

$$H_2O \xrightarrow[O_2]{SO_2} H_2SO_4\ (sulfuric\ acid) \quad \text{Equation 3.6}$$

Where R and R^1 refer to alkylic and aliphatic and/or phenylic groups that are forming the base stock of lubricants. Ramkumar and co-workers [77] found that sulphuric acid, which can be formed due to the reaction between water and additives, reacts with detergent to form a salt ($CaSO_4$) in engine oil. They determined the effect of sulphuric acid on wear compared to soot and water. They illustrated that sulphuric acid had a significant effect on wear compared to wear at different moisture conditions as shown in Figure 3.28.

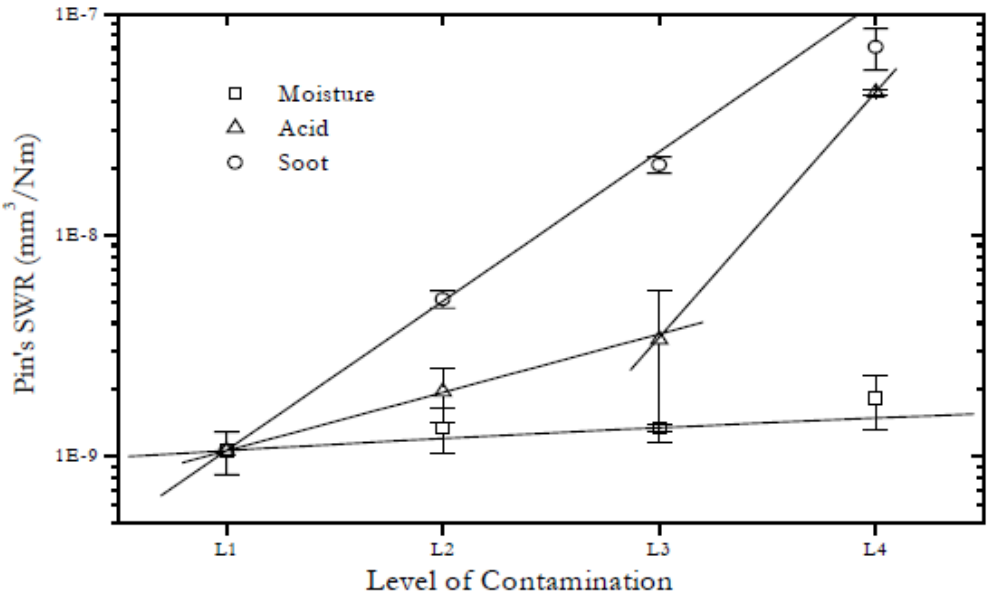

Figure 3.28: Specific wear rate (SWR) of the pin in the presence of different contaminants [77].

In general, the interactions between water and additive in engine oils have not been fully understood due to complex mechanisms that influence the interaction process. This project will cover the literature gap in terms of the amount of additives that can be removed by water and its effect on wear.

3.4 Oil additives replenishment

3.4.1 Engine oil and additive quality

Used engine oils typically contain a used additive that affects the oil performance. The additive over the oil service needs to be replenished with a fresh additive to remain working effectively. The used additive in used oils includes the additive that either evaporates, degrades, depletes, decomposes, adsorbs, or consumes over time [8], [173], [174]. By “life-extending” additive is referred to as the additive that forestalls oil degradation and maintains the oil properties and its effectiveness for a longer time [173]. Engines manufacturers recommend that engine oil should be changed at regular intervals depending on the operating conditions to keep the additive levels up. For example, General Motors Corporation advises changing the oil for gasoline engines every 12 months or 7.500 miles under normal driving conditions, and 3 months or 3000 miles under severe operating conditions (e.g. driving in dusty areas, frequent

short trips, trailer towing and frequent stop & go driving). Accordingly, most vehicle manufacturers have provided oil change reminder/warning systems to maintain the oil quality [173]. However, the vehicle consumers rely on either the recommended details about oil change intervals by Original Equipment Manufacturer (OEM), or they use the oil reminder light to remind them when the oil is required to replace. Dodge Cummins, Ford Powerstroke and GM Duramax recommend the 7,500 miles for oil change intervals for model light trucks at light duty service. At severe service conditions, the oil change intervals are less than 3,000 miles. With heavy-duty trucks, the oil can be used for 40,000 to 50,000 miles for light-duty applications compared to 15,000 to 25,000 miles under harder use conditions [175]. American Petroleum Institute (API) and European Automobile Manufacturers Association (ACEA) establish their guidelines for the oil change as follows; most USA cars are required to change the oil every 5000 miles compared to up 10000 miles for European cars. This is due to high-performance engines designed by European companies extending oil change intervals and reducing CO_2 emissions [176].

Schwartz et al.[177] recognised the effect of temperature on oil degradation and additive depletion. They suggest that excessive oil degradation occurs due to temperature extremes. At temperatures below 60 °C, water, fuel and soot tend to accumulate in engine oil causing a decrease in its viscosity and an increase in wear. At high oil temperatures (above 130 °C), the anti-oxidant additive is depleted leading to nitration and oxidation of the oil. As a result of nitration and oxidation, the oil becomes viscous and acidic, and more insoluble by-products are deposited on engine components' surfaces as sludge or varnish. Acidic oil reduces its ability to protect the engine from corrosion and rust. Schwartz et al. [177] predict the oil quality or remaining oil life depends on the thermal history of engine oil (time-at-oil temperature), where time can be calculated based on the miles driven or engine speed (Revolutions per minute). The effect of temperature on oil life is determined by the Arrhenius principle. Commercially, a computer/controller is usually used to measure the oil temperature and

revolutions per minute to determine when the oil should be changed, which is based on empirical data [177].

3.4.2 Additive replenishment

Oil additive replenishment to extend the lubricant has been an interesting topic in the manufacturing segment. There are many studies [60], [117], [178] regarding the effect of added additives to base oil to enhance the tribological performance. In contrast, the effect of additives replenishment on used oil after filtering the contaminants has not been much researched. However, several patents report different additive system suppliers can replenish the additives through a controlled injection or filters. Some methods have designed oil filters to release additives using such as colloidal suspensions of PTFE particles less than two microns in the filter (Figure 3.29) [179], polyolefin containers or capsules in flowing oil [180], other patents suggested mechanical mechanisms that can inject the additives into oil circulation systems (Figure 3.30) [122,123].

It has been proposed that by simply adding excess amounts of additives to the used oil, the oil change intervals can be prolonged. Rohde et al. [183] designed a polyolefin container that contains the additives to be added to the oil. At elevated temperatures, the additive inside the container diffuses through the wall into the oil. The amount of diffused additive is reduced as the amount of additive inside the container is reduced. Other patents, for example, Lefebvre et al. [184] and DeJovine et al. [185], provide dissolved materials consisting of a soluble composite comprising additives, for example, polymer matrix. Engine oil can pass through the soluble composite (e.g. in an oil filter), dissolving the additive from matrix polymer into the oil. The dissolved additive can be limited in oil as a soluble material contaminates the engine oil and delays subsequent dissolution over time. All of these techniques have taken into account that adding too much additive to the oil has a negative effect on tailpipe emissions and the vehicle fuel economy. Accordingly, it is important to have controlled additive release technique to keep the additive concentration within desirable limits.

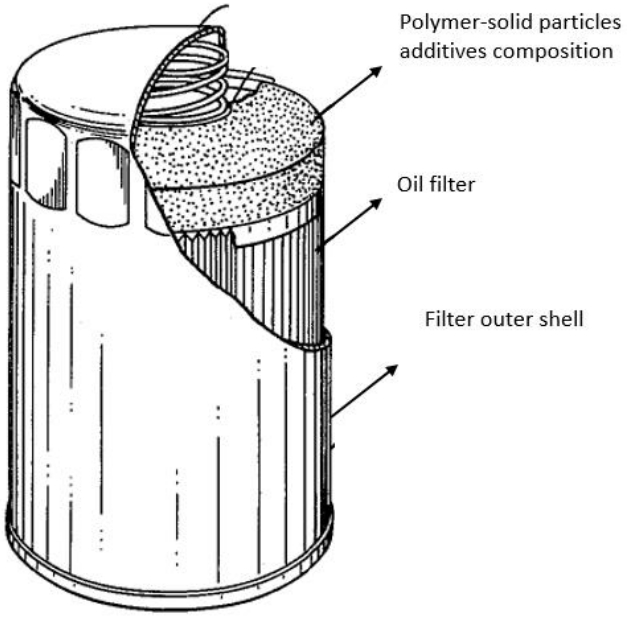

Figure 3.29: Oil filter apparatus to release additives using polymer-solid particles compositions [185].

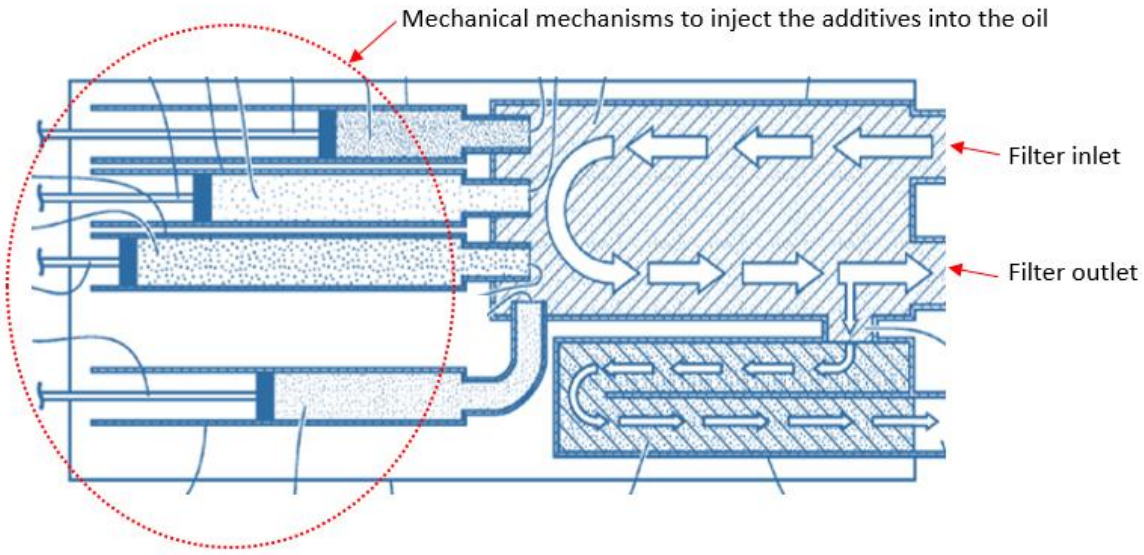

Figure 3.30: mechanical mechanisms that can inject the additives into oil circulation systems [181].

3.4.2.1 Effect of ZDDP on oil performance

Zinc dialkyl dithiophosphate (ZDDP) is the most common additive which can control wear and act as an oxidation and corrosion inhibitor [186]. ZDDP reacts on rubbing surfaces to form a quite thick tribofilm (up to 200 nm) [187]. The effect of ZDDP concentration on tribofilm

formation has been investigated by Yin et al. [188]. The results revealed that a low concentration of ZDDP (0.25 and 0.5 wt%) forms short phosphate chains, whereas a high percentage of ZDDP (1 and 2 wt%) leads to the formation of long phosphate chains in the tribofilm. Furthermore, Tomala et al.[189] found that a larger percentage of ZDDP causes thicker and rougher tribofilms. Ghanbarzadeh et al.[190] indicated that increasing ZDDP concentration increased the formation and thickness of tribofilm and reduced the wear. The formation of tribofilm derived from added ZDDP has a negative effect on friction causing an increase in friction coefficient. The reason behind this is the higher shear strength of the tribofilm [191] and the effective roughening of rubbing surfaces by the formation of uneven distribution of asperity peaks [192]. There is a synergistic effect between the MoDTC and the common anti-wear additive (ZDDP) [63]–[65]. The results demonstrated that ZDDP and MoDTC synergize well producing lower wear and friction. A very recent study found that the combination of Organic Friction Modifer (OFM), Inorganic Friction Modifer (IFM) and ZDDP can result in a synergistic effect leading to a further reduction in the friction coefficient and wear [193].

3.5 Summary

Throughout this chapter, a comprehensive review of the state-of-the-art that studied the existence of soot in engine oil has been provided. Soot effect on tribological behaviours, physical properties of engine oils and oil degradation have been discussed in detail. Most of these studies have been focused on the effect of soot on wear and friction. Chemical interactions between soot and engine oil occurred, increasing the oil degradation and reducing the oil interval periods. However, no specific study focused on the effect of chemical interactions between soot and aged oil that could change the mechanical properties of soot. Besides, no previous study investigated the impact of change in mechanical properties of soot particles on wear.

In the literature review, the possibility of reclaiming used oil using the recent filtration system has been discussed. Soot size distribution in used oil and the effect on the efficiency of filtration techniques were reviewed. Media surface filters with a full flow of engine oil can remove the large soot particles. The newest design of media filter is a depth media filter that is proposed to capture the soot particles even at a small size. There is a clear lack of literature and research on the depth filter and its efficiency to capture the soot in used oil. This literature reviewed the centrifugal filter and the effect of different parameters especially the oil temperature on its efficiency.

The existence of water and its influence on engine oil were also reviewed. Water in different states exists in engine oil influencing the lubricating system and causing further problems. Many mechanisms affect the water saturation level in engine oil for example relative humidity, pressure, oil contamination, oil additives, temperature, etc. However, there is no specific study that determined the saturation level in engine oil using an experimental method in the laboratory. A number of studies have investigated the effect of water at different levels on oil performance. The literature in several studies was focused on the effect of water on wear and tribofilm formation on rubbing surfaces. It was reported that water could influence the tribofilm even if it exists in the dissolved state. Although wear is expected to increase when the water is found at the free state in engine oil.

Oil contamination effects such as soot and water on the additives were also reviewed. Several studies have investigated the additive adsorption on soot particles. However, none of them studied the effect of the increased soot surface area on the additive adsorption and, if the additive is adsorbed on soot particles, what is the effect of removing these soot particles on the tribological performance of the resulting oil. The interactions between water and additive in engine oils have not been fully understood due to complex mechanisms that influence the interaction process. It was reported that ZDDP decomposition occurred even in a small amount of water. It was suggested that ZDDP could also be washed out by free water causing additive depletion. Dispersant/detergent depletion is expected when dispersant/detergent

molecules are attached to free water molecules due to high polarity. This project will cover the literature gap in terms of the amount of additives that can be removed by water and its effect on wear.

Engine oil change interval and the quality of engine oil were discussed in this chapter. It has been suggested that the change period of used oil was influenced by many factors such as oil contamination, oil degradation, additive depletion, etc. Several studies demonstrated that the chemical structure of bulk oil did not change over the use in the engine. It has been suggested to extend the oil life service by removing the oil contaminants and replenishing the depleted additives by adding ZDDP. In this study, the additive replenishment process in heavy-duty oil for the first time will be investigated before/after removing soot and water from the used oil.

4 Chapter (4) Materials and methods

This chapter describes the main experimental procedures of the PhD project. It provides the details of materials (engine oils, soot and water) and tests conditions, ageing procedures, filtration techniques, chemical analysis techniques (ICP, FTIR, EDX), surfaces analysis (NPFLEX, optical microscope, AFM, TEM, XRD, SEM), tribometer rig (TE77), water content measurement (KF) and In-situ nano-indention.

4.1 Materials

4.1.1 Fully formulated oil

Fully Formulated Oils (FFOs) were used in this study provided by Parker Filteration Ltd. A commercial Afton, BDS4 and VDS4 fully formulated oils with a viscosity grade 10W-40 (passenger car), 15W-40 (truck) and 15W-40 (truck) respectively were used in this project. The oils are designed to work in a diesel engine environment. The physical properties of oils are reported in Table 4.1. FFOs, which are used in this project, consist of synthetic base oil and several additives, such as antiwear additive, dispersant, detergent and extreme pressure and ant-oxidants additives. The most common contaminants in a diesel engine are soot and water, therefore the additives which are existed in these oils such as antiwear, anti-oxidation and dispersant/detergent are important to protect the engine components and prolong the service life of engine oil.

Inductively Coupled Plasma (ICP) was applied to quantify the additive concentration in the engine oils at Oil Check Laboratory Services Ltd, UK. Chemical analysis of Afton, BDS4 and VDS4 oils show the primary additive elements in these oils as reported in Table 4.1. Some primary elements such as zinc (Zn), phosphorus (P) and sulphur (S) originate from antiwear compounds (e.g. ZDDP). However, at the same time, S and P elements could also come from dispersant/detergent compounds such as sulfonates and phosphonates [50]. calcium (Ca) comes from detergent for example, calcium sulfonates [37], [39]. Magnesium (Mg) originates from detergent for instance, magnesium sulfonates [37], [39]. Other elements such as

molybdenum (Mo), silicon and sodium have been detected at a low concentration of less than 30ppm in these oils.

Table 4.1: Physical and chemical properties of fresh engine oils (FFOs).

Details	Parameters		
	Afton oil	**BDS4 oil**	**VDS4 oil**
Density at 15°C (g/ml)	0.961	0.855	0.874
Kinematic viscosity at 40 °C (mm^2/s)	80.6	95.19	113
Kinematic viscosity at 100 °C (mm^2/s)	11	15.18	15
Flash point (°C)	135	219	215
Total base number (mgKoH/g)	77	11	10
Zn concentration (ppm)	1115	1187	1306
P concentration (ppm)	1065	1060	1158
S concentration (ppm)	4140	4885	6366
Ca concentration (ppm)	--------	1114	1332
Mg concentration (ppm)	--------	846	941

4.1.2 Carbon Black Particles (CBP)

There are three different options to prepare the experiment samples such as used engine oil, carbon black mixed with new oil or extracted engine soot mixed with the new oil. Basically, CBP mixed with the oil is a well-known method of producing the test samples as it is easy to prepare, inexpensive and constant contaminated with the same particles at each time [73]. Therefore, the CBP will be used to investigate the effect of increasing the soot surface area on tribological performance and additive adsorption under the same conditions. 120 Carbon Black Particles (CBP) were used to simulate the soot particles in engine oil. Monarch 120 CB was purchased from Cabot Corporation, Massachusetts, USA. The crystal structure of CB

particles consists of a core and shell, as shown in Figure 4.1. The diameter of a single carbon black particle starts from less than 50 nm and the particles agglomerate in large clusters as shown in Figure 4.2. In the current study, the size distribution of CBP in aged oil containing 1.5 wt%CBP varies between 150 nm to 1.5 µm, as shown in Figure 4.2a and b, ageing conditions according to ASTM standard [194]. The chemical analysis of CBP consists of carbon (C), oxygen (O) and sulphur (S) as shown in Figure 4.3.

In this study, contaminated oils were prepared by blending the CB homogenously in the FFO at different CB levels and different conditions. It was important to uniformly disperse the CBP in the oil to obtain repeatable tests and reliable information. Therefore the stirring process was used to distribute the CBP in a beaker using a magnetic stirrer at 500 rpm for 1.5 hrs. In addition, an ultrasound bath was used for 15 mins to ensure the homogeneous distribution of CBP in oil before tribological experiments.

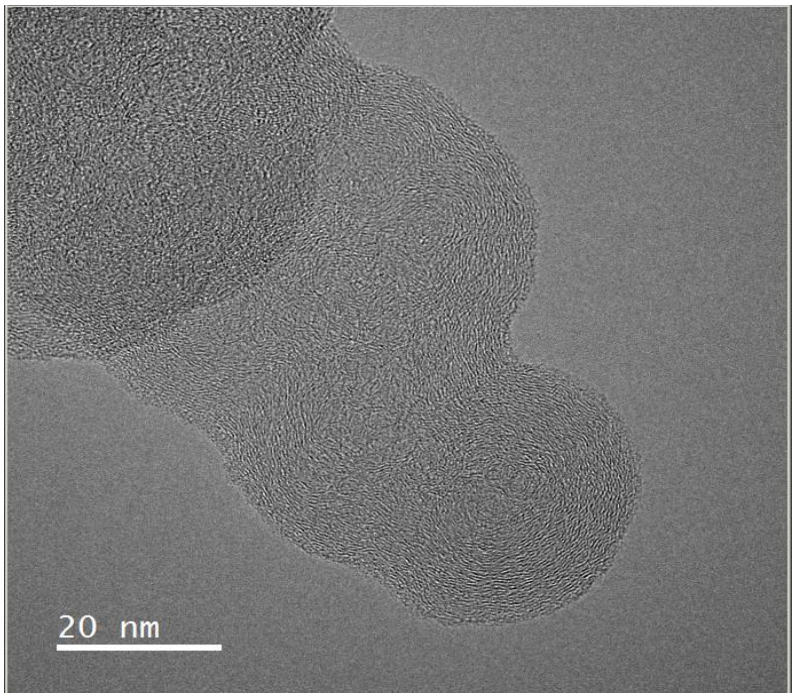

Figure 4.1: TEM image shows CB particles at a high magnification level.

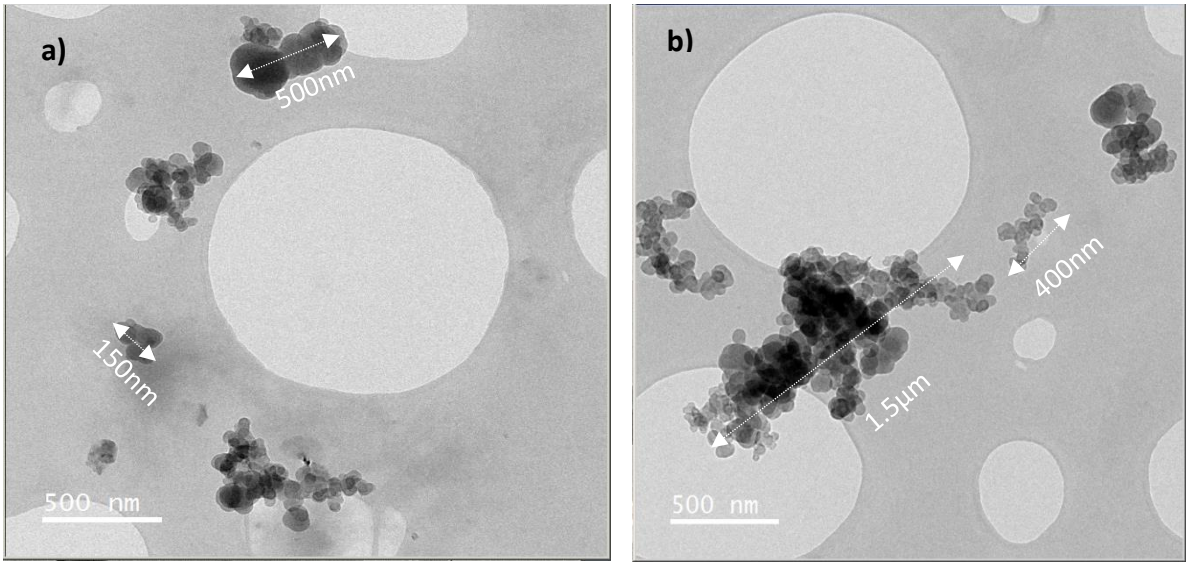

Figure 4.2: TEM images show CBP size distribution in Afton oil containing 1.5 wt% CB a) CBP agglomerates with size distribution(≤1 µm), b) CBP agglomerates in large size distribution (≤1.5 µm).

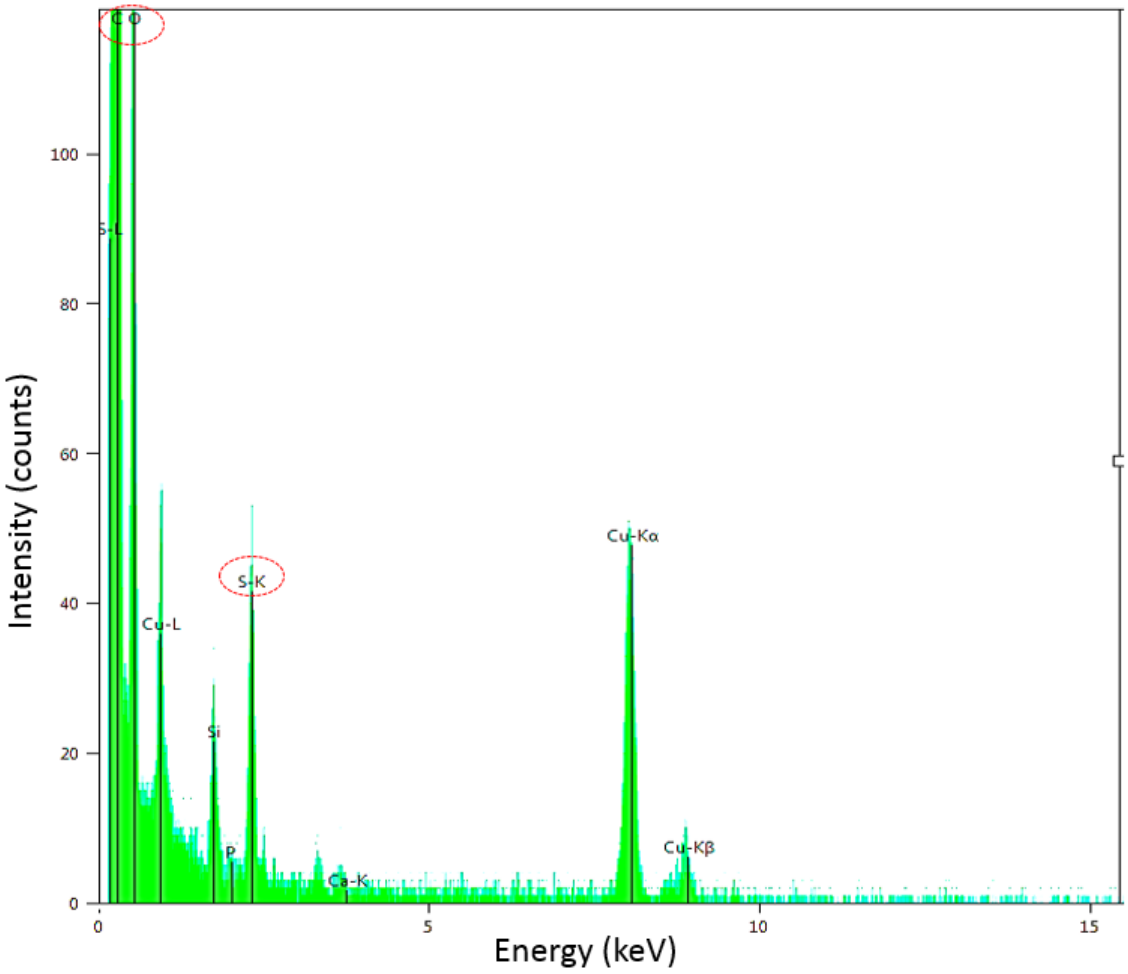

Figure 4.3: TEM spectra of fresh carbon black particles.

4.2 Experimental methods

4.2.1 Ageing oil method

The artificial ageing method of lubricating oil was used to examine the thermal-oxidation stability of the engine oil and oil degradation under severe conditions [195]. As it is difficult to get real used oils containing different levels of soot and operated under the same conditions. Thus, the ageing oil method will be used to simulate chemical interactions between the additives in the oil and soot to investigate its effects on oil degradation and additives adsorption on CBP. This method allows the investigation of increasing soot surface area on additives adsorption and oil degradation. The engine oil has been artificially aged oil in the lab exactly in accordance with ASTM D4636-99 standard [194]. The ageing oil temperature used in this method is 160 °C compared to the temperature of severe oil conditions of 120 °C in the real application [196]. The author believes that ageing oil conditions in this method are tougher than real engine conditions. Thus, the artificial ageing method is used for a part of this project for specific objectives (Chapter 5) and then the rest of the project is completed by using real aged oil drained from the heavy-duty diesel engine (Chapter 6 and Chapter 8).

This method is used to simulate the engine oil in vehicles that are working in severe conditions. As shown in Figure 4.4, 250 ml of mixed oil is placed in a beaker covered with a three-neck lid. The beaker containing oil is placed on the hot plate at a constant temperature of 160 °C. The first open neck allows the airflow (2 L/h) through the oil, providing a source of oxygen to imitate the real oxidation process. The middle neck-led is equipped with a condenser to prevent the evaporation of the oil. The last neck is used to monitor the temperature during the ageing process. Metal samples (grey cast iron material) are placed in the beaker to provide catalytic reactive surfaces. Blended oil is stirred at the speed of 500 rpm to keep lubricating liquid homogeneously over the ageing period. The ageing process is applied for oils containing different levels of carbon black (0, 0.75, 1.5, 3 and 5 wt %) for $96\ \mathrm{hrs}$. The ageing period is chosen according to the D4636 standard [197], which allows measurable

results (i.e. oxidation) to be obtained in a reasonable time [197]. The aged oils samples before and after removing CBP are used for the subsequent experiments.

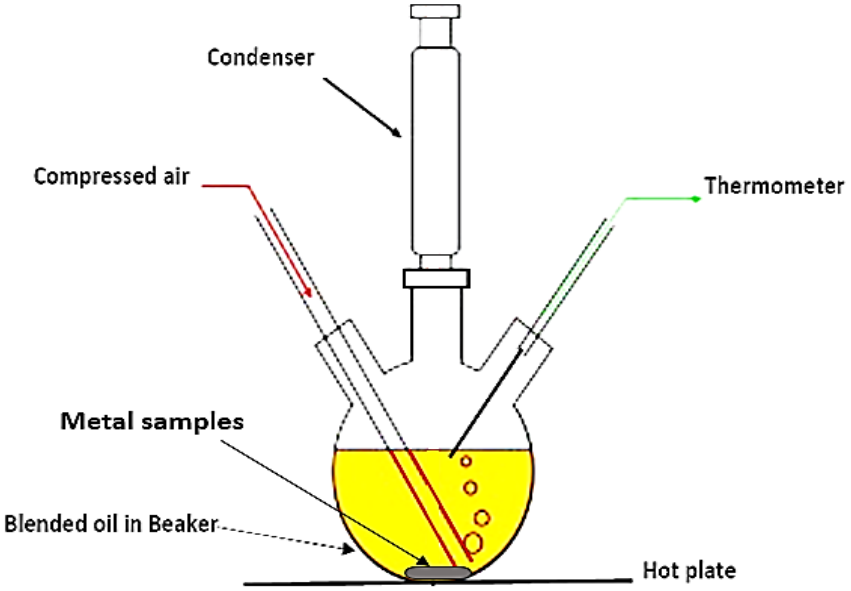

Figure 4.4: Schematic set-up of the artificial ageing process [198].

4.2.2 Water saturation method

The water saturation method helps us to distinguish between different water phases that could be existed in real lubricating oil at different temperatures. The water molecules will be dissolved in the oil naturally by using this method and then separate to free water. Therefore, the effect of water on tribochemistry of rubbing surfaces in either existing in oils as dissolved or free can be determined in the lab.

Engine oils can hold a certain amount of dissolved water depending on different conditions [128]. The maximum amount of dissolved water in the oil is referred to as its saturation point [127]. When the oil reaches its saturation level, any additional water introduced into the oil will be separated to free water that settles underneath the oil. In the lubricating system, the saturation point provides information about the moisture level surrounding the oil. If the oil reaches its saturation level, that means the moisture level is very high and free water is more likely to exist in the oil [127], [128]. In this study, water separation after reaching saturation

level has been investigated. The results will determine the effect of free water on oil performance and additives depletion.

There is no standard method to determine the saturation point in engine oil. In this study, the saturation method has been designed depending on the SAE J1488 standard [199], SAE J1488 standard was used to determine the water saturation level in the fuel, with changes in the experiment periods. In this study, the only sample preparation was used based on the SAE J1488 standard, while the method parameters such as stirring speed, time and temperature were designed depending on experiment outcomes. The saturation experiment is divided into three main stages as reported in Figure 4.5. The effect of different mechanisms on the water saturation test is discussed. These mechanisms include the effect of stirring and time on the saturation level of water in engine oil. Saturation experiment stages are described in detail as follows:

a). Sample preparation: this procedure is based on the SAE J1488 standard [199]. A glass bottle with a capacity of 250 ml was used in the saturation experiment. The bottle was washed before the test with distilled water and dried thoroughly. The 150 ml of the oil was placed into the dried bottle and a small magnetic stirrer was inserted into the oil. The syringe fitted with a long needle was used to inject 50 ml of distilled water gently underneath the oil after removing the air bubbles from the syringe. Water should be injected into the bottom of the bottle gently to create and maintain the water-oil interface with minimal agitation. Finally, the bottle was completed with engine oil. The bottle was fully sealed with two open holes. The first open hole was used for the temperature sensor. While the second hole was closed with a rubber cap which was used for sampling as shown in Figure 4.5a.

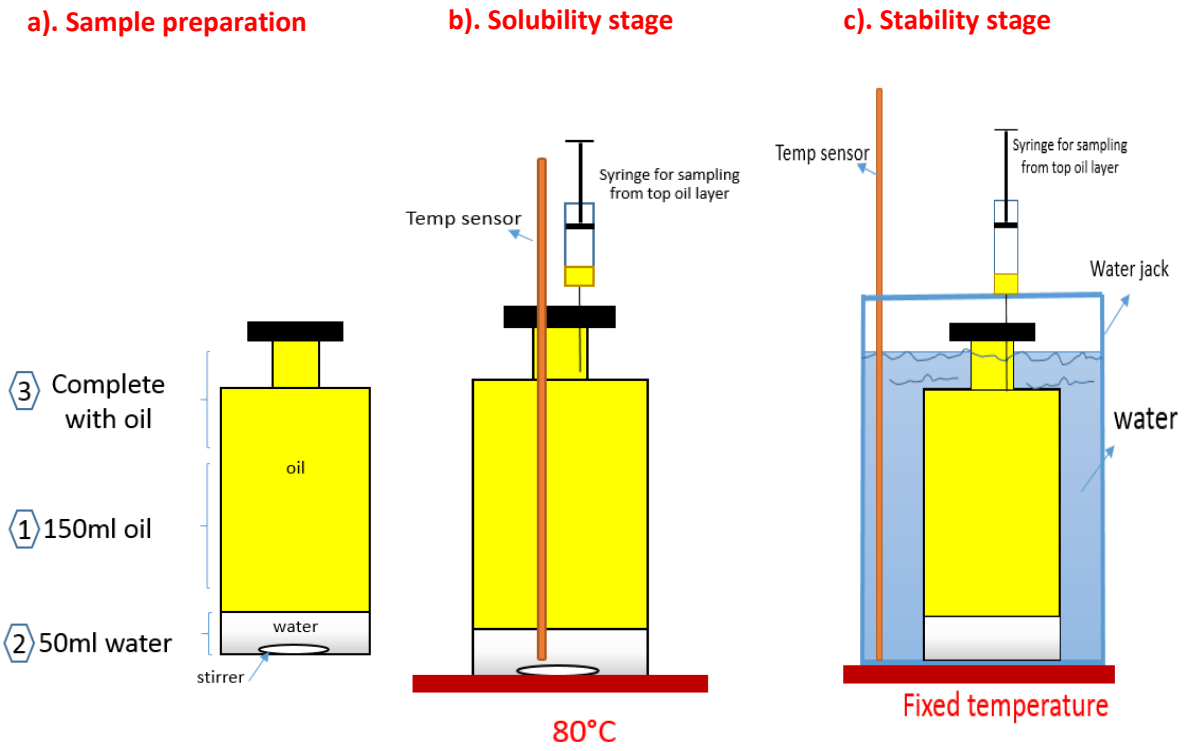

Figure 4.5: Schematic images explain the water saturation method in the oil a) sample preparation to create two separated layers of water and oil b) water solubility stage at 80 °C applied with stirring of 100 rpm c) stability stage was designed to stabilise the water in oil and separate any extra-water which cannot dissolve in oil at a fixed temperature (no stirring was used in this stage).

b). Water solubility in the oil: this stage is designed to discover the solubility and the behaviour of water in the oil over time. Two water solubility tests were run under different conditions, the first test fixed the temperature at 80 °C over time without stirring. The second test used both the temperature at 80 °C and magnetic stirring of 100 rpm as shown in Figure 4.5b. The lowest stirring speed of 100 rpm was applied to avoid agitation of the oil-water interface and the vortex as a result of stirring. The results as reported in Figure 4.6 show the increase in the level of water in engine oil progressively over time under both conditions and the water keeps increasing even without stirring. The results show that the stirring accelerates the solubility of water in oil. For the water solubility test with stirring as reported in Figure 4.7, the oil appearance exhibits that water in the oil becomes emulsified after 48hrs and reaches the milky state after 72 hrs. While water solubility test for the oil without stirring takes a longer time to reach the milky state as shown in Figure 4.6. The water solubility stage proves that water does not stabilise at saturation level even without stirring. Therefore, the next step is

used to find the stable stage where oil can hold only the dissolved water. The next stage will determine the saturation points at a fixed temperature.

C). Water stability stage (saturation level): oil appearance images, as shown in Figure 4.7, confirmed that water in the oil before 48hrs transferred from dissolved state to emulsified state. After reaching the emulsified state (after 48 hrs), the oil bottle was settled down in the water bath at a fixed temperature. For example to find the saturation level at 80 °C, the test bottle was placed in a water bath at 80°C without stirring to guarantee homogenous heating surrounding the glass bottle as shown in Figure 4.5c. The water level in the oil was measured over time until reaching the stable content of water in oil which is called the saturation level. To find the saturation level of any temperature, the test bottle should be settled down at a fixed temperature until reaching a stable level of water. The exact saturation point is calculated by finding the mean values of the stable points.

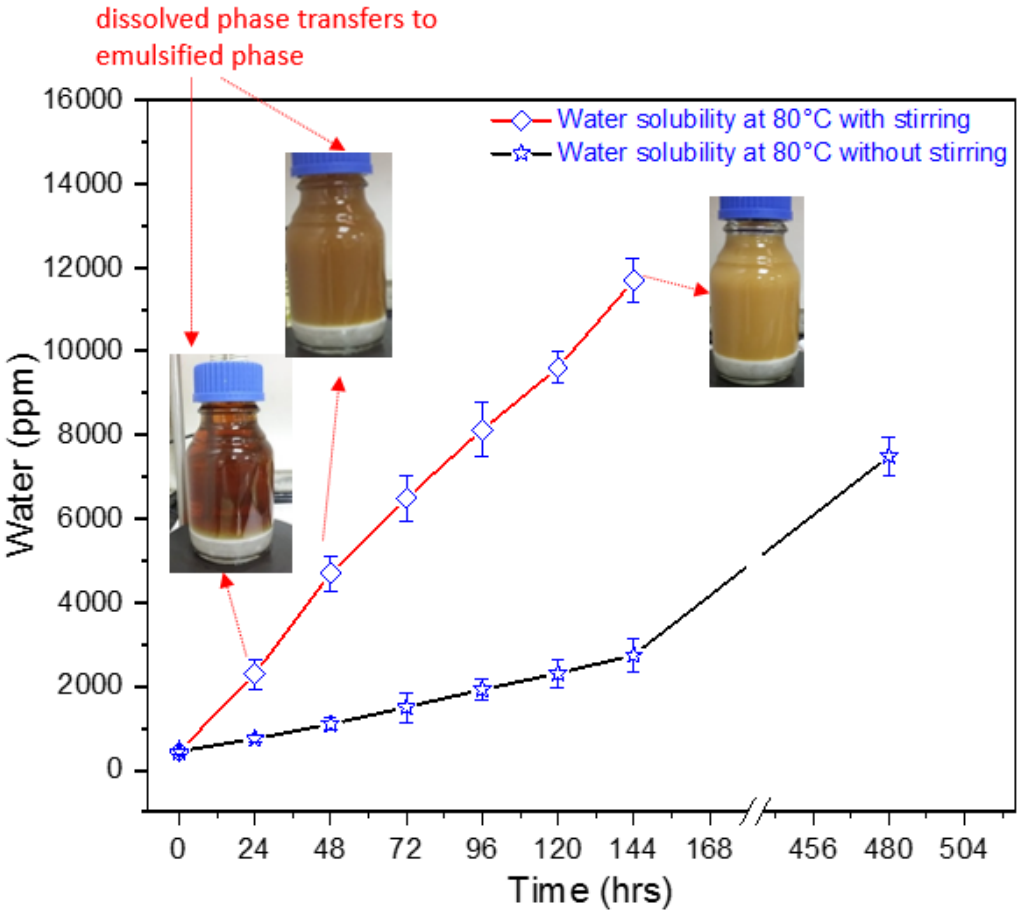

Figure 4.6: Water solubility in the oil at 80°C with stirring and without stirring.

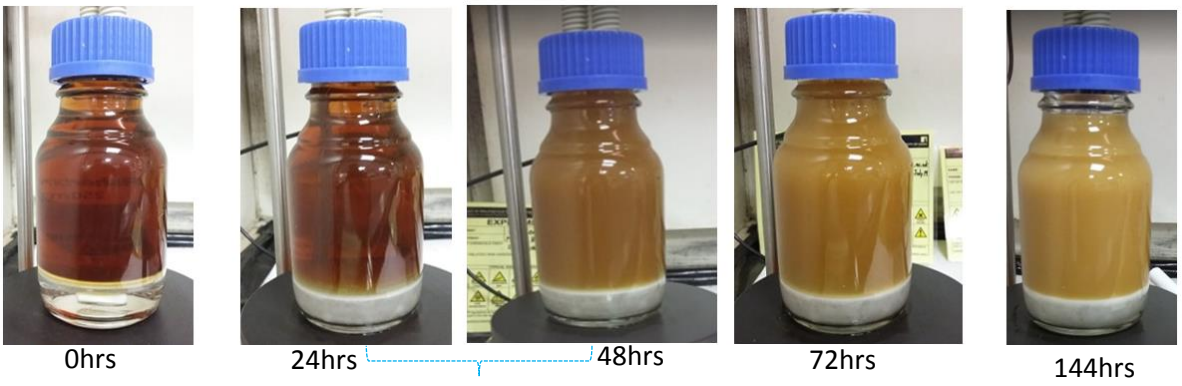

Figure 4.7: Oil appearance develops from dissolved water (clear appearance), as displayed in 0 hrs image and 24 hrs image, to emulsified state (cloudy) after 48 hrs until reaching the milky state of oil after 72 hrs.

4.2.3 Soot calibration method

FTIR technique is used to estimate the soot level in used oil according to ASTM D7844 standard [200]. Fundamentally, soot or CB level in the oil causes the shift at 2000 cm^{-1} point of FTIR spectra and the shift in the spectra is associated with soot or CB level. The CB with varied levels was blended homogeneously in Afton oil using the hotplate at the temperature of 60 °C and the speed of 500 rpm for 1.5 hrs. The Oil sample containing the known level of CB was measured using FTIR. FTIR spectra for the oil with varied levels were plotted in Figure 4.8. The results show that the higher level of CB in the oil causes an increase in the shift of FTIR spectra.

The calibration curve plotted the relationship between the known CB level in the oil and the shift at the 2000 cm^{-1} point of FTIR spectra (Figure 4.9). A similar calibration curve method using CB to determine soot percentage was described by Bordg H at al. [201]. In this study, the calibration curve was used to estimate the soot level in the used oil.

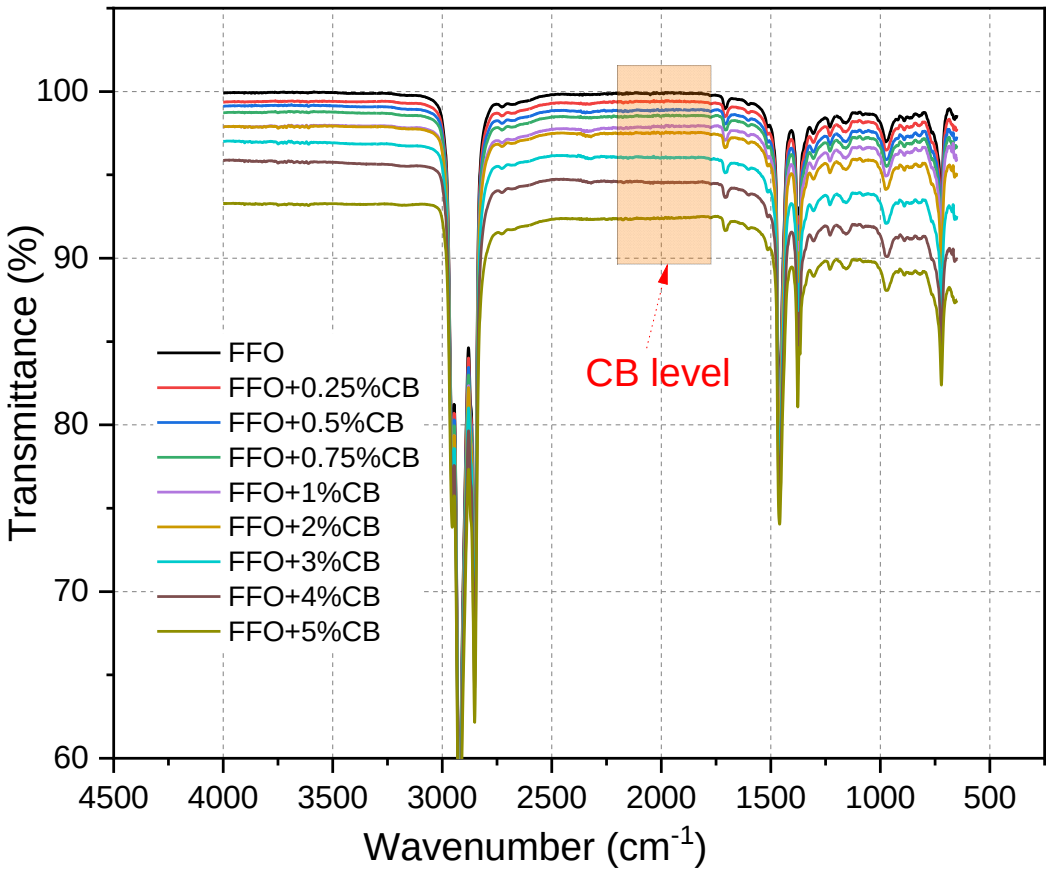

Figure 4.8: FTIR spectra for varied levels of CB.

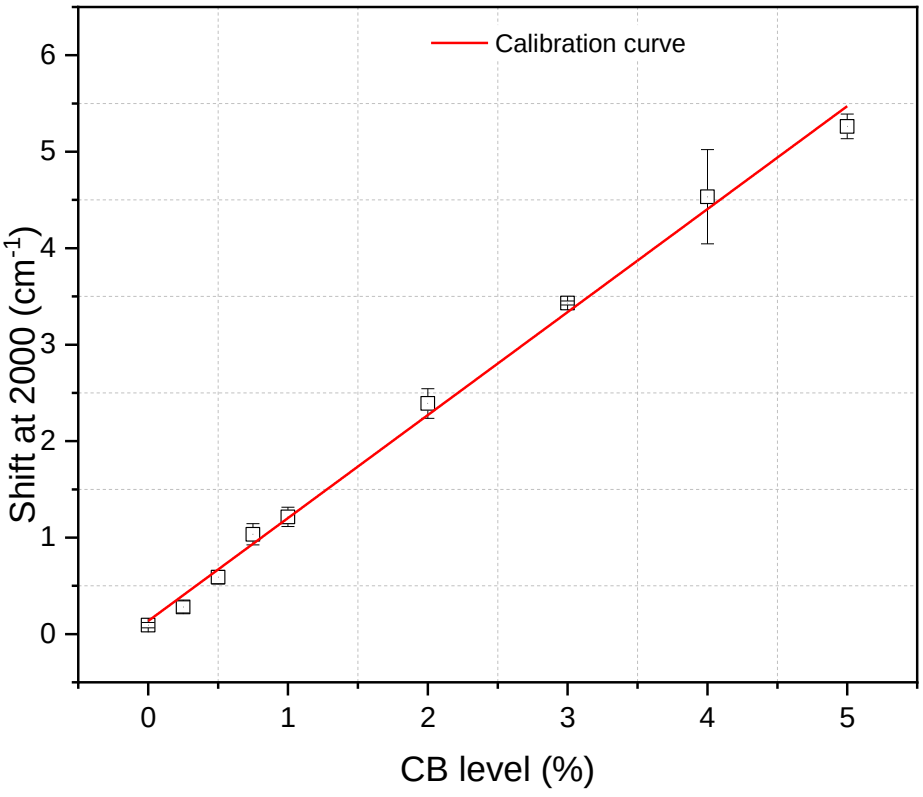

Figure 4.9: Calibration curve obtained from the shift in 2000 cm^{-1} point when the CB exists in the oil.

4.3 Fourier Transform Infrared Spectroscopy/ Attenuated Total Reflectance (FTIR/ ATR)

FTIR spectroscopy is an analytical technique that uses the beam of infrared radiation light to direct the light through the sample of material. IR beam is reflected or absorbed when the beam comes into contact with the material. The reflected/absorbed beam is directed to the detector at a certain angle. The energy of reflected or absorbed infrared light at various wavelengths is measured to identify the molecular composition or structure of materials. The adsorption of wavelengths depends on the molecular vibrations of the material [127, 128].

An ATR accessory to FTIR works by measuring the changes that occur in an internally reflected IR beam. The internal reflections produce an evanescent wave that passes through the ATR crystal underneath the material sample. In regions of the IR spectrum that absorbs the energy, the evanescent waves will be attenuated. The attenuated beam returns to the crystal and exits from the end of the crystal and is directed to the detector. The detector records the attenuated IR beam to produce the spectrum as illustrated in Figure 4.10. In the final step, the data is decoded using a mathematical technique to produce a spectrum of the material [204]. The ATR provides specific details correlated to the existence or the absence of chemical functional groups [127, 128]. However, the ATR technique is used to determine the chemical bonds of oil samples, especially in the presence of additives such as ZDDP. In this study, oil degradation, additives depletion and oil contaminants were detected using the FTIR technique. FTIR spectra within the range of 650 to 4000 cm^{-1} were applied and the resolution of collected spectra is 4 cm^{-1}.

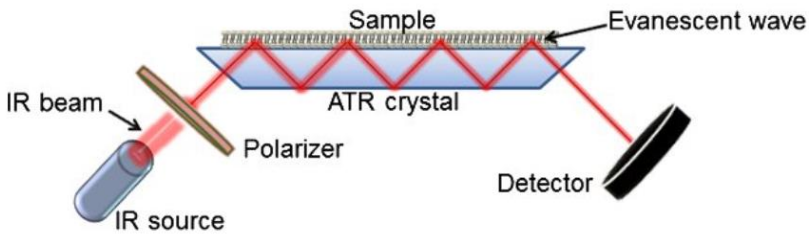

Figure 4.10: Schematic representation of the principal work of ATR/FTIR [204].

4.4 Inductively Coupled Plasma –Optical Emission Spectroscopy (ICP-OES)

ICP-OMS is a powerful tool to detect a variety of metal elements in oils. In this study, ICP is a very important technique to identify the change in the additive concentration in engine oil. The principle of this tool depends on determining how much light is absorbed or emitted by molecules or atoms when the plasma energy is changed from one state to another. The difference between the two energy states can be determined by measuring the light frequency that is absorbed or emitted by atoms. Fundamentally, a liquid sample is transported inside the instrument after the liquid is converted into aerosol through a process called nebulisation. The aerosol is then transported through the plasma chamber where then goes through several steps; vaporized, atomized and ionized or excited by the plasma rays. The ions from excited atoms release their characteristic radiation which is collected and sorted out by the wavelength of radiation. The radiation wavelength is measured and converted into electronic signals which are turned into the information of elemental concentration [205]. ICP chemical analysis for oil samples in this project was done by Oil Check Laboratory Services Ltd, UK.

4.5 Viscosity measurement

KINEXUS rheometer is used to measure the viscosity of the oil, a small quantity of engine oil approximately 0.5 ml is required for the test. The working principle depends on bringing two circular plates together leaving a small gap, then heating the bottom plate to 40 °C by rotating the top plate and repeating the test for 60 increments. The second set is done at the higher temperature of 100 °C and the average for repeated readings is calculated at both temperatures. The 40 °C and 100 °C are chosen according to the ASTM standard [206].

4.6 Surface analysis techniques

Several surface analysis techniques have been used in this project to provide high-resolution images and precise information depending on the material state and the best technical

features that can be provided. Table 4.2 summarised the surface techniques applied in this project and the main purposes of using each technique.

Table 4.2: Summary of the surface techniques that are used to provide different functions in this project.

Technique name	Service provider	Main functions used in this project
NPFLEX	IFS lab/Leeds Universty	Provides high-resolution images of surface topography. It is used to measure the wear scar diameter on pins.
Atomic Force Microscopy (AFM)	IFS lab/Leeds University	Extremely high-resolution non-optical imaging technique. AFM is used as a 3D imaging technique to measure the surface topology, especially for water contamination samples to study the effect of water on tribofilm topography.
Scanning Electron Microscope And Energy Dispersive X-ray analysis (SEM/EDX)	LEMAS lab/Leeds University	Excellent topography images of surfaces with very high resolution. SEM can detect the small cracks of the metal surface caused by water or soot. EDX equipped with SEM is used to confirm the existence or absence of tribofilm elements in the wear scar.
Transmission Electron Microscopy (TEM)	LEMAS lab/Leeds University	TEM produces details regarding nanoparticles of size <100nm, So the TEM technique was used to study the crystal structure and size distribution of CB and soot nanoparticles.
X-ray Photoelectron Spectroscopy (XPS)	Harwell labs, UK	XPS is used to identify and quantify all the surface elements of tribofilm, especially to quantify the effect of water on polyphosphate length chains.
X-ray Diffraction (XRD)	SCAPE lab/Leeds University	X-ray Diffraction (XRD) is used to identify the crystallographic structure of soot or CBP for the whole bulk of material not just for a few particles.

4.6.1 Wear measurement

An optical white light interferometer using NPFLEX from Bruker Corporation, USA was used to measure the wear volume of the pin after tribometer tests. It was not possible to measure wear on the plate due to the high surface roughness compared to the pin. NPFLEX uses one source of light to create two light beams by using a beam-splitter, half of the light beam is called a reference beam, and another is called an object beam. Objective and reference beams are reflected from the sample surface being scanned and perfect mirror respectively, then both light beams combine and travel off through optics and camera. Reflected light beams are represented on a computer screen as dark and bright bands are called fringes. The brightness fringes of the sample appear on the computer screen which means the light beams are perpendicular to the sample surface, hence the reflected lights can provide the best resolution image of tomography of the sample surface being scanned [207].

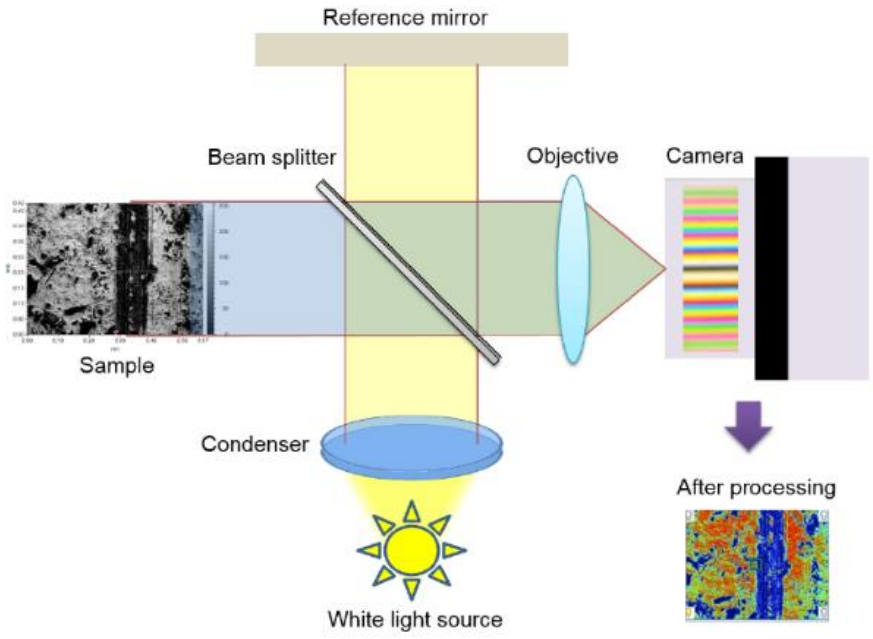

Figure 4.11:Schematic explanation of the principal work of the white light interferometry [208].

Scanned images of pin surfaces that are measured by NPFLEX have been investigated using Vision64 software from Bruker Corporation. Wear volume (spherical cap volume) on the pin is calculated using Equation 4.1 and Equation 4.2 as follows:

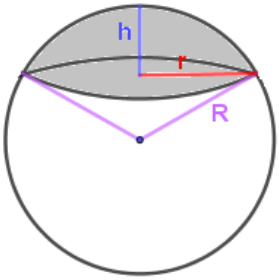

Figure 4.12: Schematic of a spherical cap shape.

$$V_{pin\ vloume\ loss} = \frac{\pi.h^2.(3R-h)}{3}$$ Equation 4.1

$$h = R - ((R^2 - r^2))^{0.5}$$ Equation 4.2

Where,

h: Spherical cap height (µm), R: sphere radius (µm), r wear scar radius (µm).

4.6.2 Atomic Force Microscopy (AFM)

Atomic force microscopy (Bruker, USA) is used as an imaging technique in this study to measure the surface topology of the sample surface with picometer high resolution. This microscope technique is based on a laser beam that is focused on the backside of the cantilever (*Figure 4.13*). The cantilever moves up and down on the substrate surface line-by-line and beam defections of the laser are captured by the sensitive photodiode. The height differences due to the z-piezo movements within a sample surface produce 3D topographic images. This technique has also the ability to measure a variety of material properties including, nanomechanical and electrical properties [209]. In this study, the AFM was used to investigate the textural and structure of tribofilm on wear scar of pins. After running tribotests, the pins were washed with heptane to remove the contaminated oil from the surface before using the AFM technique. Dimension Icon Bruker AFM was used with a nominal spring constant of 40 N/m and a resonant frequency of 2 kHz. PeakForce Quantitative Nanoscale Mechanical (QNM) maps are applied to distinguish between nanomechanical properties including adhesion and deformation with atomic resolution in the topography. High-resolution AFM images of an area of 10×10 µm^2 were captured. The AFM tip was centred in the rubbed

area of the pin surface. The images were captured at a low contact force of 45 nN and a speed of 40 $\mu m/s$. The scanning angle during the imaging was fixed at an angle of 90°.

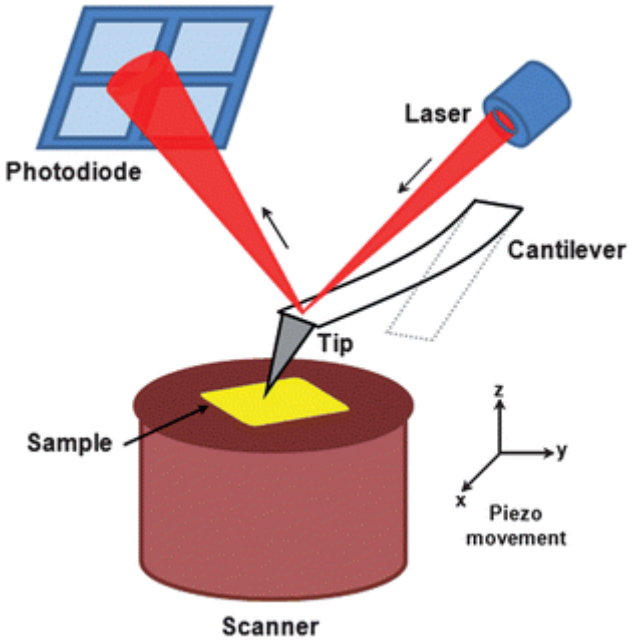

Figure 4.13: Schematic illustration of the principal work of AFM technique [210].

4.6.3 Scanning Electron Microscope and Energy Dispersive X-ray analysis (SEM/EDX)

A Carl Zeiss (Oberkochen, Germany) EVO SEM is used in this study to provide high magnification images of samples. Electron bombarded through the sample surfaces leads to secondary electron emission. This emission contains electrons with different energy levels and SEM detectors just collect secondary electrons that come from the top layer of the sample surface. This will give excellent topography images of surfaces with very high resolution. SEM can detect the small cracks of the metal surface caused by water or soot in engine oil.

While EDX chemical analyser technique is integrated into SEM and equipped with an X-ray spectrometer to identify the chemical composition of the samples. EDX principle depends on measuring the energy of an electron beam that is reflected from the sample surface. The differential in emitted electron energies determines the chemical elements of the surface.

4.6.4 Transmission Electron Microscopy (TEM)

Transmission electron microscopy (TEM) is used in this study due to its higher spatial resolution with very good quality and analytical measurements compared to SEM. The working principle of TEM is similar to the SEM technique. TEM is facilitated with high E-beam energies ranging from 60 to 350 keV travel through a thin sample (<100 nm) to produce an image onto a fluorescent screen. TEM produces details regarding nanoparticles including crystallographic information, compositional, morphologic and precise particles size. TEM provides the crystal structure on an atomic scale for nanoparticles including the inner and outer structure of nanoparticles with high resolution [211]. In this study, the TEM technique was used to study the crystal structure and size distribution of CB and soot.

4.6.5 X-ray Photoelectron Spectroscopy (XPS)

X-ray photoelectron spectroscopy (Thermo NEXSA XPS, UK) is a powerful analytical technique used to study the elemental composition of the material surface. XPS spectra represent the kinetic energy of the electrons that are emitted from the top layer (1-10 nm) of the sample surface being investigated. Chemical composition of surface characteristics as the peaks in the XPS spectrum. XPS spectra use the energy and intensity of the peaks to identify and quantify all the surface elements [212]. The working principle of the XPS technique is illustrated in Figure 4.14. In this study, the samples were analysed in the HarwellXPS lab, Cardiff University. All samples were cleaned with heptane to remove the contaminated oil from the wear scar before the XPS analysis. The tribofilm elements such as Zn, Fe, Ca, Mg, O, C, P and S were measured on the tribofilm of samples. The XPS spot of 200 µm ×100 µm was centred in the middle of the wear scar. The XPS was run at an X-ray source energy of 1486.69 eV, an X-ray strength of 19.2 W, an Iron gun current of 150 µA and a voltage of 45 V. The temperature and pressure during XPS analysis were 294 K and below 10^{-8} Torr respectively. The spectra of samples were analysed using CaseXPS software. The different parameters and constraints used for fitting the spectra and the assignments to spectra peaks are listed in

Table 4.3. The deconvolution of XPS signals was performed by fitting them with the peaks using the line shape of the Gaussian/Lorentzian (GL) formula. The fitted peaks are correlated to the available literature [213]–[217].

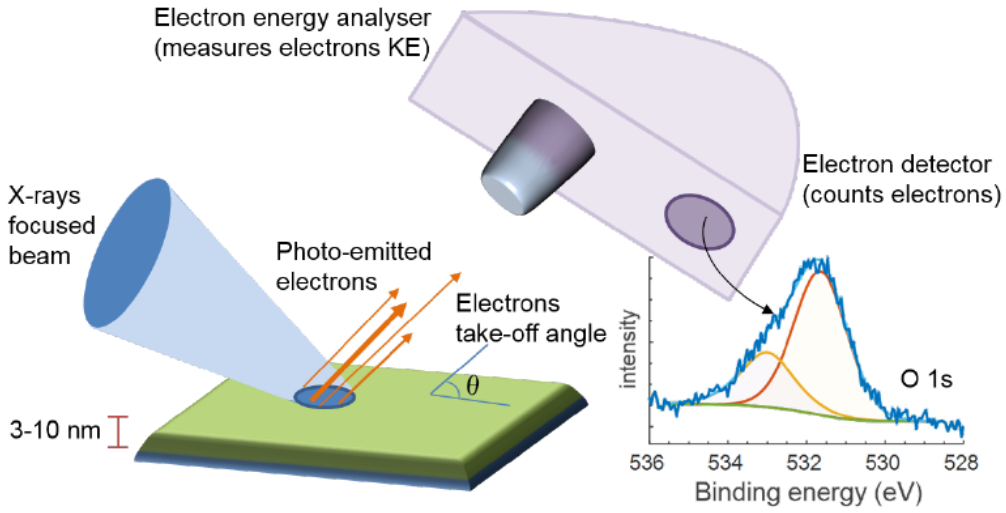

Figure 4.14: Schematic explanation of the working principle of XPS [208].

Table 4.3: The parameters used in the analysis of XPS spectra.

Element	Assignment	Binding Energy (eV)	Line shape
O1s	NBO	531–532	GL(30)
	BO	532–533	GL(30)
P 2p	Phosphate	133–134	GL(30)
	Phosphate	134–135	GL(30)
Fe 2p	FeO	529–530	GL(30)
Zn 2p	Phosphate	1022-1023	GL(30)
Zn 3s	Phosphate	140–141	GL(30)

4.6.6 X-ray Diffraction (XRD)

X-ray Diffraction (XRD) is an analytical technique used to identify the crystallographic structure of materials. XRD sample is oriented in the path of the X-ray beam. X-rays are scattered by the crystal of material into the detector. The detector and the beam are rotated at a range of angles. The scattering angles and intensities of the X-rays that refected from the sample are

recorded. The reflected X-rays correspond to the planes of atoms in the material [218]. In this study, XRD was used to determine the crystal structure of CB and soot particles. The scan angle (2θ) is ranged between 10 to 90°.

Miller indices are used to describe certain crystallographic directions and planes in a material [101]. XRD data of CB consists of only (00l) and (hk0) graphite reflections [219]. The position of the (002) peak in XRD spectra of CB is often referred to as $d_{(002)}$ which is the distance between graphite layers [219]. The peaks positions at ~25° and 43°, the diffraction patterns are composed of two board peaks, are indexed as the (002) and (100) graphite-type reflections respectively [19], [219]. These two peaks at 2θ positions ~25° and 43° are arising from turbostratic carbon structure [19], [219]. Table 4.4 demonstrates the expected peaks in XRD spectra of CB and soot particles.

Table 4.4: XRD peaks are expected in the crystal structure of CB and soot [19], [101], [219].

Peak list	Peak position (2θ deg)	Possible compound	Chemical formula	Miller indices
002	~25	turbostratic carbon	C	002
100	~43	turbostratic carbon	C	100

4.7 Filtration techniques

4.7.1 Centrifugation technique

Centrifugation efficiency has been studied to remove as much CB as possible from engine oil. Three main factors influence the centrifuge process; temperature, rotation speed and time. The speed is constricted by the design of the sample tube as the higher speed needs a special tube. While the centrifuge temperature has been proved that affects the removal of particles from the liquid [123]. Figure 4.15 demonstrates the centrifuge process at two temperatures 25 °C and 40 °C for three different samples that contained varying levels of CB. The results show

that increasing the temperature to 40 °C can remove more CB compared to the samples that are centrifuged at a lower temperature of 25 °C. Samples with darkening colour centrifuged at low temperature still contain CB in the oil. While the samples are centrifuged at a higher temperature of 40 °C characterised as light colour meaning no CB in the oil.

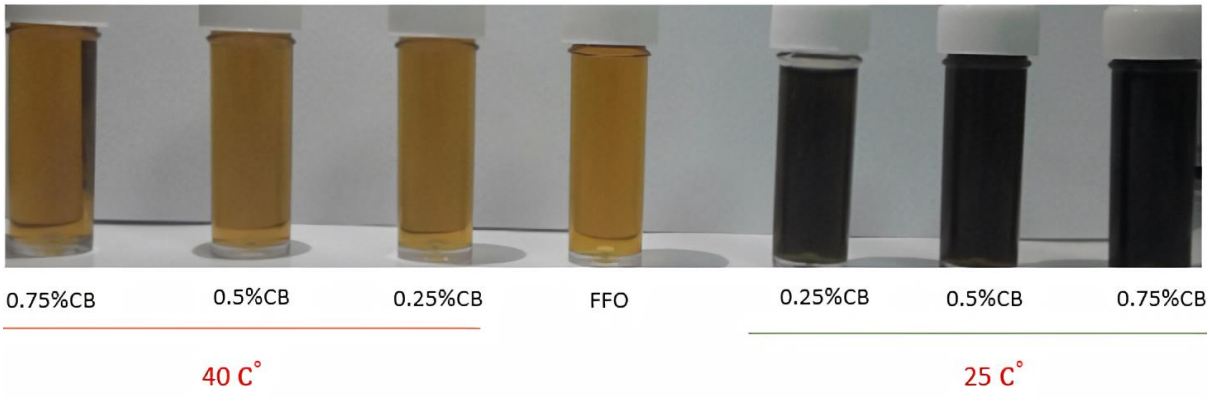

Figure 4.15: FFO mixed with CB at different levels of CB after running the centrifuge process twice at two different temperatures (25 and 40 °C) compared to fresh FFO.

In order to study the effect of oil viscosity on the removal of CB from the oil at different centrifuge temperatures. Oil viscosity at 25 and 40 °C were measured for FFO containing 0.25 %CB and 0.5 %CB. The viscosity of oils with the same level of CB reveals a decrease in the viscosity to less than a half at 40 °C compared to the oil viscosity at 25 °C as seen in Figure 4.16. This effect can be explained as the viscosity decrease, the CB movements inside the liquid become much easier hence centrifugation is more efficient to remove CB with less viscosity of oils. Therefore, the centrifuge temperature of 40 °C has been used in this project to set up a centrifuge process. Megafuge 16R machine was used to perform the centrifuge process. The centrifugation conditions to remove the CB or soot and water from the oil in this project are shown in Table 4.5.

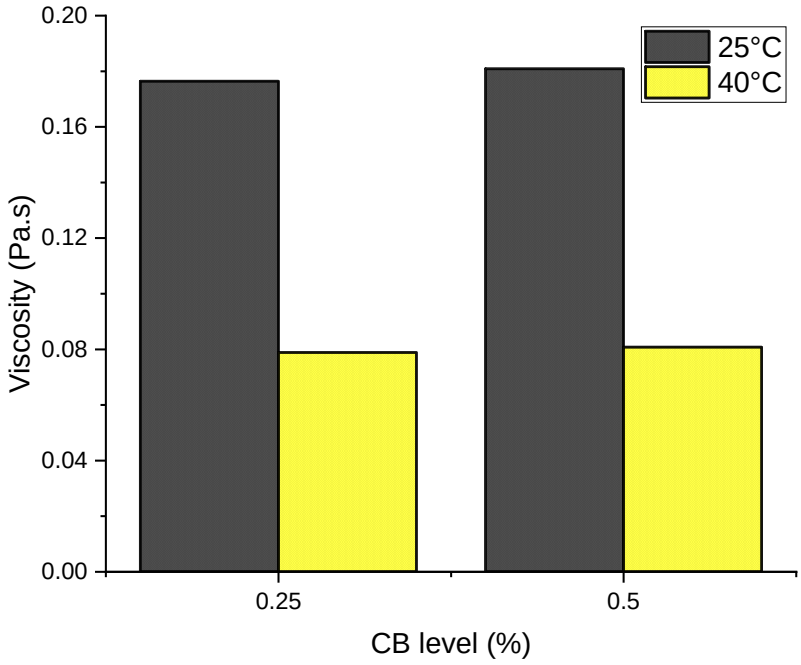

Figure 4.16: Viscosity measurements at 25 °C and 40 °C of FFO contained 0.25 %CB and 0.5 %CB.

Table 4.5: Centrifugation conditions used in this study to remove soot or CB and water from the oils.

Contamination types	Temperature (°C)	Speed (rpm)	Time (hr)	Repeated process
CB Particles	40	12000	2	X4
Water	20	12000	1	X1

4.7.2 Media filtration rig

Full-flow of the filtration rig was built based on SAE HS 806 oil filter test procedure [220] as shown in Figure 4.17. Full-flow filtration rig consists of the oil pump (5bar), oil flow meter, media filter housing, oil pressure relief valves before and after the filter and the oil tank. 5 litres of used oil were circulated through the depth filter over time. The oil samples were collected from the running test at a regular time. Soot concentration in used oil was measured consistently over time using FTIR. Manufacturing details of depth filters were used in this study illustrated in Table 4.6. The efficiency of the filter $(\mathcal{E})$ was calculated using Equation 4.4 [221].

$$V.dc = -Q\mathcal{E}C.dT$$ Equation 4.3

$$Ln(\frac{C2}{C1}) = -\frac{Q\mathcal{E}}{V}\Delta T \qquad \text{Equation 4.4}$$

Where, V (litre) tank volume, T (s) time, $C1$ (%) soot concentration before filtration, $C2$ (%) soot concentration after filtration, $\mathcal{E}$ (%) filter efficiency, Q (m^3/s) flow rate.

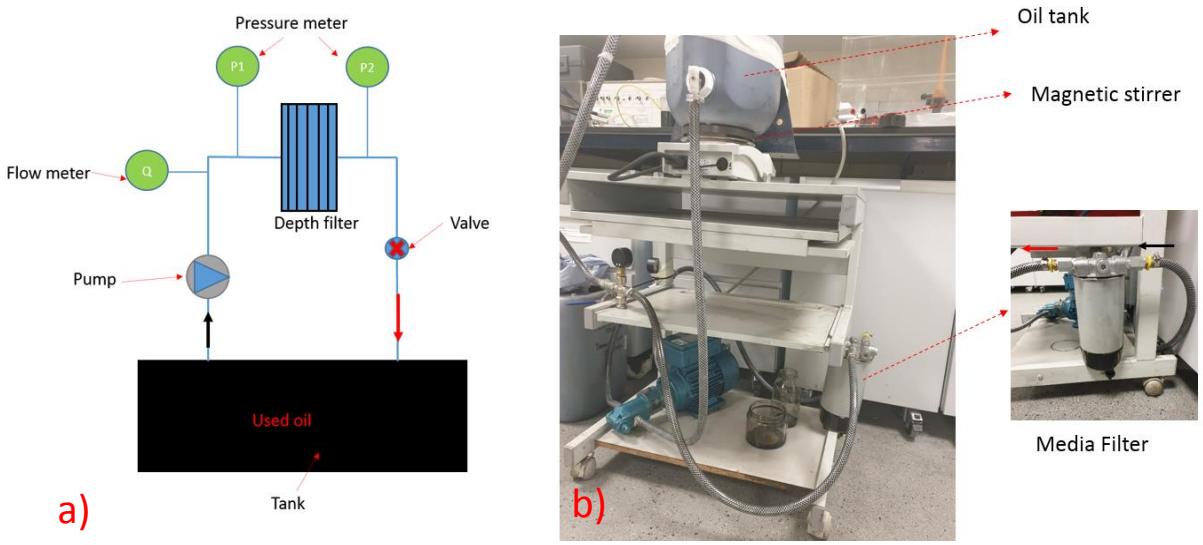

Figure 4.17: Filtration media rig used to filter the used oils using depth filters a) schematic diagram of filtration rig b) the image of filtration rig that used in this study.

Table 4.6: Depth filters details used in this study.

Filter manufacturing name	Material	Number of layers	Pore size (µm)
X175545W	Cellulose fibres	45	20
X175580W	Cellulose fibres	80	20
X175680W	Cellulose fibres	80	20
X1890	Cellulose fibres	80	20

4.8 Pin-on-Plate tribometer

TE77 tribometer is used to simulate reciprocating sliding conditions in an engine according to ASTM G 181 [222]. The tribometer was used in this study to conduct the friction tests of the piston ring and cylinder liner interface in the engine at the boundary lubrication regime and reciprocating motion. A 3D diagram of TE77 is shown in Figure 4.18a. Dimensions and

material properties of specimens are described in Table 4.7. The pin and plate samples are used to represent the contact interface between piston rings and cylinder liners respectively. Experiments are carefully designed to investigate wear and friction in a boundary lubrication regime (Lambda of FFO λ=0.27<1). The λ was calculated based on the equations Eq 2.2 and Eq 2.3 described in Chapter 2. The maximum contact pressure is calculated using the Hertzian contact equation (Equation 2.7). The test temperature is used to replicate the real working condition in the engine as shown in Table 4.7. The electric motor applies a reciprocating motion through the gearbox on the pin holder arm. The force transducer is used to measure the friction force which is used to calculate the friction coefficient. The normal load is applied by a cantilever system through the contact interface as shown in Figure 4.18b. 10ml of oil sample is used for each tribological test. The experiments are repeated at least twice to ensure the repeatability of tests. The standard deviation method of error bars for repeated tests was applied. After all the tribological tests, pins and plates are rinsed with heptane to remove the contaminated oil from the surfaces.

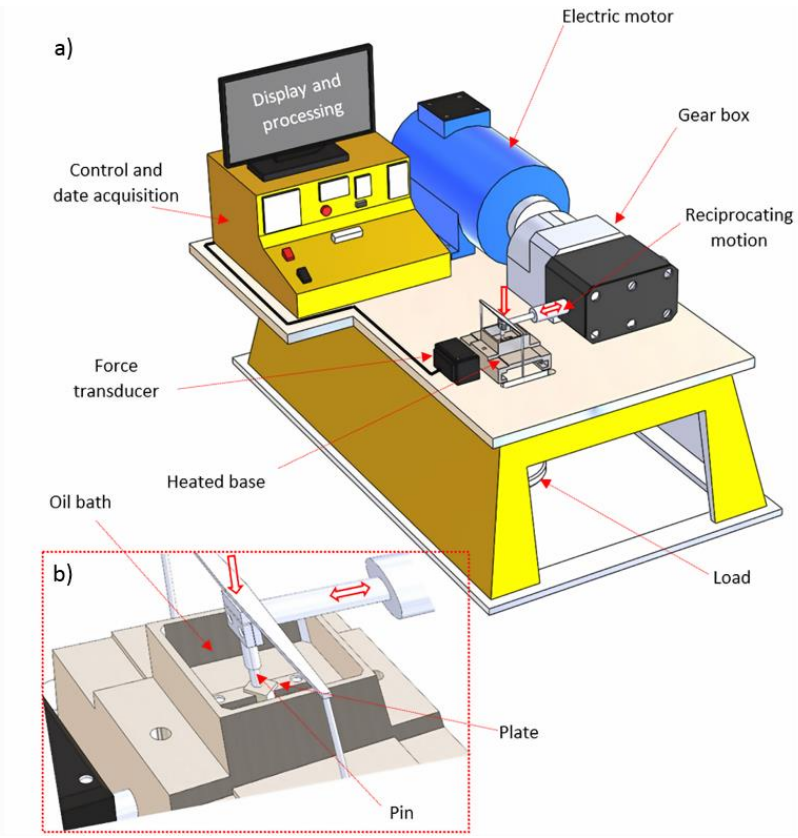

Figure 4.18: 3D schematic of TE77 experiment set up (a), the contact interface between pin and plate (b).

Table 4.7: Materials properties of specimens and TE77 set up parameters.

Material Properties	Pin	Plate	TE77 Parameters	Value
Material	Steel EN31	Steel EN31	Temperature °C	100
Dimensions (mm)	10 radius	7*7*3	Contact pressure (GPa)	1.26
Hardness (HRC)	58-62	58-62	Load (N)	22.1
Roughness (nm)	30-50	400-600	Frequency (Hz)	25
Elastic modulus (GPa)	190-210	190-210		
Poisson's ratio	0.28	0.28	Test duration (mins)	120

4.9 Water concentration measurement in oils

Coulometric Karl Fischer Titration (KFT) is a chemical analytical method that is widely used to determine water concentration in oil according to ASTM D6304 [223] with high accuracy of ±0.01 %. The KFT method detects water content due to the chemical reaction between the iodine reagent, sulfur dioxide and water in oil. The iodine reagent is consumed due to the reactions between the water and reagent. This consumed reagent was used as a gauge to determine water concentration in oil. This method is used to measure water concentration regardless of the water state if dissolved or free [223].

4.10 In-situ nano-indention

Nanoindentation experiments to investigate the mechanical properties of soot particles have been performed in this study. The particles were dispersed in iso-propanol at the ultrasonic bath for 2 mins. Silicon wedge substrate, with dimensions (10×10 mm) and thickness of 5 µm, was dipped into the solution and dried over the night. Many nanoparticles were found to stick on the wedge surface by Van der Waals forces. Nano-indenter (Alemnis Standard Assembly) is equipped and fitted into the SEM machine to provide a high resolution during the nano-indention process as illustrated in Figure 4.19b. The diamond tip, with a diameter of 1 µm and a speed of 10 nm/s, moves toward the CBPs as shown in Figure 4.19a. A single particle can be monitored during the deformation in real-time using SEM. The force to resist the

deformation in the particle shape was measured using the load sensor. The Force-displacement curve represented the particle deformation during the indention process.

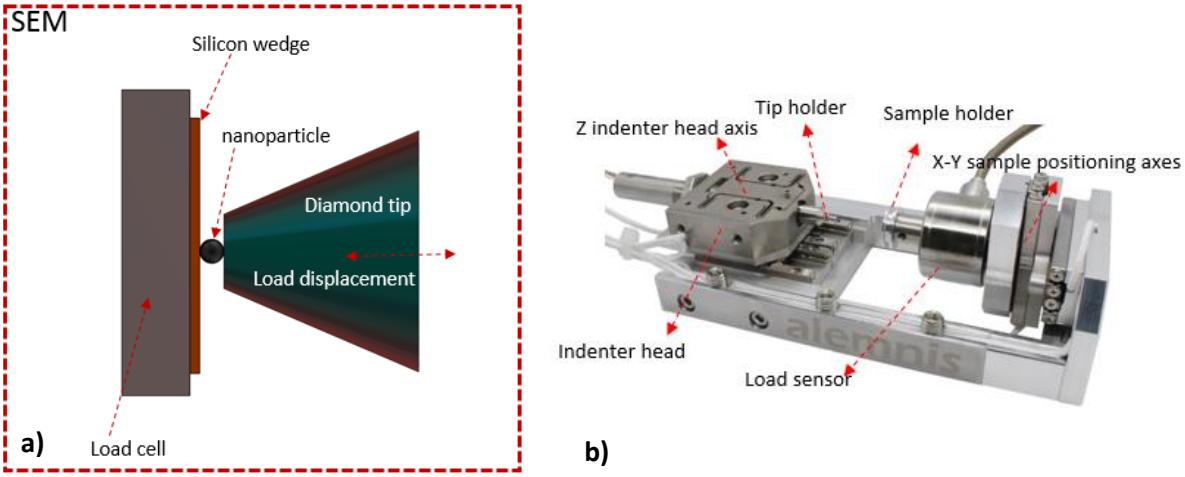

Figure 4.19: a) Schematic representation of nanoindenter performing a compression test on soot particle in the SEM b) Alemnis nanoindenter.

4.11 Soot extraction from the oil

Soot/CB particles were extracted from the oil using centrifugation. To remove the oil from the particles' surfaces after centrifugation, the particles were washed with heptane and centrifuged as shown in Figure 4.20 [110]. In the final stage, the particles were dried in the oven for 2 hrs at 100 °C for post-chemical and physical analysis.

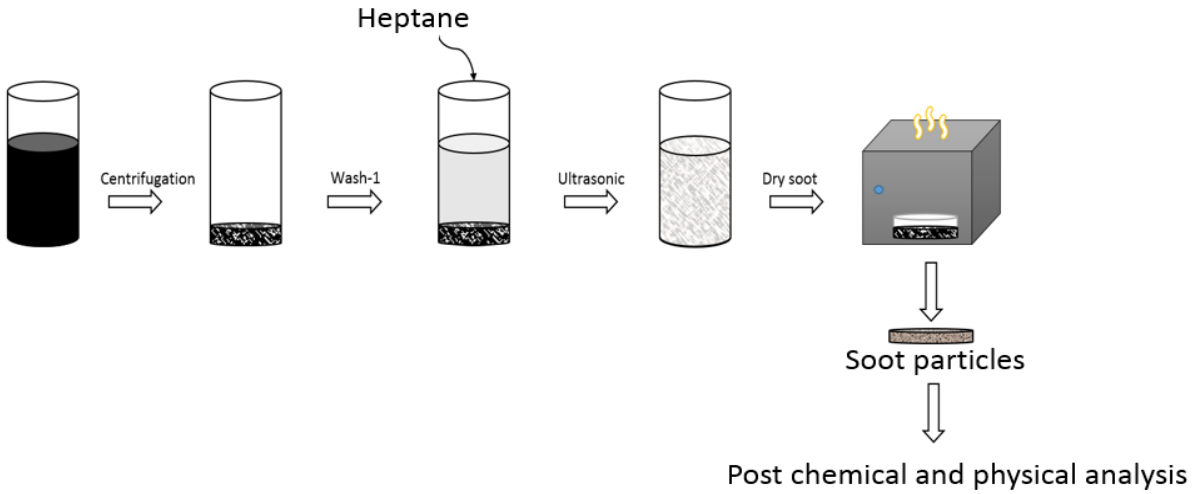

Figure 4.20: Diagram of soot extraction process from the oil.

5 Chapter (5) CBP effect on engine oil

This chapter investigates the effect of CBP on engine oil under different ageing conditions. This chapter studies the effect of CBP at varied levels at ageing conditions on tribological performance and oil degradation. The effect of oil degradation on the physical properties of engine oil is discussed. Additive adsorption on CBP is investigated using experimental techniques including ICP and EDX. The study explores how degradation products and additive adsorption can influence wear. The surface analysis and chemical composition of tribofilm of reclaimed oil samples are discussed. This chapter aims to understand whether the reclaimed oil after removal of CBP from aged oil can perform as the fresh oil. Further investigations to understand the effect of ageing oil on the crystal structure and mechanical properties of CB particles are discussed using TEM, XRD and nanoindentation techniques.

5.1 Effect of CBP on oil degradation

5.1.1 CBP removal from oils

Fully formulated oil (AFTON) of passenger vehicles with a viscosity grade 10W-40 was used in this chapter. The physical and chemical properties of fresh oil are displayed in Table 4.1. A centrifuge process was used to remove the CBP from the aged oil samples for post analysis to identify the interactions between the CBP, additives and oil. The ageing method for the oil containing CBP was described in section 4.2.4. Oil samples were centrifuged at $12000\ \mathrm{rpm}$ and at $40\ ℃$ to remove the CBP from the oil. This process was repeated four times to ensure the removal of CBP as much as possible. FTIR determines the change in soot concentration in the engine oil at the region around 2000 cm^{-1} [94]. Figure 5.1a and b demonstrate the CBP concentration before and after centrifugation with various CBP percentages in the oil. After centrifugation as shown in Figure 5.1b, the results show that all FTIR spectra have no shift at the region around 2000 cm^{-1} similar to fresh FFO. This determines that almost all CBP were removed from oils by the centrifugation process explained above. It is worth noting that there is a limitation to the FTIR technique since this method does not detect a small amount of CBP

(less than 0.1 wt%) in the engine oil [94]. However, Berbezier et al.[224] investigated the effect of low levels of CB (<0.1 wt%) on the engine oil performance, the results showed that the CBP concentration lower than 0.1 wt% in oil does not influence the wear.

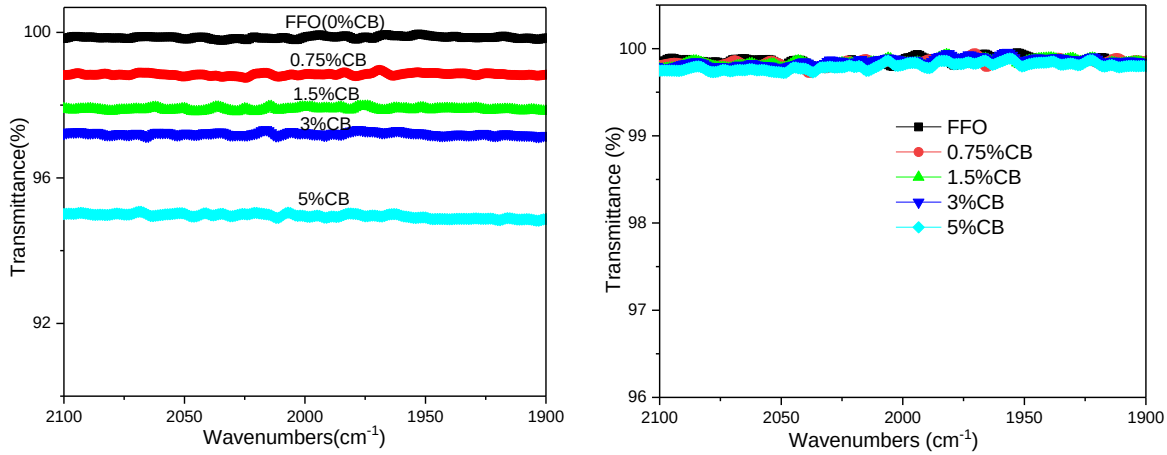

a) Before centrifugation **b) After centrifugation**

Figure 5.1: FTIR spectra of aged oil samples in the region around 2000 cm^{-1} to determine the CBP level before and after using the centrifuge compared to fresh oil (FFO) a) before centrifuge b) after centrifuge.

5.1.2 Chemical structure of the oil

The chemical structure of bulk oils was investigated using the FTIR technique. Figure 5.2 displays the overall FTIR spectra of aged oil samples containing CB before and after centrifugation. The existence of soot in engine oil causes a shift in overall FTIR spectra depending on the level of soot [94]. Figure 5.2 shows that FTIR spectra shifted down with an increase in the CBP levels in the aged oils as expected. FTIR spectra after removing CB shifted up and three influenced regions are explained in Figure 5.2. The $P-O-C$ band around 978 cm^{-1} corresponds to the antiwear additive (ZDDP) [225]–[227] as shown in Figure 5.3a. The oil samples after ageing have no peak at 978 cm^{-1} as can be seen in Figure 5.3a. This means that the antiwear additive could have either been depleted or decomposed during the ageing process. These results are in line with other studies [10], [96] showing that ageing the oil at high temperature causes decomposition or depletion of antiwear additive and as a result, the $P-O-C$ peak disappears in the FTIR at 978 cm^{-1} region. The $S-O$ and $S=O$ bands in FTIR spectra, as shown in Figure 5.3b, are identified in regions around 1150 and 1250 cm^{-1} respectively [75], [226] The $S-O$ and $S=O$ bands are referred to the formation of sulphate

by-products as an increase in FTIR intensity (shift down) in the presence of CBP in the oils. Oxidation of oils, the formation of carboxylic by-products, is indicated in the $C = O$ peak around 1720 cm^{-1} [225] as shown in Figure 5.3c. These results are in agreement with other studies that showed the formation of sulphate by-products [96] and oil oxidation [86] during the ageing process. In general, the intensity of FTIR spectres (shifting down) increases with increasing CBP levels in the oils. In the current study, the effect of CBP on degradation products during the ageing process has been observed, as seen in Figure 5.3b and c. The results confirm that the existence of CBP in the oil during the ageing process affects oil degradation and induces the formation of degradation products in the oil. There are complex chemical interactions between the additives themselves and the CBP in the existence of oxygen at high temperatures. CB surface chemistry contains chemical bonds such as carbon-oxygen and sulphur-oxygen bonds. As CB level increases in the oil, a higher density of carbon-oxygen and sulphur-oxygen bonds exist in the aged oil. This can cause higher chemical interactions between released chemical bonds from soot and the additives hence catalysing the formation of degradation products.

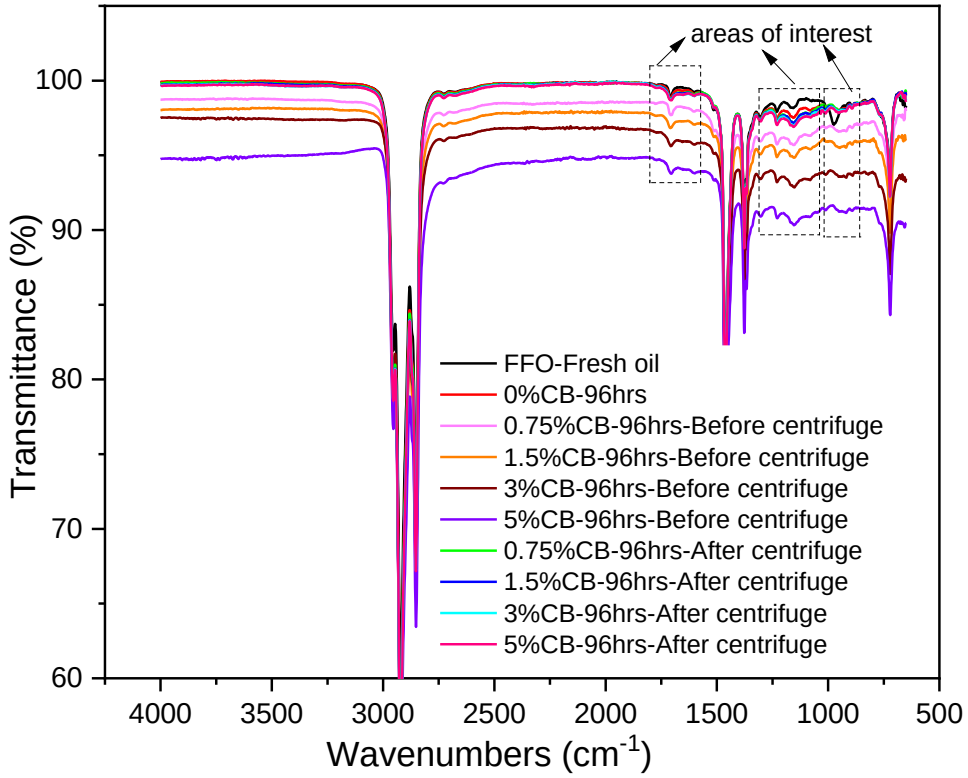

Figure 5.2: FTIR spectra for aged oil samples before and after removing CB.

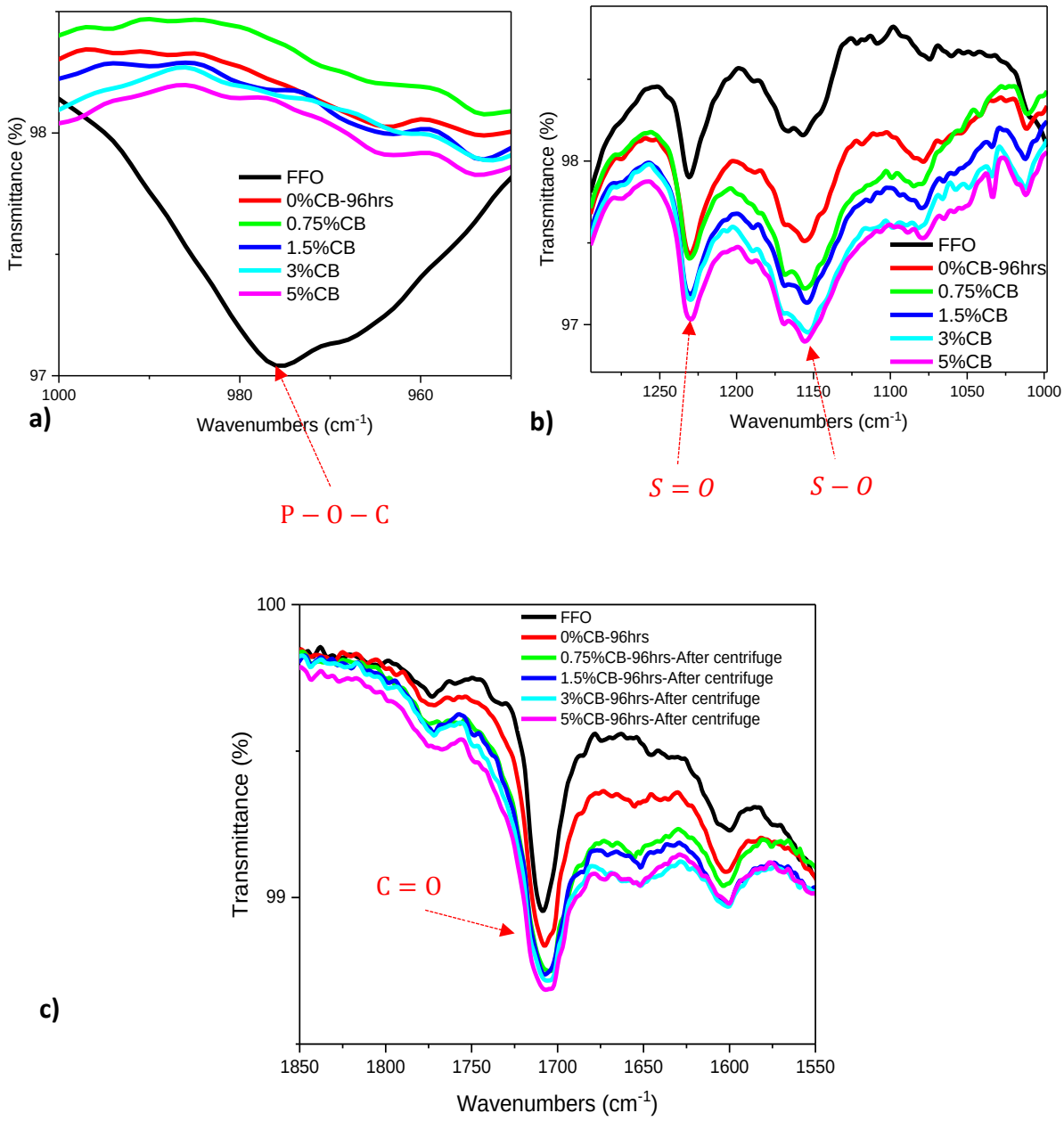

Figure 5.3: FTIR measurements of aged oils after removal of CBP at a) 978 cm^{-1} point represents the $P-O-C$ antiwear additive b) around 1150 and 1250 cm^{-1} points represent the $S-O$ and $S=O$ respectively c) around 1720 cm^{-1} point represents $C=O$ band.

5.1.3 Physical properties of oils

Viscosity is one of the most important physical properties which is used to identify signs of oil contamination and oil degradation [89]. Figure 5.4a displays the effect of the ageing process on the viscosity of the oils containing CBP. In both ageing and no-ageing conditions, the results show an increase in viscosity with increasing the level of CBP in the oils as expected

[25], [88]. These results are in line with other studies [25], [88] in terms of the effect of CB level on oil in viscosity. In general, the results show an increase in the viscosity after the oils are being aged compared to the fresh oil mixed with the same level of CBP. Since both oils (aged and non-aged) contain the same levels of CBP, this increase in viscosity is related to the ageing process and the formation of degradation products. To investigate the effect of degradation products on viscosity, CBP were removed from aged oil. Figure 5.4b displays the viscosity of oils at 40°C and 100°C after removal of CB from aged oils samples. The viscosity of oils samples decreases after removing the CBP as expected. However, these values are still higher than the viscosity of fresh oil. This is due to the formation of degradation products in oils. The results are in line with different studies that have confirmed the effect of degradation products [89], [228], [229] on the physical property of oils. The current study shows how oil degradation can influence the increase in viscosity even after soot removal as demonstrated in Figure 5.4b.

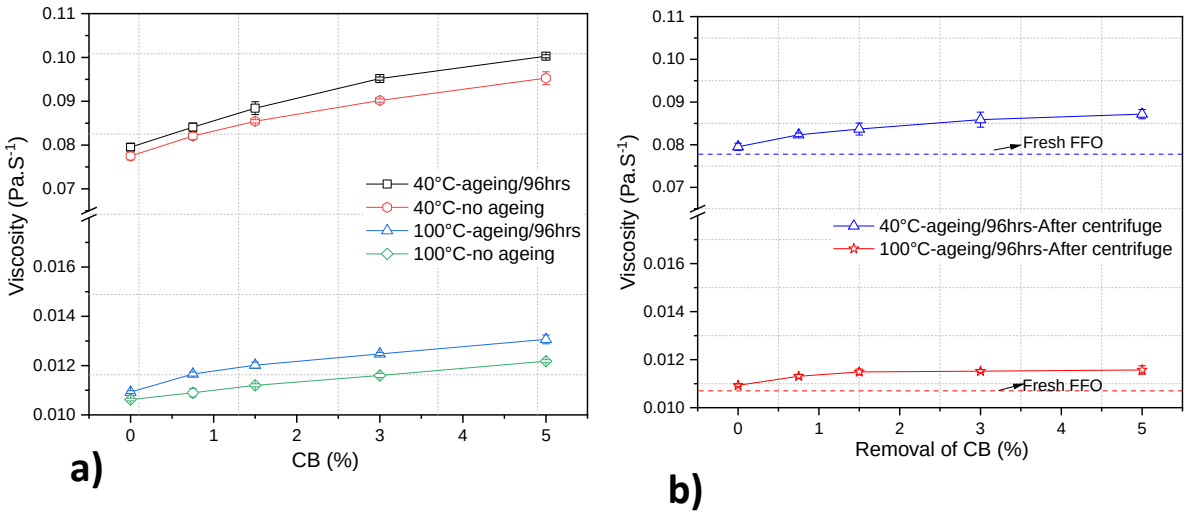

Figure 5.4: Viscosity of oils at 40 °C and 100 °C a) with increasing the CBP levels after ageing the oil for 96 hrs compared to non-aged oil samples containing the same level of CB b) after removing the CB from aged oil samples.

5.1.4 Additives adsorption on CBP

FTIR results showed the antiwear decomposition or depletion in oils with no CBP and oils containing CBP as explained in Figure 5.3a. It is not possible to detect the changes in additive concentration of oils using the FTIR technique. Therefore, ICP analysis was conducted on oil

samples to determine the additive concentration after centrifugation. ICP results in Figure 5.5 indicate the change in the concentration of S, P and Zn elements in aged oils and after removing different levels of CBP from the aged oils. The reduction in additives concentration in engine oils classifies into two types: additive depletion [157] when there is no CBP in oil and additive adsorption [10] when the CBP exists in oils. The S, P and Zn elements come from antiwear additives, for instance, Zinc dialkyldithiophosphates (ZDDP) and Zinc dithiophosphate (ZDP), while the S and P elements could also come from dispersant/or detergent compounds such as sulfonates and phosphonates [50].

The concentration of S decreased significantly in aged oil with no CB due to additive depletion as shown in Figure 5.5. ICP analysis was conducted on the aged oils containing various levels of CB after centrifugation. The results confirm the phenomenon of additive adsorption on CBP. Moreover, the results show a lower concentration of S, P and Zn in the oils containing higher levels of CB. This is due to the higher active surface area with higher CB levels in the oil leading to more additive adsorption on CB particles. This is in agreement with the function of dispersant/detergent additives with polar groups to attract the organic contaminants which are expected to be removed by CBP [47].

Additive adsorption on CBP was previously studied by Motamen Salehi et al. [10] at the same conditions. However, they used the base oil+1 wt% ZDDP to investigate the additive adsorption on CBP, instead of FFO. The results showed full adsorption of ZDDP compound on 5 wt% CB after ageing the oil [10]. In the current study, however, lower levels of additives adsorption on CBP is observed in FFO compared to the base oil and ZDDP. This is due to interactions between the additives in the presence of antiwear, dispersant and detergent, which may reduce the antiwear additive adsorption on CBP. The decomposition of additive (as shown in Figure 5.3a) could also be another factor that affects the additive adsorption on CBP.

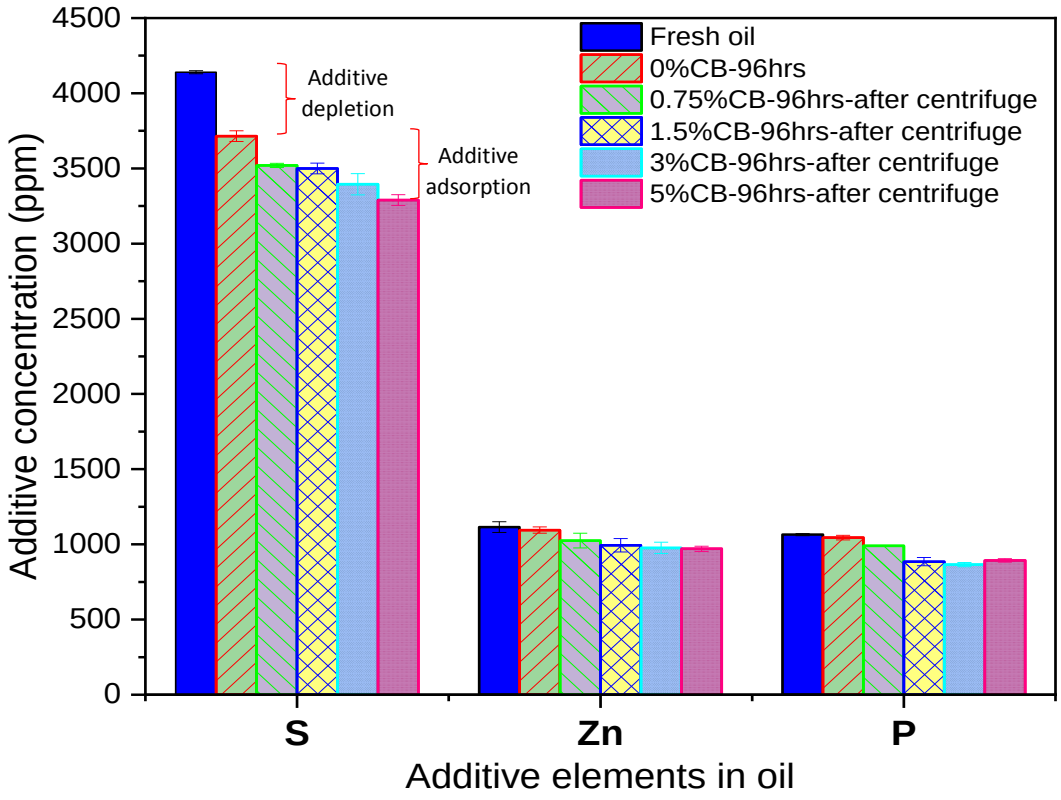

Figure 5.5: ICP results of oils after removing CBP.

Figure 5.6 shows Energy Dispersive X-ray (EDX) results on CBP extracted from the aged oil to confirm the existence of additive adsorption on CBP. The extracted CBP from oil containing 5wt% by centrifugation indicated the presence of constituents of an antiwear additive such as Zn, P and S due to adsorption of these elements on CBP. The results are in line with other studies showing the existence of engine oil additive elements on the soot particles using EDX [10], [157], [162].

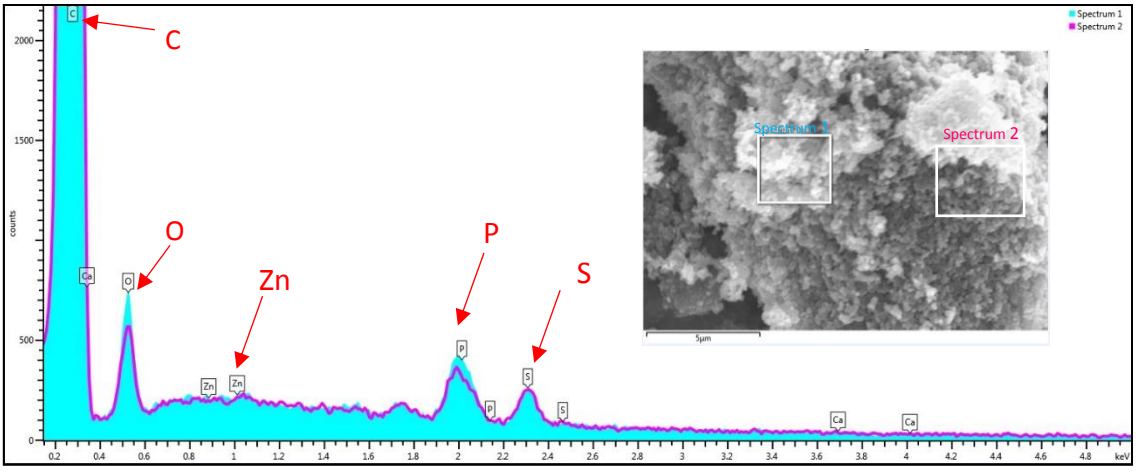

Figure 5.6: EDX chemical analysis of extracted CBP from aged oil containing 5 %wt CBP after 96 hrs ageing.

5.1.5 CBP effect on tribological performance

The effect of CBP on friction coefficient was determined over two hours of tribological tests as shown in Figure 5.7. It can be observed that the friction coefficient decreases gradually with rubbing time in the samples containing CB. For oils containing 1.5, 3 and 5 wt% CBP, the friction coefficient was high (higher than fresh oil) at the beginning of the tests and then gradually decreased over time. The length of the high friction period was increased with increasing CBP level in the oil. This can be explained by the small contact area between pin and plate (as shown in Figure 5.7) and high levels of CB which causes oil starvation at the beginning of the test. Over time, this contact area increases in size and becomes a larger flat area due to high wear. In this case, there is a possibility of moving towards a mixed lubrication regime that explains the lower coefficient of friction observed in tests with high levels of CB.

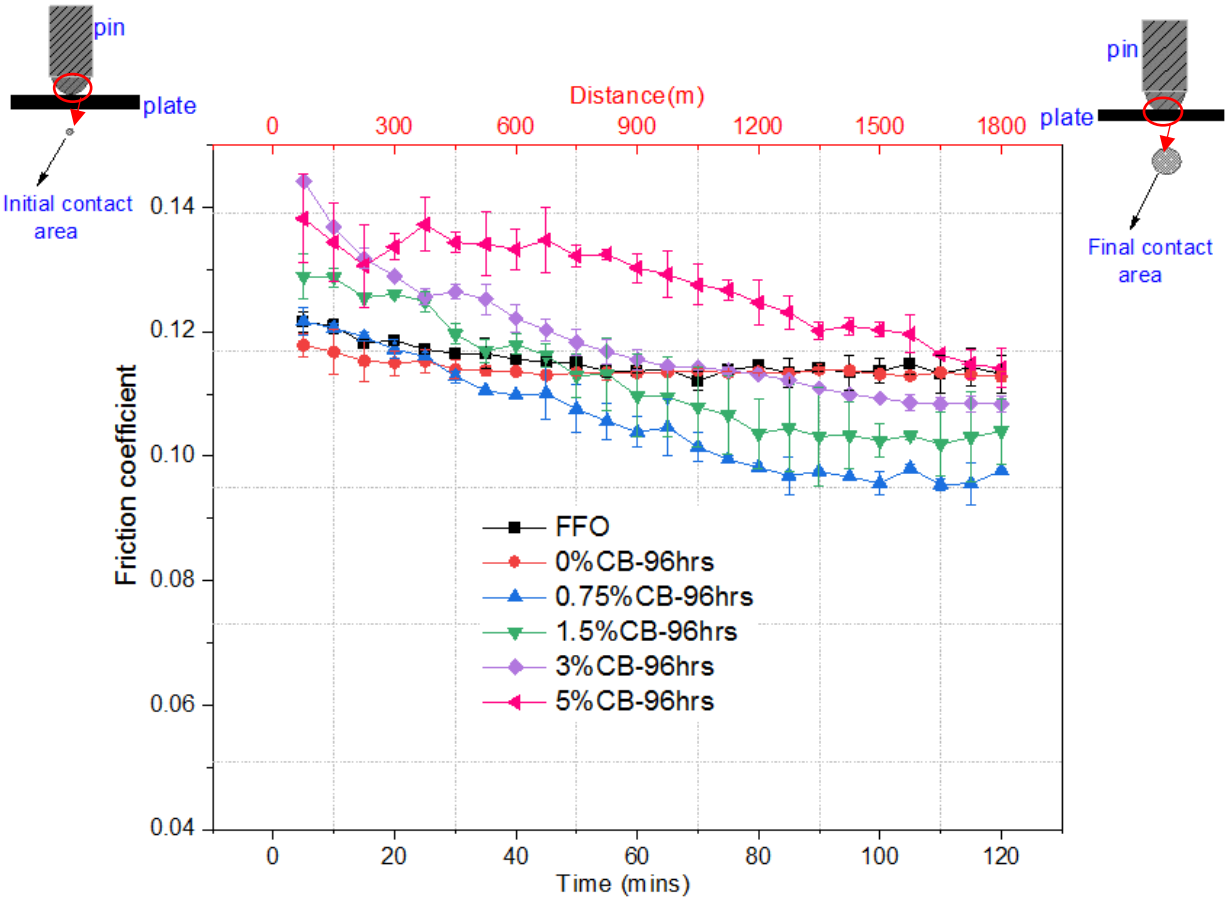

Figure 5.7: Friction coefficient of aged oils containing CBP (before centrifugation) over 2 hrs period of the test with schematic images of the contact area.

The increase in friction coefficient at the initial period and decrease over time due to starvation has also been observed in previous studies [77], [78]. While the results show that CB at level 0.75 % act as a friction modifier [75], [230] and reduces the friction coefficient between the contact surfaces over time. CBP at low concentration has less ability to form a large agglomeration and does not affect oil starvation. This is due to the dispersant's ability to disperse the particles at a low CB level preventing the coalescence into large agglomeration [91].

The effect of CBP on wear before centrifugation was investigated as shown in Figure 5.8. Wear increases with increasing the CBP level as expected. This is because more CBP and large clusters of particles exist in the oils. The increase in wear by increasing CB levels in the oil is in agreement with other studies [73], [84] as the higher level of CBP forms large clusters leading to starvation. There is also another factor of increasing wear with higher CBP as the dispersant becomes less effective to disperse the particles preventing them from approaching and coalescing into large agglomerates [91].

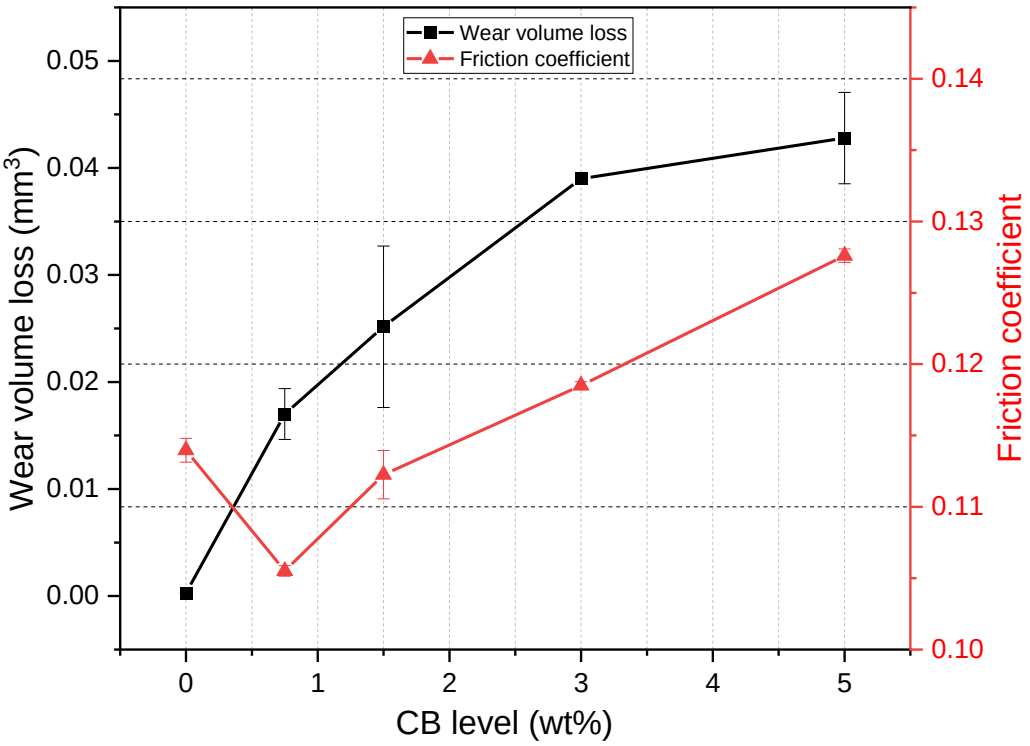

Figure 5.8: Wear volume loss with different levels of CBP correlated to the mean of the coefficient of friction over the whole test of each sample. The standard deviation method of error bars for two repeated tests was applied.

The correlation between wear and friction, as illustrated in Figure 5.8 depends on the CB level in the oils. With a low CB level, the particles act as a friction modifier producing low friction during the test in contradiction with wear. However, as the CB level increased causing starvation, both wear and the average friction coefficient over the whole test increased as shown in Figure 5.8.

5.1.6 Effect of oil degradation on wear

5.1.6.1 CBP effect at different ageing conditions

The effect of ageing the oils containing CBP on wear was investigated as shown in Figure 5.9. The ageing oil process for 96hrs was explained in detail according to ASTM D4636-99 [194] as illustrated in the 4.2.1 section. At 0 hrs ageing condition, CBP was mixed for 2 hrs, the temperature of 60 °C and stirring speed of 500 rpm before tribological tests to disperse CBP homogeneously in oils. The results compare the wear with varied levels of CBP before and after ageing the oils for 96 hrs. In both states, wear increases with increasing the CBP level as expected, since more CBP and large clusters of particles exist in the oils. There is also another factor of increasing wear with higher CBP as the dispersant becomes less effective to disperse the particles preventing them from approaching and coalescing into large agglomerates [91]. Wear of aged oils demonstrates higher values of wear compared to oils containing a similar level of CBP without ageing. This could be due to oils degradation and additive depletion discussed in Figure 5.3 resulting in changes in the physical properties of aged oils as shown in Figure 5.4. Changing the mechanical properties of CB particles after ageing causes an increase in wear is one of the proposed factors which will be investigated in this chapter. Bhowmick et al. [109] suggested that changing mechanical properties of soot particles due to interactions between additives and soot causes an increase in wear. In this study, measuring the mechanical properties of fresh CBP and aged CBP using nano-indentation will be discussed in the 5.2.2 section.

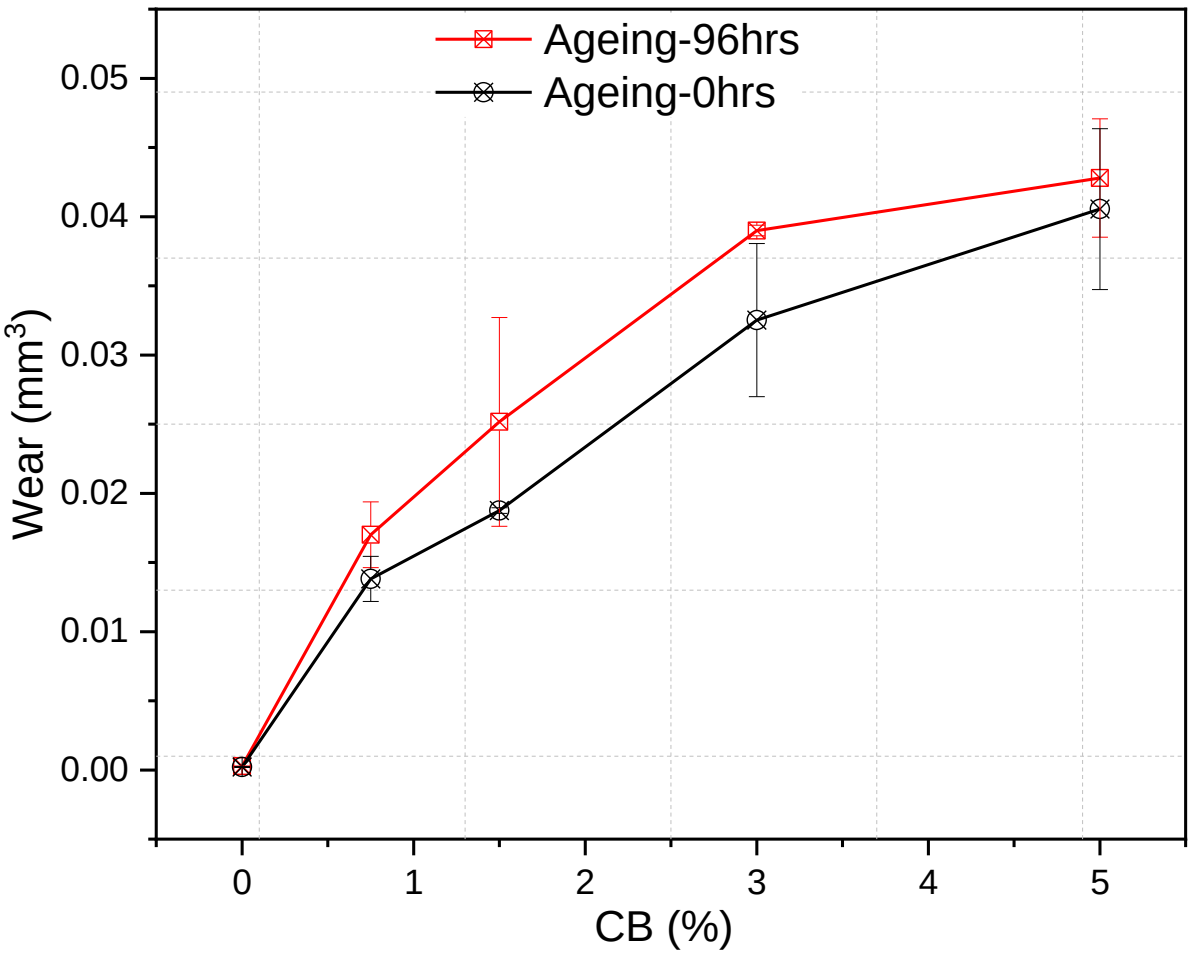

Figure 5.9: Wear volume loss with different levels of CBP at two different ageing conditions.

5.1.6.2 Oil reclamation effect on wear

Removing CBP from oils has a significant effect on decreasing the wear compared to the oil-containing CBP as shown in Figure 5.10. The increase in wear after CBP removal compared to fresh oil could potentially be due to three main mechanisms. Firstly, the increase in the additive adsorption such as Zn, P and S on CBP (as shown in Figure 5.5) leads to a reduction in antiwear additive. Secondly, the formation of sulphate by-products is due to the interactions between CBP and additives during the ageing process. Thirdly, oil oxidation (carboxylic by-products). The results show that the engine oil after removing CBP does not perform as good as the fresh oil. This is due to oil degradation and additive adsorption. However, a significant improvement in wear is expected after CBP removal as shown in Figure 5.10.

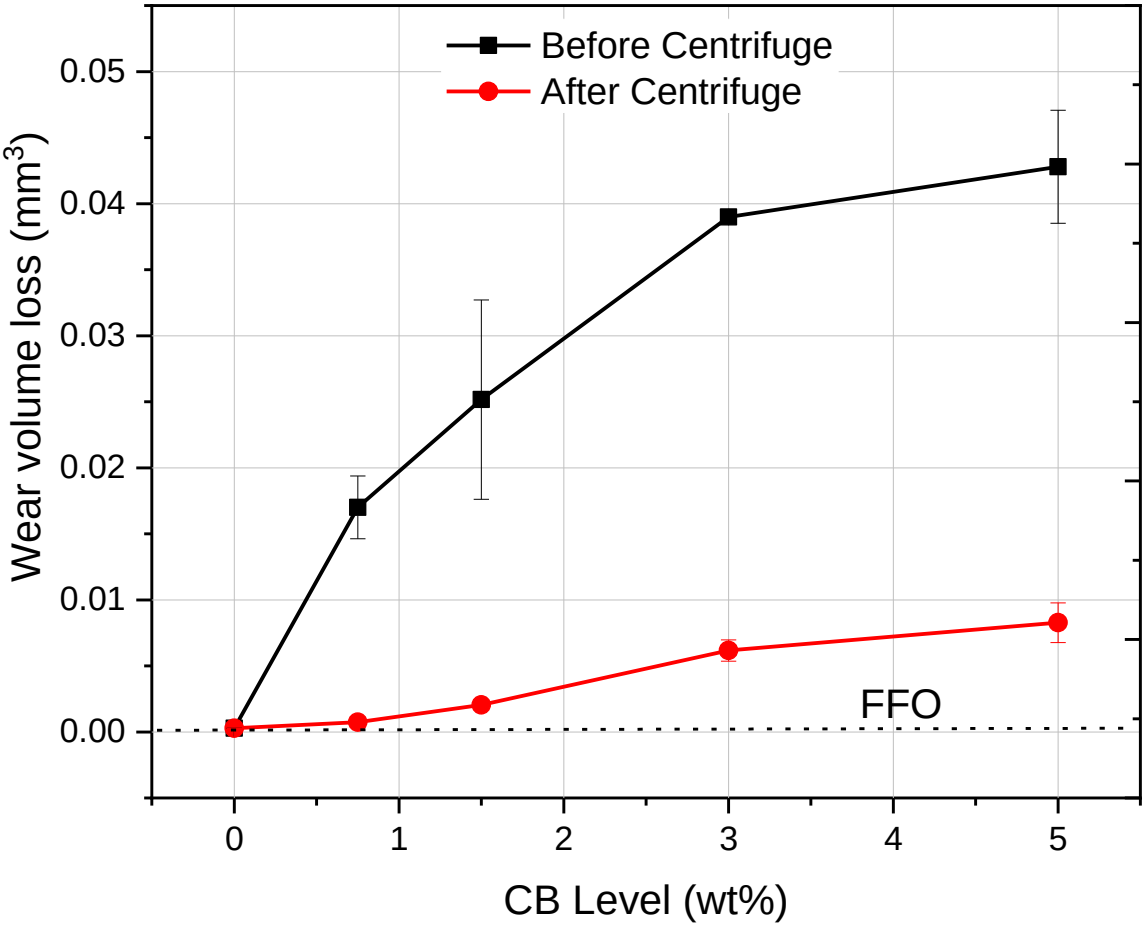

Figure 5.10: Wear with different levels of CBP in aged oil before and after centrifuge.

5.1.7 Surface characterisation

Figure 5.11 shows microscopic images of wear scars on pins for oils containing CBP and after CBP removal. The arrow on the image refers to the sliding direction of the pin-on-plate. The wear scar of fresh FFO shows no abrasive wear with full coverage of tribofilm is observed on the surface as shown in Figure 5.11a. Oil samples containing CBP demonstrate the sign of abrasive wear on the surface and more CB particles producing higher wear as expected. The wear scars showed a constant increase in the width of grooves with a higher concentration of CBP as shown in Figure 5.11b, c, d, and e in comparison to fresh oil in Figure 5.11a. This can be attributed to higher CBP concentration in oils producing more and larger CB agglomerates causing the plastic deformation by these particles. These results are in line with other studies

[75], [231]–[233] showing the effect of soot particles on the contact surfaces causing abrasive wear.

Figure 5.11a_1 demonstrates abrasive wear on wear scar after ageing the oil with no CB due to additive depletion. The wear scars are significantly smaller after removing CBP (Figure 5.11b_1, c_1, d_1 and e_1) compared to the oils samples before removing CBP as shown in Figure 5.11b, c, d, and e. It is worth noting that there are still signs of abrasive wear on the wear scars after removal of CBP, this is due to additives adsorption on CBP and oil degradation during the ageing process.

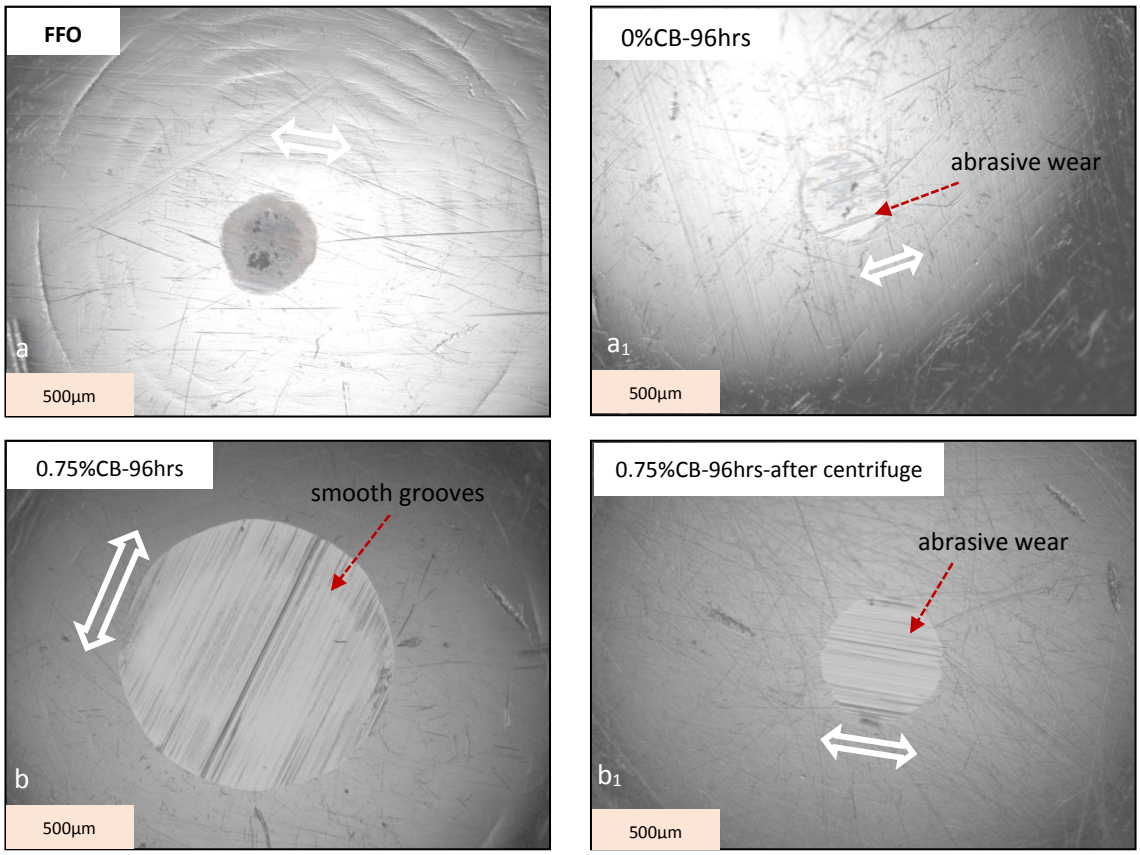

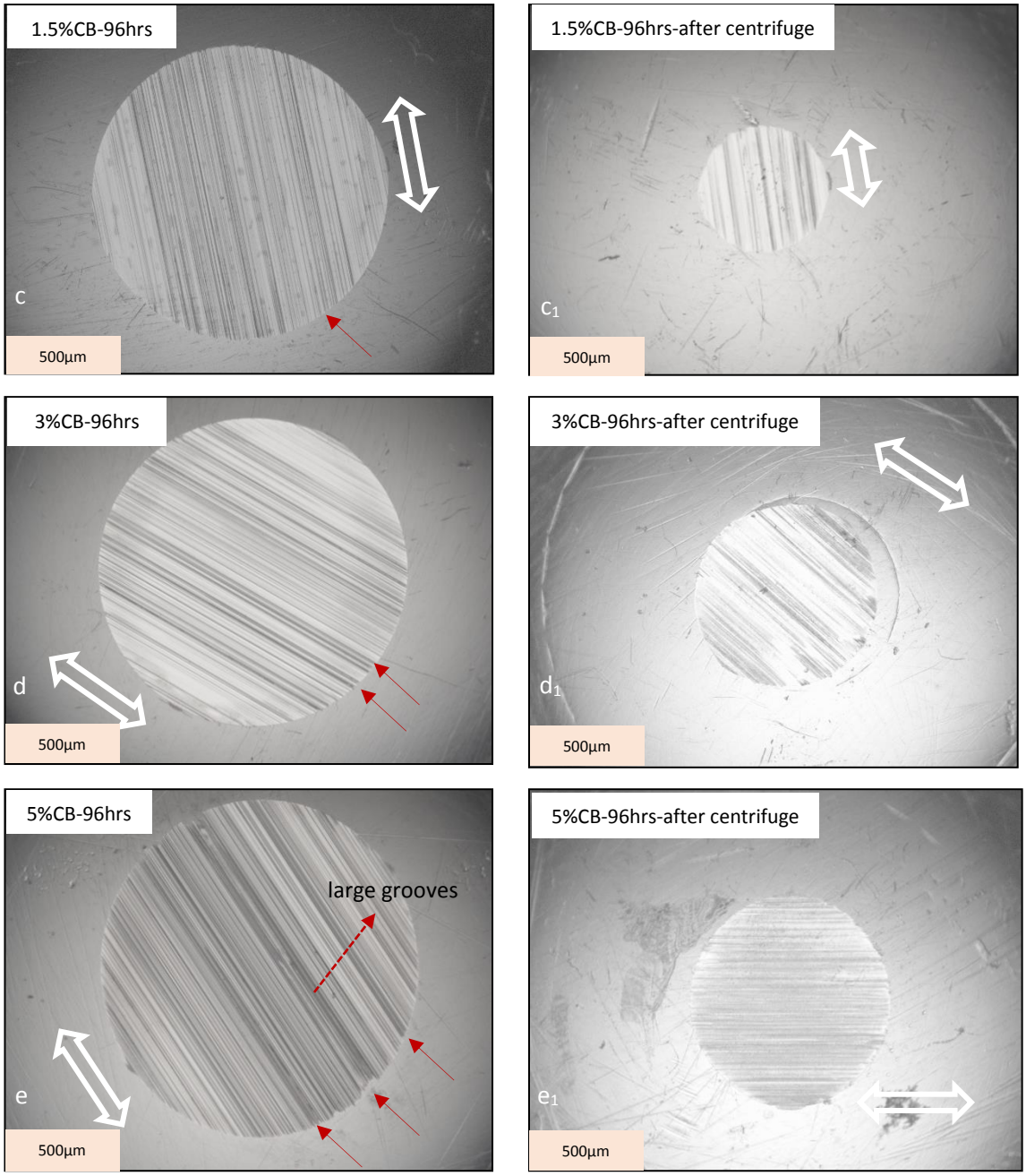

Figure 5.11: Microscope images show wear scars on pins of oils containing CBP before and after centrifuge, arrows indicate sliding direction.

Several studies [75], [231]–[233] showed the presence of CB or soot particles influences the contact surfaces causing abrasive wear. SEM images at high magnification as shown in Figure 5.12a and b confirm that abrasive wear occurs also after ageing the oil with no CBP and for aged oil containing 0.75 %CB after centrifuge. The chemical and physical changes in oils due

to additive depletion and oil degradation can affect the contact surfaces and cause hard abrasive wear on surfaces.

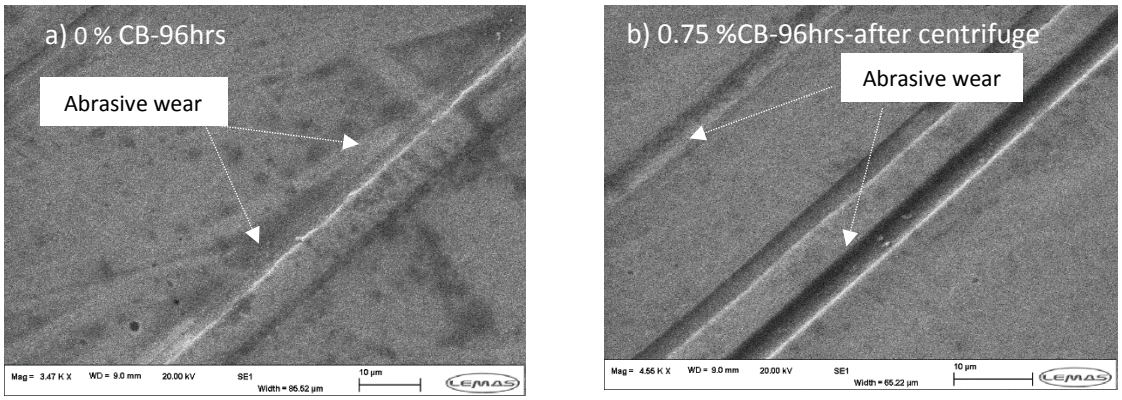

Figure 5.12: SEM images with high magnification a) abrasive wear of the oil after ageing with no CBP b) abrasive wear of aged oil containing 0.75 %CB after centrifuge.

5.1.8 Chemical composition of tribofilm

Scanning Electron Microscope SEM/EDX was conducted on pin samples to verify the observation from wear results and optical microscope images. It is believed that when CBP exists in the oil, the tribofilm is removed by CB particles causing abrasive wear [22]. Figure 5.13 demonstrates the change in the chemical composition of tribofilm inside the wear scar. In this current study, EDX analysis was conducted to assess if the additive depletion during oil ageing, additive adsorption on CBP and oil degradation can affect the chemical composition of tribofilm. Figure 5.13a_1 of the fresh oil sample shows the presence of antiwear additive elements (Zn, P and S) on the tribofilm which are originated from ZDDP. The effect of ageing oil with no CBP on tribofilm chemistry is demonstrated in Figure 5.13a_2, the result shows a significant reduction in P and S atomic concentration with the absence of Zn in tribofilm. This correlated to additive depletion and oil degradation during the ageing process at high temperatures. The result from the aged oil with 0.75 wt%CBP after centrifugation in Figure 5.13a_3 indicates the absence of all elements of tribofilm. This result confirms that both additive adsorption on CB particles and oil degradation reduce the ability of the lubricant to protect the contact surfaces.

Elements/Wt%	EDX

a1

Element	Wt.%
Fe	71.38
O	5.83
Si	4.29
P	3.04
S	3.85
Ca	2.52
Cr	5.01
Zn	4.08
Total	100

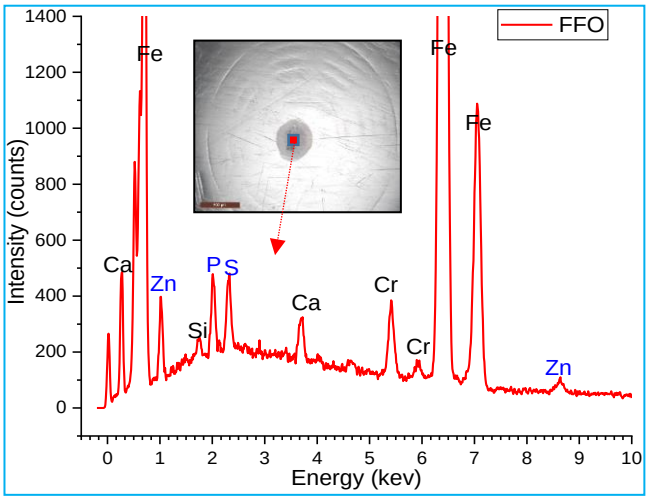

a2

Element	Wt.%
Fe	89.84
O	3.81
Si	0.94
P	1.03
S	0.85
Ca	1.52
Cr	2.01
Zn	0
Total	100

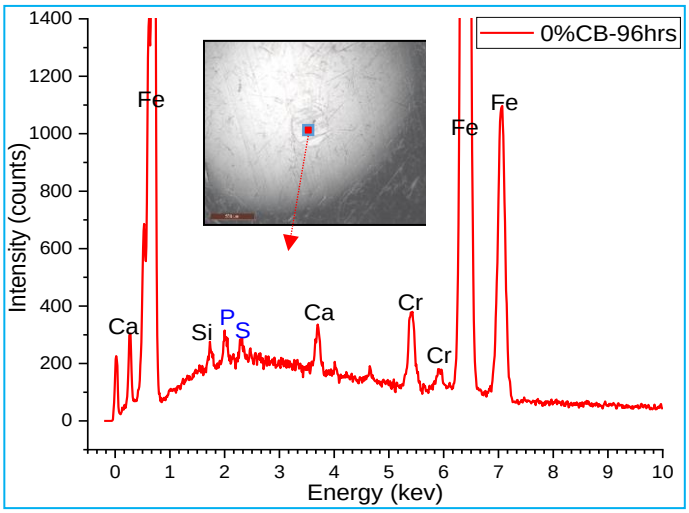

a3

Element	Wt.%
Fe	93.55
O	2.61
Si	0.71
P	0
S	0.02
Ca	2.52
Cr	0.59
Zn	0
Total	100

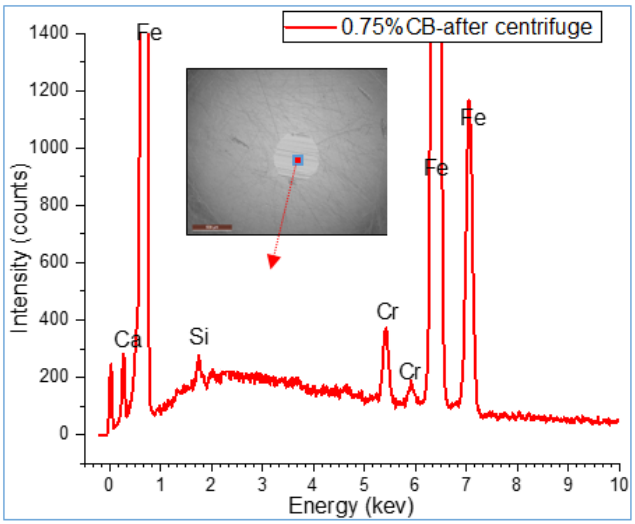

Figure 5.13: SEM/EDX to identify the chemical composition of tribofilm of wear scar on pins a_1) fresh oil, a_2) aged oil for 0 wt% CB-96hrs, a_3) aged oil containing 0.75 wt% CB-after centrifuge.

5.2 Effect of ageing the oil on CBP

5.2.1 Physical characterisation of CBP and soot

5.2.1.1 TEM crystal structure

Soot particles are related materials and usually obtained from the incomplete combustion of hydrocarbons [219]. CB particles, used in this study to simulate the real soot, are simply produced from a fine-grained form of crystalline graphite [219]. In this study, the TEM technique was used to investigate the crystal structure of fresh CB, aged CB and soot particles. Aged CB and soot particles were extracted from aged oil and used oil respectively by centrifugation. Used oil details are displayed in Table 5.1. The particles were washed with heptane using an ultrasound bath for 15 mins to remove the contaminated oil. The particles were dried overnight at 100 °C in the oven. The primary of CBP agglomerate in clusters of particles as shown in Figure 5.14a, b, c and d. The crystal structure of primary CB particles (fresh and aged) consists of inner core and outer shell. The inner core and the outer shell can be observed in Figure 5.14 a, b, c and d. The shell thickness is ≤7 nm. CB shell displays groups of graphite planes arranged concentrically around the core in parallel. The internal structure of CB particles reveals turbostratic domains with unordered graphite layers.

TEM images of aged CB particles show the formation of the layer with a thickness of ≤3 nm as displayed in Figure 5.14c, d. This layer resulted from the oxidation of CB surface or/and ageing impurities. A similar layer was found around the outer soot shell in previous studies [234], [235]. Some studies [234], [236] reported that large particles with a higher degree of crystalline can block O_2 diffusion through their outer shell. They proposed that O_2 diffusion is only possible for small particles since O_2 atoms react with edge-site atoms of shell particles. The passivated shell does not allow O_2 to access and diffuse through the reactive amorphous core [234]. This causes the formation of an oxidation layer on the outer shell of CB or soot.

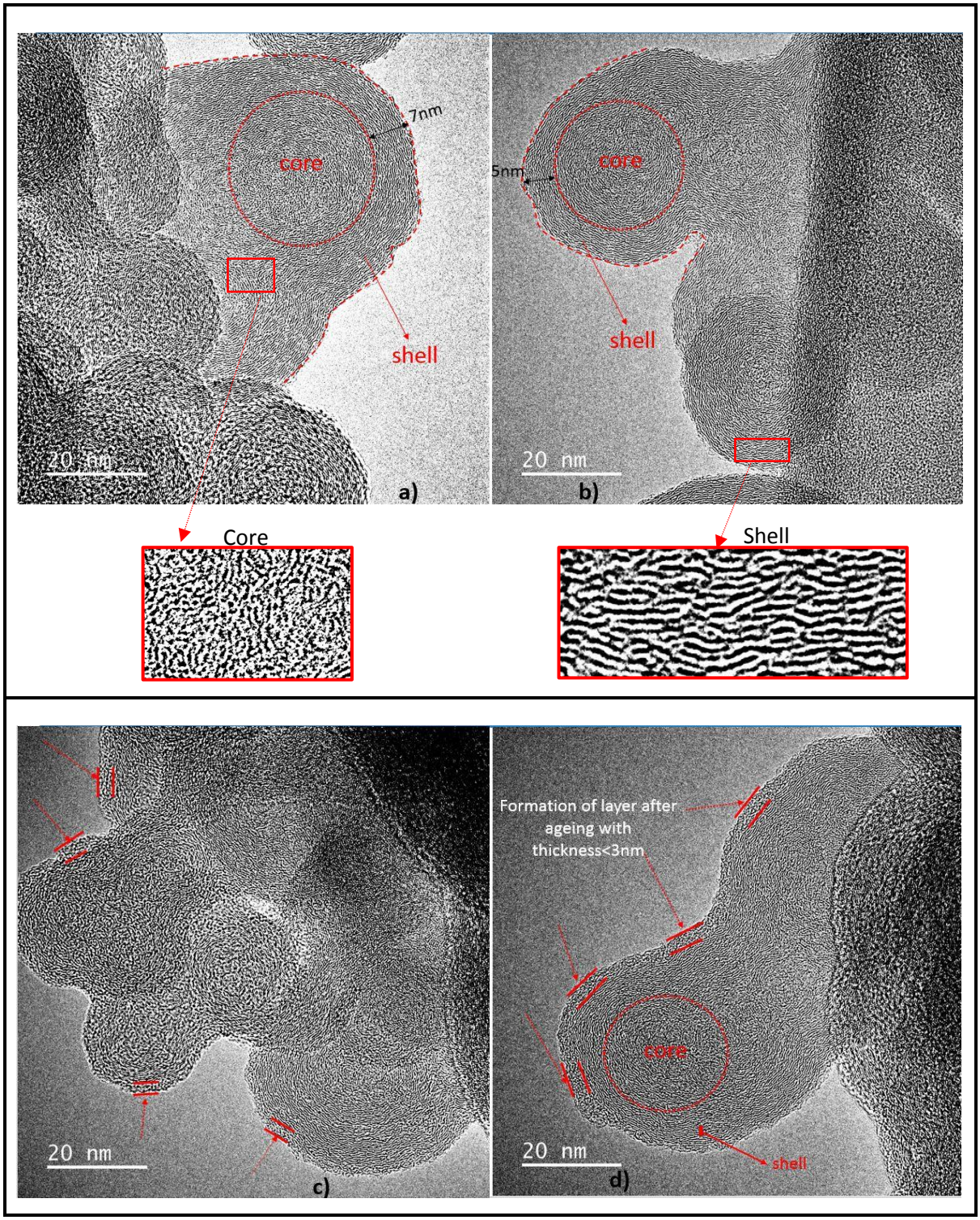

Figure 5.14: TEM images of a), b) fresh CB primary particles and c), d) aged CB primary particles.

Figure 5.15a and b indicate that the crystal structure of soot consists of core and shell. CB and soot particles show to have the same crystal structure. Shell thickness of soot particles varies and reaches up to 10 nm in some particles as shown in Figure 5.15e. Soot particles display an unordered structure layer surrounding the shell with a thickness of less than 2 nm.

This outer layer is similar to the layer found after ageing CBP in the oil as displayed in Figure 5.14c and b. This is in line with several studies [234]–[236] that reported as this type of layer resulted from soot oxidation. This layer consists of an unordered structure (amorphous) opposite to the structure of the particle shell. The layer surrounding the soot shell could also contain impurities or crystalline species. Post analysis using XRD in the next section will determine the crystalline species in soot particles.

Table 5.1: Soot extracted from the used oil that drained from a truck engine.

Truck used oil	Fill (7.12.18)	Drain (22.5.19)
YK16 XSB	334470	383110

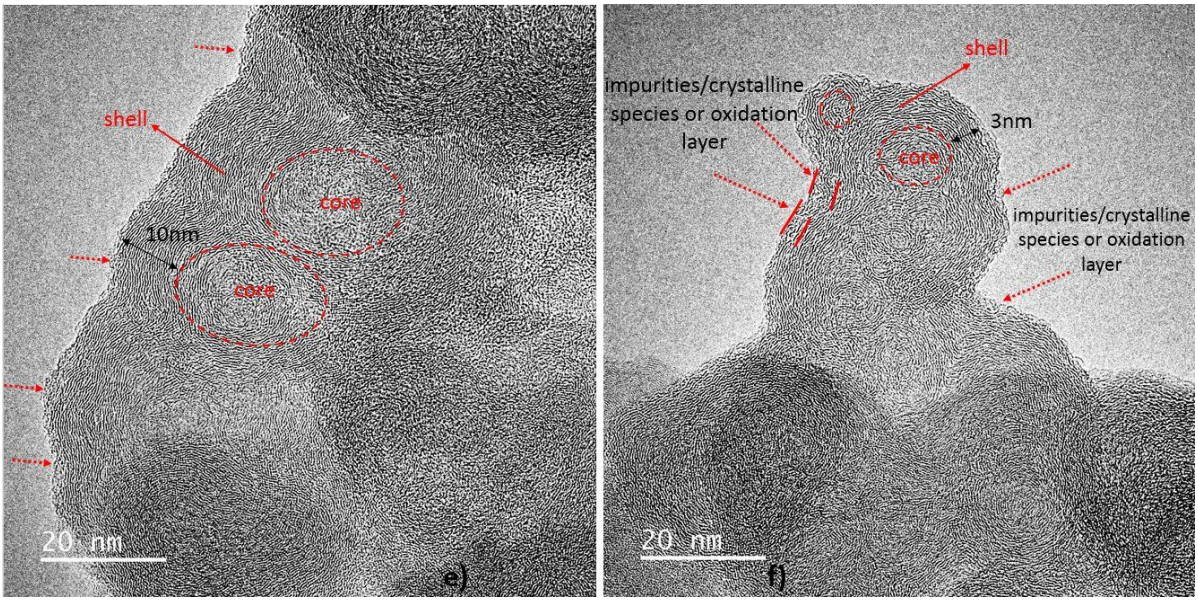

Figure 5.15: TEM images (e, f) of the primary soot particles.

5.2.1.2 Effect of ageing oil on CBP

XRD technique in this study was employed to identify the internal structure of CB, the crystalline organization of carbon inside the material, and the effect of the ageing process on the internal structure of CB. TEM results, as displayed in Figure 5.14 and Figure 5.15, focused on a tiny part of materials due to the extremely high magnification applied. To get a clear

picture of bulk materials, which are usually combinations of many crystallites, particles and other nano-objects. Therefore, the XRD technique is used to guarantee this analysis. The obtained data about the atomic structure are averaged over the whole sample volume under probe [219]. In this study, both fresh CB and aged CB particles were investigated using XRD. XRD information was recorded for the entire scan range of 10-90°θ as shown in Figure 5.16a and b.

Miller indices are used to describe certain crystallographic directions and planes in a material [101]. XRD data of CB consists of only (00l) and (hk0) graphite reflections. The peaks at (00l) are related to the inter-layer correlation and peaks at (hk0) are related to the in-plane correlations [219]. The position of the (002) peak in XRD of the CB is often referred to as $d_{(002)}$ which is the distance between graphite layers [219]. The peaks positions at ~25° and 43°, the diffraction patterns are composed of two board peaks, are indexed as the (002) and (100) graphite-type reflections respectively [19], [219]. These two peaks at 2θ positions ~25° and 43° are arising from turbostratic carbon structure [19], [219]. XRD results show broad humped peaks and none of them sharp peaks as shown in Figure 5.16a and b, which refer to turbostratic carbon structure for both fresh and aged CB particles [19], [219]. TEM images, as displayed in Figure 5.14a,b,c and d, confirmed the turbostratic structure of CB (fresh and aged).

XRD results of CB after ageing as shown in Figure 5.16b displays a change in peak width (dispersive shoulder peak ranging from 15° to 21.5°). XRD data of aged CB is similar to the study that showed defects of atomic of CB in this orientation [237]. Zhang et al. [237] showed that the crystal structure of CB was changed and the crystal degree of CB was enhanced at the higher temperature. In this study, CB was aged at a high temperature in the presence of additives and oxygen, which could also influence the CB structure. Jurkiewicz et al. [219] showed that the $d_{(002)}$, the distance between graphite layers, of heated CB increases with an increase in temperature. XRD data of the oxidation of graphite in oils at the same 2θ orientation was investigated by Gupta et al. [238]. The shoulder at 2θ of 15° to 21.5° in graphite oxide

results [238] is similar to aged CB data. This correlated to the intercalation of oxygen groups or water molecules that existed in the oil causing increase in interlayer spacing. In this study, TEM results confirmed the CB oxidation after the ageing process. Both TEM and XRD results show the change of CB crystal structure after ageing in the oil due to oxidation.

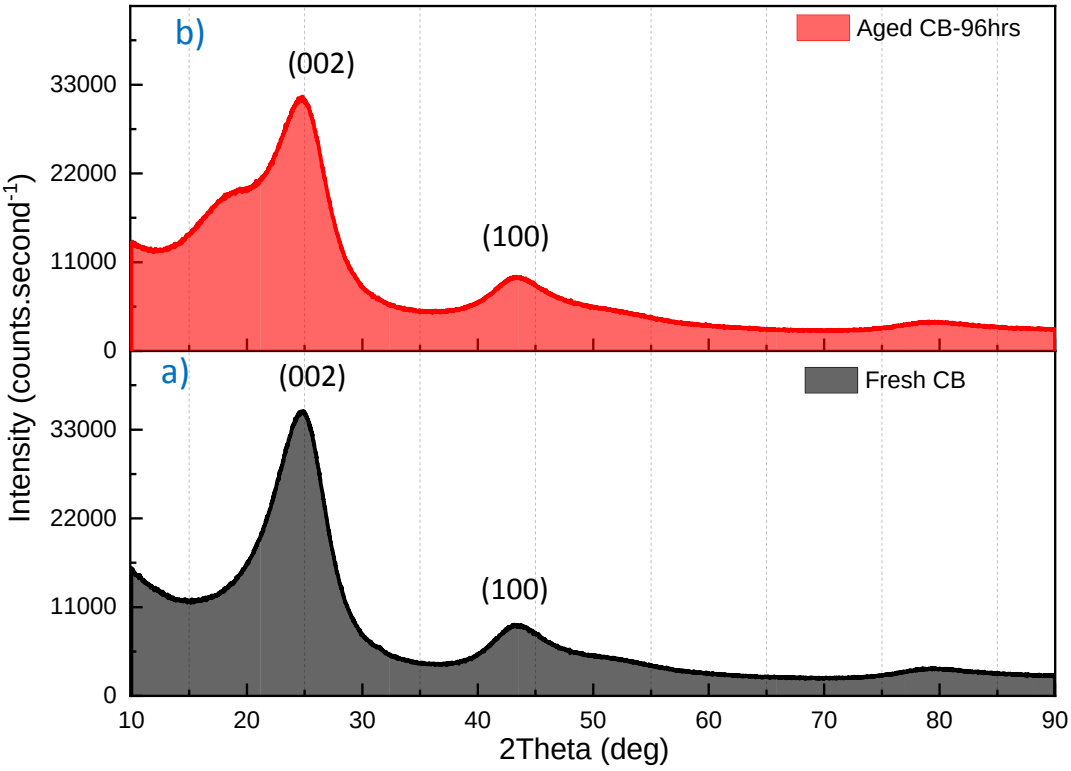

Figure 5.16: XRD results to demonstrate the crystal structure of aged CB (b) compared to fresh CB (a).

5.2.1.3 Crystal structure of CBP and soot

Figure 5.17 reveals the crystal structure of soot extracted from truck used oil compared to fresh CBP and aged CBP. Similar to fresh and aged CBP analysis, two main peaks at 2θ positions ~25° and 43° are observed in the soot spectrum as shown in Figure 5.17c. Soot spectrum at ~25° and 43° reveals turbostratic carbonaceous structure [101], [239]. The small sharp peaks (A,B,C,D) represent various crystalline species or impurities such as (calcium-based compounds) [101], [239]. These peaks (A,B,C and D) indicate that various crystalline species were embedded into turbostratic carbonaceous soot. Similar to XRD spectra of soot analysis was investigated by Sharma et al. [101], [239]. XRD data of soot showed also a dispersive shoulder peak ranging from ~15° to 21.5° which is approximately similar to the

aged CB spectrum as displayed in Figure 5.17b and c. Dispersive shoulder peak reveals the oxidation of soot particles and increase in interlayer spacing [238]. The results are in line with TEM images (Figure 5.15) that confirmed the presence of a thin layer surrounding the soot particles and aged CBP.

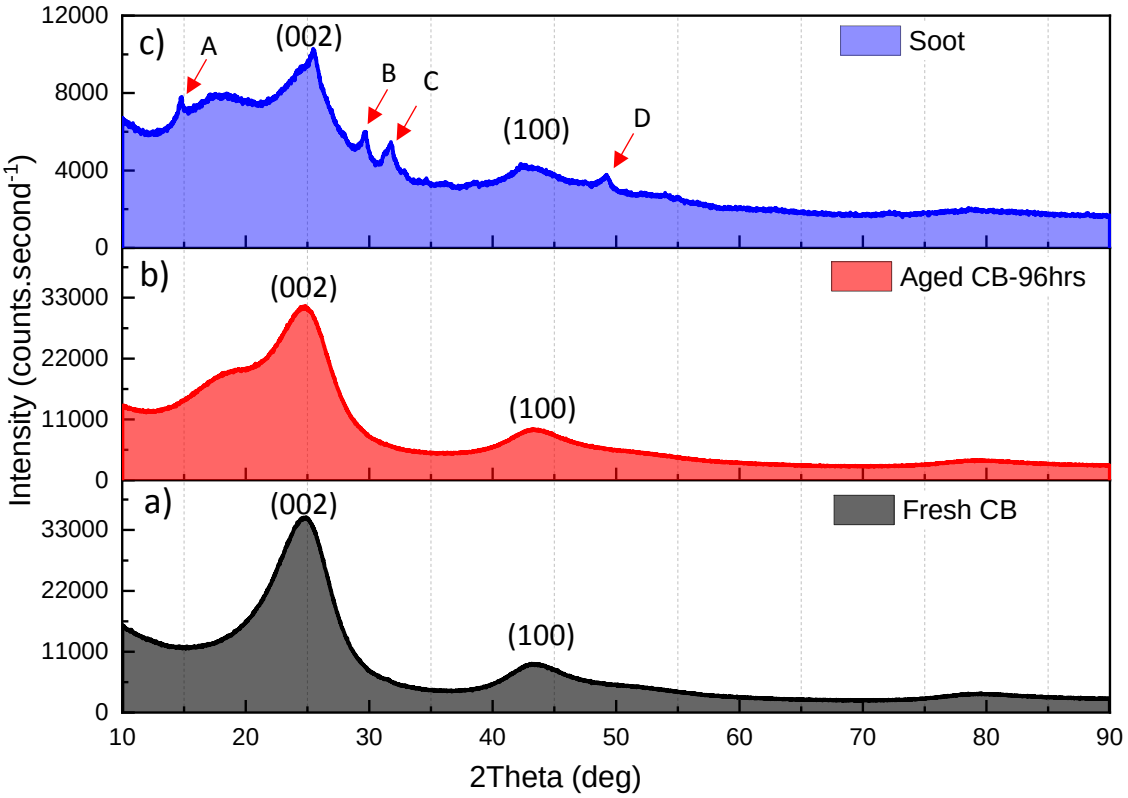

Figure 5.17: XRD results of the crystal structure of fresh CB (a), aged CB-96hrs (b) and soot (c).

5.2.2 In-situ nanoindentation of CBP

5.2.2.1 Nano-compression of fresh CBP

In-situ nanoindentation experiments of fresh CB were performed at different particle sizes (130-140 nm) and (200-240 nm). The deformation of CB particles was investigated to understand the effect of CB hardness on abrasive wear of contact surfaces. It is important to understand the correlation between the soot mechanical properties and the wear mechanisms. In this study, 100 nm displacement was used for nano-compression tests at a loading rate of 10 nm/s. The corresponding load-displacement curve recorded during the compression experiment is reported in Figure 5.18. Figure 5.18 shows the recorded load-

deformation after compressing (200-240 nm) CB particle. The results display a crack in the particle after approximately 70 nm compressing displacement corresponded to 100 µN of recorded load. It is worth noting that the increase in the load after breaking the CBP is correlated to continue indention in the deformed particle and Si substrate. Afterwards, when the CBP was unloaded, the particle was deformed and stuck on the tip. The CB particle under compression undergoes elastic-plastic deformation. In this study, it was difficult to calculate the hardness of the particles due to the unknown of the contact area after compression. As the applied/deformation load is the main factor that affects the hardness [240]. Thus, the judgment of the change in hardness in this study was linked to the change in the deformation load.

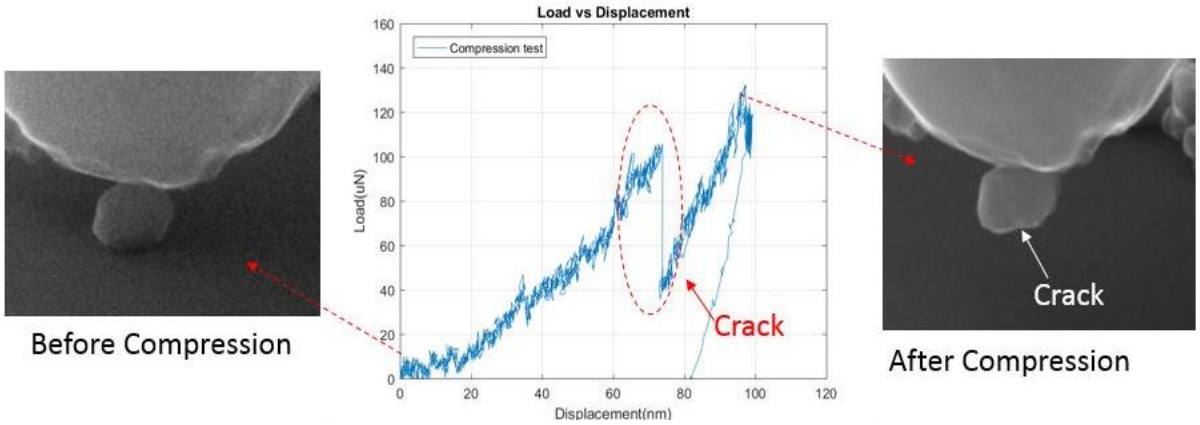

Figure 5.18: Nano-compression test of fresh CB particle at size 200-240 nm, particle deformation under the diamond tip was captured from a video recording during the compression experiment.

In-situ nano-compression test of CB particle was carried out to measure the deformation force of CB at smaller particle size (130-140 nm). The corresponding load-displacement curve shows the deformation in CB particle after approximately 40 nm compressing displacement corresponded to 20 µN recorded load. The CB particle after compression is oblate. Similar to the (200-240 nm) compression test, the increase in the load after breaking the CBP was correlated to continue indention in the Si substrate underneath the particle as illustrated in Figure 5.19b. Figure 5.19a demonstrates the deformation force to break or/and deform the CBP at different particles sizes (130-140 nm) and (200-240 nm). The results show that the larger CBP has more resistance to deform compared to the smaller CBP (130-140 nm). The

load of the larger particle is 100 µN compared to 55 µN of the smaller CBP. It is important to note that the compaction of the particles is partially reversible as shown in Figure 5.19a. Lahouij et al [107] studied nanocompression test on soot particles using the TEM nanoindenter. The results showed that soot particles resisted the contact pressure until 7 GPa. The results showed that soot particles exhibited elastic-plastic behaviour. While Bhowmick et al [109] determined the maximum applied load on soot particles using nanoindentation. The results demonstrated that the maximum applied load on the soot particle is 100 µN before the deformation in the soot particle occurred.

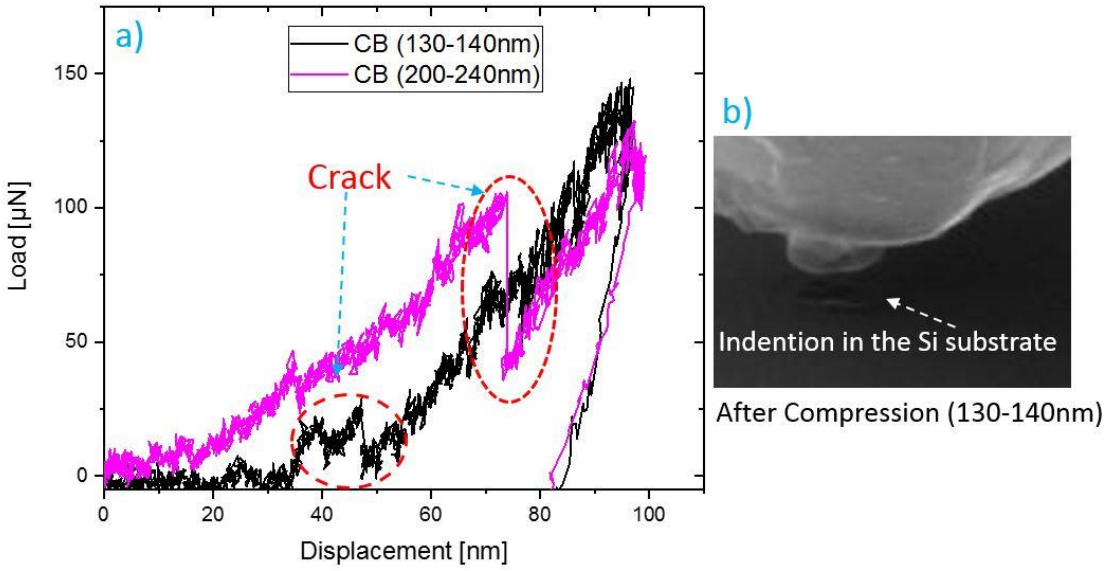

Figure 5.19: a) Nano-compression tests of fresh CBP at different particles size, b) indention in Si substrate after compressing (130-140 nm) particle.

5.2.2.2 Nano-compression of ageing CBP

In-situ nano-compression experiments of aged CB particles were conducted. Aged CB particles were extracted from aged oil and dried overnight in the oven. TEM and XRD results exhibited a change in the crystal structure of CBP after ageing as illustrated in Figure 5.14 and Figure 5.16. TEM images showed the formation of an oxidation layer around aged CB particles. Besides, there is an increase in wear after ageing the oil at the same level of CB as displayed in Figure 5.9. In addition to oil degradation and additive depletion after ageing the oil, there is the possibility that the change in mechanical properties of CBP could affect the

wear. Previous studies [10], [99] suggested that soot interactions with additives might affect the mechanical soot hardness. The interactions between the additives, oil and soot surface can contribute to ambiguous analytical results. There is no previous study that proved the effect of soot interactions with additives in the engine and its influence on the mechanical properties of soot particles.

Nano-compression of the aged CBP at different sizes (130-140 nm) and (210-220 nm) were performed to investigate the effect of the ageing process on the mechanical properties of CBP. The corresponding load-displacement curve of the (210-220 nm) compression test was reported in Figure 5.20. The result shows that during the compression process, the recorded load increases progressively and linearly. Particle deformation occurs approximately at 90 nm compressing displacement accommodated to 200 µN recorded load. After the compression test, the crack can be observed in the aged CB particle as displayed in Figure 5.20.

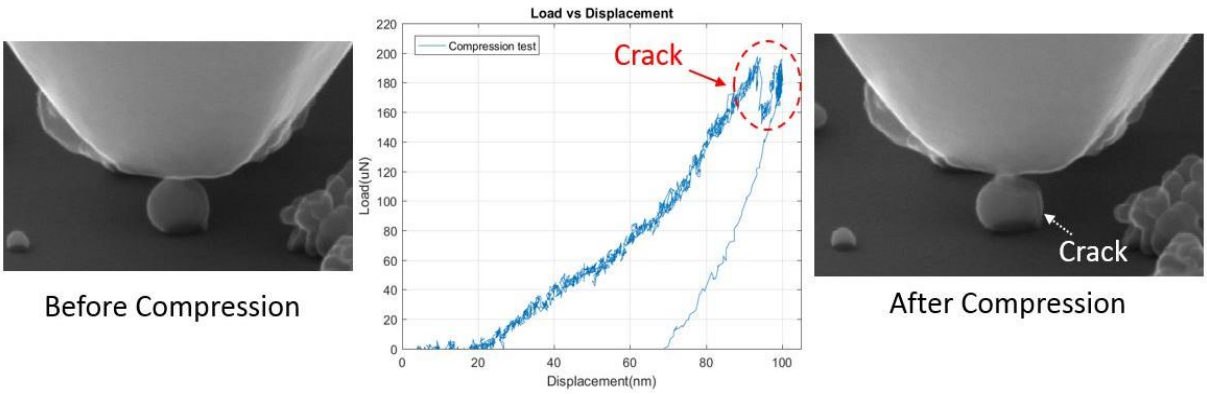

Figure 5.20: Nano-compression test aged CBP at size (210-220 nm).

Load-displacement curves of two different sizes of aged CB particles (130-140 nm) and (210-220 nm) have been reported in Figure 5.21a. Figure 5.21a indicates that the larger aged-CB particle (210-220 nm) required a higher deformation load to break the particle compared to the smaller aged-CB particle (130-140 nm). Similar to fresh CB, the larger particle has more resistance to deform compared to smaller CBP. The (130-140 nm) aged-CB particle was deformed and oblate after compression as shown in Figure 5.21b. The compression of the (130-140 nm) particle had an impact on the Si substrate underneath the particle as highlighted

in Figure 5.21a, b. The deformation load of the larger aged-CB particle is 200 µN compared to 100 µN of the smaller aged-CB particle. The results demonstrate that the aged-CB particle under nano-compression undergoes elastic-plastic deformation.

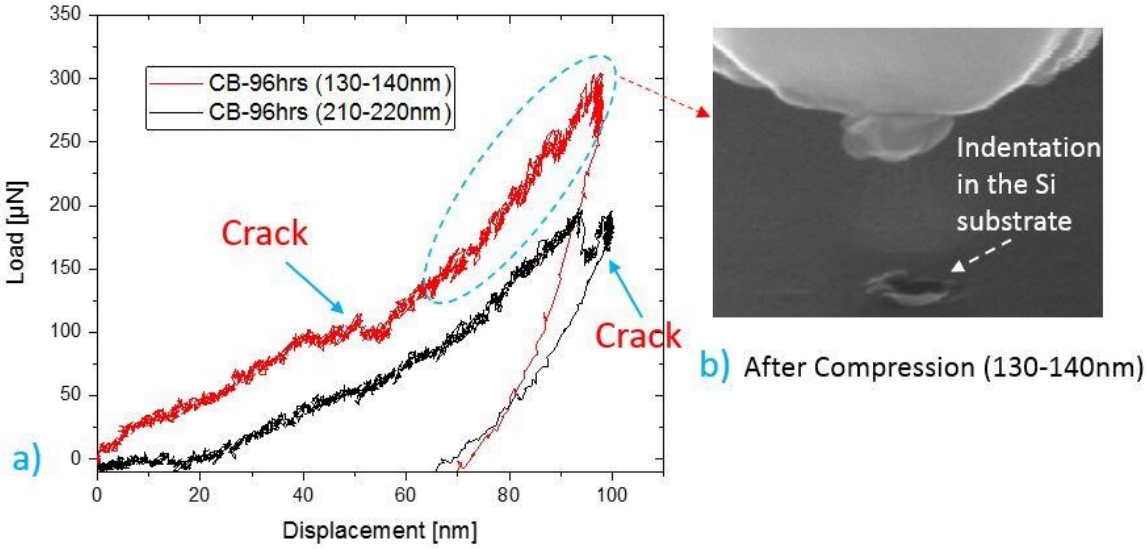

Figure 5.21: a) Nano-compression tests of aged CBP at different particles size, b) indention in the Si substrate after compressing 130-140 nm particle.

5.3 Summary

In this chapter, the effect of CBP contaminants at varying levels was investigated. It was observed that adding CBP to FFO at ageing conditions affected the engine oil performance as expected. The results proved that removing the CBP from oils will certainly improve the performance of the oil and reduce the wear value significantly. It is worth noting that oil performance after the removal of CBP was still not as good as the fresh oil. This is due to the fact that the aged oil after removing the CB is experiencing other problems such as additives depletion, additive adsorption and degradation products in oils that influence the performance of the oil. The crystal structure and mechanical properties of CBP were changed after ageing the oil. The following key points summarise this part of the study:

- Chemical analysis of aged oils revealed decomposition of antiwear additive and the formation of degradation products depending on the amount of CBP presented in the oil.

- Additives were adsorbed on CBP. This study proved for the first time the relationship between the increase in the surface area of CB and additive adsorption.

- Friction, in the presence of a high level of CBP, increases at the beginning of the tests due to the high impact of oil starvation on the inlet of contact surfaces and then decreases over the remaining duration of the test.

- After removing CB, the aged oils performed higher wear compared to fresh oil due to additive adsorption on CB and oil degradation. These results were investigated for the first time in this study.

- The crystal structure of CBP after ageing in the oil was changed. The crystal structure of aged CBP was similar to soot extracted from used oil. The results found for the first time the effect of chemical interactions between additives and soot under the ageing condition on the crystal structure of soot.

- Nano-compression experiments revealed that the deformation load applied to break the CBP particle after ageing was approximately double compared to the deformation load of fresh CBP. The findings proved for the first time that the changes in crystal structure due to chemical interactions caused changes in the mechanical properties of CBP.

6 Chapter (6) Soot effect on heavy-duty used oils

This chapter investigates the effects of soot on the performance of heavy-duty engine oil. Used oil drained from the truck is studied to determine the change in the oil after being used in the heavy-duty engine. According to the latest research [77], [80], [81], [83], [84], it is well accepted that the existence of soot in the engine oil can increase the wear of components in the engine, however, it is important to determine the effect of removing the soot from used oil on wear. In order to overcome the issue of soot contamination in the diesel engine, various filtration techniques have been introduced to filter the soot particles from engine oil. Before using the soot filtration techniques, the soot size distribution in heavy-duty engine oil is determined using the TEM technique. The size distribution of soot is compared to the size distribution of CB at ageing conditions. This comparison helps to understand the efficiency of depth filters to remove the soot or CB that agglomerated at different sizes. As soot is removed from the used oil, additives adsorption on soot is investigated. Reclaimed oil (after removing the soot from used oil) will be used to study the ZDDP replenishment process of used oil in Chapter 8.

6.1 Chemical analysis of used oil

Fully formulated oil (VDS4) of heavy-duty vehicles with viscosity grade 15W40 was used in this study. The physical and chemical properties of fresh oil are displayed in Table 4.1. The engine oil after being used in the heavy-duty diesel engine of a truck was drained for further investigations. The drained oil was provided by Parker Ltd. The millage details of drained oil are shown in Table 6.1. A chemical investigation to study the chemical structure of used oil was conducted using FTIR. FTIR results demonstrate the change in the oil spectrum after being used in the truck as shown in Figure 6.1. Figure 6.1 reveals two interesting areas in the used oil spectrum compared to fresh oil. The 978 cm^{-1} region is correlated to the P-O-C bond which refers to antiwear additive and the 2000 cm^{-1} region is related to soot level in used oil [94]. Figure 6.2a shows no peak in used oil at the 978 cm^{-1} region which could be due to depletion or decomposition of antiwear additive. Figure 6.2b confirms the formation of soot

particles in the used engine oil as there is a shift in the FTIR spectra at 2000 cm^{-1} according to the ASTM D7844 standard [200]. KINEXUS rheometer was used to investigate the change in the viscosity at test temperature (100 °C) after being used in the heavy engine. The viscosity values as displayed in Table 6.1 show a small decrease in the viscosity of used oil compared to fresh oil. The decrease in the viscosity of used oil is due to the loss of Viscosity-Index Improver (VII) at high temperature causing the decrease in the viscosity [241]. Further chemical analysis to determine the change in additive concentration in the used oil will be discussed later in this chapter.

Table 6.1: Used oil (YK63UFD) details, (YK63UFD is the number of the truck's plate).

Truck oil change	Oil filling	Oil draining
Date	21.06.2019	29.11.2019
Mileage (km)	524604	563842
Viscosity (Pa.s)	0.0097±0.0006	0.0092±0.00007

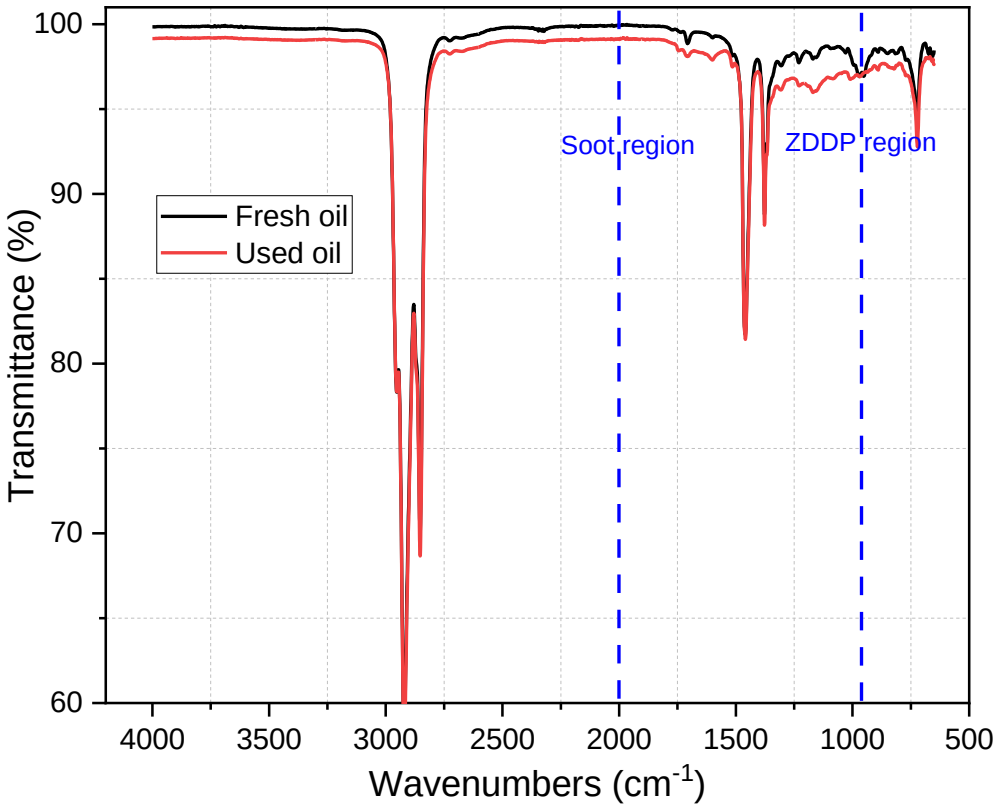

Figure 6.1: FTIR chemical analysis of used oil (YK63UFD) compared to fresh oil (VDS4).

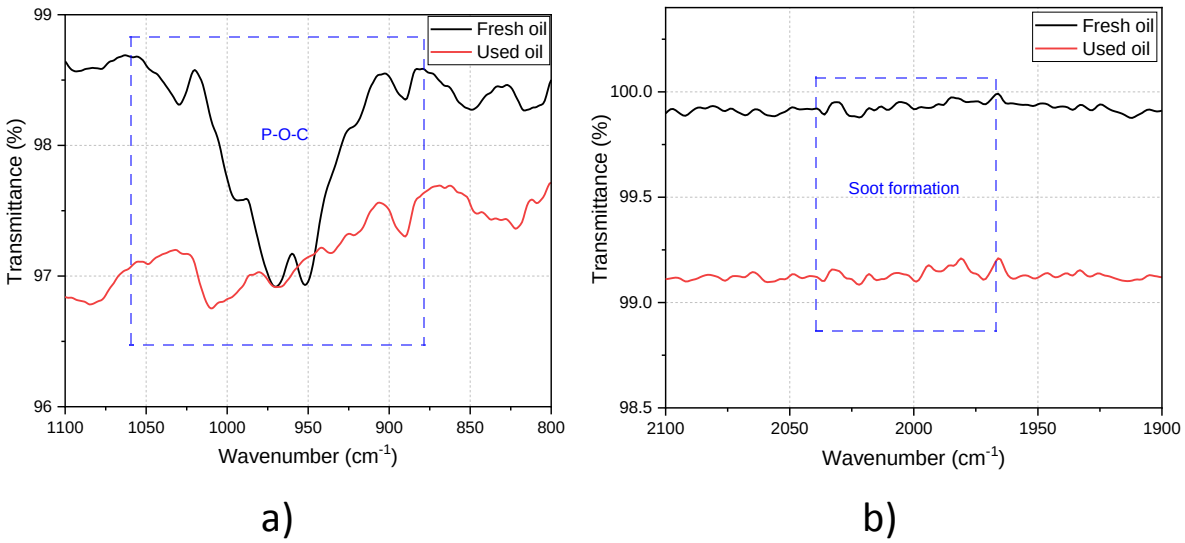

Figure 6.2: a) Antiwear additive area at 978 cm^{-1} point, b) Soot formation area at 2000 cm^{-1} point.

6.2 Soot size distribution

6.2.1 Soot in used oils

TEM technique was applied to determine the soot size distribution in used engine oil. The specification of drained oil was described in Table 6.1. A few droplets of used oil were diluted in heptane solvent with a dilution ratio (1:60) to produce a solution with lower oil content that contains soot particles [110]. The used oil and heptane solvent were mixed using an ultrasound bath for 3 sec. The TEM grid of graphene oxide was dipped in the prepared solution and dried over the night. Soot particles were stuck on the TEM grid by Van der Waals forces.

An example of TEM images is presented in Figure 6.3a and b, which were analysed to measure soot size distribution in used oil. More than 20 TEM images at different positions were taken to obtain the soot size distribution in used oil. There were plenty of primary particles with a diameter of less than 50 nm which were difficult to be counted. The data of soot size distribution in this used oil were plotted in Figure 6.4. The primary soot particles are agglomerated in a mixture of chain-like clusters of spherules. The length of the chain-like particles was measured for all soot clusters within a size larger than 50 nm. The results indicate that soot size distribution concentrated in the range of less than 200 nm. Used oil contains some soot clusters that reached up to 600 nm. The crystal structure of this soot and

the primary size particles were shown in Figure 5.15. As explained earlier, the soot consists of a core and shell and the primary size of some soot particles was 10 nm agglomerated in a large cluster. The result is in the agreement with other studies [242]–[245] that reported the size distribution of soot agglomerates was less than 400 nm of clusters. However, the size of primary particles was smaller than 50 nm [242]–[245].

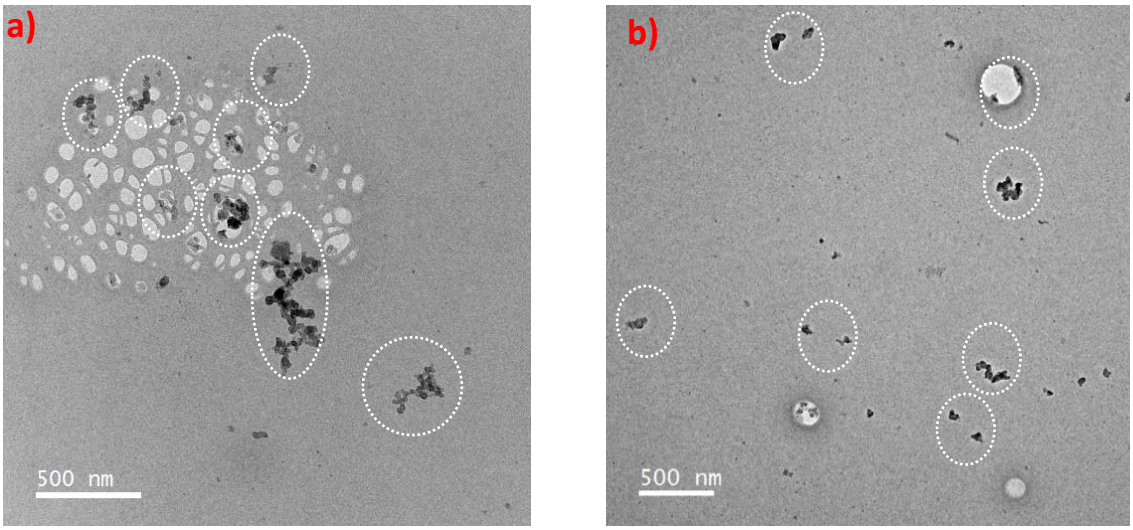

Figure 6.3: TEM images (a and b), as an example of TEM images, which are used to measure the size distribution of soot clusters in used oil.

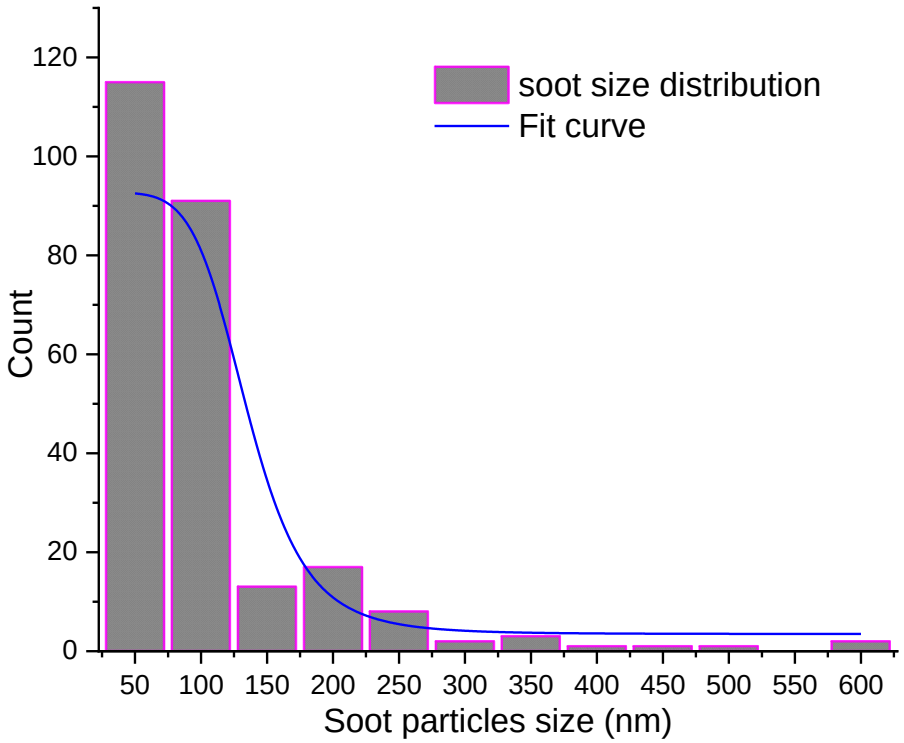

Figure 6.4: Soot size distribution in used oil.

6.2.2 CBP in aged oil

The size distribution of CBP after ageing in the oil was measured using TEM. Engine oil (AFTON oil) +1.5 wt%CB was aged for 96hrs in the lab according to ASTM D4636-99 standard [194]. TEM sample preparation was explained in the previous section 6.2.2. A few droplets of aged oil were diluted in heptane solvent with a dilution ratio (1:60) to produce a solution with lower oil content that contains CBP particles [110]. The aged oil and heptane solvent were mixed using an ultrasound bath for 3 sec. The TEM grid of graphene oxide was dipped in the prepared solution and dried over the night. CBPs were stuck on the TEM grid by Van der Waals forces. More than 20 TEM images were analysed to measure CB size distribution in aged oil. Primary particles with a diameter less than 50 nm were not counted. Size distribution of CB in aged oil is reported in Figure 6.6, an example of TEM images is presented in Figure 6.5a and b. The length of chain-like particles is determined in Figure 6.6. The results show that CBP size distribution in aged oil is concentrated in a size less than 800 nm. The size distribution of some CB clusters in aged oil reached up to 2 µm as shown in Figure 6.6. The specification of manufactured CBP is displayed in the methodology. The diameter of single carbon black particles varies and reaches up to 250 nm as shown in Figure 5.18. CB particles are agglomerated in large clusters as shown in Figure 6.5b.

The primary particles of soot and CB have sized up to 50 nm and 250 nm respectively. Both soot in used oil and CB particles in aged oil were agglomerated in large clusters as displayed in Figure 6.4 and Figure 6.6. The size of soot and CB clusters shows that soot clusters are concentrated in a smaller size smaller (less than 200 nm) compared to 800 nm of CB clusters.

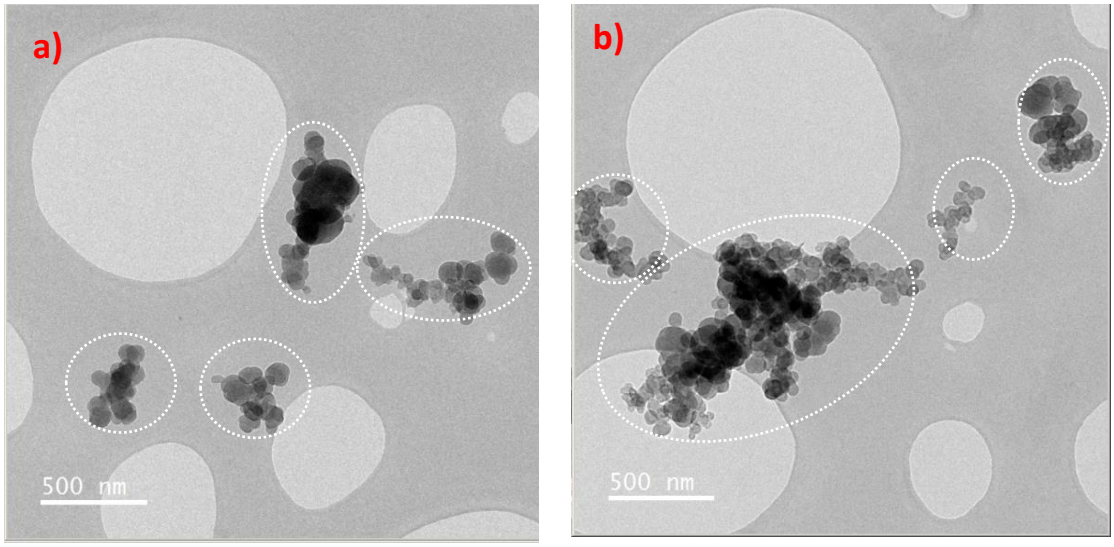

Figure 6.5: TEM images (a and b), as an example of TEM images, which are used to measure the size distribution of CBP clusters in aged oil.

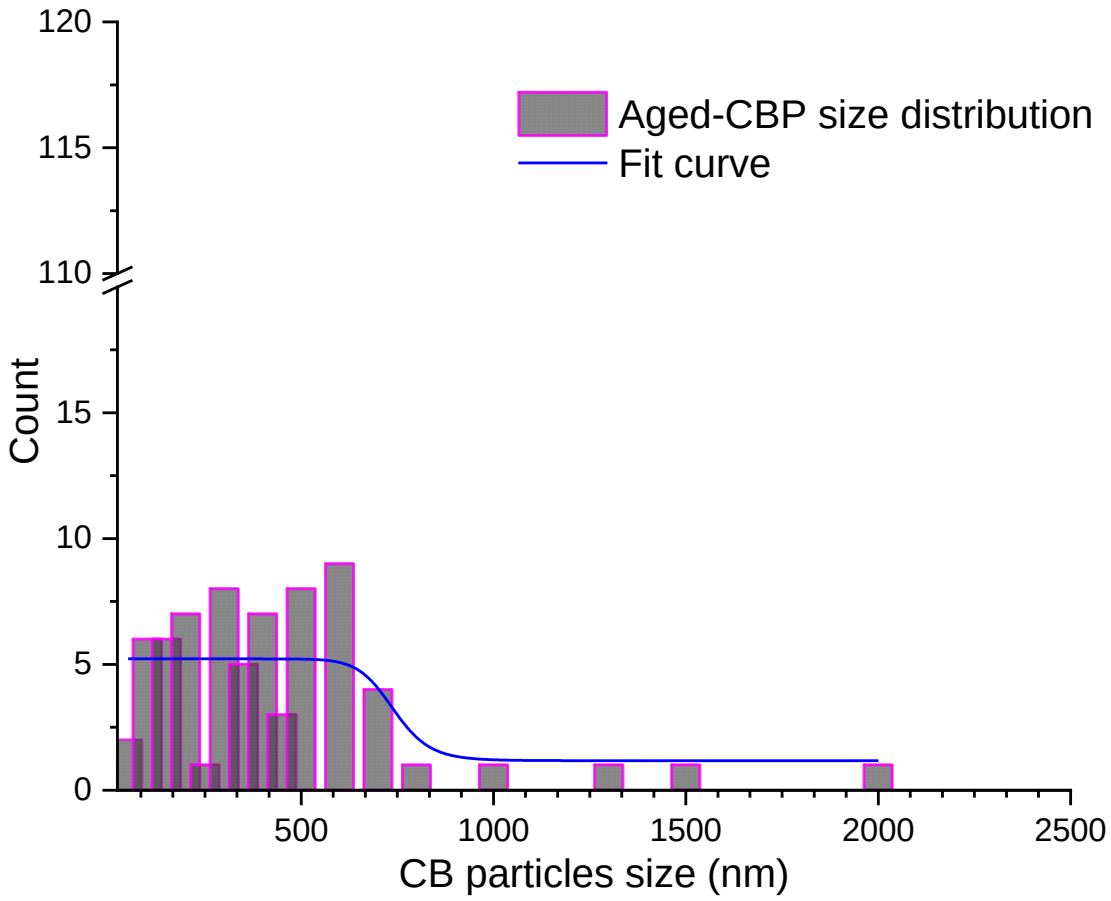

Figure 6.6: CB size distribution in aged oil.

6.3 Soot filtration techniques

6.3.1 Soot removal using centrifugation

A centrifuge was used to remove soot particles from the used oil. The centrifuge was conducted at 40 °C with a speed of 12000 rpm for 2 hrs. This centrifugation process was repeated six times to ensure that most of the soot has been removed from the oil. FTIR was used to measure the soot level in the used oil according to the ASTM D7844 standard [200]. The calibration curve method to determine the level of soot in the oil was explained in the methodology (section 4.2.3). Figure 6.8 shows the calibration curve to estimate the soot percentage in used oil plotted between different levels of carbon black (CB) and the shift at the 2000 cm^{-1} point. The calibration curve was applied in this study to measure the soot level in drained oil after every centrifuge run. Figure 6.7 shows a decrease in soot percentage in used oil after every centrifuge run as the oil curve shift-up at the 2000 cm^{-1} point. Drained oil contained 0.62 wt% soot after being used in the truck. The soot level decreased gradually after every centrifuge run and the soot level after 6-times centrifugation became 0.05 wt% as shown in Figure 6.8.

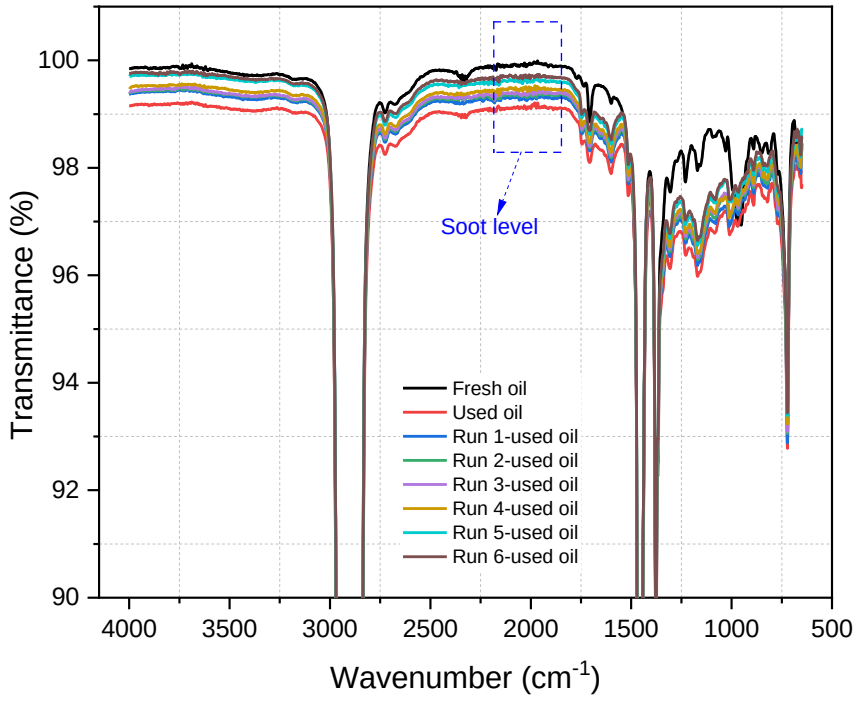

Figure 6.7: Centrifugal process was repeated 6-times at the same conditions and the soot level was measured after every run, the shift at 2000 cm^{-1} point was used to estimate the soot percentage in used oil.

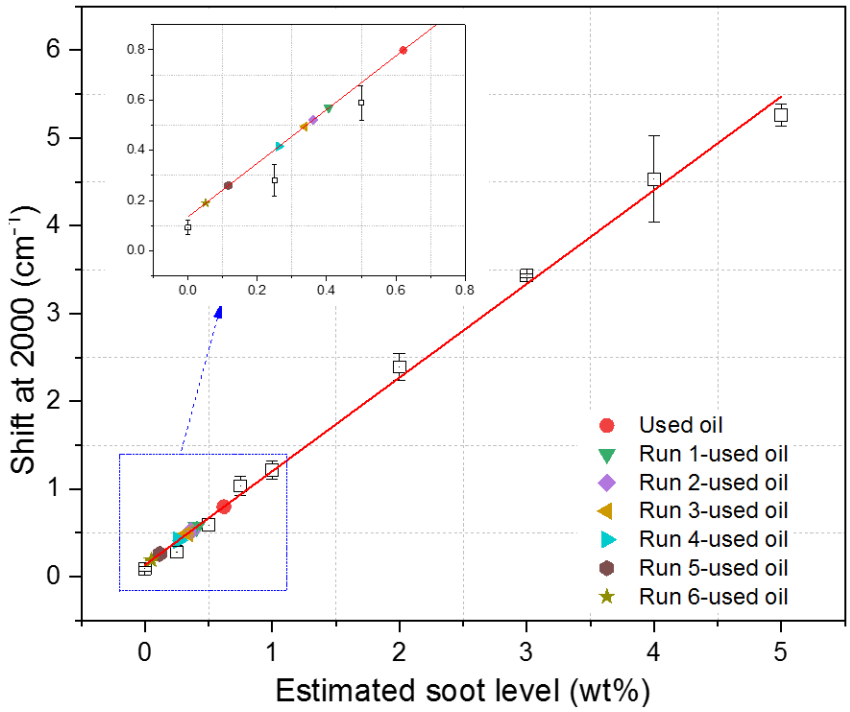

Figure 6.8: Soot level in used oil was measured at 2000 cm^{-1} point after every centrifuge run by FTIR and plotted on the calibration curve to obtain the soot level in the oil.

6.3.2 Soot removal effect on used oil performance

Soot in real engine oil has been investigated in serval previous studies [77], [80], [81], [83], [84] to determine its effects on wear. The results showed an increase in wear as the soot level increased in the oil. Conversely, removing soot from used oil reduced the amount of wear. Figure 6.9 shows a decrease in soot level by repeating the centrifuge process. The results reveal a decrease in the wear value with a decrease in the soot level in the used oil with no further decrease in wear after 4-centrifuge runs. It is worth noting that wear after removing soot is still higher than the wear of fresh oil sample. This is due to the additive adsorption on soot and/or antiwear decomposition as FTIR results showed in Figure 6.2a. As there was no change in wear values after 4-centrifuge runs, thus the used oil after 4-centrifuge runs is used for further additive replenishment tests. Soot level in used oil was 0.62 wt% after draining the oil from the truck and reduced to 0.26 wt% after 4-centrifuge runs. The results are in line with the study [224] confirmed the low level of soot (0.2 wt%) in engine oil does not have a significant effect on wear and agreed with other studies [118], [175], [246] found that removing the soot from used oil reduced its effects on wear.

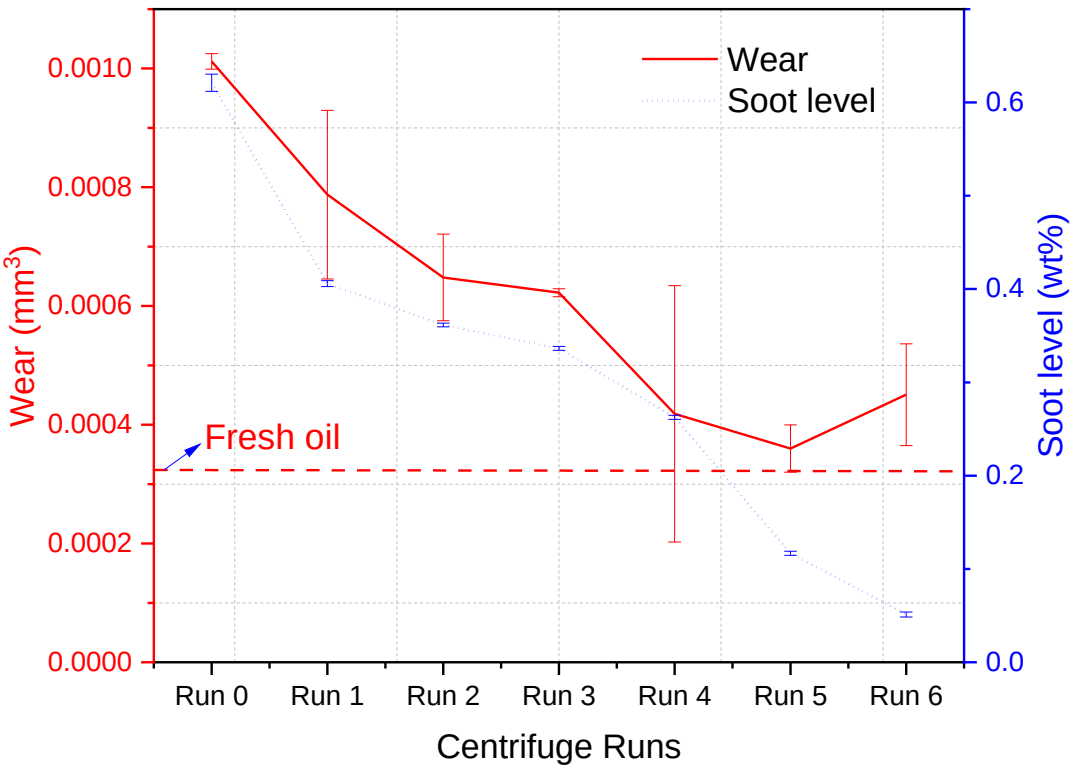

Figure 6.9: The effect of repeated centrifuge process on both soot level and wear.

6.3.3 Soot removal using depth media filter

The used engine oil drained from the truck contains 0.62 wt% soot that was used to run the media filtration experiments. Depth filters and used oils were provided by Parker filtration Ltd, Dewsbury. Two different depth filters were manufactured for these tests with different multilayers thicknesses of cellulose fibres. The bores in each layer are 20 µm which allows the full flow of oil and transfers throughout multilayers without affecting the oil pressure which needs to force the oil to go through the media filter. The depth filter was designed to capture the varied soot sizes through multilayers of the filter. Soot size distribution in used oil was less than 200 nm as shown in Figure 6.4. Depth filters at two different multilayers thicknesses were used in this study. The first depth filter consists of 45 layers (X17545w) and the second filter is made from 80 layers (X175580w). Soot level was measured constantly over time using FTIR. In this study, 5 litres of used oil was cycled through the depth filter. The efficiency of depth filters was calculated using Equation 4.3 and Equation 4.4 as displayed in Table 6.2. Figure 6.10 presents the filtration data using depth filters with a different number of layers.

The results show the relative soot level over time. Where Ct (%) represents the soot concentration after the period and $Cinit$ (%) represents the initial soot concentration. The depth filter (X17545w) with 45 layers shows no change in soot level after running the filtration process for 312 hrs. Increasing the number of cellulose fibres layers to 80, as displayed in filter data (X175580w), demonstrates a small decrease in soot level. There was no change in oil pressure, ΔP=2.2 Pa was constant over time, at the beginning and the end of the filtration process (P_1=4.2Pa is the oil pressure before the filter and P_2 = 2 Pa is the oil pressure after the filter). It is important to mention that the size of soot particles is less than 200 nm (Figure 6.4) which is too small to be removed by these designed filters.

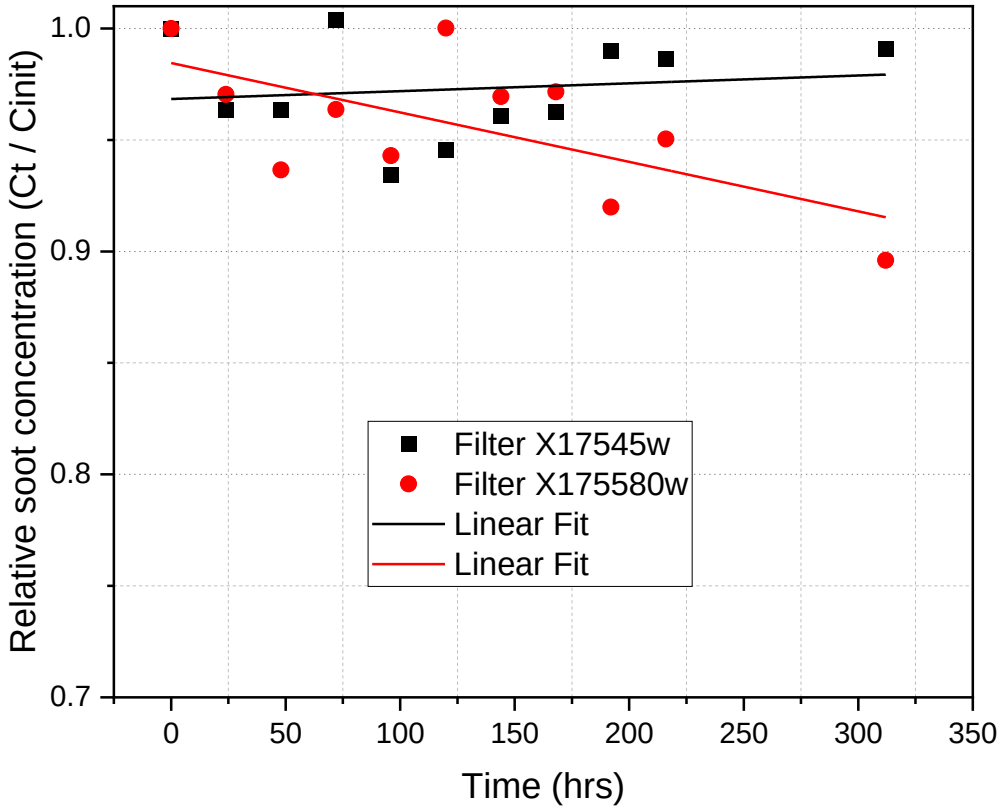

Figure 6.10: Relative soot concentration (Ct/Cinit) using filter X17545w and X175580w.

Further investigation was explored by cycling different used oil with a higher level of soot (1.57 wt%) and using 80 layers of depth filter as shown in Figure 6.11. The test was run for 500 hrs and soot was measured constantly. Figure 6.11 shows the same depth filters (80 layers) with different levels of soot in used oil as presented in Table 6.2. The depth filter (X1890) displayed a similar filter efficiency compared to the same filter (X175580w) that was used to filter the

used oil with lower soot content as in Table 6.2. The results in Table 6.2 demonstrate a small change in soot level after running the experiment for 500 hrs. This comes from the fact that soot particles in this used oil are too small to be removed by these filters even in the existence of a high level of soot (1.57 wt%) in the oil.

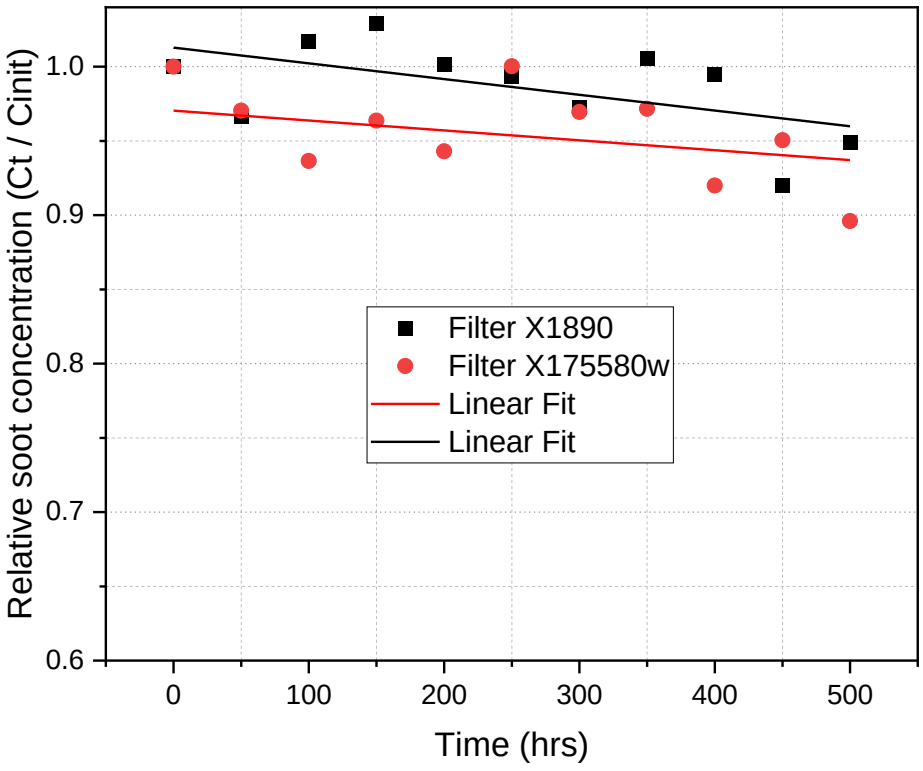

Figure 6.11: Relative soot concentration (Ct/Cinit) using filters X1890 and X175580w.

Table 6.2: Filtration process details for three different depth filters.

Filtration parameters	X17545w	X175580w	X1890
Number of layers (layer)	45	80	80
Flow rate Q (L/min)	1.28	1.18	0.81
Tank vol V (L)	5	5	5
Efficiency e %	0.0003	0.001	0.001
Soot before filtration %	0.62	0.62	1.57
Soot after filtration %	0.62	0.55	1.49

6.3.3.1 Depth filtration after adding CB

The presence of CB in engine oil was agglomerated in larger clusters compared to soot clusters as shown in Figure 6.3 and Figure 6.5. Therefore, 1.5 wt% CB was mixed with used oil containing 0.62 wt% soot which will agglomerate at larger clusters. The same depth filter with 80 layers was used to remove both soot and added CB from the oil. The results after adding CB show that the depth filter has higher efficiency to remove the particles as shown in Table 6.3.

Table 6.3: Filtration process details for depth filters with 80 layers before and after adding CB.

Filtration parameters	X175680w	X175680w/+1.5%CB
Flow rate Q (L/min)	1.18	0.32
Tank vol V (L)	5	5
Efficiency e %	0.001	0.13
Soot+CB before filtration %	0.62	1.99
Soot +CB after filtration %	0.55	1.62

This comes from the fact that larger clusters were formed after adding CB. The filter displayed a higher ability to remove the (soot and CB) clusters as shown in Figure 6.12. The soot+CB concentration in used oil decreased from 1.99 wt% to 1.62 wt% after filtering the oil for 360 hrs. While a small amount of soot was removed from used oil before adding CB, the soot level decreases from 0.62 wt% to 0.55 wt%.

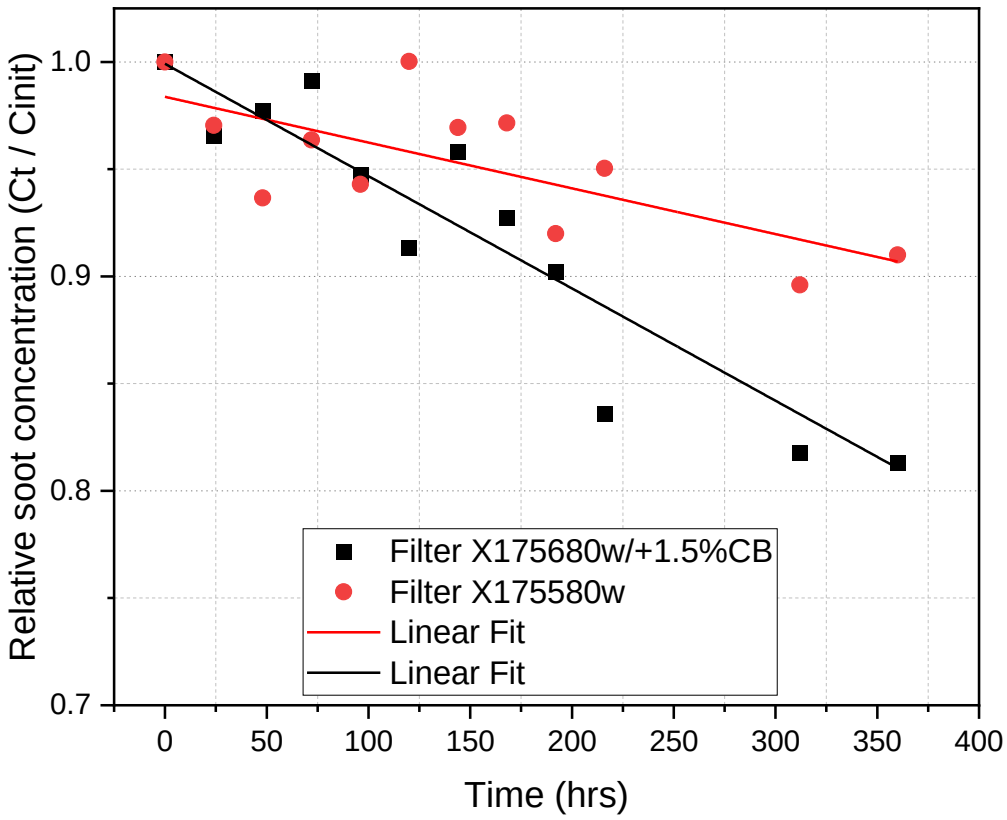

Figure 6.12: Relative soot concentration (Ct/Cinit) using filter X175680w for used oil after adding 1.5 %CB.

6.4 Additives adsorption on soot

ICP chemical analysis was conducted for used engine oil (0.62 wt%soot) and reclaimed oil (after removing soot from the used oil). Figure 6.13 indicates the change in the concentration of oil additive after being used in the engine as expected. The results show a decrease in the additive concentration of Zn, P, S and Mg except for Ca concentration. Zn, P and S elements come from the antiwear additive, such as Zinc dialkyl dithiophosphate, and it is expected to be consumed to protect the tribological surfaces. P and S elements could also come from dispersant/detergent compounds such as sulfonates and phosphonates [50]. The main function of detergent additives is to clean and neutralize oil impurities [50]. Ca and Mg elements originate from the detergent compounds. Figure 6.13 shows an increase in Ca level after being used in the truck. This could come from impurities, rainwater, fuel or road dust. There is a significant drop in Mg concentration that may be used to overcome impurities and other contaminants that caused an increase in the Ca level.

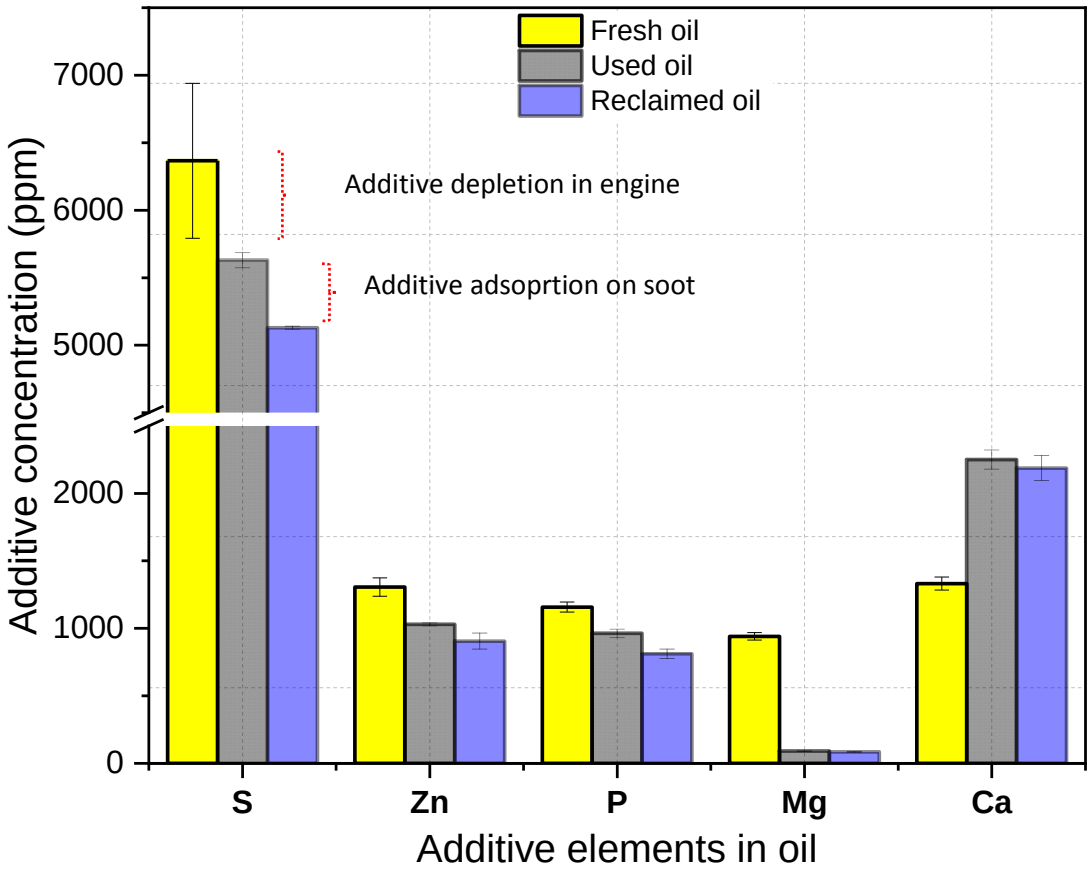

Figure 6.13: ICP chemical analysis of fresh oil, used oil (YK63 UFD) and reclaimed oil (after removing soot from the used oil).

A similar fresh oil was used in a different truck (YK16XSP), YK16XSP is the number of the truck's plate, to investigate the depletion and additive adsorption by soot. ICP analysis as displayed in Figure 6.14 proves that additives concentration was influenced after using the oil in the truck and after removal of soot from used oil. Figure 6.14 shows that a high level of S was depleted significantly in the engine. The S may come from dispersant/detergent compounds such as sulfonates and phosphonates [50] or/and antiwear compounds such as ZDDP. Other elements Zn, P, Mg and Ca were slightly decreased. All elements decreased after removing soot due to additive adsorption on soot. Soot level before and after centrifugation was measured in Table 6.4.

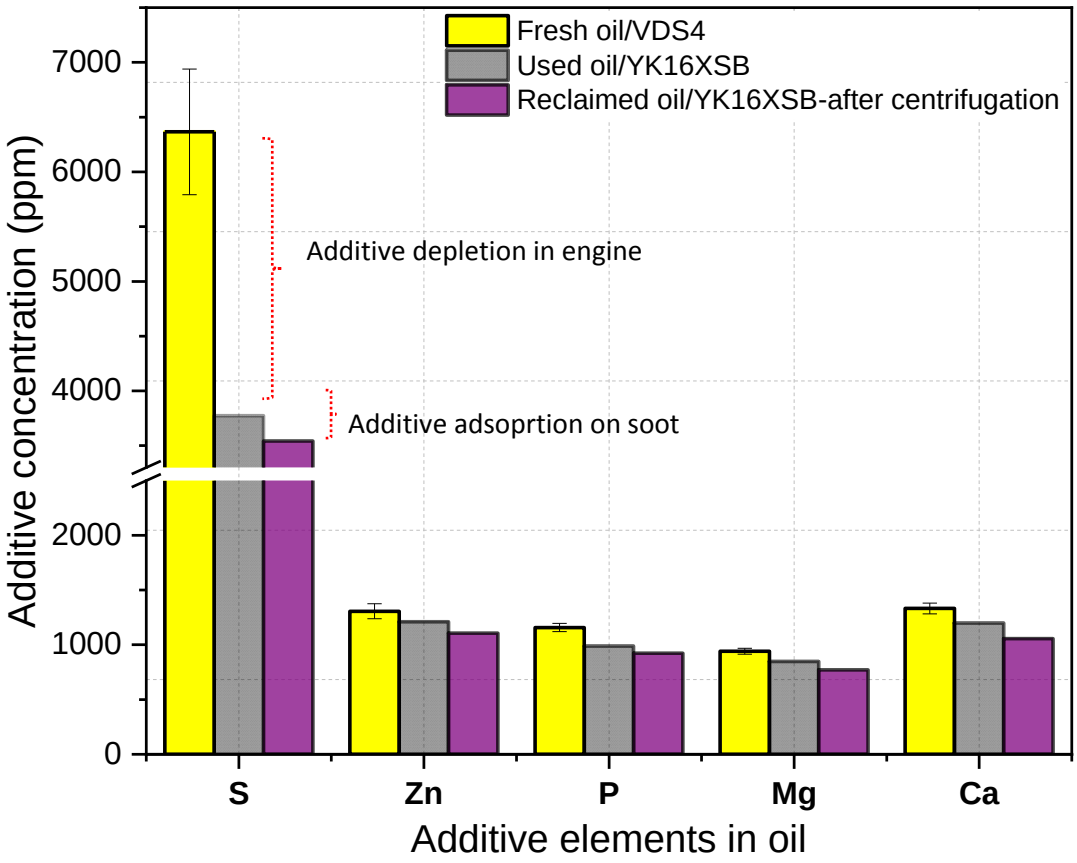

Figure 6.14: ICP chemical analysis of fresh oil, used oil (YK16XSB) and reclaimed oil (after removing soot from the used oil).

Additives adsorption on soot particles has been studied before [10]–[13]. Thus, there is a possibility of removing the additives that are adsorbed on the soot particles during the centrifugation process [47]. Additives adsorption occurs due to the high polarity and surface activity of soot surfaces [247]. Additive adsorption on soot was observed in this study after removing soot as shown in Figure 6.13 and Figure 6.14. In general, there was a decrease in the concentration of all elements that originated from both antiwear and dispersant/detergent. The results agree with several studies [10]–[13] that investigated additives adsorption on soot. The effect of additive depletion and additive adsorption on wear was observed in Figure 6.9.

Table 6.4: Used oils details from two different trucks that were filled with the same fresh oil**.**

Truck plate	Oil filling mileage (km)	Oil draining mileage (km)	Soot before centrifuge (%)	Soot after centrifuge (%)
YK63 UFD	524604	563842	0.62	0.26
YK16 XSB	334470	383110	0.89	0.25

6.5 Summary

In this chapter, the effect of soot on engine oil and the ability to reclaim heavy-duty used oil using different filtration techniques were investigated. The main conclusions were summarised as follows:

- The chemical analysis of heavy-duty engine oil showed no change in the chemical structure of used oil after being used in the truck. However, chemical analysis of used oil exhibited the existence of soot and decomposition or depletion of antiwear additives.
- The findings showed for the first time that the media filter with an increase in depth filter improved the filter efficiency to remove the soot from used oil compared to the media filter with less depth.
- Soot size distribution in used oil influenced the efficiency of the depth filter.
- Removing the soot from used oil caused a decrease in additive concentration due to additive adsorption on soot.
- At the lower level of soot (<0.26 wt%) in used oil, there was no significant effect came from soot level on wear.
- The findings proved for the first time that the reclaimed oil after removing soot did not perform similar to the fresh oil due to the additive adsorption on soot and antiwear decomposition.

7 Chapter (7) Water effect on engine oil

This chapter investigates the existence of different water phases in engine oil, water effect on tribological performance and additive depletion by water. In this chapter, the dissolved water content in heavy-duty used oils is monitored at different mileages. In order to understand the effect of temperature on water saturation level in engine oil, the water saturation method is conducted at different temperatures. Water effect on wear at different levels is investigated in the absence and existence of CB. This helps to identify the critical level of water that affects the wear. Water effects on oil degradation and antiwear decomposition are presented at ageing conditions. The previous studies [47], [136] proposed that the change in water phases from free water to dissolved water can affect the additives in the oil causing additive depletion. Thus, additive depletion by water is studied in this chapter. In addition, the effects of additive depletion on wear and tribofilm formation are investigated. Further investigations to understand the effect of water on the chemistry and tribofilm formation are utilised.

7.1 Water in heavy-duty engine oils

Water content in the used engine oil of two trucks has been determined in real working conditions as displayed in Figure 7.1 and Figure 7.3. Used oil samples were provided by Parker Filtration LTD, Dewsbury, England. Water content in the used oil of the truck-YJO8WJC was determined at different oil changes as shown in Figure 7.1. The results indicate the dissolved water level in the used oils. Fresh fully formulated oil (Morris oil), which was used in this truck, contains 2270 ppm of dissolved water. As the truck runs, water content increases after the first sampling at each oil change and starts levelling between 3500 to 3900 ppm until draining the oil. It seems that dissolved water in these oil samples reached its saturation level as it did not have a significant change in water content over truck running as illustrated in Figure 7.2. The dissolved water level was high in these used oils samples due to the high level of water in the filled fresh oil (2270 ppm). Other factors may influence the water level in these used oils such as soot level, oil oxidation and driving in different humid conditions [127], [131].

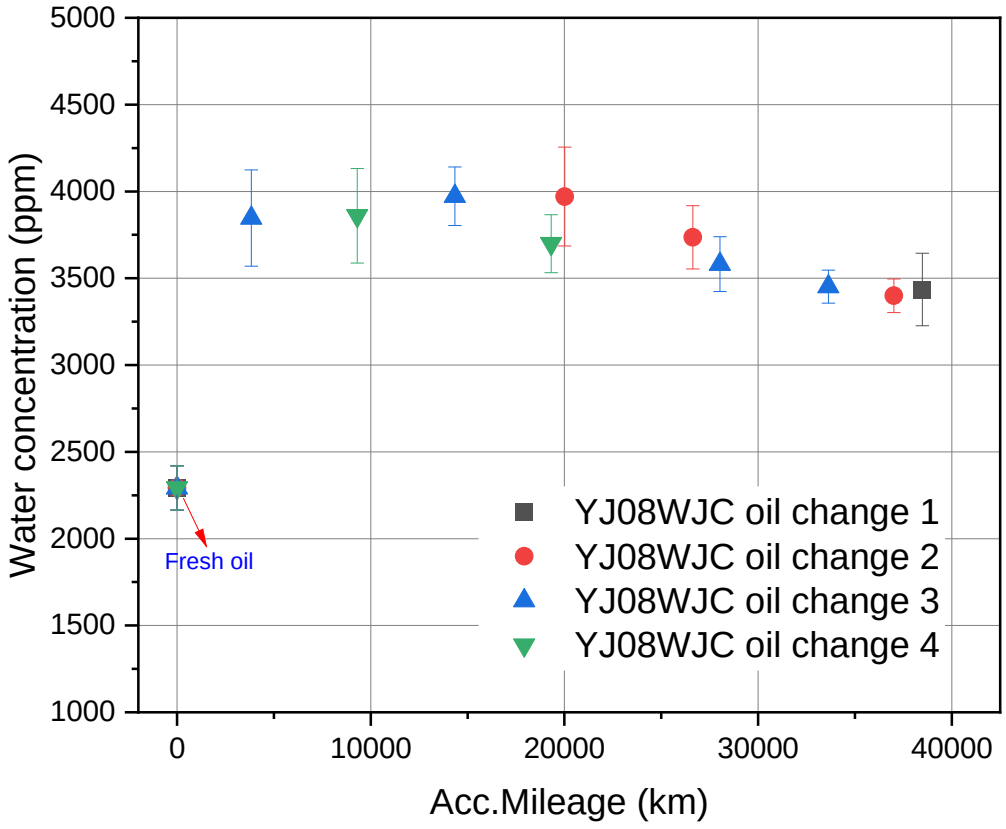

Figure 7.1: Water content in used engine oils. Four oil changes for the same truck (YJO8WJC) were reported. At each oil change, the water level was measured over the accumulated mileage at different points.

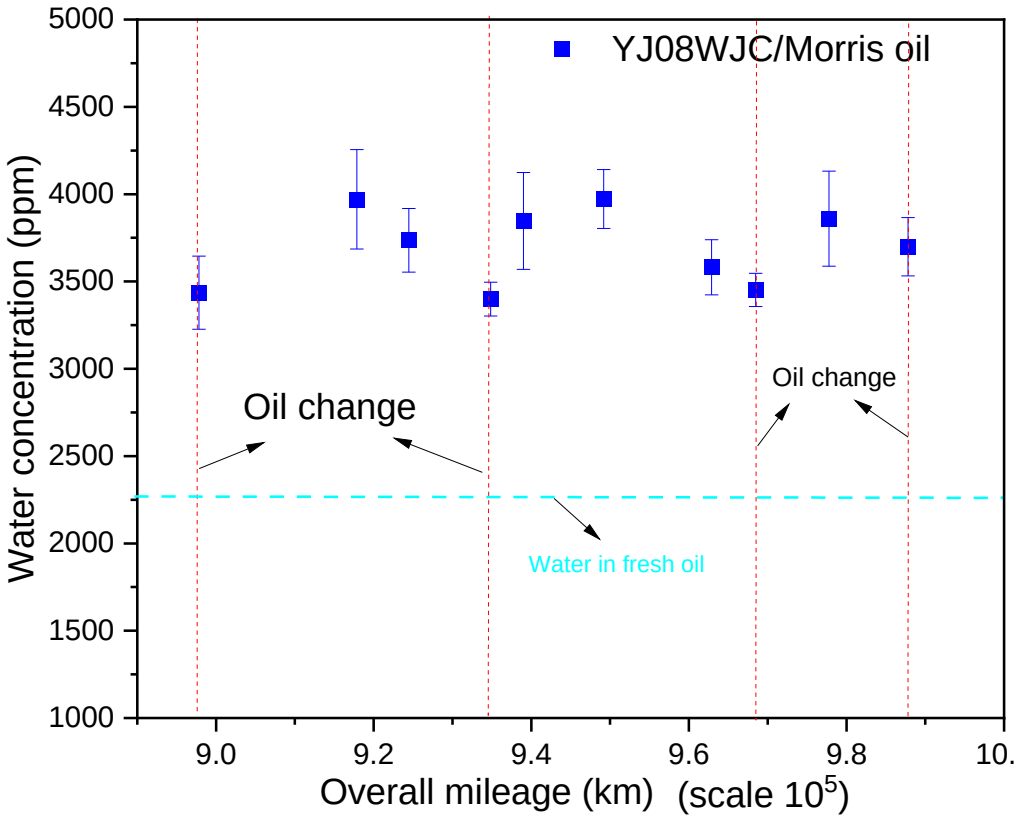

Figure 7.2: Water content in used oil of truck-YJO8WJC over the mileage. The used oil was drained four times during the overall mileage.

Water content in used oil of the tuck-YD140RK was measured at different oil changes reported in Figure 7.3. Fresh fully formulated oil (Rubia oil), which was used in this truck, contains 550ppm of dissolved water. As the truck runs, the water content of each oil change increases over the accumulated mileage. The water level had been increased until draining the oil and it seems that water still did not reach its saturation level as displayed in Figure 7.3. Figure 7.4 shows that the used oil was drained four times during the overall mileage. The water content ranged between 1500 ppm to 3000 ppm during the overall truck run. It could be also influenced by the increase in both additives decomposition, oil oxidation and soot level over time [127], [131]. The reason behind this is that soot particles have high polarity and active surface which attract more water molecules and remain in the oil as dissolved water.

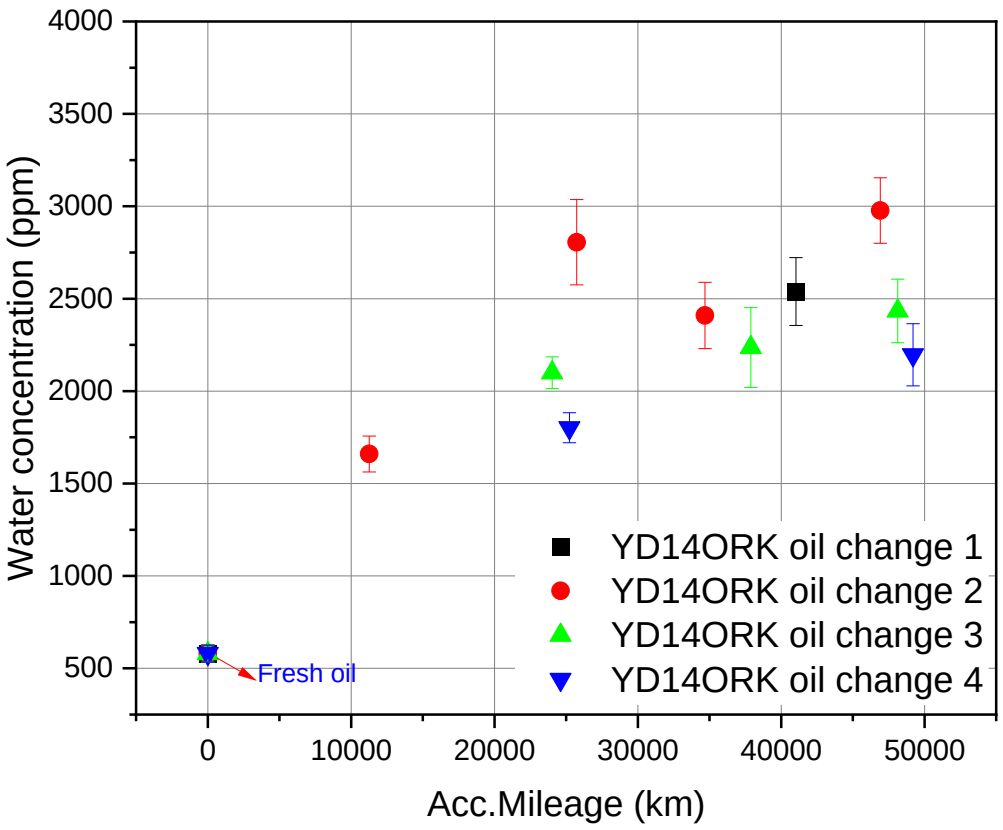

Figure 7.3: Water content in used engine oils. Four oil changes for the same truck (YD140RK) were reported. At each oil change, the water level was measured over the accumulated mileage at different points.

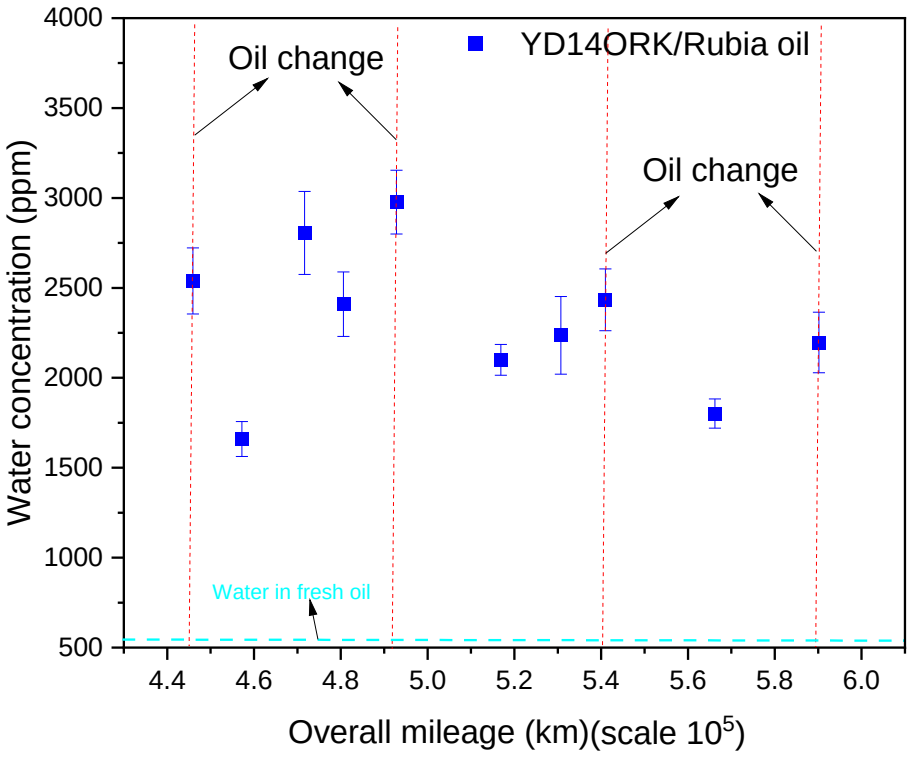

Figure 7.4: Water content in used oil of truck-YD140RK over the mileage. The used oil was drained four times during the overall mileage.

Disloved water concentration in both used oils (truck-YJO8WJC and truck-YD140RK) was high reaching up to 3900 ppm and 3000 ppm respectively. In service limits, manufacturing requirements suggested that dissolved water above 2000 ppm has to give attention. It is commonly agreed that water content in truck engine oils does not exceed 2000 ppm [132]. In the oils of the truck-YJO8WJC, the water seems to reach its saturation level and free water was separated from the used oil. As free water is separated from used oil, this may lead to additive depletion by water. Further investigations in this chapter are important to understand the water saturation level in engine oils, the effect of water at a level higher than 2000 ppm on tribological performance and additive depletion by free water.

7.2 Water saturation in engine oil

7.2.1 Effect of temperature

The water saturation method was explained in the methodology. Three main stages; the preparation stage, solubility stage and stability stage, were used to calculate the saturation

level in the oil. To calculate the saturation level at any fixed temperature, firstly the water level reached the emulsified state at the solubility stage with 5049 ppm of water in the oil as displayed in Figure 7.5a. Secondly, the test bottle was settled down in the water bath at a fixed temperature as shown in Figure 7.5b. The water level in the oil was measured over time until reaching the stable water level in the oil which is called the saturation level. To find the saturation level of 80 °C, the test bottle was calmed down at 80 °C until reaching a stable level of water as shown in Figure 7.6. The exact saturation point was calculated by finding the mean values of the stable points (the last 4-points in the curve as shown in Figure 7.6). Oil appearance at the beginning of the test was cloudy (emulsified state), as illustrated in the test bottle image in Figure 7.6, compared to a clear appearance of oil after reaching the saturation level by the end of the test. At the end of the saturation test, only dissolved water existed in the oil. The amount of dissolved water in oil at 80 °C is 2881±88 ppm and any water in the oil above this level was separated into the free water settled in the bottom of the glass bottle.

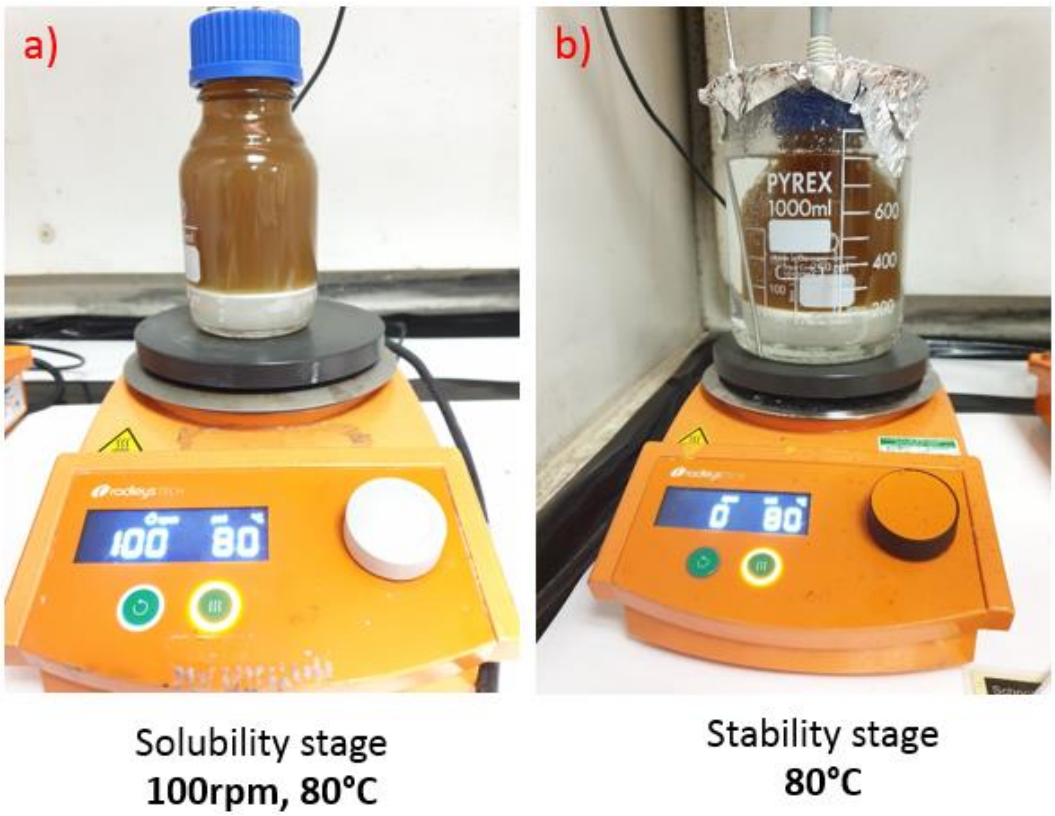

Figure 7.5: (a) Solubility stage, the oil reached the emulsified state (after48hrs), (b) stability stage, test bottle was settled down in the water bath at 80 °C.

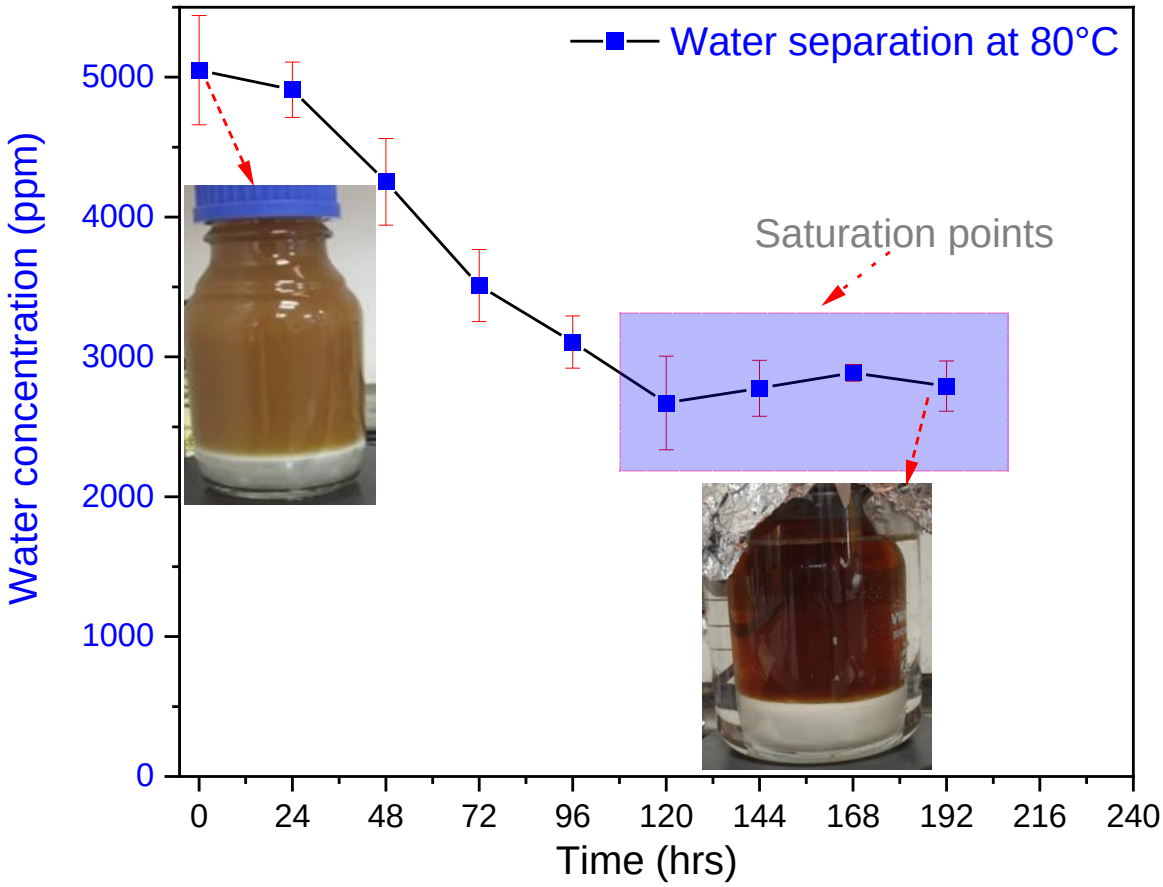

Figure 7.6: Water stability test after the oil reached the emulsified state. The test bottle was moved to a water bath at 80 °C to obtain the saturation points.

After calculating the water saturation test at 80 °C, the water bath temperature was set at 60 °C to determine the saturation level at 60 °C. The water level in the oil was measured over time until reaching the stable content of water in the oil. Water readings at 60 °C, as shown in Table 7.1, stabilise after 24 hrs and the results were reported over 120 hrs. Similar processes were repeated to calculate the saturation level at 40 and 20 °C. The results in Table 7.1 displayed the water level over 120 hrs using the stability stage at different temperatures. It is worth noting that the water level at 60, 40 or 20°C was stabilised after 24 hrs. To calculate the water saturation level at each temperature, the mean values of water readings after stabilisation were used to calculate the saturation level. The stabilized values of each temperature were highlighted in Table 7.1.

Table 7.1: After reaching the saturation level at 80 °C test, the temperature was fixed at 60 °C over 120 hrs and water readings were reported in the table over time. Similar processes were repeated at 40 °C and 20 °C.

Time (hrs)	60°C	40°C	20°C
0	2881 ± 88	2400 ± 212	2077 ± 146
24	2284 ± 316	2021 ± 160	1734 ± 130
48	2509 ± 253	2045 ± 78	1626 ± 66
72	2527 ± 218	1968 ± 4	1624 ± 76
96	2447 ± 153	2030 ± 113	1654 ± 146
120	2400 ± 212	2077 ± 146	1647 ± 102

After calculating the saturation levels at 80, 60, 40 and 20°C, the saturation points were used to draw the water saturation curve at different temperatures shown in Figure 7.7.

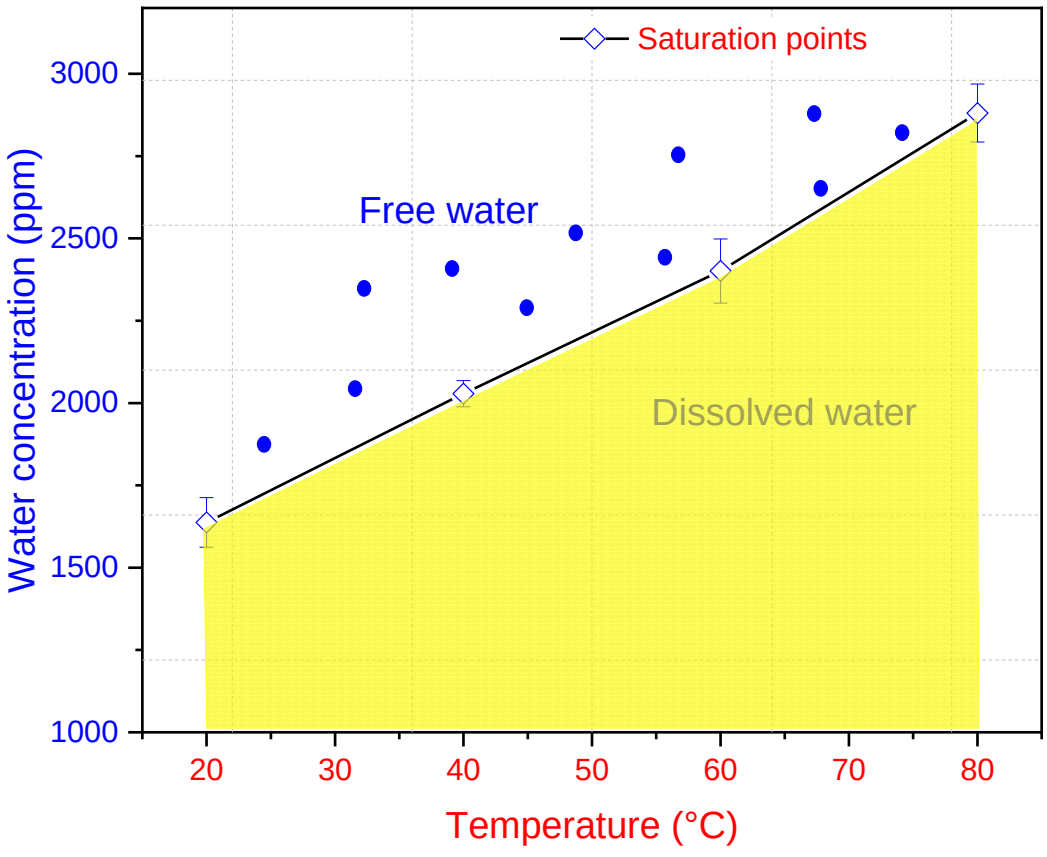

Figure 7.7: Water saturation level at different temperatures.

The results exhibit that dissolved water content in engine oil increases with an increase in temperature. This can prove as the temperature of engine oil decreases, free water is separated into the oil. Regardless of the saturation level of the oil, the saturation curve

provides a true indication of the risk when the free water starts to exist in engine oil. The results are in agreement with the oil property that shows the variation of temperatures causes differences in the amount of dissolved water in oils. The higher temperature of engine oil can hold more dissolved water compared to the lower temperature [29].

7.3 Water effect on tribological performance

7.3.1 Water effect on wear

Water effect on the tribological performance of engine oils has been investigated in several studies [149]–[151]. The results showed an increase in wear [149]–[151] and a decrease in the tribofilm thickness [75], [150] with an increase in water content in the oil. Some studies [165], [166] reported that the presence of water in oils can degrade the oil at a temperature (>60°C). In this current study, water was blended in the oil at room temperature without heating. Different levels of water 0.2,0.3,0.5 and 1 wt% were mixed in engine oils at room temperature for 30 mins and 500 rpm of stirring speed. The tribological test conditions are demonstrated in Table 4.7 and the actual water content in the oils was measured by KF as shown in Table 7.2. The tribological tests were run using two different oils, Afton and BDS4 oils which are used in passenger car and the truck respectively. The physical and chemical properties of these fresh oils are displayed in Table 4.1. Figure 7.8 shows an increase in wear with an increase in the water level in both oils (Afton and BDS4). From the saturation curve as reported in Figure 7.7, the water saturation point at 20 °C of the BDS4 oil was 1637 ppm. Any extra water above this level is free water.

It is important to note that an increase in wear at the level of water above 2500 ppm due to the free water has existed in oils. The results are in line with different studies [127], [132] that considered the water content effect with a concentration higher than 2000 ppm (0.2 wt%) on oil performance [132]. The acceptable water level is approached the dissolved water level in automotive oils and a higher level of water should be taken into account. At the higher level of water above 2000 ppm, more free water exists in oils causing a thinner tribofilm thickness

hence higher wear. While the corrosive wear on contact surfaces can be observed in the presence of water in the oil in the previous studies [29], [128].

Table 7.2: Water content in both oils is measured by KF.

Engine oils	Fresh oil	Added water			
		0.2%	0.3%	0.5%	1%
KF-Afton oil (ppm)	350	2747	3750	5681	10802
KF-BDS4 oil (ppm)	370	2541	3642	5873	10651

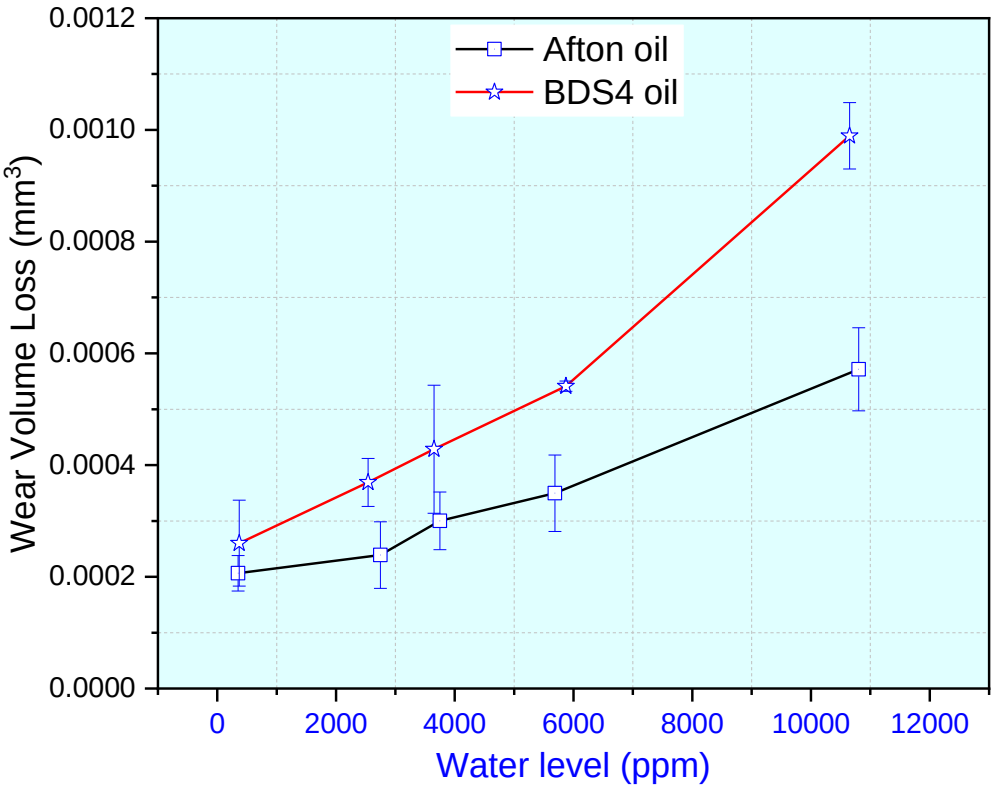

Figure 7.8: Wear volume loss with an increase in the level of water in passenger (Afton) and truck (BDS4) oils.

7.3.2 Water effect on wear in the existence of CBP

The effect of water at different levels on the engine oil performance in the presence of 1 wt%CB is plotted in Figure 7.9. In this study, 1 wt% of the CBP was mixed in the oil for 2hrs to guarantee homogeneously distribution of CBP. Before the tribological tests, water at

different levels was blended in the oil-containing 1 %CB. The results display an increase in wear with an increase in the water level in oil-contaminated by CB. It can be understood from Figure 7.8 and Figure 7.9 graphs that water affects fresh oil and contaminated oil respectively.

Water influences the performance of the additives, the formation of tribofilm on the surface and promotes corrosion [26], [168], [169]. Water is known as the polar molecule that can impede the dispersants/detergents due to the formation of reverse micelles. When the water content in the oil increases, more reverse micelles are generated [171]. The formation of reverse molecules affects the efficiency of dispersants/detergents causing agglomeration of CBP hence the starvation phenomenon. In addition, the high polarity of water molecules also affects the formation and adhesive of tribofilm on contact surfaces [26], [168], [169]. The contact surfaces may face more abrasive wear caused by CBP without the primary protection which comes from the formation of tribofilm on the contact surfaces.

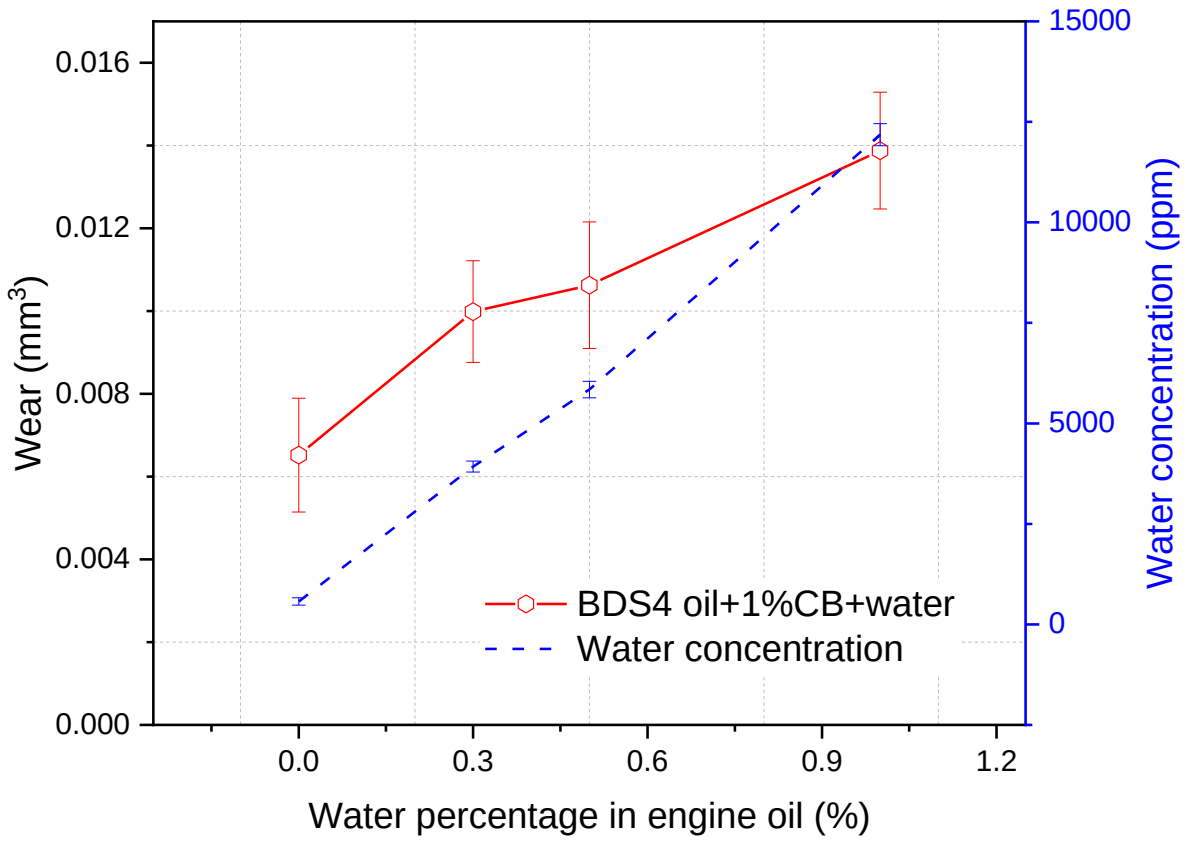

Figure 7.9: Wear values with an increase in the level of water on the oil containing 1 wt%CB.

7.4 Water effect on the oil at ageing conditions

7.4.1 Additives depletion by water

In the current study, the results showed that the saturation level of water is correlated to the oil temperature. The change in oil temperature over time causes a separation of free water which settles down in the bottom of the oil tank. Free water could affect the concentration of the additive due to the high polarity of water molecules [171]. This can be explained when the heads of additives latch onto water molecules surrounding the water molecules. Additives can be depleted when the free water separates from the oil. To study the effect of free water on additive depletion, the oil (BDS4 oil) was aged with different levels of 0.3, 0.5, and 1 wt% of water for 48 hrs and stirring speed of 500 rpm at the temperature of 80 °C as displayed in Figure 7.10. Ageing parameters were chosen to ensure that water molecules in oils can interact with additives sufficiently [165], [166]. The test bottle was filled completely with oil containing different levels of water and sealed to avoid the evaporation of water during the ageing process. The oils after ageing were centrifuged for 2 hrs to remove the free water from the oil. Water content before and after centrifugation was determined by KF as shown in Table 7.3.

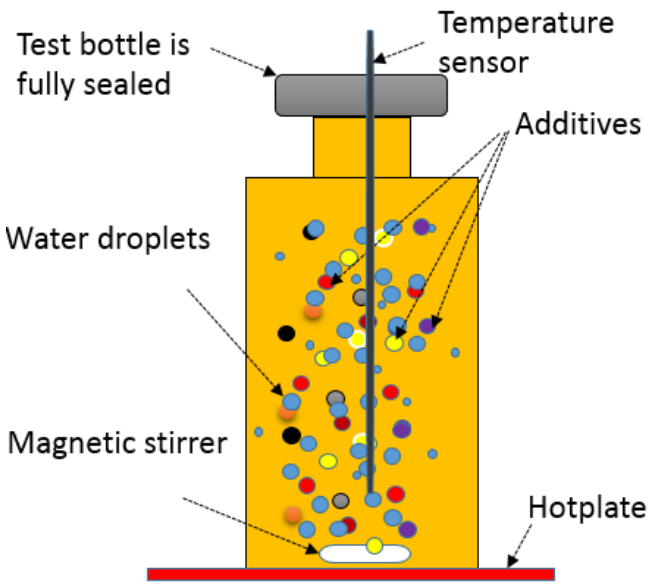

Figure 7.10: Schematic of the ageing process set-up of water in engine oil at 80 °C and with a speed of 500 rpm for 48 hrs.

Table 7.3: Water content in oils was measured by KF before and after centrifugation.

Details	Added water		
	0.3%	0.5%	1%
Water in oil before ageing (ppm)	3828	6268	11875
Water in oil after 48hrs-ageing (ppm)	2790	4648	7509
Water in oil after centrifuge (ppm)	2045	2651	2637

ICP analysis was conducted on oil samples after centrifugation to determine the change in the additive concentration as shown in Figure 7.11. The results show generally a reduction in the additive concentration of elements after removing the free water. The S, P, Zn and Mg concentrations decrease with an increase in the amount of removed water with no significant change in Ca concentration. The results proved that additives depletion by water occurred after removing the water from the oil. The reduction of S, P and Zn, as demonstrated in Figure 7.11, comes from the depletion of antiwear additive such as ZDDP. While the S and P could also originate from dispersants/detergents such as sulfonates and phosphonates [50]. While the reduction in Mg concentration originates from depletion in detergents/dispersants such as magnesium sulfonates [248].

Water is known as a polar molecule which is similar to the additives that have polar heads. The heads of additives latch easily onto water molecules and surround them as illustrated in Figure 7.12 [171]. When the water content in oil exceeds the saturation level, water molecules surrounded by additives separate from the oil causing additives depletion. The results are in line with the function of dispersants/detergents where more polar groups capture or attach to the organic contaminants. It is expected to be removed by water as illustrated in Figure 7.12 [47], [136]. Zn is originated from an antiwear additive and could be washed out by removed water. The results exhibit the effect of change in water level after reaching saturation level on

additive depletion as demonstrated in Figure 7.11. As much water above the saturation level separates from the oil, more additives are depleted. The reduction in additive concentration could affect engine oil performance. Table 7.3 displayed that remained water is above 2000 ppm after centrifugation which could influence the wear. Post investigations have been done to understand the effect of additive depletion and remained water on wear.

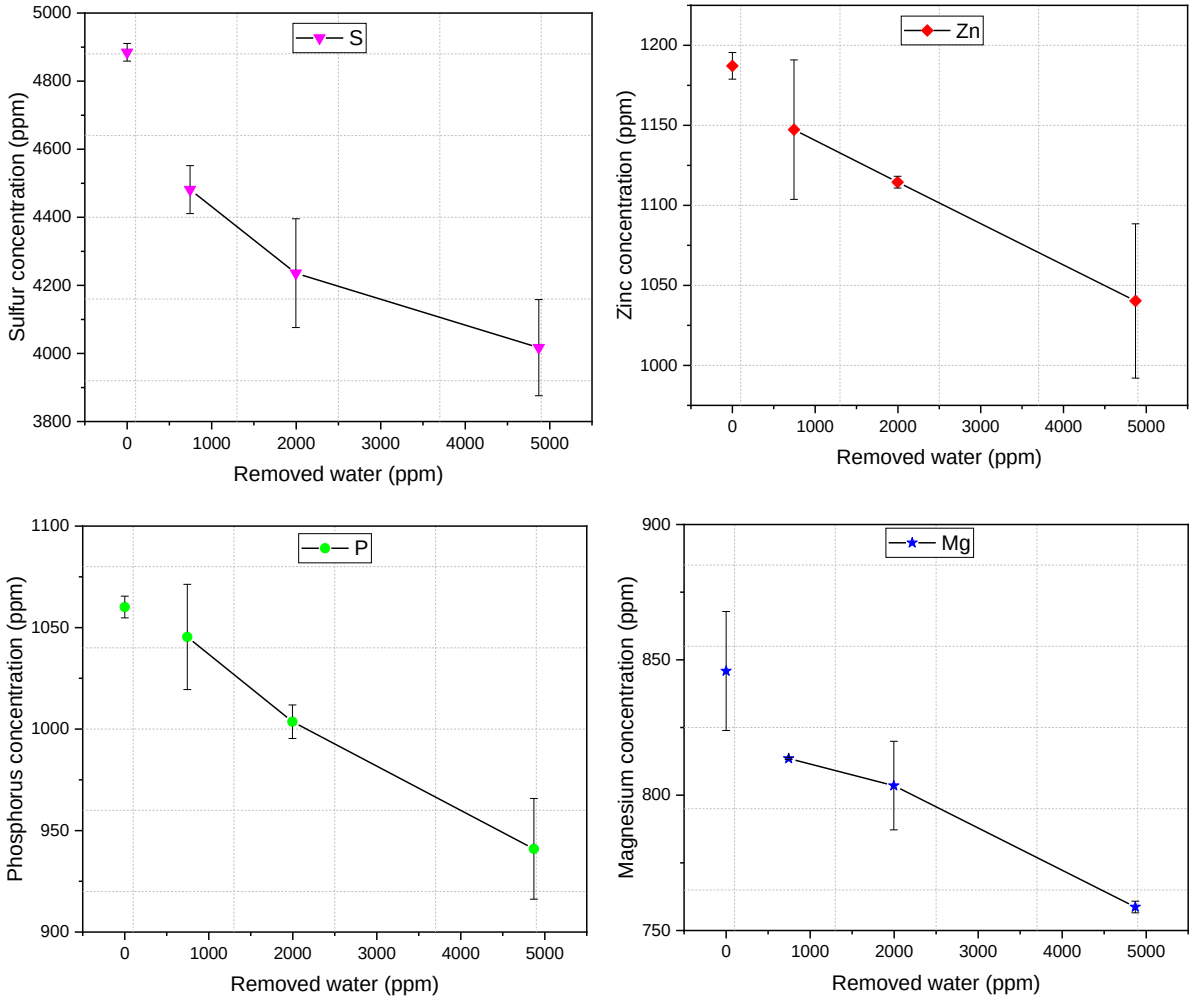

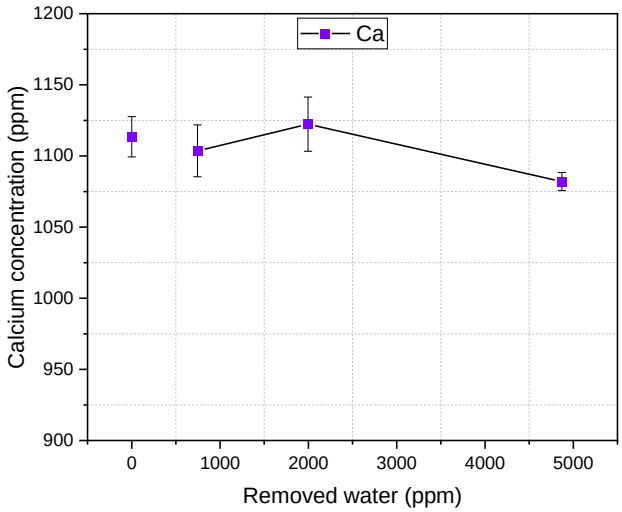

Figure 7.11: ICP results of additive elemental concentration after removing the water from oils.

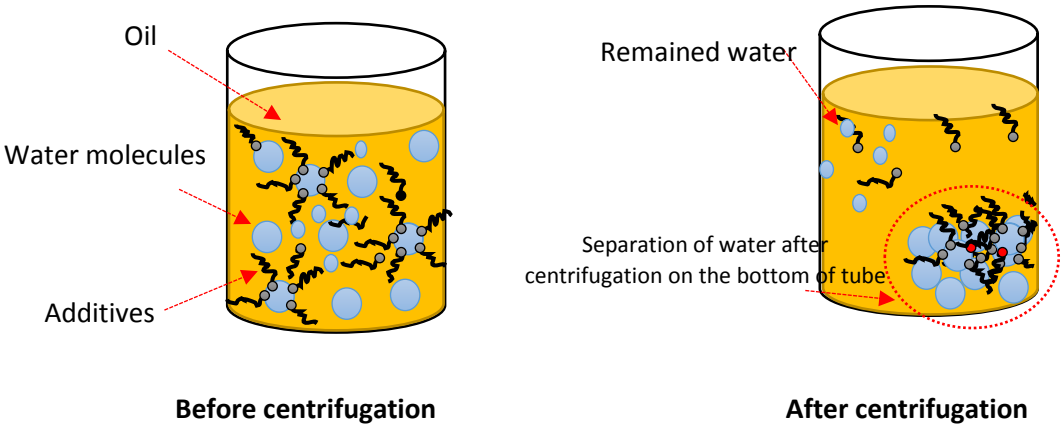

Figure 7.12: Schematic images explain the principle of additive depletion by water.

7.4.2 The effect of water on oil degradation

The effect of water on the bulk oil after ageing the oil with different levels of water (0.3, 0.5 and 1 wt%) at a temperature of 80 °C for 48 hrs was investigated in this study. Ageing oil procedures with water were demonstrated in section 7.4.1. Ageing parameters were chosen to ensure that water molecules in the oil can interact with additives sufficiently [165], [166]. FTIR data of bulk oil after removing the free water from the oil by centrifugation are plotted in Figure 7.13. The results show no change in the chemical structure of oils after ageing with water at 80 °C compared to the chemical structure of fresh oil. The results indicate that the

anti-wear additive at the 978 cm^{-1} region did not decompose. Chemical analysis of oils demonstrates no degradation products (such as oxidation or sulfation products) caused by water at ageing conditions. The results in contrast with other studies [165], [166] proposed that ZDDP (antiwear additive) decomposition occurred or was accelerated not only by the thermal decomposition but also due to the hydrolysis process. The previous studies [165], [166] suggested that water can destruct the antiwear additive when it reacts with water at a temperature of 60 °C and above.

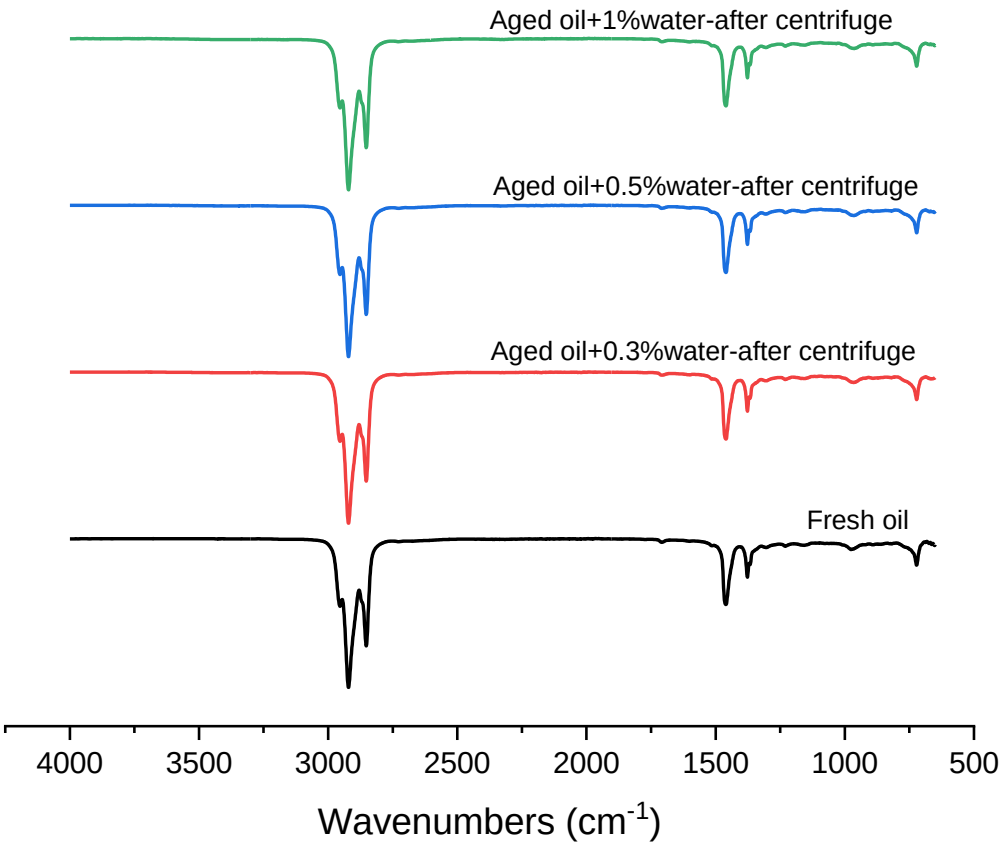

Figure 7.13: FTIR chemical analysis of aged oils with different levels of water after removing the free water from oil samples by centrifuge, water level before and after centrifugation was measured by KF as shown in Table 7.3.

7.4.3 Effect of additive depletion on wear

Tribological tests were performed using the TE77 tribometer for aged oils containing water. TE77 working conditions are demonstrated in Table 4.7. The purpose of these tests is to investigate the effect of ageing oil containing water and additive depletion by water on wear. The wear tests were run before and after removing the water from the oil. Based on the wear

results shown in Figure 7.14, it can be noted that wear increases with an increase in water content in the oil as expected. The results are in line with other studies [149]–[151] that stated that water contamination had a significant effect on wear and tribofilm formation. Water contamination influenced the formation and growth of tribofilm producing higher wear in the existence of temperature in the tribological test [249]. Fitch and Jaggernauth [26] showed that antiwear additive, which forms tribofilm at a high temperature, can be destroyed even by a slight amount of water in the oil.

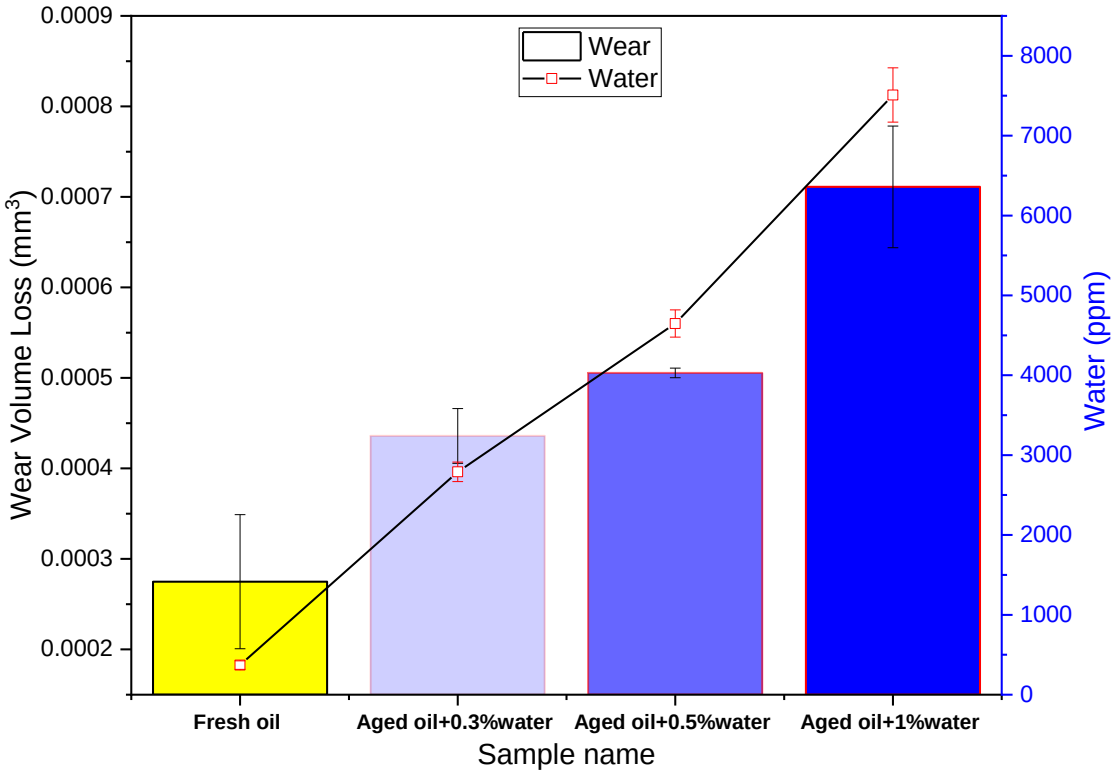

Figure 7.14: Wear volume loss after ageing the oil with different levels of water.

According to saturation tests, the water level was changed depending on oil temperature by releasing free water at a lower temperature. Water separation from the oil caused additive depletion as shown in Figure 7.11. Water level after centrifugation was measured by KF, the results show that the remaining water in oils (which is less than 2500 ppm) represents the dissolved water in the oil. To investigate whether the additive depletion and remaining water influence the wear rate, wear tests after removing the free water from aged oil were conducted. Figure 7.15 shows the increase in wear with an increase in the level of removed water from

oil due to additive depletion and remaining water. When the dissolved water presents in the oil, more hydrolysis of polyphosphates occur resulting in more formation of short-chain polyphosphates and phosphoric acid [249]. This can be associated with depolymerisation of longer polyphosphate chain to shorter polyphosphate chain causing higher wear. Chemical analysis of the tribofilm will result in gaining insights into the real mechanism involved.

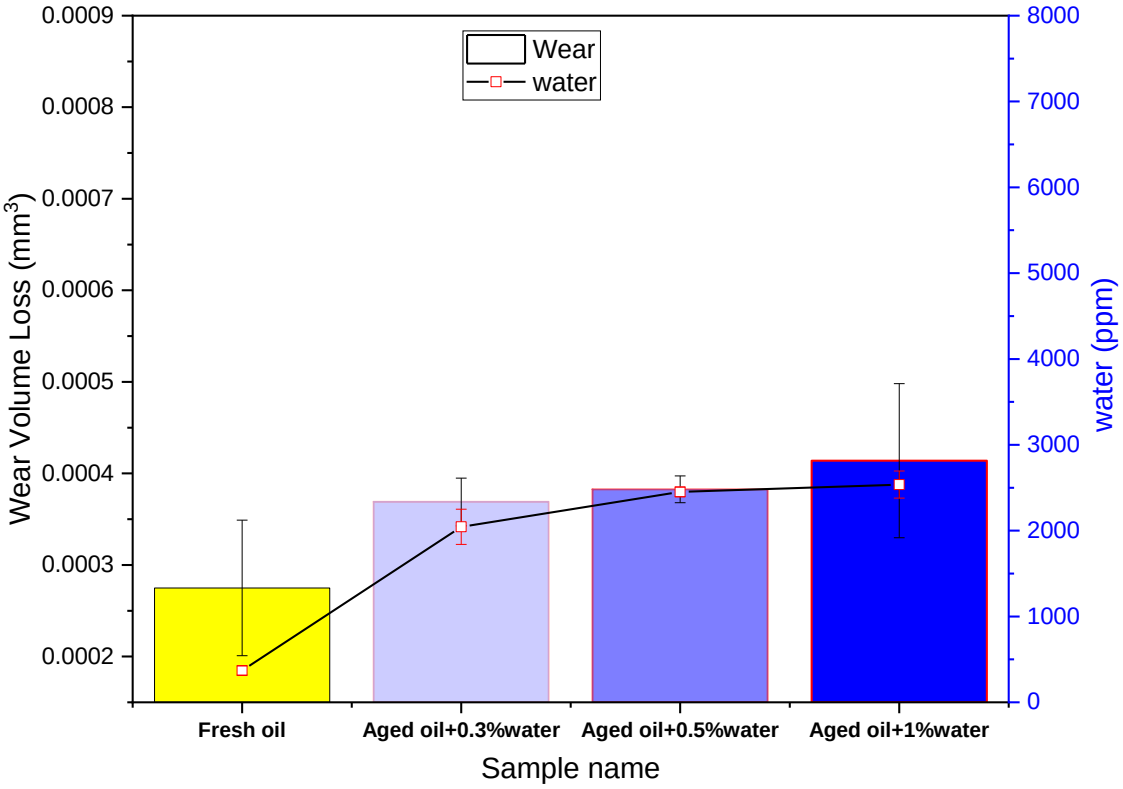

Figure 7.15: Wear volume loss after removing the free water from oils by centrifugation.

7.4.4 Tribofilm topography

Topography features of tribofilm were characterized using the AFM technique as shown in *Figure 7.16*. The images represent an area of 10×10 μm^2. Wear results demonstrated an increase in wear with the increase in the level of the water as displayed in Figure 7.14. The presence of water in oils accelerates the decomposition of antiwear additives and the formation of shorter polyphosphate chains in tribofilm [166]. Tribofilm formation was influenced by water according to previous studies [149], [151] in terms of thickness of tribofilm and covering or continuity of antiwear film on the metal surface.

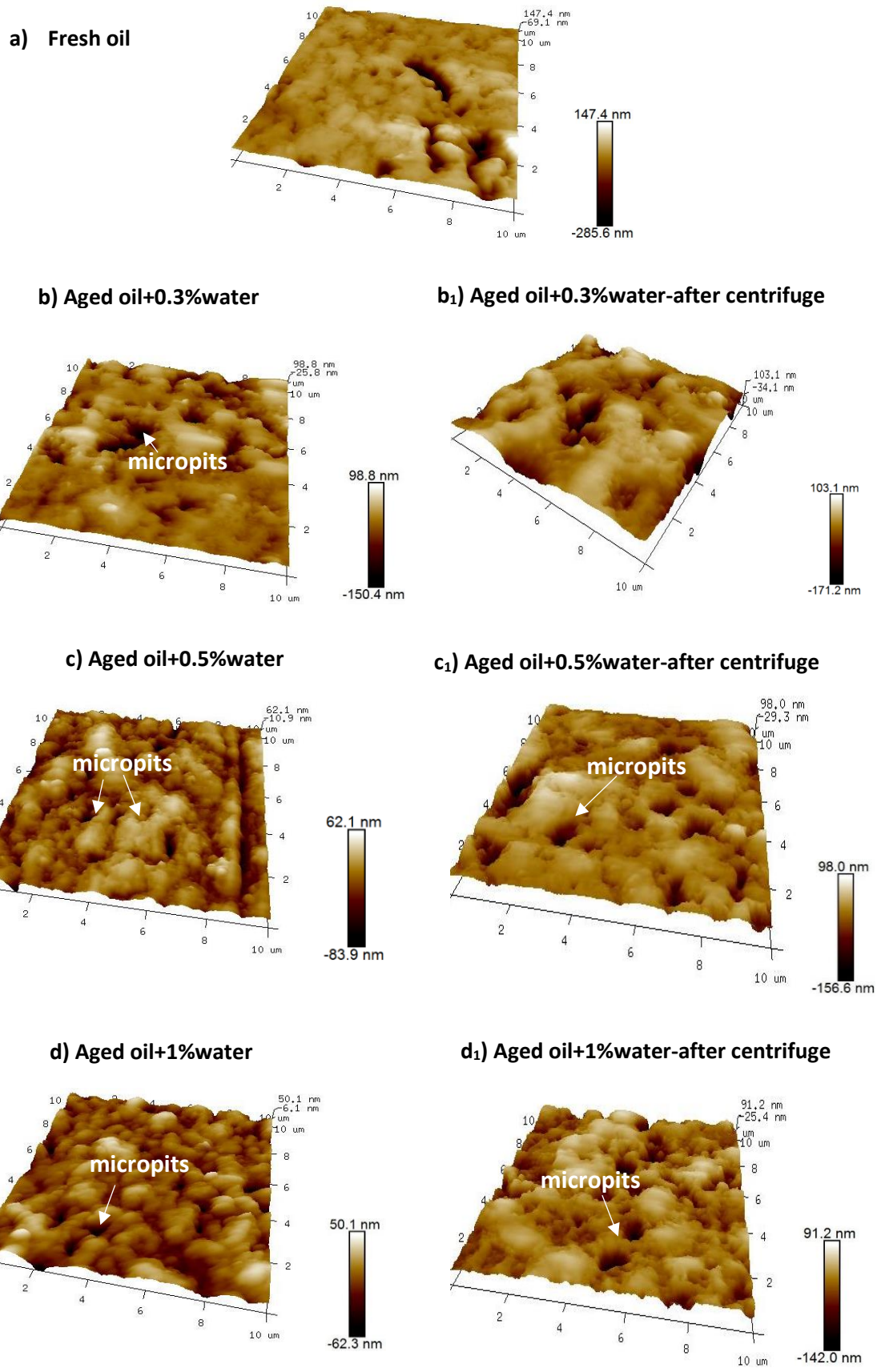

Figure 7.16: AFM images of tribofilm formed on pin surface a) Fresh oil, b) Aged oil+0.3 wt%water, c) Aged oil+0.5 wt%water, d) Aged oil+1 wt%water, AFM images of the oils samples after centrifuging the free water b1) Aged oil+0.3 wt%water, c1) Aged oil+0.5 wt%water, d1) Aged oil +1 wt%water.

Figure 7.16 b,c and d demonstrate AFM images of tribofilm on the wear scar of pins for oils containing different levels of water. The images show a discontinuity or micropits in the tribofilm (distribution of dark spots) in the existence of water compared to the tribofilm of fresh oil displayed in Figure 7.16a. Water level influences the discontinuity of tribofilm and more micropits can be observed with an increase in the water content. The results reveal a decrease in tribofilm thickness with the increase in water content in the oil as displayed in Figure 7.16 b,c and d. The results are in agreement with other studies that reported a decrease in tribofilm thickness and an increase in wear depth with higher water concentration in the oil [151], [152].

Oils after removing the water influence the oil performance causing an increase in wear as shown in Figure 7.15. AFM images as shown in Figure 7.16 b_1, c_1 and d_1, of oil samples after centrifugation show less effect on tribofilm. There is still discontinuity or mircopits in the tribofilm due to additive depletion and remaining dissolved water. The growth rate and morphology of these films, which are formed on steel substrates, are distinguishable and influenced by dissolved water and additive depletion.

7.4.5 Effect of water on tribochemistry

The surface chemistry of tribofilm mainly consists of zinc polyphosphates chains [213]. Zinc polyphosphates in the tribofilm can be determined using the XPS technique [213]–[215]. The oxygen 1s signal from XPS data is fitted by two peaks bridging (P-O-P) and non-bridging oxygen (P=O and P-O-M, with M being a metal) [214], [215]. It has been proved that the chain length of zinc polyphosphates can be characterised based on the intensity ratio of the bridging oxygen/non-bridging oxygen (BO/NBO) and the binding energy difference between Zn3s - $P2p_{3/2}$ [214], [250]. This combined method is applied to characterise the polyphosphate chain ranging from zinc orthophosphate to zinc metaphosphate depending on BO/NBO values [214], [250]. Crobu et al. [214], [251] assessed the length of polyphosphate chains depending on the (BO/NBO) vales. If the BO/NBO values are less than 0.2, the short chains of polyphosphate will be formed which is called orthophosphate chains. While if BO/NBO values are larger than

0.37, the long chains of polyphosphate will be found in the tribofilm which is called metaphosphate chains.

In this study, the chemistry of tribofilm on pins for all the above-mentioned tests in section 7.5.3 was conducted using XPS analysis. The oxygen 1s peaks from XPS data were plotted and fitted by BO and NBO peaks as shown in Figure 7.17a,b and c. The results show that fresh oil is responsible for the longest polyphosphate chains and metal oxide [215], [250] was found on the surface as demonstrated in Figure 7.17a. Table 7.4 demonstrates the results for BO/NBO and the binding energy difference between Zn3s - $P2p_{3/2}$ at different levels of water and after removing the free water from oils. It can be noted that BO/NBO values decrease and Zn3s - $P2p_{3/2}$ values increase in the presence of water. Figure 7.17b reveals that the presence of water in oil affects the length of polyphosphate chains to form the short chains. This can be interpreted that the presence of water causing the formation of shorter orthophosphate chains. The length of orthophosphate chains can be affected by the water percentage presented in the oil as shown in Figure 7.18. The results are in line with studies in terms of the formation of short orthophosphate chains in the presence of water [216], [217]. It also supports the fact that a higher concentration of water in the oil could also influence the length of glassy phosphates chains [249].

The chemistry of tribofilm of tests after removing the free water by centrifugation was analysed. Based on the BO/NBO ratios represented in Table 7.4 and Figure 7.19, the results indicate that dissolved water and additive depletion by water can also affect the length of polyphosphate chains. Figure 7.17c reveals that the intensity of the BO peak decreases after removing the water due to the removal of P-O-P compounds (BO bridge). Figure 7.19 shows a decrease in BO/NBO values and an increase in Zn3s - $P2p_{3/2}$ values which refer to the formation of short polyphosphate chains.

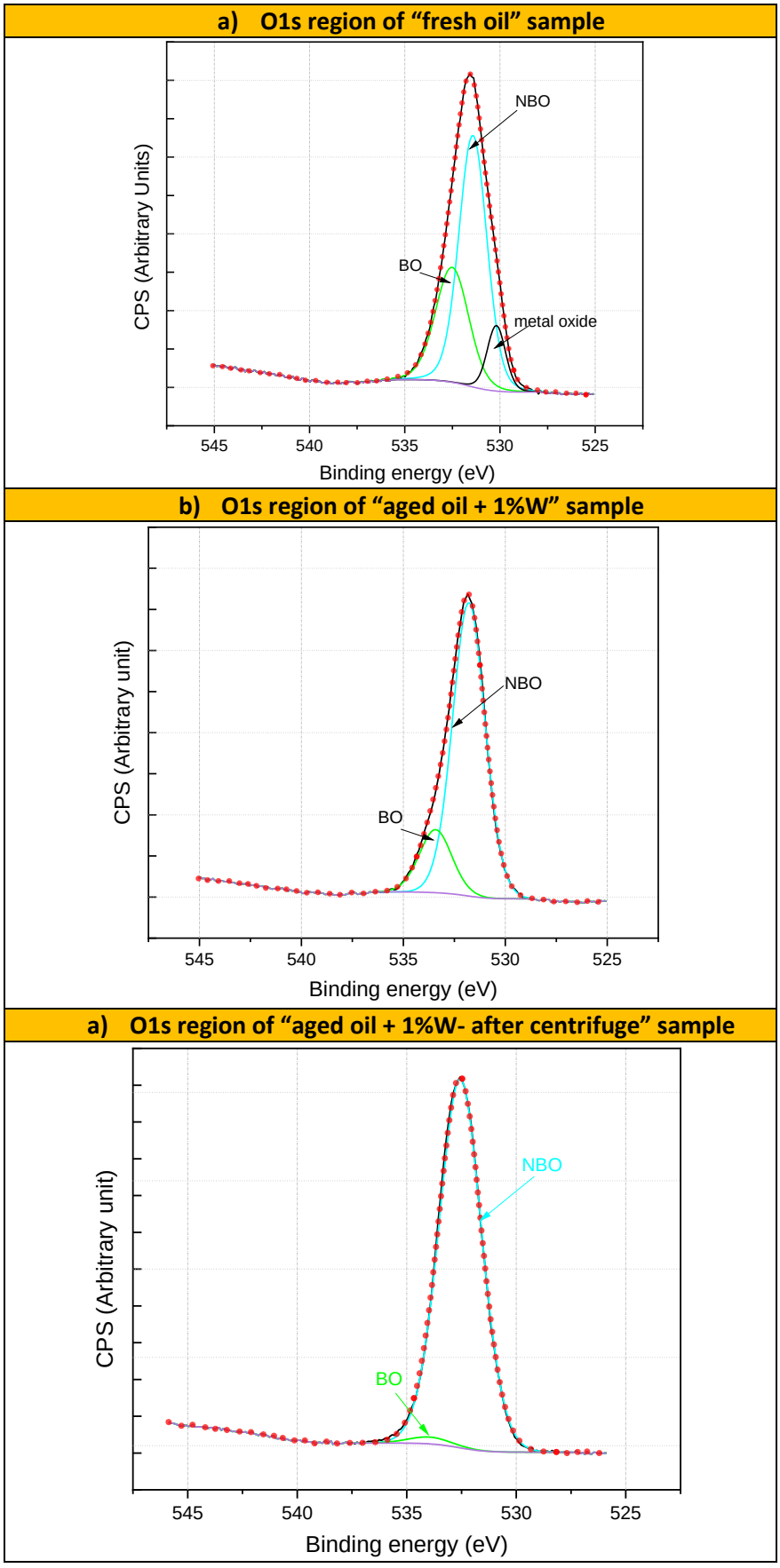

Figure 7.17: XPS oxygen 1s spectra from pins surface for oil samples a) fresh oil b) aged oil +1 %water c) aged oil+1 %water-after centrifuge.

Table 7.4: BO/NBO ratios and (Zn3s - P2p3/2) binding energy difference for the oil at different levels of water and after removing free water by centrifugation.

Tests	BO/NBO	Zn3s-P2p$_{3/2}$ Binding energy difference (eV)
Fresh oil	0.56	5.8
Aged oil + 0.3%water	0.19	6.84
Aged oil + 0.5%water	0.16	6.98
Aged oil + 1%water	0.19	6.86
Aged oil + 0.3%water-after centrifuge	0.11	6.99
Aged oil + 0.5%water-after centrifuge	0.1	6.78
Aged oil + 1%water-after centrifuge	0.03	6.85

The results are in line with other studies [252], [253] which claimed that the chain polyphosphates can be depolymerised by water to shorter chains. Equations 7.1 and 7.2 describe the mechanisms of depolymerisation of polyphosphates chains in the existence of water. The hydrolysis of polyphosphates in the presence of water occurs producing short-chain polyphosphates and phosphoric acids.

$$Zn(PO_3)_2 + 6H_2O \rightarrow Zn_7(P_5O_{16})_2\ (\text{short} - \text{chain polyphosphates}) + 4H_3PO_4 \quad 7.1$$

$$Zn(PO_3)_2 + 3H_2O \rightarrow Zn_2P_2O_7\ (\text{short} - \text{chain polyphosphates}) + 2H_3PO_4 \quad 7.2$$

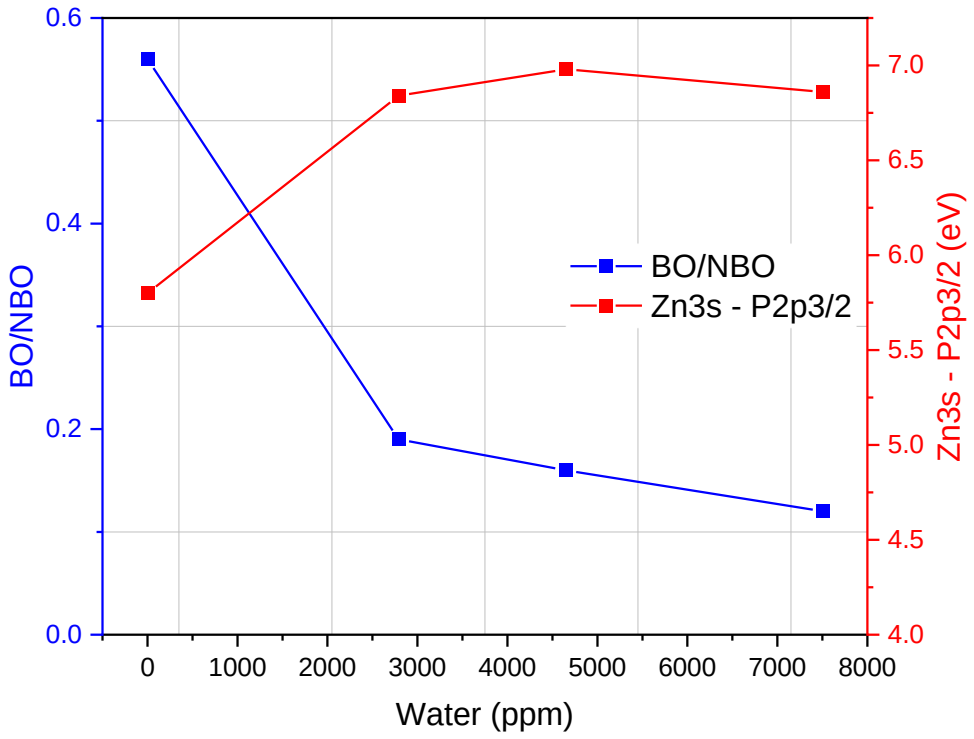

Figure 7.18: Water concentration effect on polyphosphate chain length.

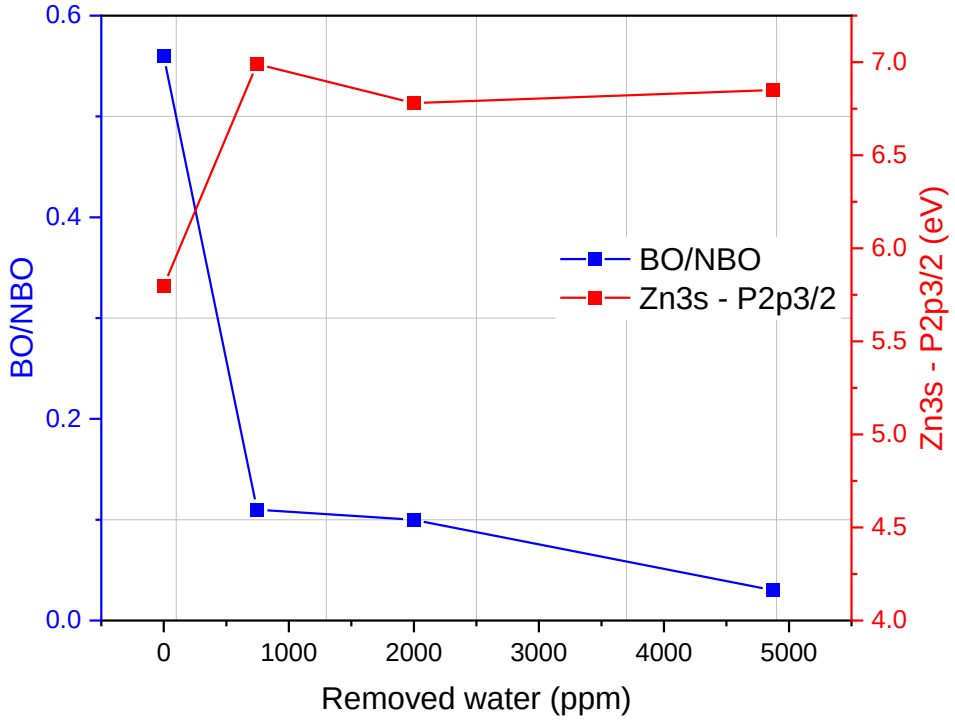

Figure 7.19: Effect of remaining water after centrifugation and additive depletion on polyphosphate chain length.

7.5 Summary

In this chapter, the existence of water in engine oil and its effects on wear, oil degradation and additive depletion were studied. The results showed that the level of dissolved water in heavy-duty used oils increased over the accumulated mileage until reaching saturation level. The water saturation curve in engine oil at different temperatures was plotted. The concentration of dissolved water in the oil was increased with an increase in the oil temperature. Wear increased with an increase in water level in the fresh oil and the oil-contaminated by CB.

After removing free water from the oil, the results proved for the first time that additives were depleted by free water. The amount of depleted additive correlated to the amount of removed water from the oil. Water in engine oil influenced the discontinuity of tribofilm, formation of short-chain polyphosphates and more micropits were observed with an increase in the water content. However, after removing free water from the oil, the results demonstrated discontinuity in the tribofilm and formation of short-chain polyphosphates due to additive depletion by water and remaining dissolved water.

8 Chapter (8) ZDDP replenishment

This chapter investigates the ZDDP replenishment process at different levels in used oil drained from the heavy-duty engine. The effect of soot on the replenishment process in the used oil is discussed. Chemical analysis of oils after replenishing with ZDDP, tribological experiments and post-surface investigations are studied. This chapter determines the critical level of added ZDDP to regain the oil performance of used oil contaminated by soot. The study explores the effect of removing soot from used oil on ZDDP replenishment. The surface analysis and chemical composition of tribofilm for reclaimed oil (without soot) after adding different levels of ZDDP are investigated. In addition, the effects of water on ZDDP replenishment in the existence of soot in used oil and after removing both soot and free water from the oil are studied. This chapter determines the main mechanisms that influence the additive concentration after reclaiming the oil from soot and water. Additive depletion in the engine, additive adsorption on soot and additive depletion by water are discussed in this chapter. The effect of depleted additive after removing contaminants (soot and water) from used oil on ZDDP replenishment is investigated. The summary of the ZDDP replenishment process in this chapter is illustrated in Figure 8.1.

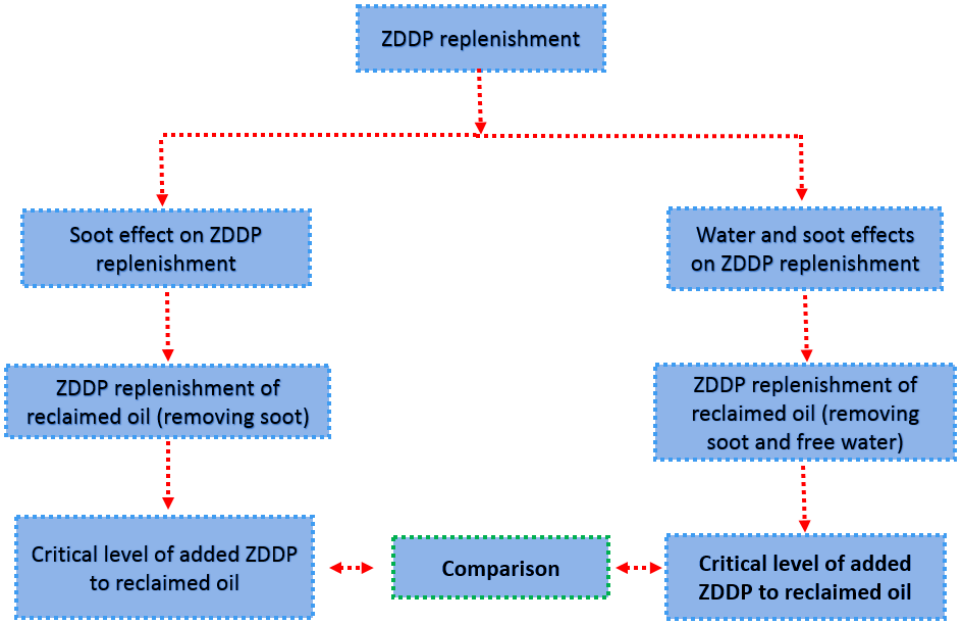

Figure 8.1: ZDDP replenishment plan used in this study.

8.1 ZDDP replenishment of used oil

8.1.1 Chemical analysis of oils

Used engine oil was drained after approximately 40000 km of driving the truck as shown in Table 6.1. ICP analysis of used oil showed a decrease in most additive elements concentration due to additives depletion as shown in Figure 6.13. ZDDP was used in this study to replenish the consumed additive in the used oil and improve its tribological performance. ZDDP contains three main elements Zn, S and P. Thus, it is expected that adding ZDDP to used oil will increase the concentration of these elements. ICP analysis after adding different levels of ZDDP was conducted as shown in Figure 8.2. The results show an increase in the concentration Zn, S and P with no change in Ca and Mg. As the level of ZDDP increases in the used oil, an improvement in the performance of used oil is expected. The reason behind this is that ZDDP promotes the formation of antiwear tribofilm to protect the rubbing surfaces from oil contamination.

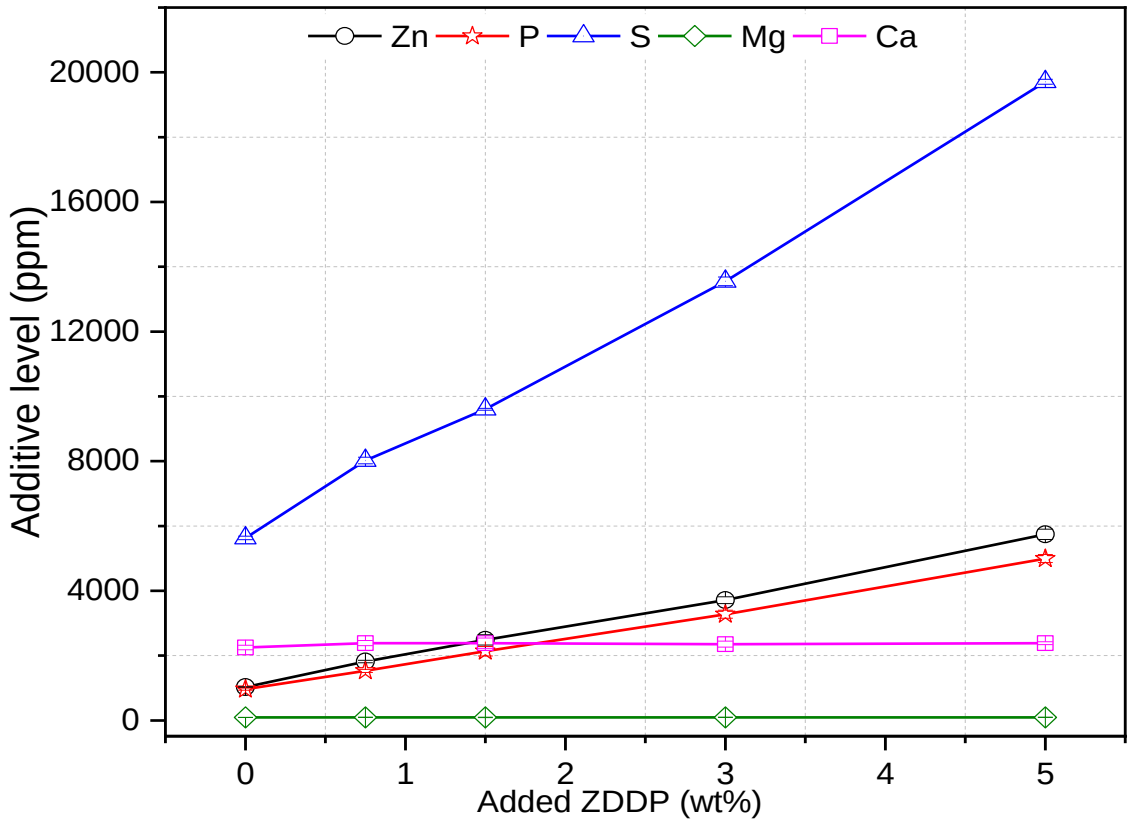

Figure 8.2: The concentration of additive elements in used oil after adding different levels of ZDDP.

8.1.2 Tribological performance

Tribological tests of used oil before and after adding different levels of ZDDP have been conducted as shown in Figure 8.2. In this study, there is the synergy of two main mechanisms that influence wear and affects the oil functionality after being used in the truck. Firstly, additive depletion or decomposition of antiwear additive that is consumed or decomposed in used oil over time causes an increase in wear as illustrated in Figure 6.9. Secondly, the existence of 0.62 wt% soot influences tribological performance and causes hard abrasive wear on the rubbing surfaces. After replenishing depleted additives in the used oil, the results demonstrate a consistent decrease in wear with the increase in the level of ZDDP in used oil. Figure 8.3 reveals that wear of used oil after adding 3 wt% ZDDP performs almost similar to the fresh oil. In this study, it can be concluded that replenishing used oil by adding 3 wt% ZDDP or more was sufficient to renew the oil functionality even in the existence of 0.62 wt% soot.

On the other hand, the soot effect on friction is variable depending on the soot level in the oil [24], [85], [254]. The higher level of soot can cause oil starvation and increase the friction coefficient [24], [85]. While it has been observed a decrease in the friction coefficient with low soot levels as soot particles act as friction modifier [254]. In this study, the friction coefficient of used oil containing 0.62 wt% soot decreases before adding ZDDP as shown in Figure 8.3. The results are in line with studies [22], [254] that demonstrated the effect of soot on friction in the existence of low soot levels. Soot acts as a friction modifier causing a decrease in friction coefficient. However, as the ZDDP is added to the oil, a higher friction coefficient resulted [191], [192]. The higher friction coefficient after adding ZDDP can be explained due to the formation of tribofilm derived from ZDDP. The reason behind this is the higher shear strength of tribofilm [191] due to an effective roughening of rubbing surfaces by the formation of uneven distribution of asperity peaks [192]. The effect of shear strength of tribofilm on friction coefficient was less when 1.5 wt% ZDDP or more existed in the used oil as shown in Figure 8.3. It appears that tribofilm roughness had a limiting effect on friction with a ZDDP level of ≥1.5 wt%.

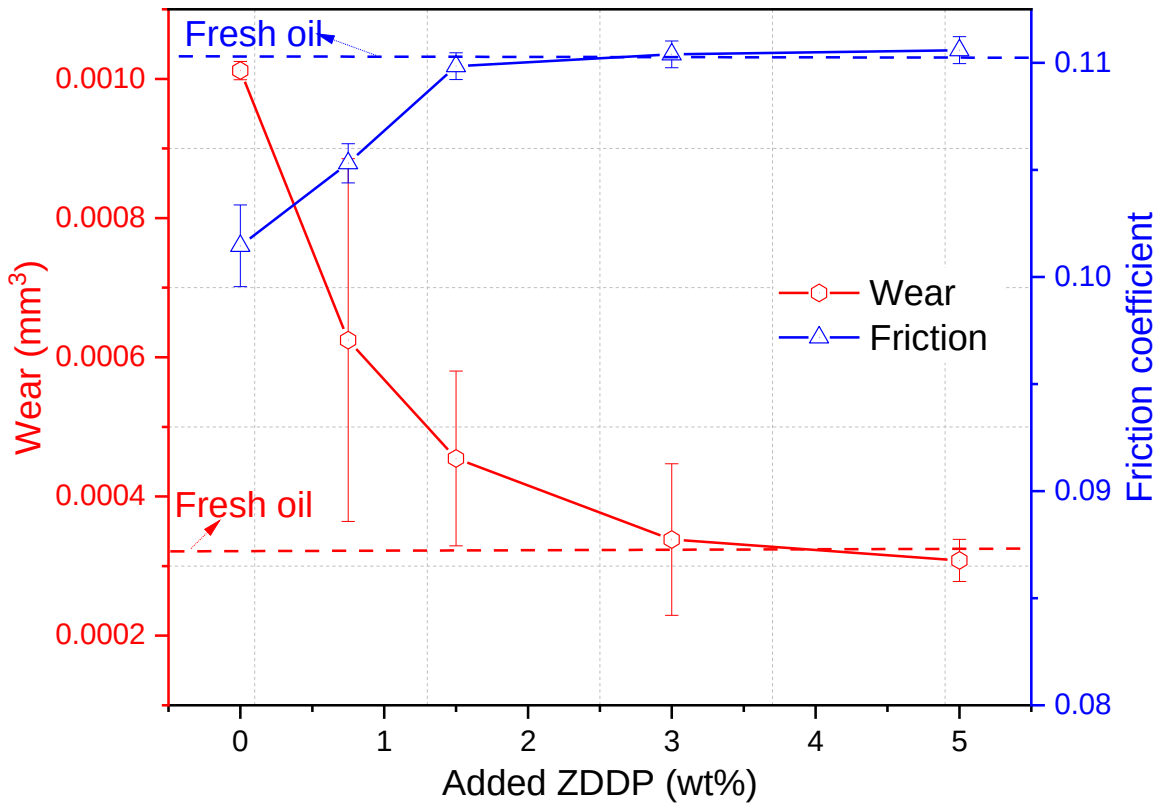

Figure 8.3: Wear and friction of used oil after adding different levels of ZDDP.

8.1.3 Surface analysis

Previous studies [24], [85] revealed that soot in engine oil causes abrasive wear on rubbing surfaces. Figure 8.4 shows SEM images of wear scar on pins of used oil and after adding ZDDP at different levels. It is expected to see abrasive wear on the surface of used oil in the existence of soot as seen in Figure 8.4a_1. Adding ZDDP to the used oil reduces the effect of soot on the surface due to the formation of the tribofilm. As known that the ZDDP level increases in the oil, a higher rate of tribofilm growth is expected and this could help to protect the surfaces from soot particles and improve the oil functionality. Figure 8.4b shows that adding 0.75 wt%ZDDP to the used oil reduces the effect of soot on surfaces significantly. There is still a few signs of abrasive wear on the surface as soot overcomes the triboflim formation and abrades on the surface as shown in Figure 8.4b. A higher rate of tribofilm formation to overcome the abrasive wear caused by soot occurred with the level of ≥1.5 wt%ZDDP. This can protect the surfaces from abrasive wear caused by soot as shown in

Figure 8.4b_1, c and c_1. No abrasive wear was detected on surfaces with the formation of uneven tribofilm as shown in Figure 8.4c_1. Adhesive wear on surfaces after adding ZDDP has been noted as displayed in Figure 8.4c, c_1. This could be due to the higher shear strength of ZDDP tribofilm between the rubbing surfaces causing adhesive wear [189], [255].

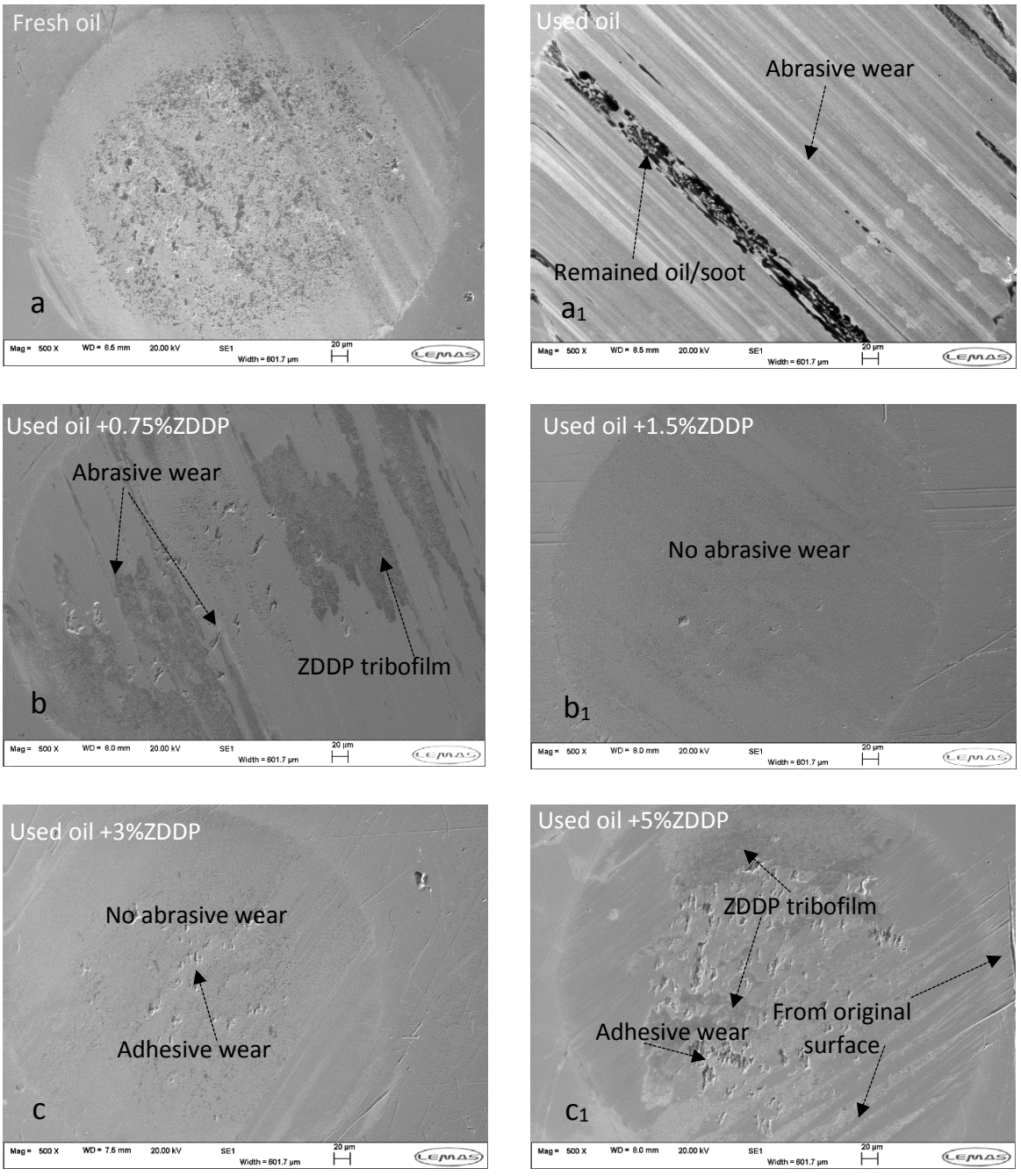

Figure 8.4: SEM images of wear scar on pins a) fresh oil a_1) used oil b) used oil+0.75 wt%ZDDP b_1) used oil+1.5 wt%ZDDP c) used oil+3 wt%ZDDP c_1) used oil+5 wt%ZDDP.

Microscope images confirm the distribution of tribofilm after adding ZDDP to the used oil compared to the fresh oil as shown in Figure 8.5. Where some regions are covered by tribofilm as shown in a dark area in wear scar, while other tribofilm regions are removed by soot. It is worth noting that ZDDP tribofilm attempts to protect the surfaces from soot particles, but soot abrades and removes the tribofilm from wear scar in some regions. Further chemical analysis of the dark area to confirm the presence of tribofilm was carried out as demonstrated in Figure 8.6b. The results prove that the dark area on the rubbing surface represents the existence of tribofilm elements on the surface compared to the light area on wear scar as shown in Figure 8.6b.

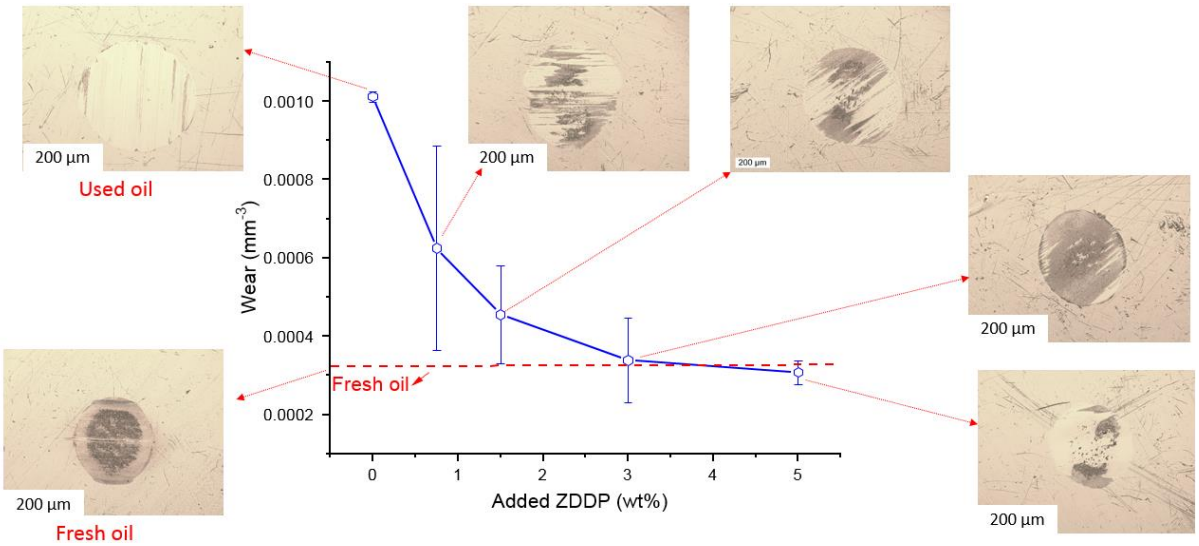

Figure 8.5: Microscope images of wear scar on pins after adding different levels of ZDDP.

8.1.4 Chemical composition of tribofilm

Energy Dispersive X-ray (EDX) analysis was conducted on the wear scar of pins to analyse the chemical composition of tribofilm. The chemical composition of the fresh oil sample at different positions demonstrates the uniform distribution of tribofilm as displayed in Figure 8.6a. EDX results revealed fully removal of the whole tribofilm causing abrasive wear on the surface in the existence of soot as shown in Figure 8.4a_1.

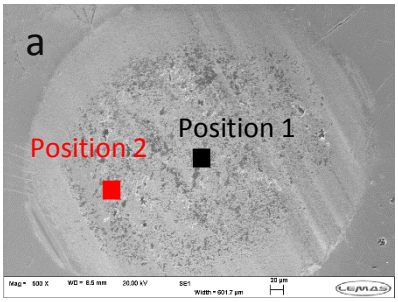

Elements	Position 1 (wt. %)	Position 2 (wt. %)
Zn	1.09	0.94
P	1.02	0.33
S	0.77	1.21
Ca	0.45	0.19
Fe	82.03	76.78
C	6.94	16.02
O	4.83	2.84
Cr	1.52	1.16
Si	0.23	0.14
Mg	1.13	0.39
Total	100	100

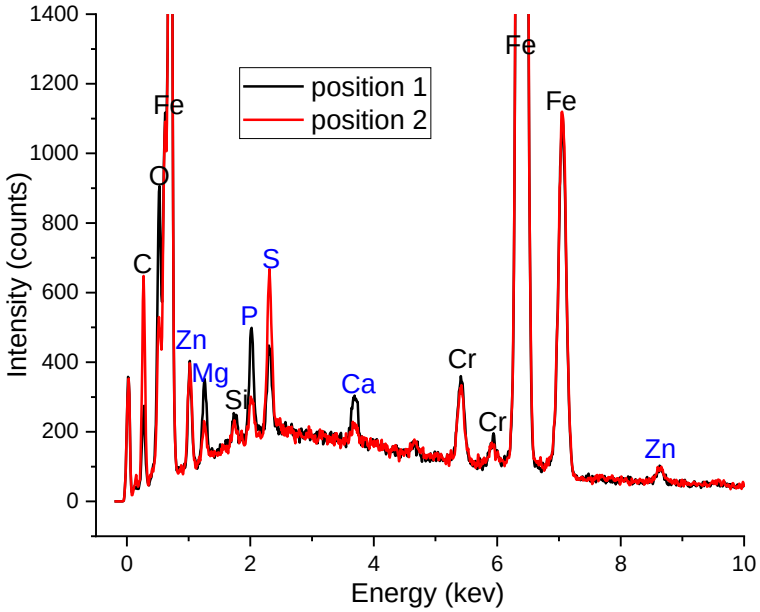

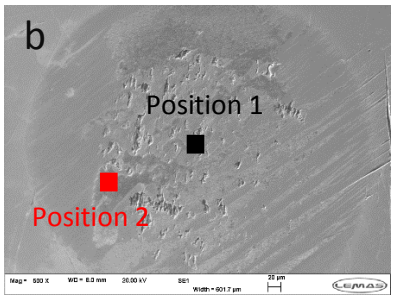

Elements	Position 1 (wt. %)	Position 2 (wt. %)
Zn	0	7.72
P	0	3.95
S	0.2	1.6
Ca	0	0.47
Fe	88.92	62.55
C	9.26	7.88
O	0	14.5
Cr	1.36	1.13
Si	0.27	0.2
Total	100	100

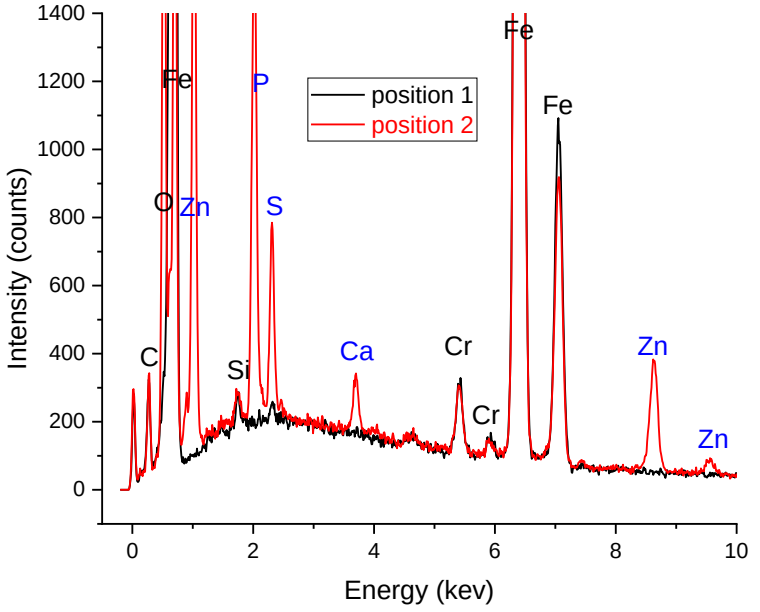

Figure 8.6: EDX chemical composition of tribofilm of wear scar on pins a) fresh oil b) used oil+5 wt%ZDDP samples at two positions. The probed depth in EDX analysis is around 1-3 µm compared to tribofilm thickness which is mostly thinner than 200 nm, which leads to much lower concentrations of P, S and Zn compared to Fe.

Adding ZDDP increased the concentration of three main elements S, Zn and P in the used oil as shown in Figure 8.2. Therefore, the concentration of these elements in the tribofilm composition is also increased compared to fresh oil as expected (Figure 8.6b at position 2). Tribofilm was not uniform on the surface after adding ZDDP (Figure 8.5) and this was confirmed by chemical analysis of tribofilm at different positions. The results proved the distribution of tribofilm is uneven in wear scar after replenishing with ZDDP in the presence of soot (Figure 8.6b). The chemical composition of tribofilm reveals the coverage of the tribofilm in some regions and the removal of tribofilm by soot in other regions. The results indicate that there is no full coverage of tribofilm on the surfaces even after adding a high level of ZDDP (5 wt%) in the existence of soot particles. Soot can overcome the formation of tribofilm and remove the tribofilm in most surface regions.

8.2 ZDDP replenishment of reclaimed engine oil

8.2.1 Tribological performance

Used oil after removing soot (reclaimed oil) performed higher wear compared to fresh oil due to the decomposition of antiwear additive and additive depletion as displayed in Figure 6.1 and Figure 6.13 respectively. Adding ZDDP at different levels to the reclaimed oil had a positive effect and decreased the amount of wear significantly as shown in Figure 8.7. As the ZDDP level increased in the oil, the amount of wear decreased gradually and the replenished oil performed better than fresh oil after adding 0.75 wt% ZDDP. Replenishing the reclaimed oil with a level ≥0.75 wt% ZDDP is sufficient to improve wear and extend the oil function. Further surface investigations are discussed in the next section to ensure no abrasive wear and fully tribofilm coverage on the surface after replenishing the additives.

Friction results as shown in Figure 8.7 reveal that the friction coefficient of reclaimed oil was less than the friction coefficient of fresh oil due to the presence of 0.26 wt% soot. Existence of these particles in oils acted as a friction modifier between rubbing surfaces reducing the friction. However, it is good to mention that the existence of 0.26 wt% soot did not affect wear

value as shown in Figure 8.7. Friction increased with an increase in the amount of ZDDP in reclaimed oil as shown in Figure 8.7. Friction coefficient starts levelling with the amount of ≥3 wt%ZDDP. The increase in friction coefficient after adding ZDDP to the reclaimed oil is due to the high roughing of tribofilm [192] or the higher shear strength of tribofilm [191]. The effect of the increase in ZDDP level on the coefficient of friction at the higher level is limited. The results are agreed with studies [189], [255] that demonstrated the effect of tribofilm on the friction coefficient can be stabilized at the high level of ZDDP.

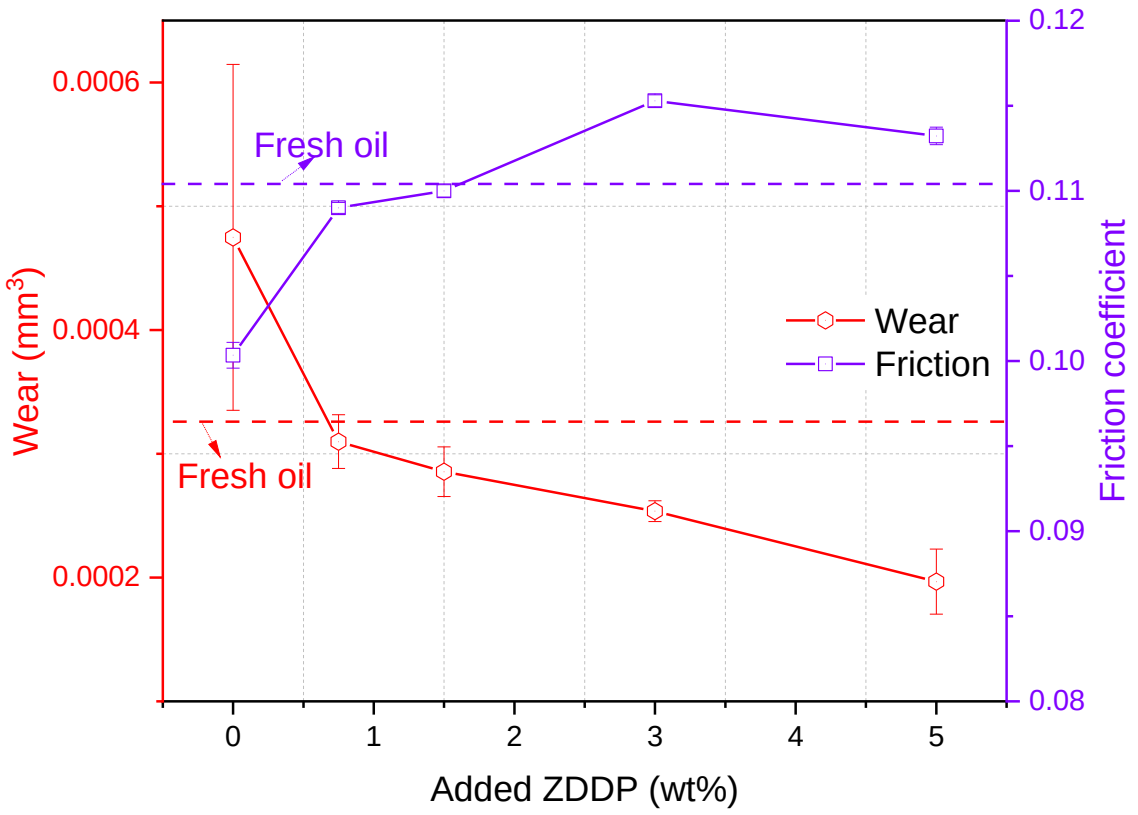

Figure 8.7: Wear and friction of reclaimed oil after adding different levels of ZDDP.

8.2.2 Surface analysis

Figure 8.8 shows the wear scar of pins after replenishing the reclaimed oil at different levels of ZDDP compared to reclaimed and fresh oil samples. Abrasive wear was detected on the wear scar surface of reclaimed oil (Figure 8.8a_1) due to the depletion and decomposition of additives. It was found that the wear value reduced significantly after adding 0.75 wt%ZDDP and the oil performed better than fresh oil as shown in Figure 8.7. The surface of wear scar

after adding 0.75 wt% ZDDP showed no abrasive wear and full coverage of tribofim as shown in Figure 8.8b. Additive replenishment at higher ZDDP percentages of 1.5, 3 and 5 wt% revealed no abrasive wear and uniform tribofilm formation as shown in Figure 8.8b_1,c, and c_1. Adhesive wear is observed after replenishing the reclaimed oil as displayed in Figure 8.8b, b_1,c, and c_1. This mostly comes from the higher shear strength of ZDDP tribofilm between the rubbing surfaces causing adhesive wear [189], [255].

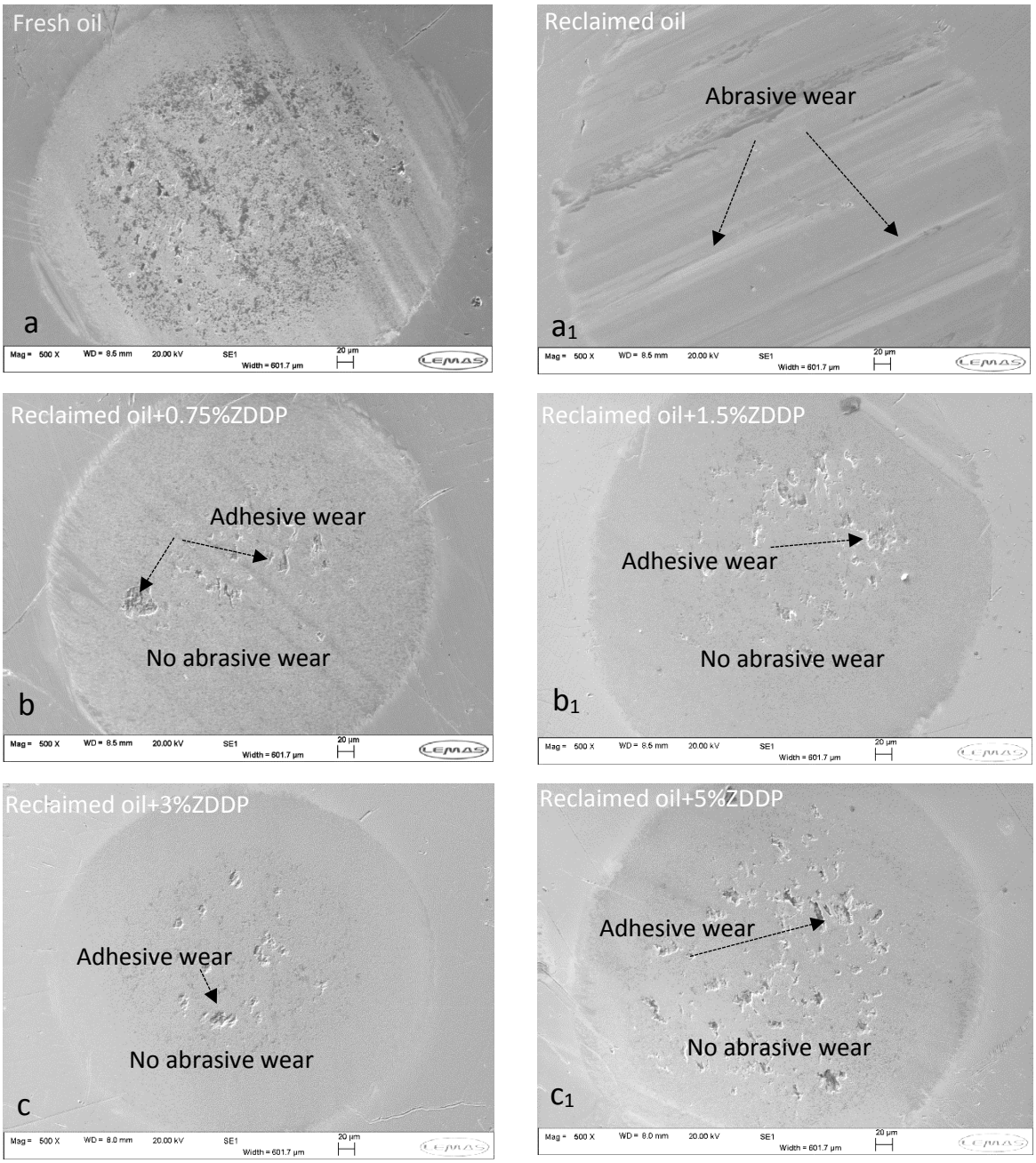

Figure 8.8: SEM images of wear scar on pins a) fresh oil a_1) reclaimed oil b) reclaimed oil+0.75 wt%ZDDP b_1) reclaimed oil+1.5 wt%ZDDP c) reclaimed oil+3 wt%ZDDP c_1) reclaimed oil+5 wt%ZDDP.

Microscope images display the distribution of tribofilm after adding ZDDP to the reclaimed oil compared to fresh oil as shown in Figure 8.9. All regions on the wear scar are protected by tribofilm represented as a dark area on the wear scar. It is evident that no abrasive wear and full coverage of ZDDP tribofilm after replenishing the reclaimed oil. Further chemical analysis of the wear scar to confirm the presence and distribution of tribofilm is carried out in the next section.

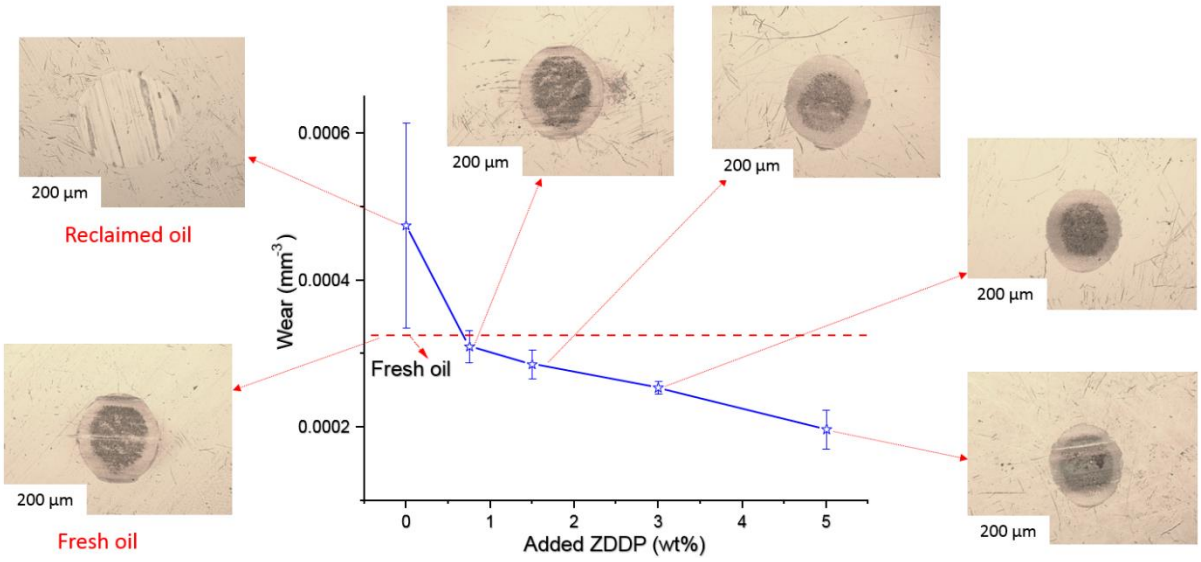

Figure 8.9: Microscope images of wear scar on pins after adding different levels of ZDDP to reclaimed oil.

8.2.3 Chemical composition of tribofilm

EDX analysis of the wear scar of pins after adding ZDDP at different levels to the reclaimed oil is presented in Figure 8.10. The results obtained from the chemical analysis of tribofilm of the reclaimed oil sample showed no ZDDP tribofilm on the surface (Figure 8.10). Chemical analysis of tribofilm after adding ZDDP to the reclaimed oil confirms the existence of tribofilm on the surface. The improvement in wear values after adding ZDDP (Figure 8.7) is reflected in the improvements in the chemistry of tribofilm. The reduction in the amount of wear after adding ZDDP (Figure 8.7) is due to an increase in the thickness of the ZDDP tribofilm. The presence of ZDDP in the reclaimed oil influences the chemical concentration of main tribofilm elements such as S, Zn and P. Figure 8.10 revealed that the higher level of ZDDP in the reclaimed oil was, the higher concentration of ZDDP elements was found in tribofilm.

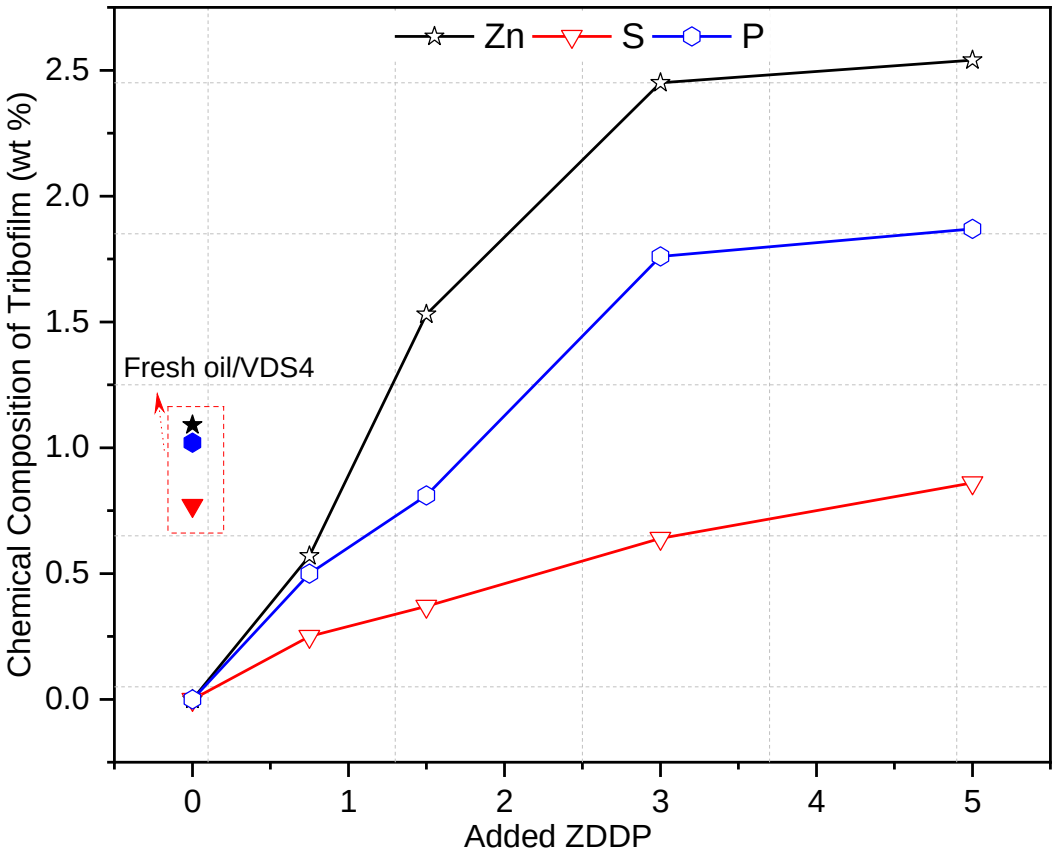

Figure 8.10: EDX chemical composition of tribofilm of wear scar on pins after adding ZDDP to the reclaimed oil.

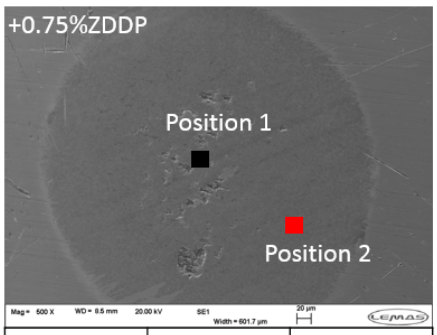

Elements	Position 1 (wt.%)	Position 2 (wt.%)
C	4.31	4.22
O	2.54	2.71
Si	0.23	0.19
P	0.56	0.72
S	0.23	0.2
Ca	0.33	0.33
Cr	1.52	1.68
Fe	89.53	88.88
Zn	0.74	1.07
Total:	100	100

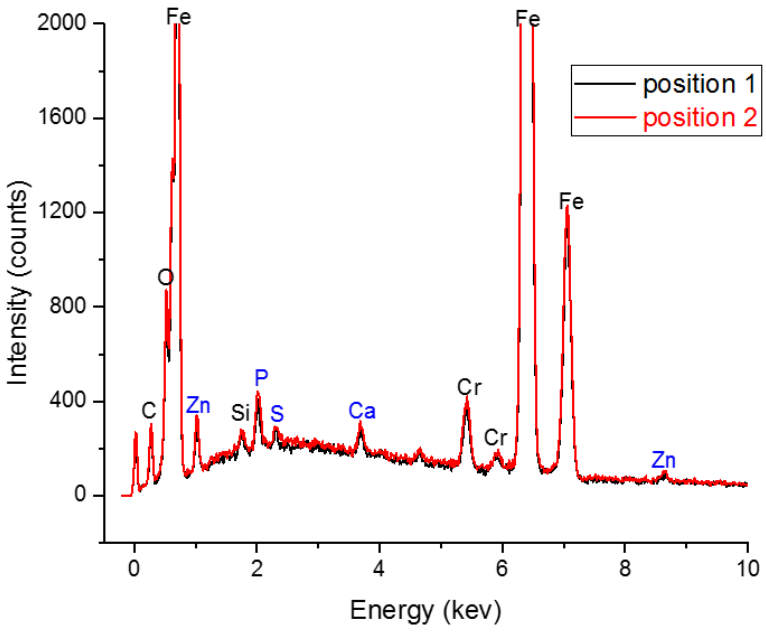

Figure 8.11: EDX chemical composition of tribofilm on the pin for the reclaimed oil+0.75 wt%ZDDP sample at two positions.

The tribofilm distribution on the surface after adding ZDDP to reclaimed oil was uniform as shown in Figure 8.11. Figure 8.11 demonstrates that the chemical analysis of tribofilm at different positions approximately has similar chemical concentrations of Zn, S and P. This leads to the conclusion that replenishing the reclaimed oil can improve the tribological performance and protect the surface by forming uniform tribofilm similar to fresh oil.

8.2.4 Critical level of added ZDDP

8.2.4.1 Chemical analysis of oils

ZDDP replenishment for reclaimed oils at the high ZDDP concentration (0.75,1.5,3 and 5 wt%) was studied in this project. The results showed adding 0.75 wt% ZDDP was enough to regain the oil performance similar to the fresh oil. Additives concentration after adding 0.75 wt% ZDDP to reclaimed oil is higher than the additive concentration in fresh oil as shown in Figure 8.12. It is important to keep the additive within desirable limits at least close or similar to the concentration of the additives in fresh oil. Therefore, adding ZDDP at a lower concentration is important to determine the critical level of added ZDDP to reclaimed oil. Adding ZDDP to reclaimed oil at the levels of 0.25,0.5 and 0.75 wt% was investigated. ICP results after adding ZDDP were demonstrated in Figure 8.12. The results identify the additive concentration in reclaimed oil at point 0 wt% added ZDDP compared to the concentration of the additive in fresh oil presented as dotted lines.

ICP analysis for oil samples after adding 0.25, 0.5 and 0.75 wt% of ZDDP shows an increase in the concentration of Zn, S and P with no change in Ca and Mg levels. This is correlated to the fact that adding ZDDP affects the concentration of Zn, S and P elements as expected. It is important to note that antiwear additive in the reclaimed oil decomposed as shown in Figure 6.2a and other additives such as dispersants/detergents could be influenced when it was used in the engine. Figure 8.12 distinguishes between the additive concentration which is already existed in the reclaimed oil and the fresh added ZDDP (shaded area). ICP results demonstrate that the critical level of adding ZDDP to reclaimed oil to be similar to the concentration of ZDDP

elements in fresh oil is located between 0.25 and 0.5 wt%. The performance of replenished oils at low levels of ZDDP will be investigated in the following sections.

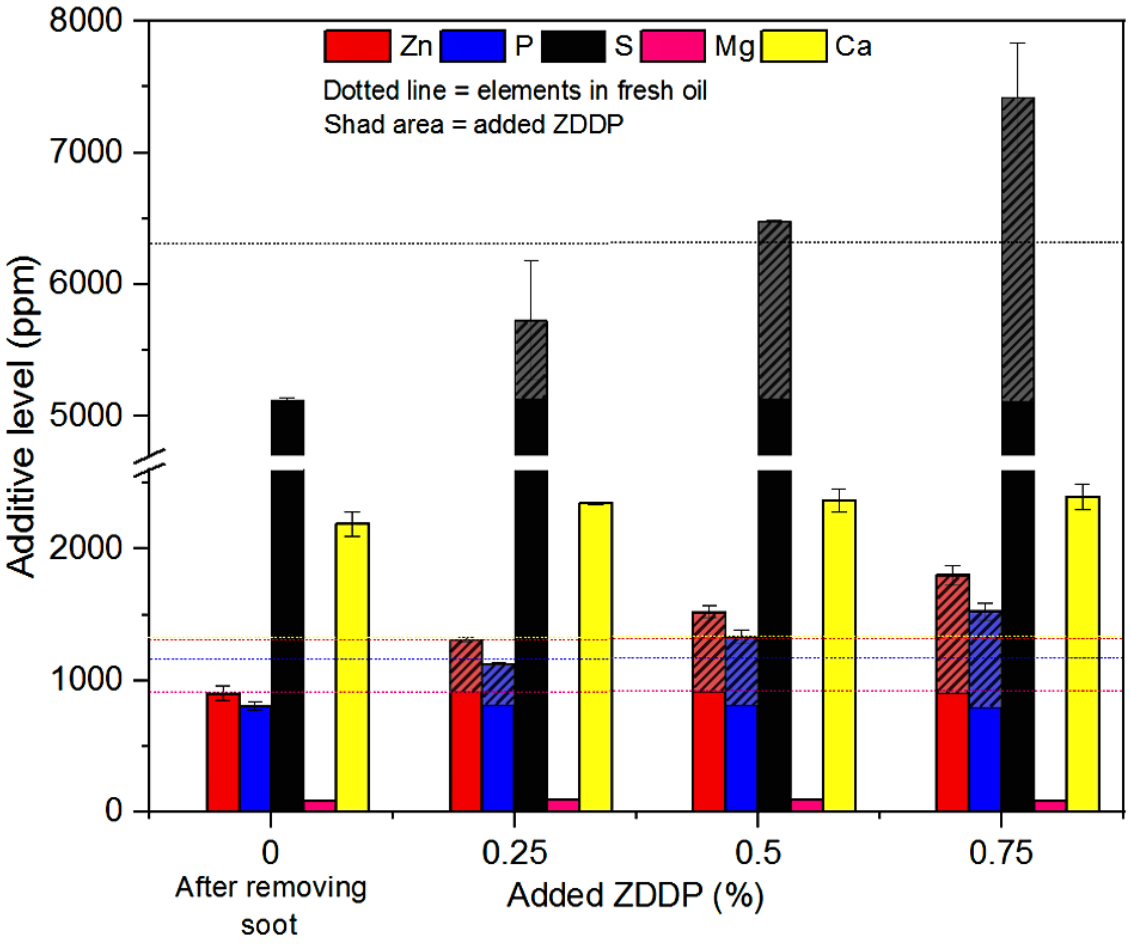

Figure 8.12: ICP results show the concentration of additive elements in the reclaimed oil after adding low levels of ZDDP. The shaded area represents the added ZDDP and the dotted lines are the concentration of additive elements in the fresh oil.

8.2.4.2 Tribological Performance

Reclaimed engine oil (after removing soot) performed higher wear, as displayed in Figure 8.13, compared to fresh oil due to the reduction in additive concentration and antiwear decomposition. Replenishing the reclaimed oil with 0.25, 0.5 and 0.75 wt% ZDDP demonstrates a decrease in the wear as shown in Figure 8.13. The results reveal that adding 0.5 wt% ZDDP to the reclaimed oil performed similarly to the fresh oil in terms of the amount of wear. There is no significant change in wear after adding 0.75 wt% ZDDP to the reclaimed

oil. Post-surface analysis for the replenished oil sample of 0.5 wt% ZDDP will provide more details about the tribofilm coverage of the rubbing surface compared to the fresh oil sample.

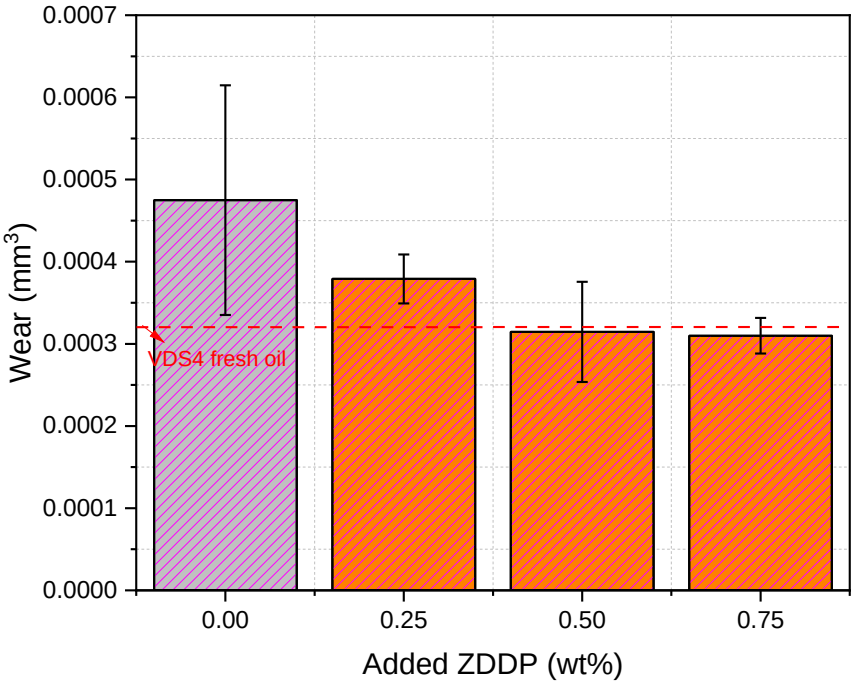

Figure 8.13: Wear of reclaimed oils after adding low levels of ZDDP.

8.2.4.3 Surface Analysis

Figure 8.14 shows surface analysis of the wear scar of pins after replenishing the reclaimed oil with different levels of ZDDP. There is no abrasive wear observed in the fresh oil sample with full coverage of tribofilm on the wear scar as shown in Figure 8.14a and a_1. Abrasive wear was detected on the wear scar of the reclaimed oil due to the reduction in additives concentration and antiwear decomposition as illustrated in Figure 8.14b and b_1. As the level of added ZDDP was increased in the reclaimed oil, the formation of ZDDP tribofilm started to cover the surface protecting the surface from abrasive wear. The surface analysis of reclaimed oil with 0.25 wt% ZDDP reveals less effect of abrasive wear compared to reclaimed oil sample as shown in Figure 8.14b and d. With the higher level of added ZDDP (0.5 wt%), a higher rate of tribofilm formation was produced to protect the surface from abrasive wear as displayed in Figure 8.14d and d_1.

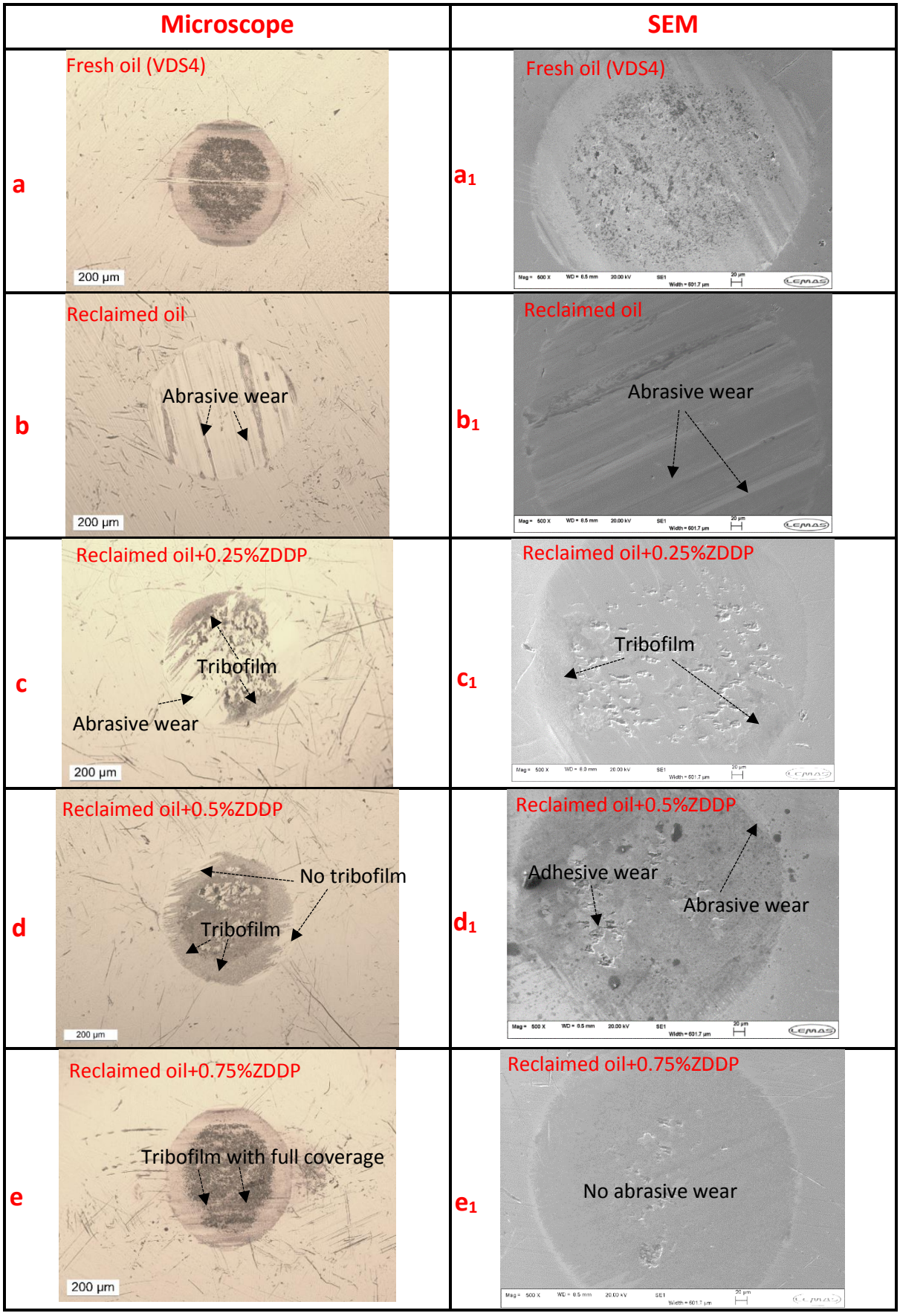

Figure 8.14: Surface analysis of wear scar on pin (microscope and SEM images) for reclaimed oils after adding 0.25, 0.5 and 0.75 wt% of ZDDP.

ZDDP replenishment of the reclaimed oil with the level of 0.75 wt% performed similarly to the fresh oil sample as shown in Figure 8.14e,e_1 and a,a_1. No abrasive wear was observed after adding 0.75 wt% with full coverage of tribofilm as shown in Figure 8.14e,e_1. Post chemical analysis using EDX will provide insightful information about the tribofilm formation on the surface.

8.2.4.4 Chemical Composition of Tribofilm

EDX results for reclaimed oils replenished with 0.25, 0.5 and 0.75 wt% ZDDP were conducted to study the chemical composition of tribofilm as shown in Figure 8.15a,b and c. EDX surface analysis was performed at different positions. The chemical composition of tribofilm demonstrated the full coverage of tribofilm after adding 0.75 wt% ZDDP to the reclaimed oil as shown in Figure 8.15c. Abrasive wear disappeared after adding 0.75 wt% ZDDP to the reclaimed oil. The chemical composition of tribofilm of 0.75 wt% ZDDP sample at different positions confirms the existence of tribofilm at the high concentration of tribofilm elements (Zn, S and P). However, surface analysis after adding 0.25 or 0.5 wt% ZDDP to reclaimed oil showed that abrasive wear in some regions exists with partial coverage of tribofilm. EDX results show the absence of tribofilm elements (Zn, S and P) at position-2 compared to position-1 on the same surface, as illustrated in Figure 8.15a and b. This leads to the conclusion that adding 0.25 or 0.5 wt% ZDDP to the reclaimed oil was not enough to form tribofilm on the whole surface.

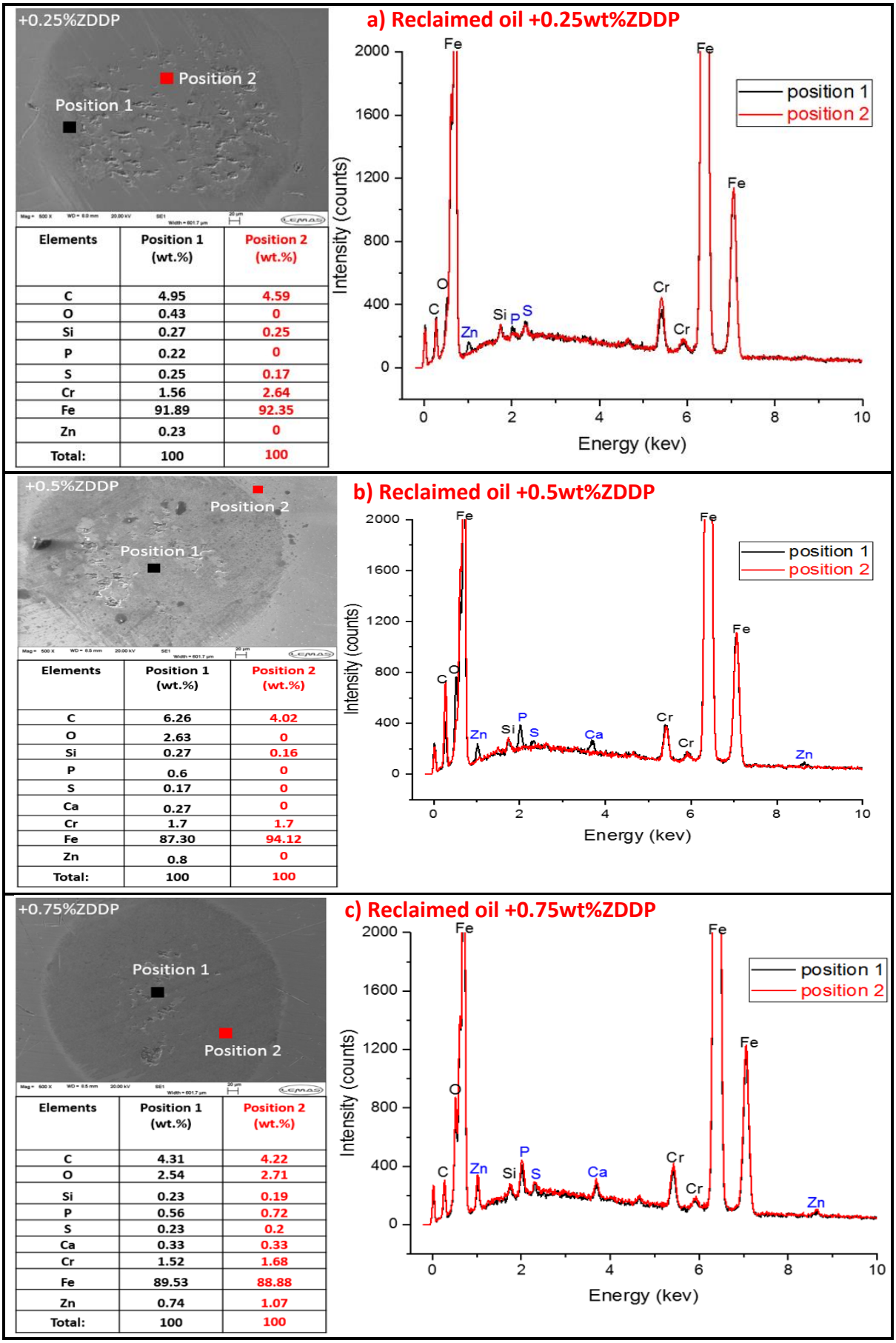

Elements	Position 1 (wt.%)	Position 2 (wt.%)
C	4.95	4.59
O	0.43	0
Si	0.27	0.25
P	0.22	0
S	0.25	0.17
Cr	1.56	2.64
Fe	91.89	92.35
Zn	0.23	0
Total:	100	100

Elements	Position 1 (wt.%)	Position 2 (wt.%)
C	6.26	4.02
O	2.63	0
Si	0.27	0.16
P	0.6	0
S	0.17	0
Ca	0.27	0
Cr	1.7	1.7
Fe	87.30	94.12
Zn	0.8	0
Total:	100	100

Elements	Position 1 (wt.%)	Position 2 (wt.%)
C	4.31	4.22
O	2.54	2.71
Si	0.23	0.19
P	0.56	0.72
S	0.23	0.2
Ca	0.33	0.33
Cr	1.52	1.68
Fe	89.53	88.88
Zn	0.74	1.07
Total:	100	100

Figure 8.15: EDX chemical composition of the tribofilm of wear scar on pins after adding ZDDP (0.25, 0.5 and 0.75 wt%) to the reclaimed oil.

8.3 Water effect on ZDDP replenishment

8.3.1 Water effect on ZDDP replenishment in the existence of soot

The effect of water on the performance of fresh oil was investigated in Chapter 7. The results showed an increase in wear with the increase in the water level in the oil and no significant change in wear at a level less than 2000 ppm as revealed in Figure 7.8. Moreover, water at different levels caused an increase in wear even in the existence of 1 wt% CB in the oil as demonstrated in Figure 7.9. The effect of water on ZDDP replenishment in the used oil containing soot was studied as shown in Figure 8.16. In this study, 1 wt% of water was aged with used oil for 48 hrs and 500 rpm of stirring speed at the temperature of 80 °C. Ageing parameters were chosen to ensure that water molecules in oil can interact with additives sufficiently [165], [166]. Used oil (YK63UFD) details are presented in Table 6.1. While water and soot levels before and after ageing are demonstrated in Table 8.1.

ZDDP replenishment for used oil and used oil after ageing with 1 wt% water has been investigated as shown in Figure 8.16. ZDDP replenishment results for used oil revealed a decrease in wear with the increase in the percentage of added ZDDP. At 3 wt% percentage of added ZDDP, where the performance of replenished oil produced approximately similar the amount of wear compared to the fresh oil. Ageing the used oil with 1 wt% water shows higher wear performance compared to the wear of the used oil sample as demonstrated in Figure 8.16. This is due to the high polarity of water molecules that can affect the formation and adhesion of tribofilm on contact surfaces [26], [168], [169]. The contact surfaces might face more abrasive wear caused by soot without the primary protection which comes from the formation of tribofilm on the contact surfaces.

However, ZDDP replenishment for used oil containing 1 wt% water demonstrates a decrease in wear with the increase in the percentage of added ZDDP as shown in Figure 8.16. The presence of water influences the wear even after adding ZDDP at varied levels causing higher wear compared to ZDDP replenishment of the used oil. It can be noted that it was difficult to

perform similar to fresh oil even after adding 5 wt% ZDDP. The results are in line with other studies [149]–[151] that stated that water contamination had a significant effect on wear and tribofilm formation. Water in the oil in the existence of temperature affects the formation and growth of tribofilm leading to higher wear [249]. Fitch and Jaggernauth [26] showed that antiwear additive, which forms tribofilm at a high temperature, can be destroyed even by a slight amount of water in the oil.

Table 8.1: The details of used oil (YK63UFD) that was aged with 1 wt% water for 48hrs and centrifuged 4-times to remove both soot and free water from the used oil.

Contamination	Before ageing	After ageing (48hrs)	After centrifuge(4x)
Soot (wt%)	0.62	0.62	0.26
Water (ppm)	11720	8154	3400

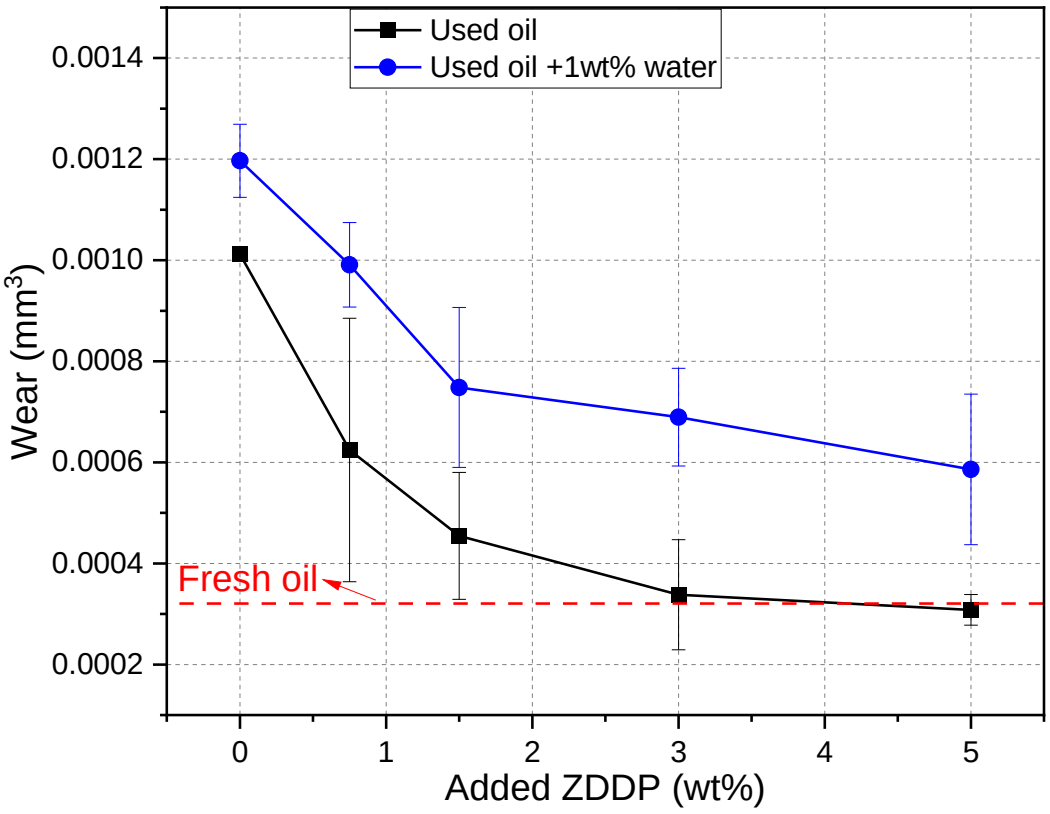

Figure 8.16: Wear of used oil replenished with different levels of ZDDP in the existence of soot and 1 wt% water compared to ZDDP replenishment of used oil in the absence of water.

8.3.2 Additive depletion by soot and water

Additives adsorption on soot and additive depletion by water were studied individually when it existed in the oil as shown in Figure 6.13 and Figure 7.11 respectively. In order to study the effect of both soot and water on additives depletion, additives elemental concentration was measured using ICP before and after the removal of both soot and water from the oil. The concentration of soot and water in the oil was also measured before and after centrifugation as displayed in Table 8.1. Additives adsorption on soot was already studied in detail in section 6.5. The results showed a decrease in the elemental concentration due to additives adsorption on soot as demonstrated in Figure 6.13.

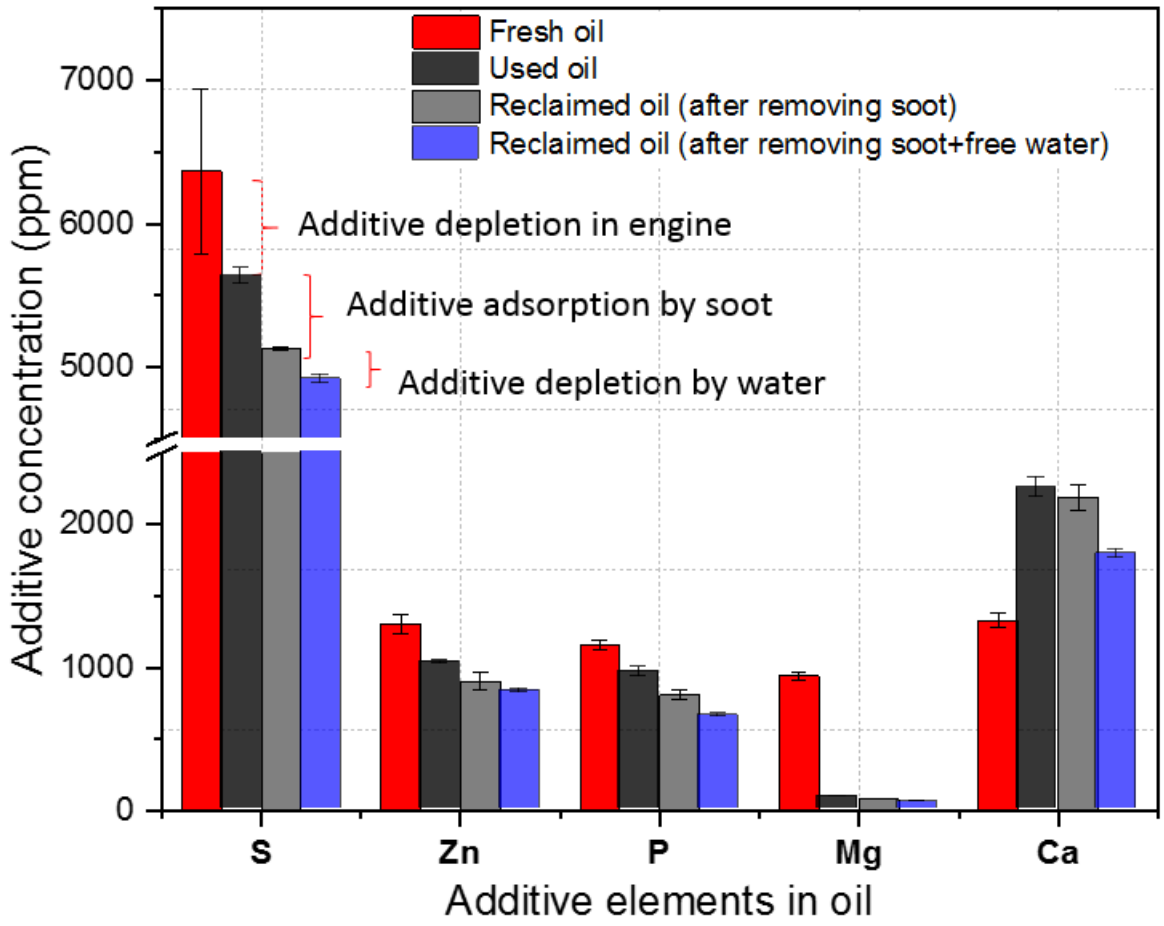

Figure 8.17: ICP chemical analysis of the reclaimed oil after removing soot and free water compared to the reclaimed oil after removing just soot.

ICP results in Figure 8.17 demonstrate much additives were depleted when both soot and water were removed from the oil. The decrease in the elemental concentration of additives,

as shown in Figure 8.17, is due to both additive adsorption on soot and additive depletion by water. The results in this study prove that additive concentration in engine oil can be decreased due to additive depletion during the use in the engine, additive adsorption on soot and additive depletion by water.

8.3.3 ZDDP replenishment of reclaimed oil

ZDDP replenishment of reclaimed oil after removal of soot was studied in Figure 8.7. The results showed that adding 0.75 wt% ZDDP was sufficient to regain the oil functionality as demonstrated in Figure 8.13. While additives were depleted after removing the free water from the oil and caused an increase in the wear as shown in Figure 7.11 and Figure 7.15. Further investigations showed that additives adsorption on soot and additive depletion by water (see Figure 8.17) occurred after removing soot and free water from heavy-duty used oil. The remained soot and water after centrifugation are presented in Table 8.1. The remained soot in the oil is 0.26 wt% which did not affect the wear as revealed in Figure 6.9. There is also still dissolved water (3400 ppm) in the reclaimed oil which is difficult to be removed from the oil.

ZDDP replenishment after removing both soot and water to a certain level from used oil was performed as shown in Figure 8.18. The used oil after removing both soot and free water demonstrates higher wear performance due to additive adsorption on soot, additive depletion by water and remaining dissolved water in the oil. Replenishing the reclaimed oils after removing soot or after removal of both soot and water demonstrate a decrease in wear with an increase in ZDDP percentage to the oil as expected. However, the reclaimed oils almost performed similarly to fresh oil after adding 0.75 wt% ZDDP. ZDDP replenishment at a percentage lower than 0.75 wt% after removing both soot and water will be discussed in the next sections.

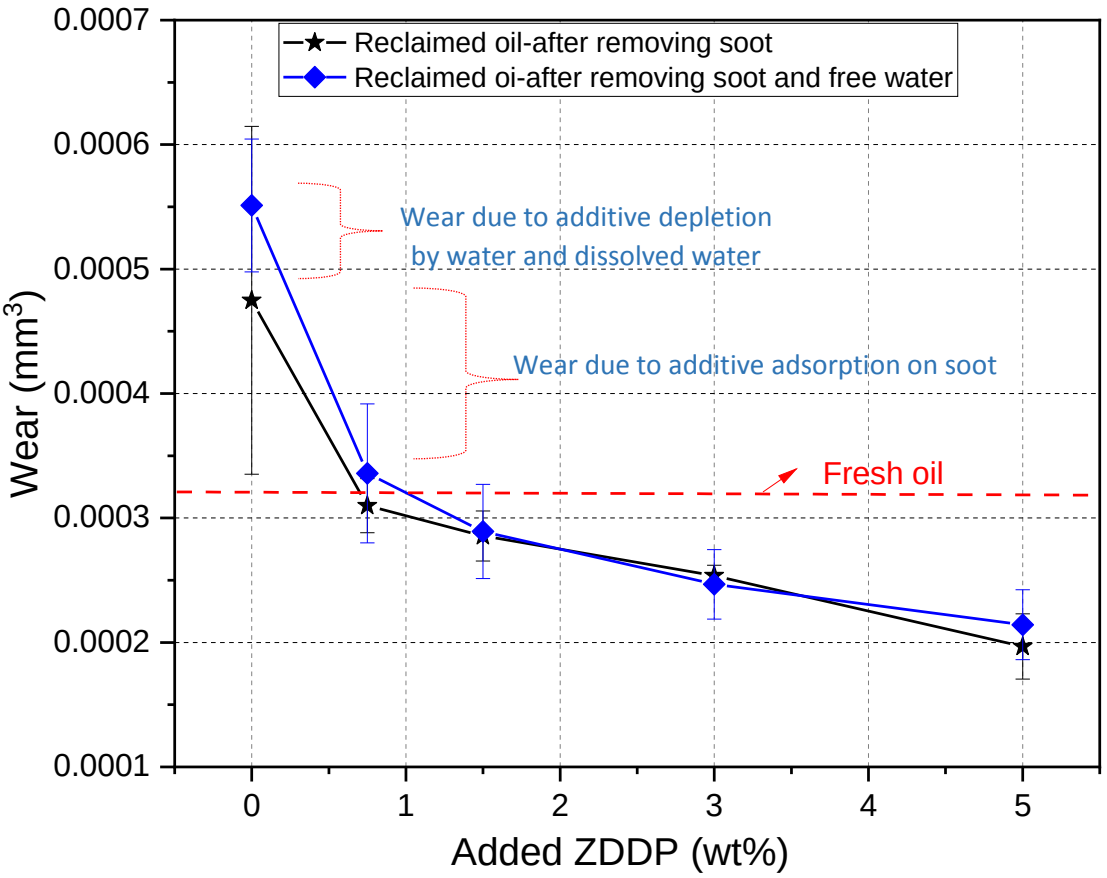

Figure 8.18: Wear of the reclaimed oils after replenishing with ZDDP at different levels.

8.3.4 Critical level of added ZDDP

8.3.4.1 Chemical analysis of oils

ZDDP replenishment of reclaimed oil after removing both soot and water at the high concentration (0.75,1.5,3 and 5 wt%) was studied in the previous section. The results showed that adding 0.75 wt% ZDDP was almost enough to regain wear value similar to the fresh oil as shown in Figure 8.18. Additives concentration after adding 0.75 wt% ZDDP to the reclaimed oil is higher than the additive concentration in the fresh oil as shown in Figure 8.19. It is important to keep the additive within desirable limits close or similar to the concentration of the additives in fresh oil. Therefore, adding ZDDP at low concentrations is important to determine the critical level of added ZDDP to the reclaimed oil. Adding ZDDP to the reclaimed oil at the levels of 0.25,0.5 and 0.75 wt% was investigated. ICP results after adding ZDDP were demonstrated in Figure 8.19. The results determine the additive concentration in the

reclaimed oil (after removing soot and free water) at point 0 wt% added ZDDP compared to the concentration of the additive of the fresh oil represented as dotted lines.

ICP analysis for oil samples after adding 0.25, 0.5 and 0.75 wt% of ZDDP shows an increase in the concentration of Zn, S and P with no change in Ca and Mg levels. This is correlated to the fact that adding ZDDP affects the concentration of Zn, S and P elements as explained before. It is important to note that antiwear additive in the reclaimed oil decomposed as shown in Figure 6.2a and other additives such as dispersants/detergents could be influenced when it was used in the engine. Therefore, it is important to distinguish between the antiwear additive which is already existed in the reclaimed oil and the fresh added ZDDP (shaded area). The critical level of adding ZDDP in the reclaimed oil is located between 0. 5wt and 0.75 wt% to get a similar level of ZDDP in the fresh oil. The performance of replenished oils at low levels of ZDDP will be investigated in the following sections.

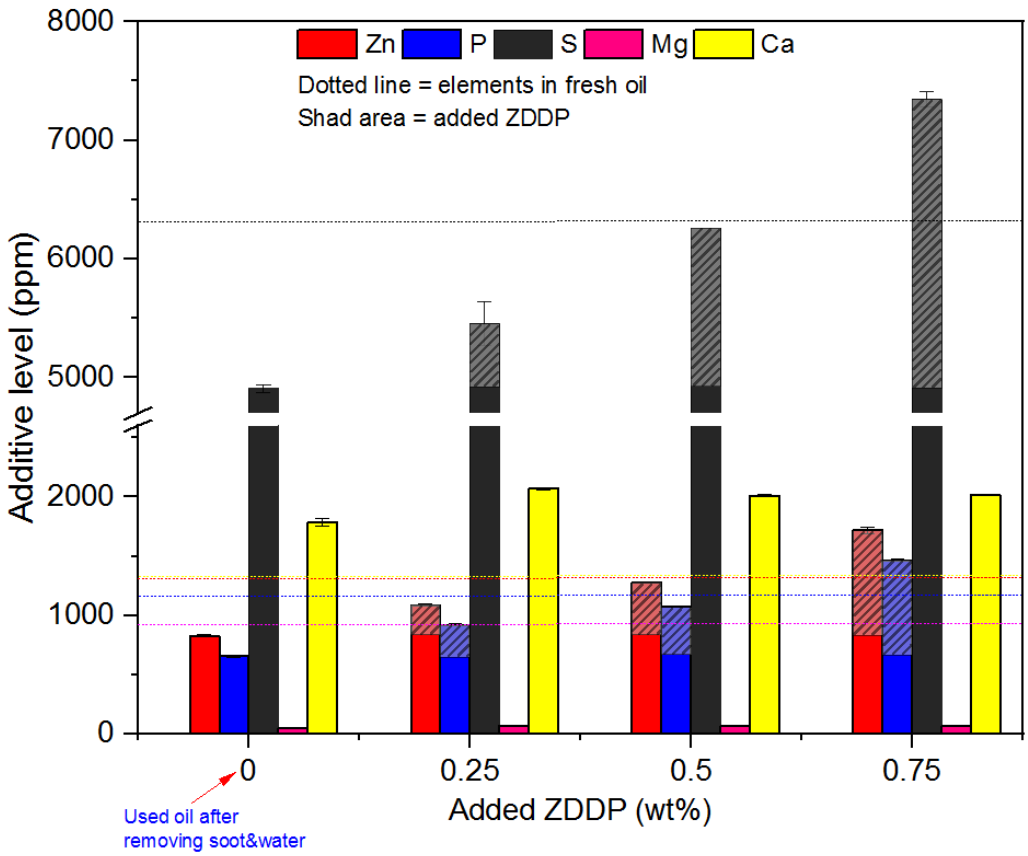

Figure 8.19: ICP results show the concentration of additive elements in the reclaimed oil after adding low levels of ZDDP. The shaded area represents fresh added ZDDP and the dotted lines are the concentration of additive elements in the fresh oil.

8.3.4.2 Tribological performance

ZDDP replenishment process at low levels of ZDDP was investigated after removing soot and water from the used oil. The reclaimed oil performed higher wear (see Figure 8.20) compared to fresh oil due to the reduction in additive concentration and remaining contaminants. Replenishing the reclaimed oil with 0.25,0.5 and 0.75 wt% ZDDP demonstrates a decrease in the amount of wear as shown in Figure 8.20. The results reveal that wear after adding 0.75 wt% ZDDP to the reclaimed oil has approximately similar to wear of the fresh oil. Post-surface analysis for the replenished oil sample of 0.75 wt% ZDDP will provide more details about the tribofilm coverage of the rubbing surface compared to the fresh oil sample.

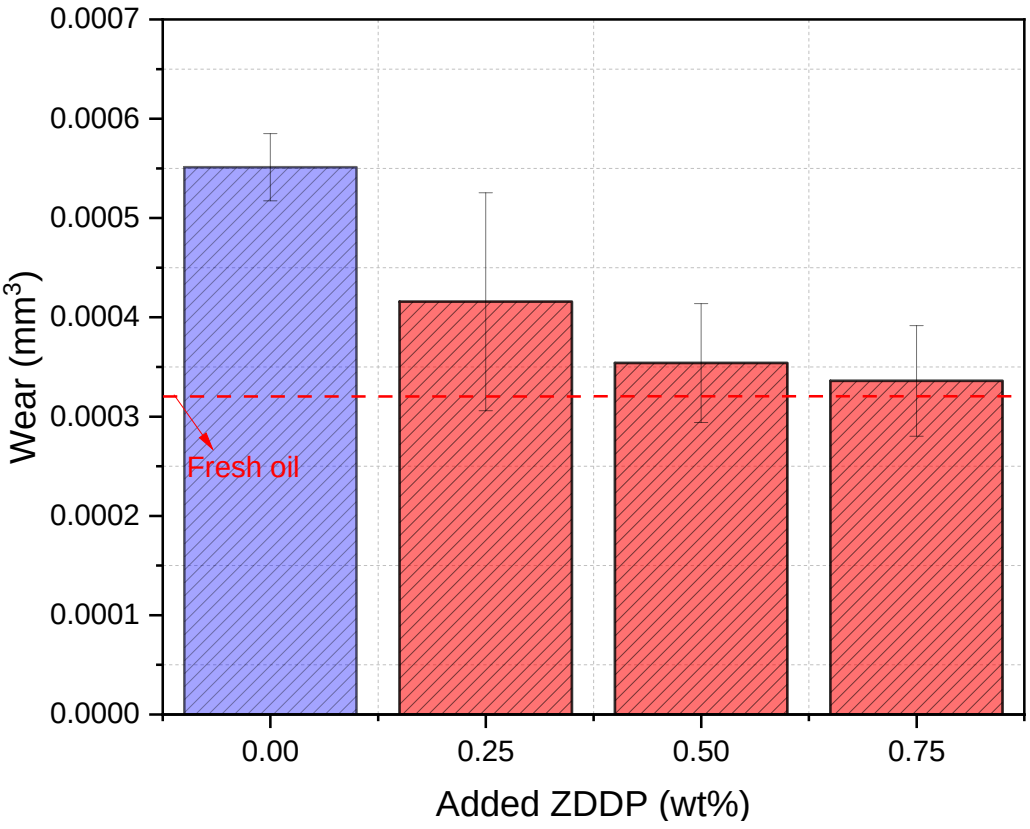

Figure 8.20: Wear of reclaimed oil (after removing soot and free water) after adding low levels of ZDDP.

8.3.4.3 Surface analysis

Figure 8.21a a_1,b b_1 and c c_1 show the surface analysis of the wear scar of pins for fresh oil, reclaimed oil (after removing soot and free water) and after replenishing the reclaimed oil with 0.75 wt% ZDDP respectively. Microscope and SEM images of fresh oil sample as displayed

in Figure 8.21a and a_1 reveal full coverage of tribofilm and no abrasive wear was detected on the surface. The results demonstrate abrasive wear in wear scar of the reclaimed oil with no tribofilm was observed in Figure 8.21b and b_1. Three main mechanisms caused the abrasive wear on the contact surface firstly, additive depletion in the engine secondly, additive adsorption on soot and finally additive depletion by water. Replenishing the reclaimed oil after adding 0.75 wt% ZDDP reduced the amount of wear as shown in Figure 8.20.

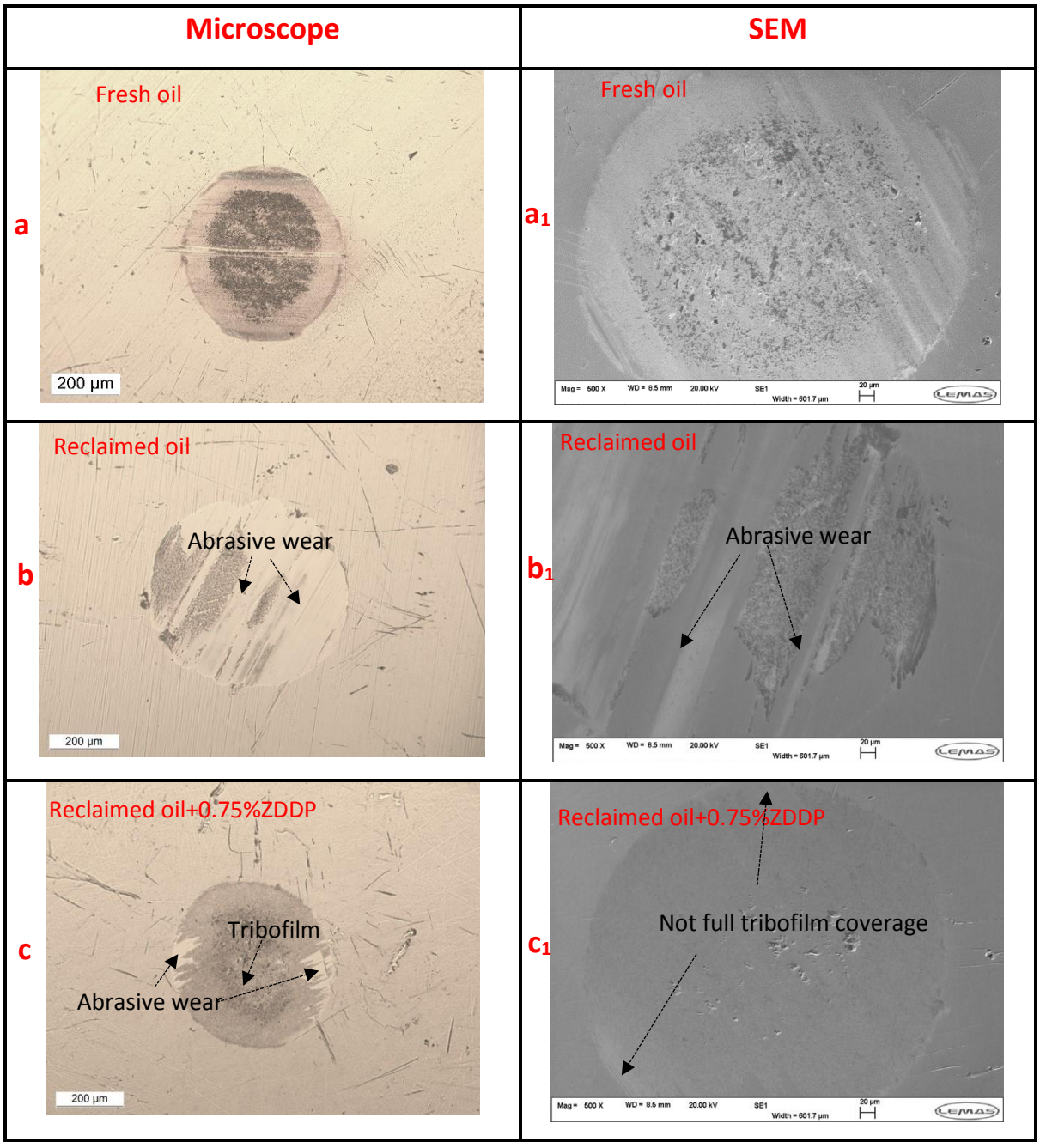

Figure 8.21: Surface analysis of wear scar on pins (microscope and SEM images).

Microscope and SEM images confirm the improvement in the contact surface compared to the reclaimed oil sample as illustrated in Figure 8.21c and c_1. The results show that the surface was mostly covered by tribofilm with existing abrasive wear in small regions. Chemical analysis of tribofilm in the next section can confirm further details about tribofilm coverage on the surface after replenishing with 0.75 wt% ZDDP.

8.3.4.4 Chemical composition of tribofilm

Surface analysis of reclaimed oil sample reveals no tribofilm on the surface as shown in Figure 8.21c and c_1. Replenishing the reclaimed oil by adding 0.75 wt% ZDDP indicates a significant improvement in the tribofilm formation covering the wear scar. However, abrasive wear was observed in some regions. EDX results after adding 0.75 wt% ZDDP confirm the absence of tribofilm in these regions (position1) as shown in Figure 8.22 compared to the rest regions of the wear scar (position2).

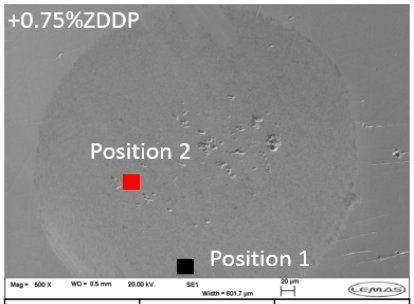

Elements	Position 1 (wt.%)	Position 2 (wt.%)
C	4.23	4.68
O	0	2.13
Si	0.25	0.21
P	0	0.36
S	0	0.23
Ca	0	0.15
Cr	1.46	1.37
Fe	94.06	90.25
Zn	0	0.62
Total:	100	100

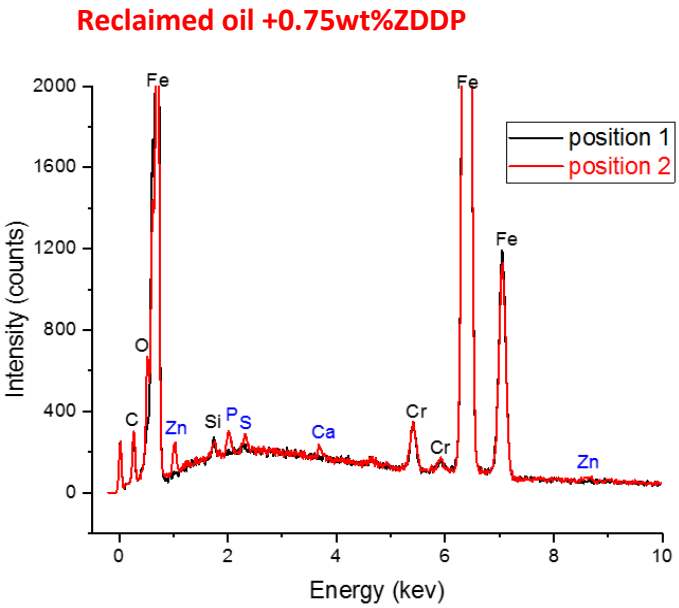

Figure 8.22: EDX chemical composition of tribofilm of wear scar on pin after adding 0.75 wt% ZDDP to the reclaimed oil.

The results prove that replenishing the reclaimed oil by adding 0.75 wt% ZDDP did not perform as well as the fresh oil. This comes from the fact that removing the soot and free water causes

additive adsorption on soot and additive depletion by water as revealed in Figure 8.17. In addition, dissolved water is another factor in the reclaimed oil that can influence tribofilm formation inducing higher wear [26], [168], [169].

8.4 Summary

In this chapter, the effect of ZDDP replenishment on the tribological performance of heavy-duty used oil was investigated for the first time. The findings from this study have not been published or investigated before. Tribological and surface analysis of the oil sample after adding 3 wt% ZDDP showed the possibility of regaining the oil function even in the presence of soot. Removal of soot to a certain level and replenishing the reclaimed oil reduced the wear and improved the oil function. The chapter investigated the critical level of added ZDDP to the reclaimed oil which can perform similar to the fresh oil. The results showed that replenishing the reclaimed oil with 0.75 wt% ZDDP was enough to regain the oil performance. However, adding 0.5 wt%ZDDP to the reclaimed oil reduced wear value to be similar to the fresh oil, but there was no complete tribofilm coverage on rubbing surfaces.

The effect of water on the ZDDP replenishment process in heavy-duty used oil was studied in this chapter. The results showed that water contamination influenced the replenishment process causing higher wear. Removing the soot and water contamination from the oil caused additive adsorption on soot and additive depletion by water. Replenishing the reclaimed oil showed that dissolved water and additive depletion by water influenced ZDDP replenishment at a level of less than 0.75 wt%. Adding 0.75 wt% ZDDP to the reclaimed oil was enough to reduce the amount of wear to get a similar wear value to the fresh oil, but there was no full coverage of tribofilm.

It can be summarised that adding 0.75 wt% ZDDP to the reclaimed oil was enough if the soot was considered as the only contaminant in the used oil. However, if both water and soot existed in the used oil, a higher level of ZDDP (>0.75 wt%) is required to regain the fresh oil function.

9 Chapter (9) Discussion

This chapter summarises and discusses the most important findings presented throughout the thesis. The discussion will be concentrated on the data obtained from experimental techniques. The chapter is divided into four main sections. The first section discusses oil degradation, additive adsorption on CBP, the effect of oil degradation on oil performance, the effect of CBP on engine performance and the link between the mechanical properties of CBP and wear. Section two discusses the effect of soot on the reclamation of heavy-duty oils. This section considers the efficiency of depth filters to remove the soot from the oil and the link between removing soot and the reclamation of used oil. Section three discusses the effect of water contamination on engine oil. This section includes the relationship between water saturation level and additive depletion, the effect of water on wear and the effect of water on oil reclamation. The final section discusses ZDDP replenishment in heavy-duty used oils. This section discusses the effect of soot and water on ZDDP replenishment in engine oils.

9.1 CBP effect on engine oil

The effects of CBP on tribological performance, additive adsorption on CBP, and oil degradation according to experimental ageing standards are investigated in Chapter 5. This section provides a detailed discussion of the results presented in Chapter 5. This is important in order to understand the effect of soot on engine oil degradation, additive adsorption and oil reclamation using a lab-based artificial ageing method.

9.1.1 Engine oil degradation

The chemical structure of bulk oils was investigated under ageing conditions with different levels of CBP. Chemical analysis of the oils showed three influenced regions in FTIR spectra, which correlate to antiwear decomposition and formation of degradation products, as illustrated in Figure 5.2. The $P-O-C$ band corresponds to the antiwear additive (ZDDP) [225]–[227] as shown in Figure 5.3a. The $P-O-C$ band in oil samples after ageing disappeared as shown in Figure 5.3a. This means that the antiwear additive has been either

depleted or decomposed during the ageing process. These results are in line with other studies [10], [96], showing that ageing the oil at high temperature (>100 °C) causes decomposition or depletion of antiwear additive. Degradation products such as sulphate by-products and oxidation (carboxylic by-products) were found in aged oils as illustrated in Figure 5.3b and c. These results are in agreement with other studies that showed the formation of sulphate by-products [75], [96], [226], [256] and oil oxidation [86], [225], [256] in engine oils. Degradation products were found in used oil due to the interactions between the oil, soot and additives [73], [257]. In the current study, the effect of CBP on degradation products during the ageing process has been observed as seen in Figure 5.3b and c. The results confirmed that the existence of CBP in the oil during the ageing process affects oil degradation and induces the formation of degradation products. There are complex chemical interactions between the additives themselves and the CBP in the presence of oxygen at high temperatures. CB surface chemistry contains chemical bonds such as carbon-oxygen and sulphur-oxygen bonds (see Figure 4.3). As CB level increases in the oil, a higher density of carbon-oxygen and sulphur-oxygen bonds exist in the aged oil. This can cause higher chemical interactions between released chemical bonds from CBP and the additives hence catalysing the formation of degradation products. Oil oxidation is accelerated in the presence of CBP. Salehi et al.[10] demonstrated that ageing oil containing CBP increased the oil oxidation compared to oil aged with no CBP. The effect of soot level on oil oxidation has shown that a higher level of soot in the engine oil causes a higher oxidation rate [9].

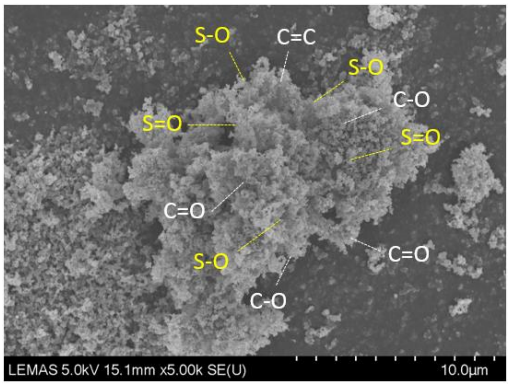

Figure 9.1: Fresh CB particles contain functional groups of carbon-oxygen and sulphur-oxygen bonds according to the chemical analysis of CB as illustrated in Figure 4.3.

Oil degradation and its effect on the physical property of the oil were studied by measuring the oil viscosity. The results showed an increase in the viscosity of the aged oil with CBP compared to the fresh oil mixed with the same level of CBP as shown in Figure 5.4a. Since both oils (aged and non-aged) contain the same levels of CBP, this increase in viscosity was related to the ageing process and formation of degradation products. To investigate the effect of degradation products on viscosity, CBP were removed from aged oil. The viscosity of oil samples decreased after removing the CBP as expected as demonstrated in Figure 5.4b. However, these values are still higher than the viscosity of fresh oil. This is probably due to the formation of degradation products in oils. The results are in line with several studies [89], [228], [229], [256] that have confirmed the effect of degradation products on the physical property of oils. The current study shows how oil degradation can influence the increase in viscosity even after removing CB as demonstrated in Figure 5.4b.

9.1.2 Additives adsorption on CBP

The antiwear additive was seen to decompose or deplete in the oil with no CBP and the oil samples containing CBP as shown in Figure 5.3a. The results presented in Figure 5.5 demonstrated that additive adsorption on CB occurred after removing different levels of CBP from the aged oils. This study is in line with other studies [8], [173], [174] that proved additives adsorption on soot and decomposition of antiwear additive. In this study, additive adsorption on CB could be confirmed for elements that originated from antiwear additive (such as ZDDP) and dispersant/detergent compounds such as sulfonates and phosphonates. The results showed a lower concentration of S, P and Zn in the oils after removing the higher level of CB. This is due to the higher active surface area of CB in the oil leading to more additive adsorption on CB particles [239], [247]. This is in agreement with the function of dispersant/detergent additives with polar groups to attract the organic contaminants which are expected to be removed by CBP [47]. Rounds [258] proposed that antiwear adsorption on soot causes higher wear. In contrast, Gautam et al. [71] and Hosonuma et al. [158] believed that antiwear additive adsorption on soot only occurred for Zn compounds with the remaining P compounds in oils.

Additive adsorption on CBP was previously studied by Motamen Salehi et al. [10] at the same conditions. However, they used the base oil+1 wt% ZDDP to investigate the additive adsorption on CBP, instead of FFO. The results showed full adsorption of ZDDP compound on 5wt% CB after ageing the oil [10]. In the current study, however, lower levels of additives adsorption on CBP were observed in FFO compared to the base oil and ZDDP. This is due to the existence of other additives such as antiwear, dispersant and detergent in the oil and the interaction between them, reducing the chance of adsorption of antiwear additive on CBP.

9.1.3 The effect of oil degradation and additives adsorption on wear

It has been suggested that additives adsorption and degradation products affect the wear inducing abrasive wear. The results after removing the CBP from aged oils proved that wear increased due to additive adsorption on CBP and degradation products as reported in Figure 5.10. Decomposition and adsorption of antiwear additive influence the formation of tribofilm to protect the rubbing surfaces producing abrasive wear as shown in Figure 5.11b1, c1, d1 and e1. This agrees with [177], [256], [259] studies demonstrating that oil degradation and the formation of degradation products influence oil performance. In this current study, wear of aged oils containing different levels of CBP showed higher values of wear compared to oils containing a similar level of CBP without ageing. This is due to oils degradation and additive depletion discussed in Figure 5.3 resulting in changes in the physical properties of aged oils as shown in Figure 5.4. There is another factor such as the changes in mechanical properties of CB particles after ageing.

The degradation of the oil is in line with Schwartz et al. [177] and Dörr et al. [259] studies who also reported the effect of temperature on oil degradation and additive depletion. They suggested that excessive oil degradation occurs due to the high oil temperature. At high oil temperatures (above 130 °C), the anti-oxidant additive is depleted leading to nitration and oxidation of the oil. The oil as a result of nitration and oxidation becomes viscous and acidic,

and more insoluble by-products are deposited on engine components' surfaces as sludge or varnish [177].

Oil degradation was monitored by Dörr et al. [259], who investigated the artificial ageing of the oil-containing antiwear additive (ZDDP) over time. The results showed the formation of antiwear compounds or/and degradation products as a result of the decomposition of ZDDP during the ageing process (Figure 9.2), where dihexyl dithiophosphate (DDP, negative ion) is the main antiwear compound in ZDDP. Other compounds such as butylhexyl dithiophosphate, dihexyl thiophosphate, hexyl dithiophosphate and dibutyl dithiophosphate were also found in the aged oils. These compounds originated from DDP degradation and were identified as degradation products. Sulfuric and phosphoric acids increased over time in aged oil. Tribology tests showed an increase in wear and the presence of abrasive wear on the surfaces [259].

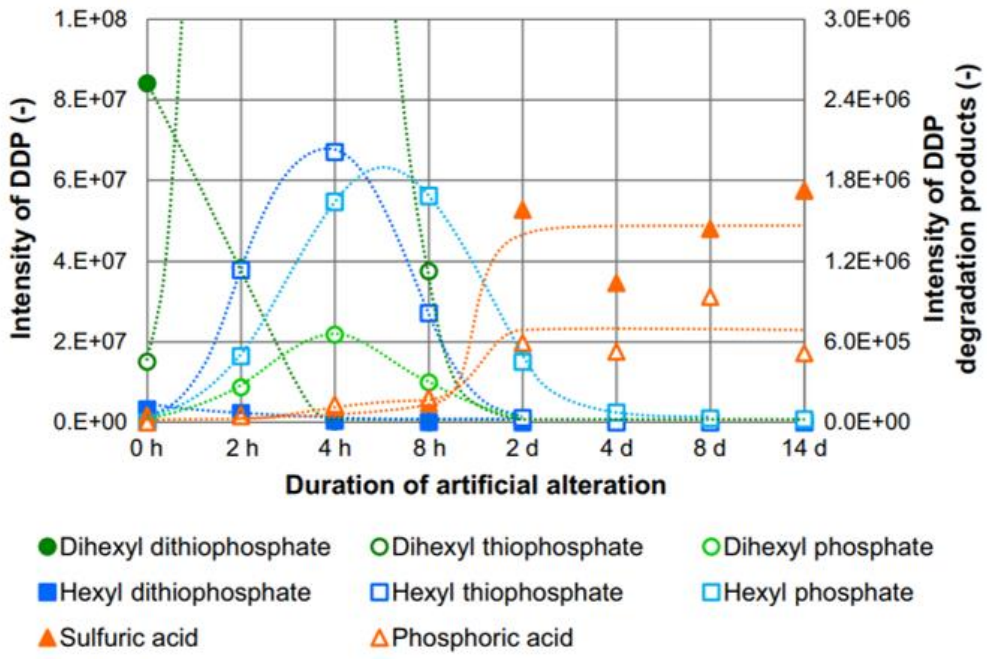

Figure 9.2: ZDDP deterioration during the ageing process and the formation of degradation products [259].

9.1.4 Effect of CBP on friction and wear

The results presented in chapter 5 showed that friction was correlated to the CBP level in the oil. CBP at the level of 0.75 wt% reduced the friction coefficient. However, CBP at high levels caused oil starvation (Figure 9.4b) and increased the friction coefficient over the whole test as

shown in Figure 5.8. The results displayed that CB at level 0.75 wt% act as a friction modifier and reduced the friction coefficient between the contact surfaces over time. This comes to the fact that CBP at low concentration has less ability to form a large agglomeration and does not affect oil starvation (Figure 9.4a). This is due to the dispersant ability to disperse the particles at a low CB level preventing the coalescence into large agglomeration.

Several studies [75], [91], [230], [260] have found different factors that affect the friction in the existence of soot/CB in engine oil. Some factors are correlated to the type of tribocontact (the interaction at these interfaces between different surfaces) [254], others associated to soot/CB level in the oil [75], [230], [260] and oil formulations (causing particles agglomeration) [77], [78], [91], [261] (Figure 9.3). Green et al. [262] and Ramkumar et al. [260] showed that increasing the CB levels in engine oil causes an increase in friction coefficient. They explained the increase in friction is due to high levels of CB causing oil starvation as a result of the agglomeration of CB particles. In contrast, CB at lower concentrations was uniformly dispersed in engine oil resulting in a decrease in friction coefficient. Liu et al. [263] and Uy et al. [264] found that the friction coefficient also was related to CBP content and the oil formulations.

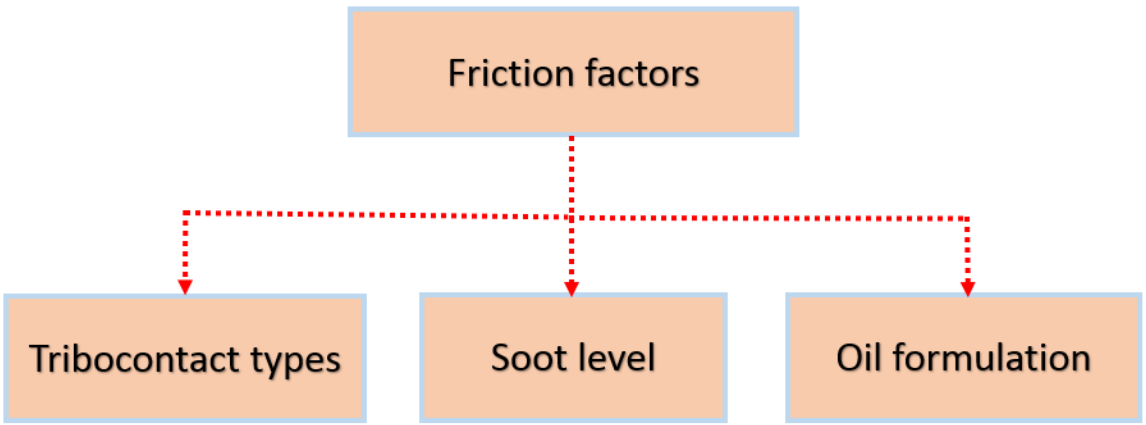

Figure 9.3: Friction factors influence the friction coefficient in the existence of soot/CB in the oil.

As shown in Figure 5.8, wear increases with increasing CBP level in oil, which is not something unexpected. The increase in wear by increasing CB levels in the oil is in agreement with other studies [73], [84] as the higher level of CBP forms large clusters leading to starvation as shown schematically in Figure 9.4b. There is also another factor of increasing wear with higher CBP

is that dispersant becomes less effective to disperse the particles preventing them from approaching and coalescing into large agglomerates [91]. The correlation between wear and friction, as illustrated in Figure 5.8 depends on the CB level in the oils. With a low CB level (Figure 9.4a), the particles act as a friction modifier producing low friction during the test in contradiction with wear. However, as the CB level increased causing starvation (Figure 9.4b), both wear and the average friction coefficient over the whole test increased (Figure 5.8).

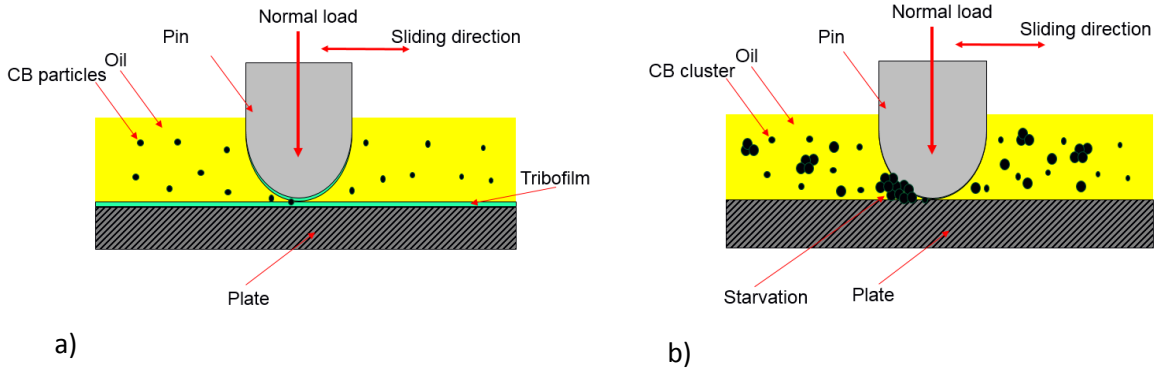

Figure 9.4: 2D-schematic explains the pin-on-plate contact with oils containing a) low CBP level b) high CBP level.

9.1.5 The link between mechanical properties of CB and wear

It has been proposed that the mechanical properties of soot are changed when in the oil at different conditions leading to an increase in wear [109]. Bhowmick et al. [109] suggested that chemical interactions between soot and additives affect wear. Sharma et al. [101] indicated that the interaction between calcium phosphates, which is a detergent compound and is considered as a hard material in nature, and soot particles could change the abrasive characteristics of these particles [101]. Several studies [234]–[236], [265]–[268] reported the formation of an oxidation layer around soot particles due to soot oxidation could affect the mechanical properties of soot particles. There are no previous experimental studies that investigated the effect of the change in the crystal structure of soot on the mechanical properties of soot particles.

In this study, TEM images (Figure 5.14c, d) and XRD data (Figure 5.16) proved that the crystal structure of CB changes after ageing the oil. TEM images (Figure 5.14c, d) showed the

formation of a layer with a thickness of ≤3 nm around aged CB particles. The comparison between the crystal structure of soot and aged CBP demonstrated that the CBP crystal structure is similar to soot. The change in the crystal structure of soot/CB particles after ageing resulted from the oxidation of the soot/CB surface. The O_2 diffuses through the outer shell of the particles to react with edge-sites atoms of shell particles. The passivated shell did not allow O_2 to access and diffuse through the reactive amorphous core forming the oxidation layer on the outer shell of CB or soot [265]–[268]. The results are in line with other studies that demonstrated the formation of the oxidation layer around soot particles [234]–[236], [265]–[268].

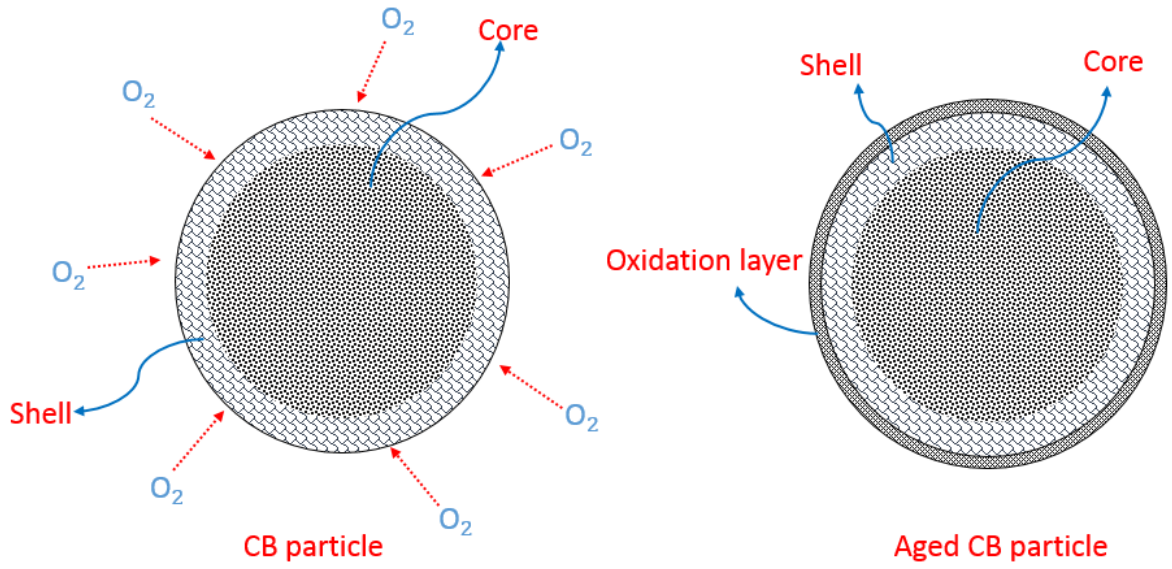

Figure 9.5: Schematic of the CBP oxidation after being aged in engine oil.

The results displayed in Chapter 5 revealed that the deformation load of CB after ageing increased for particles in two different sizes (Figure 9.6). The increase in the deformation load means a higher compression load is needed to deform/break the CB particles after ageing in the oil. Hardness is defined as the ability of the material to resist the deformation load [269]. The hardness of the CB is increased due to the change in the crystal structure of CB particles after ageing. One possible factor of the increase in wear after ageing the oil with CBP is the change in the hardness of CB particles. The current study reveals three main factors that

influence wear correlate to ageing the oil containing CB. These are additive adsorption on CB, degradation products and an increase in CBP hardness.

The results prove experimentally the hypothesis of several studies [97], [101] that proposed the change in mechanical properties of soot and its effect on wear. This is the first study that investigated the relationship between the change in the crystal structure of CB/soot after ageing in the oil, mechanical properties of CB/soot and wear. These findings are in line with Uy et al. [97] who showed that different types of soot, extracted from various oils, had different morphology which could affect the hardness of particles and hence the wear.

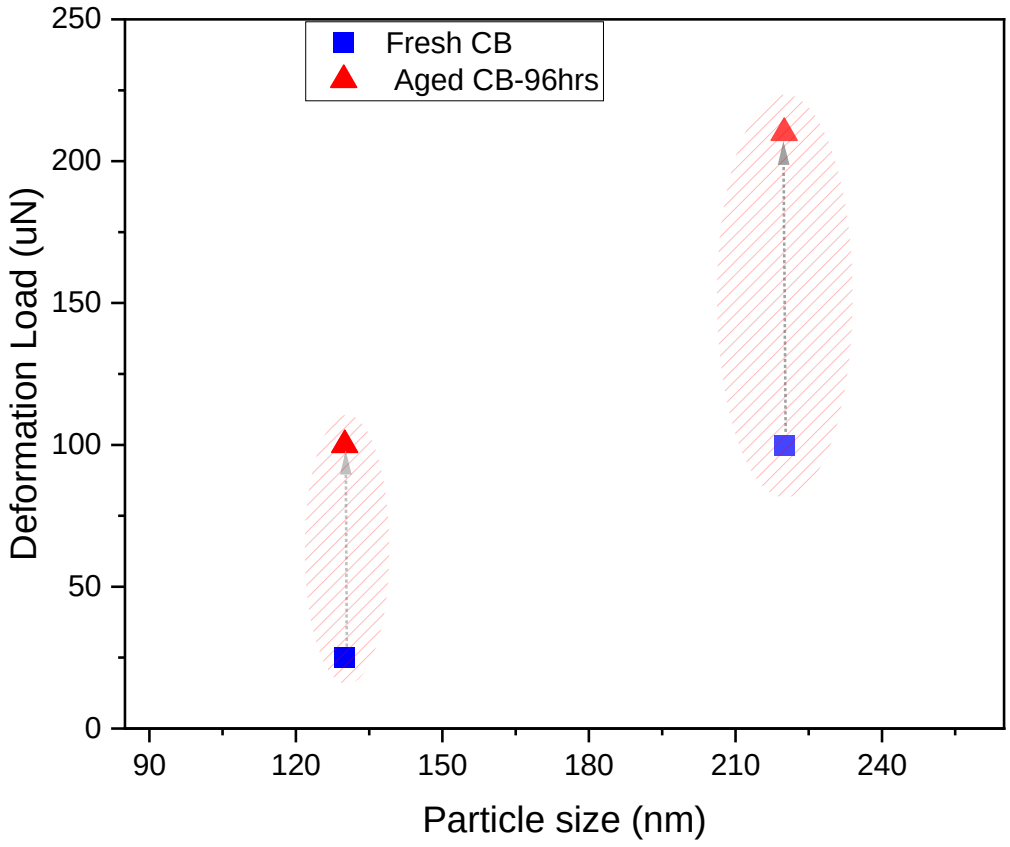

Figure 9.6: Deformation load of CB after ageing for two different particles sizes. Deformation load was calculated at the point where the CB particles were deformed/broken during nano-compression tests.

9.2 Soot effect on the reclamation of heavy-duty used oils

The link between removing soot and the reclamation of used oil is investigated in Chapter 6. This section provides a detailed discussion of the results presented in Chapter 6. The findings

in this section discuss the ability to remove the soot from heavy-duty used oil and its effects on tribological performance.

9.2.1 The efficiency of depth filters

Several previous studies [242]–[245] have reported that the soot size distribution is less than 400 nm for the clusters and less than 50 nm for single primary particles [242]–[245]. The surface filter is designed to trap the contaminants with a size of 30 µm and larger [122]. Filters manufacturers have investigated the ability to capture different sizes of soot particles using media filters. They proposed a new design of a media surface filter that can capture the smaller size of soot particles. Butler et al. [270] suggested that adding depth to the filtration media can increase the effectivity to capture the heterogeneous range of particles sizes. A depth filter consists of multi-layers to allow the contaminants to travel within the filter resulting in a high holding capacity of the contaminants [121]. Loftis et al. [118] reported that depth bypass filter shows a decrease in wear of rod bearing in engine compared to other types of filtration systems.

The results of depth filter tests presented in Chapter 7 explored the efficiency of depth filters at different depth thicknesses (45 layers and 80 layers) (Figure 6.10). Figure 9.7 demonstrates that the depth filter with 80 layers performed better than the depth filter with 45 layers. Both depth filters did not affect the oil pressure during the filtration process (ΔP=2 Pa was consistent over the test period). However, there was not a significant decrease in the soot level even after an increase in the depth filter thickness. The results reveal that the increase in the thickness of the depth filter will not necessarily improve filtration efficiency without changing the pore size of each layer. In this study, the soot size distribution in heavy-used oil is less than 200 nm (Figure 6.4). This study shows that the size distribution of soot has a high effect on the efficiency of the depth filter. Furthermore, the efficiency of the same depth filter is improved after adding 1.5 wt% (Figure 9.7). This comes from the fact that adding 1.5 wt% of CB influences the size distribution of particles (soot+CB) (Figure 6.6). The size distribution of particles (soot+CB) concentrates in the range of less than 800 nm compared to 200 nm of the

size distribution of soot in used oil (Figure 6.6). Thus, it can be concluded that the depth filter of 80 layers performed better after adding 1.5 wt%CB to the used oil due to the larger size distribution of particles captured by the filter (Figure 9.7).

This study discusses two main mechanisms that affect the efficiency of depth filter apart from the test period such as the size distribution of soot and depth filter thickness. In this study, the pore size of each depth filter layer is 20 µm and there was no drop in the oil pressure over the test period. However, reducing the pore size of each layer could improve the efficiency of the filtration process, but a drop in the oil pressure is expected [271]. The flow rate of oil decreased when the number of layers increased and after adding 1.5 %CB to the used oil (Figure 9.7). It is known that the flow rate of any liquid depends directly on the pressure and inversely on flow resistance [272]. For constant pressure in this study, increasing the number of layers of depth filter causes higher resistance for the oil to flow and hence less flow rate. Where adding 1.5 wt% to the used oil increases the oil viscosity (resistance of oil to flow) causing a decrease in the flow rate (Figure 9.7).

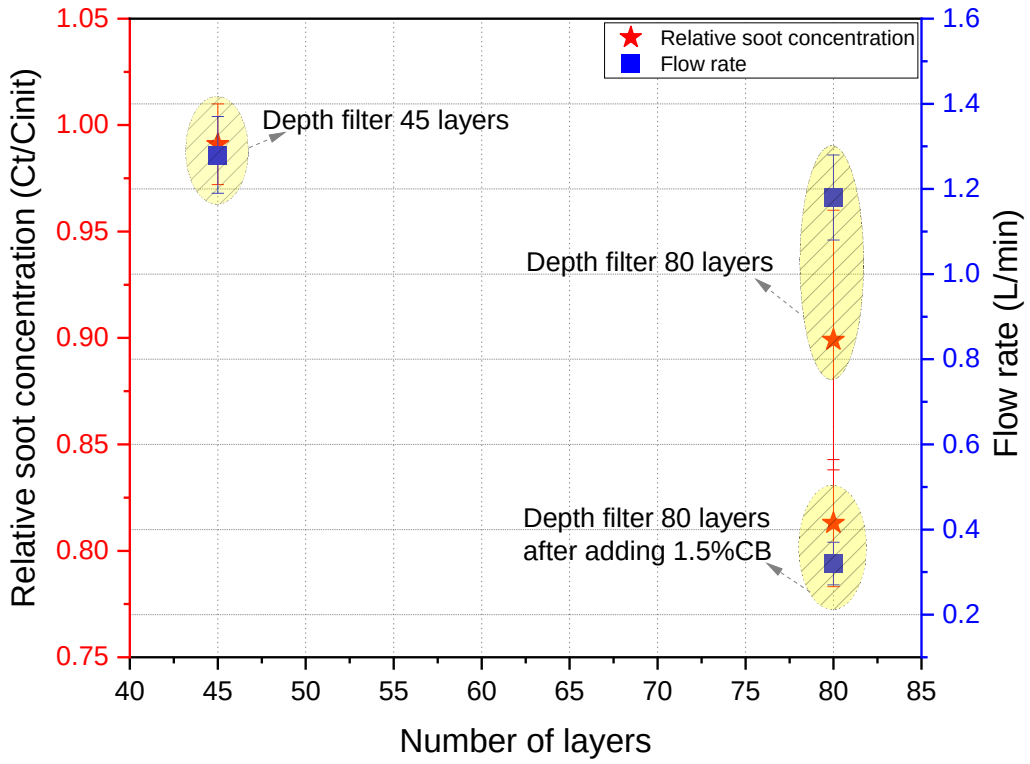

Figure 9.7: Comparison between the relative soot/CB concentration and oil flow rate for depth filters with a different number of layers and after adding 1.5 %CB.

9.2.2 The link between removing soot and the reclamation of used oil

The effect of soot on wear in real engine oils has been investigated in serval studies [77], [80], [81], [83], [84]. Setten et al. [18] reported that soot concentration in engine oil affects the oil drain interval. Other studies [2]–[5] found that oil degradation influences oil service life. The filtration system can potentially remove soot particles from engine oils. However, there is still unknown whether engine oil can perform as a fresh oil after reclamation. This is because other contaminants such as degradation products are difficult to remove by filtration and can influence oil performance. On the other hand, several studies [10]–[13] reported that removing soot from engine oil causes additive adsorption on soot which also influences the tribological performance.

The results presented in Chapter 6 indicated no change in the oil structure with decomposition and/or depletion in antiwear additive (Figure 6.1). The results (Figure 6.9) proved that reclaiming the used oil is possible after removing soot from the used oil to a certain level. As the soot level in used oil decreased, oil performance improved as expected. This is in agreement with other studies [118], [221], [246] that found removing the soot from used oil reduced its effects on wear and improve the oil function. There was no change in the oil performance with a level of <0.26 wt% soot. The results are in agreement with [224] who confirmed that the low levels (<0.2 wt%) of soot in oil do not have a significant effect on wear. Chemical analysis of engine oils demonstrated additive depletion in used oil after being used in the engine and additive adsorption on soot after removing the soot (Figure 6.13 and Figure 6.14). The results are in line with several studies [10]–[13] that investigated additives adsorption on soot discussed in Section 9.1.3. It can be summarised that removing the soot to a level less than 0.26 wt% can reclaim the oil performance. However, the reclaimed oil does not perform as well as the fresh oil due to additive adsorption and depletion.

9.3 Effect of water contamination on engine oil

In this section, the existence of dissolved water in heavy-duty used oils and water saturation at different temperatures will be studied in detail. The effects of water on additives depletion and tribological performance are presented in Chapter 7. This section provides a detailed discussion of the results demonstrated in Chapter 7. This is important to better understand the effect of water contamination on the reclamation of used oil and the tribofilm formation.

9.3.1 The relationship between water saturation and additive depletion

Water content at room temperature in heavy-duty used oils of two trucks at different oil changes was presented in Figure 7.1 and Figure 7.3. The results indicated that the level of dissolved water at room temperature increased with an increase in the accumulated mileage of trucks. This could be due to an increase in soot level and/or oil oxidation with higher accumulated mileage. This is in agreement with other studies [128], [273] that proposed a higher level of dissolved water in the oil is expected with the higher accumulated mileage. One of the trucks' oils (Figure 7.2), which contained a high level of dissolved water (2270 ppm) in fresh oil, seems to reach its saturation level (3500-3900 ppm) as there was no significant change in the level of dissolved water in the used oil for all oil changes. The results provide strong evidence that dissolved water levels in used oils varied depending on oil conditions.

The results presented in Figure 7.7 proved that the water saturation level in the engine correlated to oil temperature. Higher dissolved water levels were observed at higher temperatures (Figure 7.7). As known, water molecules are polar and attract to each other due to their polarity compared to non-polar oil molecules which are also strongly attracted to each other [47], [136]. The effect of temperature on dissolved water level can be explained that heating up causes the water molecules to gain kinetic energy and break apart allowing more dissolved water into the oil [274]. Water in engine oil over the saturation level (dissolved water level) was separated to free water as expected [128].

Henry's law [130] demonstrated several factors such as relative humidity, pressure, oil additives, contaminants and temperature that influence the amount of dissolved water in engine oils. Henry's reported the linear relationship between the humidity in the air and dissolved water for different oils containing different types of additives. Cantley et al. [131] showed that the concentration of dissolved water in engine oil is correlated to air humidity and time. Several additive compounds that have polar extremities can markedly increase the water's ability to dissolve in oil. When water molecules, which are also polar, attach to additive molecules in the oil, any extra water molecules without attachment separate and settle at the bottom of the tank as free water [128]. It can be concluded that the amount of dissolved water in the oil are associated by the amount of polar molecules in the oil in either additives or/and contaminants such as soot or oxidation products.

Another observation in Chapter 7 is that water saturation level is depending on the oil temperature causing separation of water at lower temperatures. The results proved that the removal of free water from the oil at different levels causes depletion in additives (Figure 7.11). The results showed that as much water above the saturation level separates from the oil, more additives are depleted. There are no previous experimental works that investigated the additive depletion by water. The results can be linked with the function of dispersant/detergent in the oil where more polar groups capture or attach to the contaminants such as water. Thus, it is expected to be removed by water contamination [47], [136]. However, other additives (nonpolar molecules) such as calcium-based compounds could be washed out by removed water. Evans [136] suggested that free water can wash the additives from engine oils. Almost all additive compounds are formulated to have the ability to dissolve in the oil's base stock, while the additives have less or limited solubility in water. However, some additives still have a solubility in water; which means some additives can be removed from the engine oil during the water filtration process [136]. Smiechowski et al. [171] proposed that the heads of additives latch easily onto water molecules and surround them. When the water content in oil exceeds

the saturation level, water molecules surrounded by additives separate from the oil causing the depletion in additives as explained schematically in Figure 9.8a and b.

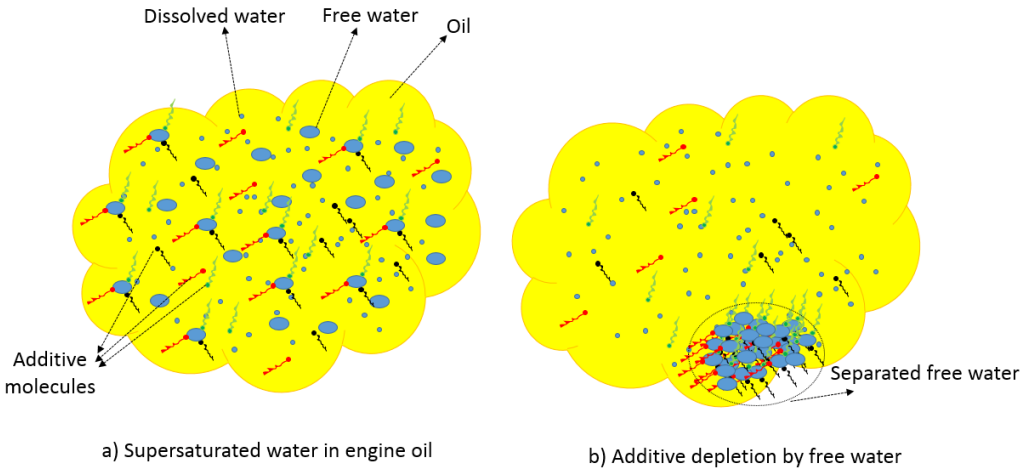

Figure 9.8: Schematic images demonstrate the additive depletion by water, when the free water is separated from the engine oil a) supersaturated water in engine oil, b) additive depletion by free water.

9.3.2 Effect of water on wear

The effect of water on the tribological performance of engine oils has been investigated in several studies [149]–[151]. The results showed an increase in wear [149]–[151] and a decrease in the tribofilm thickness with an increase in water content in the oil [75], [150]. It has been reported that water molecules adsorb to the metal surface faster [75]. This reduces the ability of additives to form tribofilm due to the higher polarity of water molecules compared to the additives [26], [168], [169]. However, the corrosive wear on contact surfaces in the presence of water was also observed after the tribology tests [29], [128].

The results presented in Figure 7.8 reveal that wear increases with an increase in water content in oils. The significant importance of these findings is that water at a level above 2500 ppm causes an increase in wear. The results are in line with different studies [127], [132] that considered the water content effect with a concentration higher than 2000 ppm(0.2 wt%) on oil performance [132]. The acceptable water level in automotive oils is approached the dissolved water level, and a higher level of water can influence the oil performance [127],

[132]. At the higher level of water above 2000 ppm, more free water exists in oils, causing a thinner tribofilm thickness hence higher wear [151].

The effect of water on contaminated oil by CB is presented in Figure 7.9. The results proved an increase in wear with the increase in water content even in the existence of CB. This is due to the polarity of water molecules that impede dispersant/detergent compounds as a result of the formation of reverse micelles [47], [136]. Therefore, the higher level of water that exists in the oil, the more reverse micelles are expected to form [171]. The formation of reverse micelles affects the efficiency of dispersants/detergents causing agglomeration of CBP hence the oil starvation phenomenon. In addition, water molecules attach to rubbing surfaces due to high polarity affecting the formation and adhesion of tribofilm on the surfaces [26], [168], [169]. Thus, the contact surfaces face more abrasive wear caused by CBP without the primary protection which comes from the formation of tribofilm on the contact surfaces.

It can be summarised that water in the oil affects wear when the water exists such as free water (above 2000 ppm). Water can dissolve in the oil at room temperature until approximately 1700 ppm as proved by the water saturation test (Figure 7.7). Figure 9.9 compares the effect of water in fresh and contaminated oil by CB on wear. The results demonstrate that water has a higher impact on contaminated oil by CB due to the formation of reverse micelles (between water molecules and dispersant/detergent molecules), causing CB agglomeration. This study observes two main synergy factors that influence oil performance; first of all, the formation of reverse micelles causes CB agglomeration hence oil starvation [171] and secondly, the presence of water can also influence the formation and adhesion of tribofilm on the surfaces [26], [168], [169].

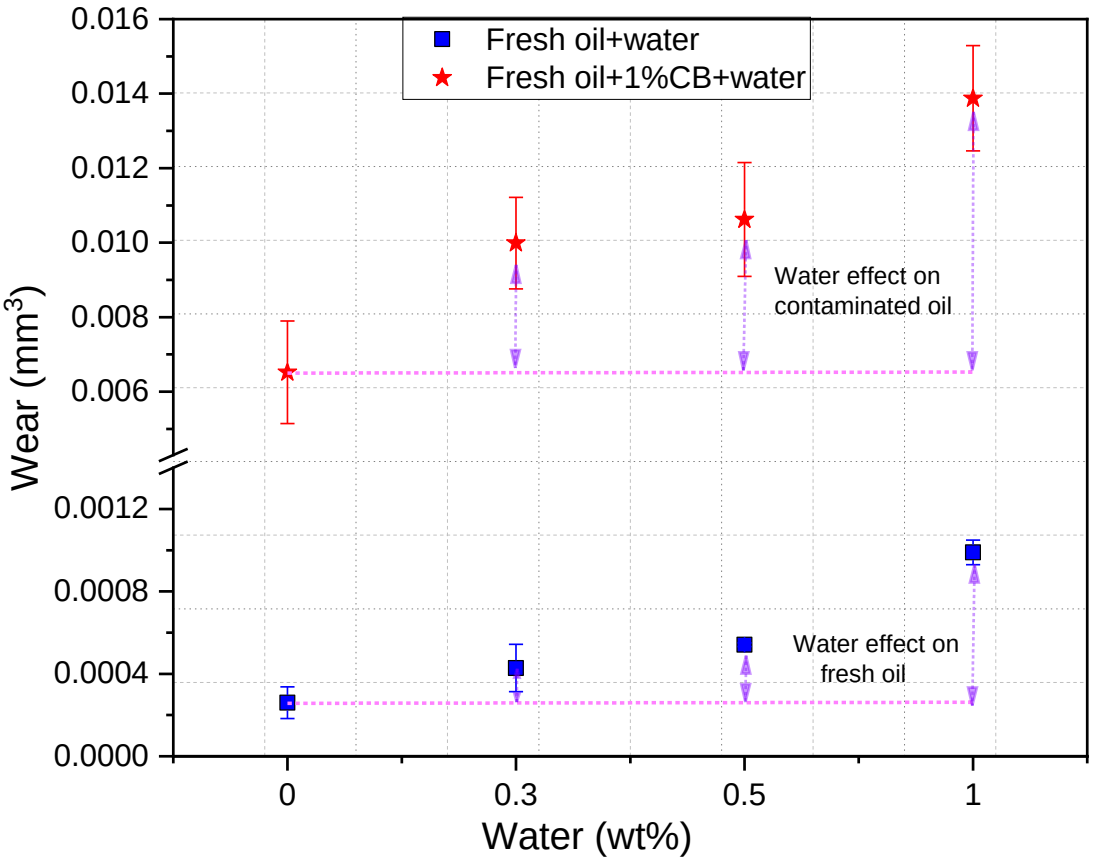

Figure 9.9: The effect of water at different levels in fresh oil and fresh oil containing 1wt%CB on wear.

9.3.3 Effect of water on oil reclamation

The effect of water on oil performance is discussed in section 9.3.2. The results presented in Figure 7.14 confirm the previous studies [149]–[151] in terms of the effect of an increase in water level on wear. The existence of water in oil at ageing conditions does not affect the chemical structure of the oil (Figure 7.13), while there were no degradation products detected in aged oil (Figure 7.13). Removing the free water from the oil at varied levels causes additive depletion (Figure 7.11). The concentration of depleted additive was increased with an increase in the amount of removed water from the oil as discussed in section 9.3.1. The results showed an increase in wear in the presence of water in oil (Figure 7.14), however, the oil samples after removing the free water performed higher wear compared to the fresh oil (Figure 7.15). The study indicated two main mechanisms that affect wear after removing the free water. These are additive depletion by water and remaining water (mostly dissolved water) in oil.

This is the first study that proves that additive depletion and the remaining dissolved water can influence wear and tribofilm formation. Evans [136] proposed that additives depletion due to the separation of free water could influence the oil performance. Minami et al. [34] and Evans et al. [8] believed that oil performance might be affected due to using up the additive to protect the oil from water contamination, especially the polar groups additive such as dispersant/detergent. However, other studies [78, 79] found that water contamination at a level higher than 0.2wt% water influences wear and tribofilm formation. Parsaeian et al.[150] demonstrated an increase in wear and a decrease in tribofilm thickness in low humid conditions. The results are in line with the study [152] that showed water contamination can decay the stability of tribofilm by reducing the tribofilm adhesion on metal surfaces.

The effect of water on the tribofilm chemistry was assessed depending on the change in the length of the zinc polyphosphates chain [213]–[215]. It has been proved that the chain length of zinc polyphosphates can be characterised based on the intensity ratio of the bridging oxygen/non-bridging oxygen (BO/NBO) and the binding energy difference between Zn3s - P2p3/2 [214], [250]. The effects of water contamination and additive depletion on the chemistry of tribofilm showed the formation of short-chain polyphosphates (orthophosphate chains) before and after removing the free water from oils (Figure 7.18, Figure 7.19 and Table 7.4). The results agree with other studies [252], [253]. These studies pointed out that chain polyphosphates can be depolymerised by water to shorter chains. Equations 7.1 and 7.2 describe the mechanisms of depolymerisation of polyphosphates chains in the existence of water. The hydrolysis of polyphosphates by water contamination occurs, producing short-chain polyphosphates. This study concluded that the remaining dissolved water in oils and the additive depletion by free water influence the reclamation of engine oils.

Dorgham et al. [275] and Parsaeian et al.[276] found that low and high humidity conditions affect the length of glassy phosphate chains formed in the ZDDP tribofilm. They indicated that water molecules have larger polarity and affinity to the rubbing surface than ZDDP, affecting the chemistry and tribofilm formation [275]. ZDDP adsorption on the rubbing surfaces was

delayed because the water molecules adsorbed and covered steel surfaces faster than ZDDP. As more water evaporated with time as rubbing continued, more free sites on rubbing surfaces were available for ZDDP adsorption and subsequent decomposition to form short chains of polyphosphate (orthophosphate chains) [275], [277]. On the other hand, in the absence of water in oil, ZDDP can be adsorbed on rubbing surfaces without delay. Over time and as rubbing continues, the short chains of orthophosphate polymerise to produce long chains of polyphosphate called metaphosphate chains [275]. The effect of water at different stages on the tribofilm formation and length of polyphosphate chains is described schematically in *Figure 9.10*.

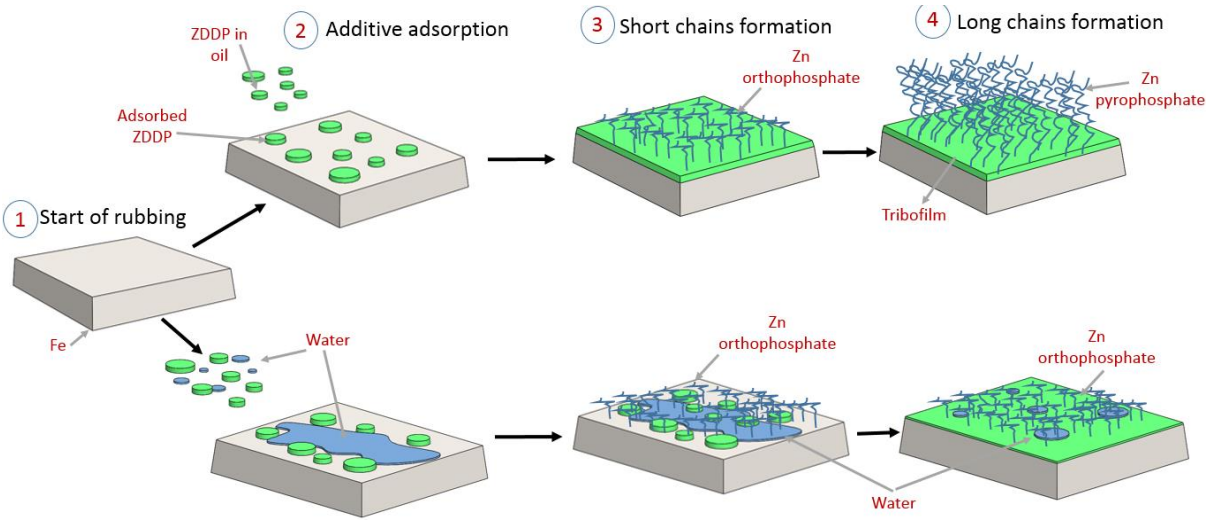

Figure 9.10: The effect of water on the different stages of the decomposition reaction of antiwear additives (ZDDP) before the tribofilm formation.

9.4 ZDDP replenishment in heavy-duty oils

The effect of soot and water on the ZDDP replenishment process is presented in Chapter 8. This section provides a detailed discussion on the results demonstrated in Chapter 8. This is important to better understand the effect of ZDDP replenishment on the tribological performance of heavy-duty used oil in the existence of oil contamination.

9.4.1 Effect of soot on ZDDP replenishment

This study assesses the replenishment process in the existence of soot and after removing the soot from heavy-duty used oil. The study details its applicability to extend the oil drain interval after applying the filtration process and replenishing the additives. The filtration process is used to filter the oil from engine contamination such as soot and hence reduce its effects on tribological performance [118], [175], [246]. While removing the soot from engine oil causes additive adsorption on soot as demonstrated in several studies [10]–[13]. Additives could also be consumed to form tribofilm on contact surfaces and to protect the engine oil from oxidation, sulfation, corrosion, etc [178], [278]. Over the use, additives concentration decreases, which influences the oil performance until the oil is no longer fit for continued service. The current study offers additional insight into the effect of soot on wear after removing different levels of soot from used oil. This study provides complementary information about the amount of depleted additive in real working conditions and its effect on the service life of engine oil. Particularly, this requires measuring the concentration of depleted additives in used oil and investigating the effect of ZDDP replenishment before and after removing soot.

In this study, the chemical analysis of heavy-duty used oil revealed no change in the chemical structure of the oil compared to fresh oil (Figure 6.1). There was a decrease in the viscosity of used oil compared to fresh oil (Table 6.1) due to the loss of Viscosity-Index Improver (VII) at high temperatures, causing the decrease in the viscosity [241]. Carden et al.[279] showed that a small change in the oil viscosity did not influence the wear and friction. However, the ultra-low oil viscosity test revealed an increase in wear. The results detected the decomposition of antiwear additive and the existence of soot particles (Figure 6.2). Decomposition of antiwear additives at engine conditions (high temperatures) was similarly found in the studies [8], [247]. However, it is expected that the presence of soot in oil causes an increase in wear value and abrasive wear on rubbing surfaces (Figure 8.4a1). The results are in agreement with studies [77], [80], [81], [83], [84] that showed an increase in wear due to the existence of soot in the oil. The centrifuge process was able to remove soot gradually from used oil (Figure 6.9). There

was no further decrease in wear values after removing the level of <0.26 wt% soot. The results is in line with Berbezier et al.[224] confirmed the existence of (<0.2 wt%) soot in engine oil does not have a significant effect on wear value. Other studies [118], [175], [246] found that removing the soot from used oil reduced its effects on wear and improve the oil function. There was a reduction in additive concentration due to additive depletion in the truck and additive adsorption after removing soot (Figure 6.13). Additives adsorption on soot has been investigated in several studies [10]–[13] and discussed in Section 9.3.3. While additive depletion in the truck during the use is expected, the additive could be used to form tribofilm on the contact surfaces and prevent oil oxidation or corrosion [154], [156], [157]. Previous studies [10]–[13] have not investigated the effect of additive depletion and additive adsorption on oil performance. In this study, the used/consumed additives cause an increase in wear and the absence of tribofilm on the surface (Figure 8.8a_1).

In this study, the ZDDP compound was used to replenish the additives in used oil before and after removing soot. The results showed a significant reduction in wear after replenishing with the ZDDP compound at different levels. The used oil after adding 3 wt% ZDDP performs almost similar to the fresh oil regarding wear values (Figure 9.11). However, an uneven distribution of tribofilm formation was observed on the rubbing surfaces in the existence of soot (Figure 8.6b), while abrasive wear caused by soot was prevented after adding 1.5 wt% ZDDP (Figure 8.4b1). Soot level (0.62 wt%) in used oil caused a decrease in friction coefficient (Figure 8.3). The results are in line with studies [22], [254] which demonstrated the effect of low concentration soot on friction reduction. Soot at this level acts as a friction modifier causing a decrease in friction coefficient [254]. As the ZDDP is added to the oil, higher friction coefficient results are observed (Figure 8.3) [191], [192]. The reason behind this is the higher shear strength of tribofilm [191] due to an effective roughening of rubbing surfaces by the formation of uneven distribution of asperity peaks [192]. It appears that tribofilm roughness had a limiting effect on friction with a ZDDP level of ≥1.5 wt%.

On the other hand, reclaiming the used oil after removing the soot had a significant effect on wear value and improved the oil performance (Figure 6.9). The reclaimed oil required less amount of ZDDP to regain the tribological performance similar to the fresh oil. This study indicates that adding 0.75 wt% ZDDP is quite enough to reduce wear and the formation of tribofilm on the surfaces (Figure 9.11). The tribofilm distribution on the surface after adding ZDDP to reclaimed oil is uniform (Figure 8.10). The results agree with studies [24], [77], [80], [81], [83]–[85] that showed the effect of soot on the removal of tribofilm from rubbing surfaces. While removing the soot to a certain level with ZDDP replenishment is expected to regain the tribological performance hence extending the service life of engine oil.

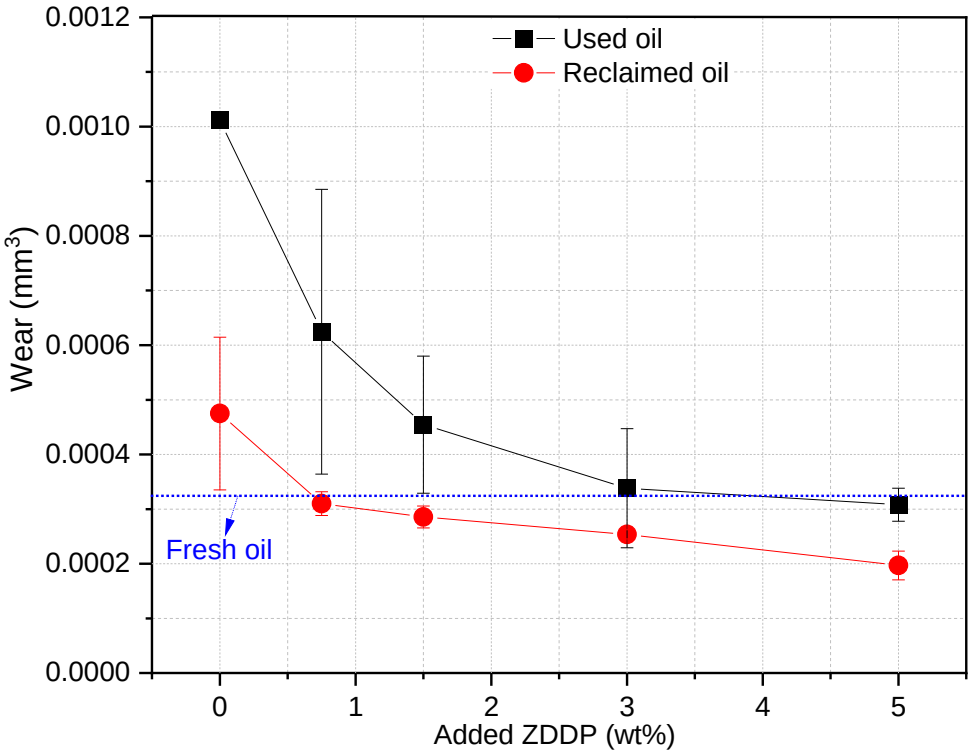

Figure 9.11: The effect of ZDDP replenishment on wear for used oil and reclaimed oil (after removing soot).

The critical level of added ZDDP to the reclaimed oil has been investigated in this study. The results determined the concentration of used and fresh additives in the reclaimed oil (Figure 8.12). ZDDP replenishment of reclaimed oil showed that adding 0.75 wt% ZDDP was enough to regain the oil performance similar to the fresh oil. Furthermore, ZDDP replenishment at the lower level of 0.75 wt% was studied in Section 8.3.5. Tribological tests and tribofilm analysis

proved that 0.75 wt% of ZDDP is the optimal added level that oil can perform similar to fresh oil. The results in (Figure 9.12) illustrated that replenishing with 0.5 wt% ZDDP can reduce the amount of wear to be similar to fresh oil. However, there is no full tribofilm coverage on the surfaces (Figure 9.12). The effect of ZDDP concentration in reclaimed oil or used oil performance has not been investigated in previous studies. While the effect of ZDDP concentration in fresh oil on tribofilm formation was studied by Yin et al [188]. The results revealed that a low concentration of ZDDP (0.25and 0.5 wt%) forms short phosphate chains, whereas a high percentage of ZDDP (1 and 2 wt%) leads to the formation of long phosphate chains. Furthermore, Tomala et al.[189] and Ghanbarzadeh et al.[190] found that the larger percentage of ZDDP causes thicker and larger roughness of tribofilm.

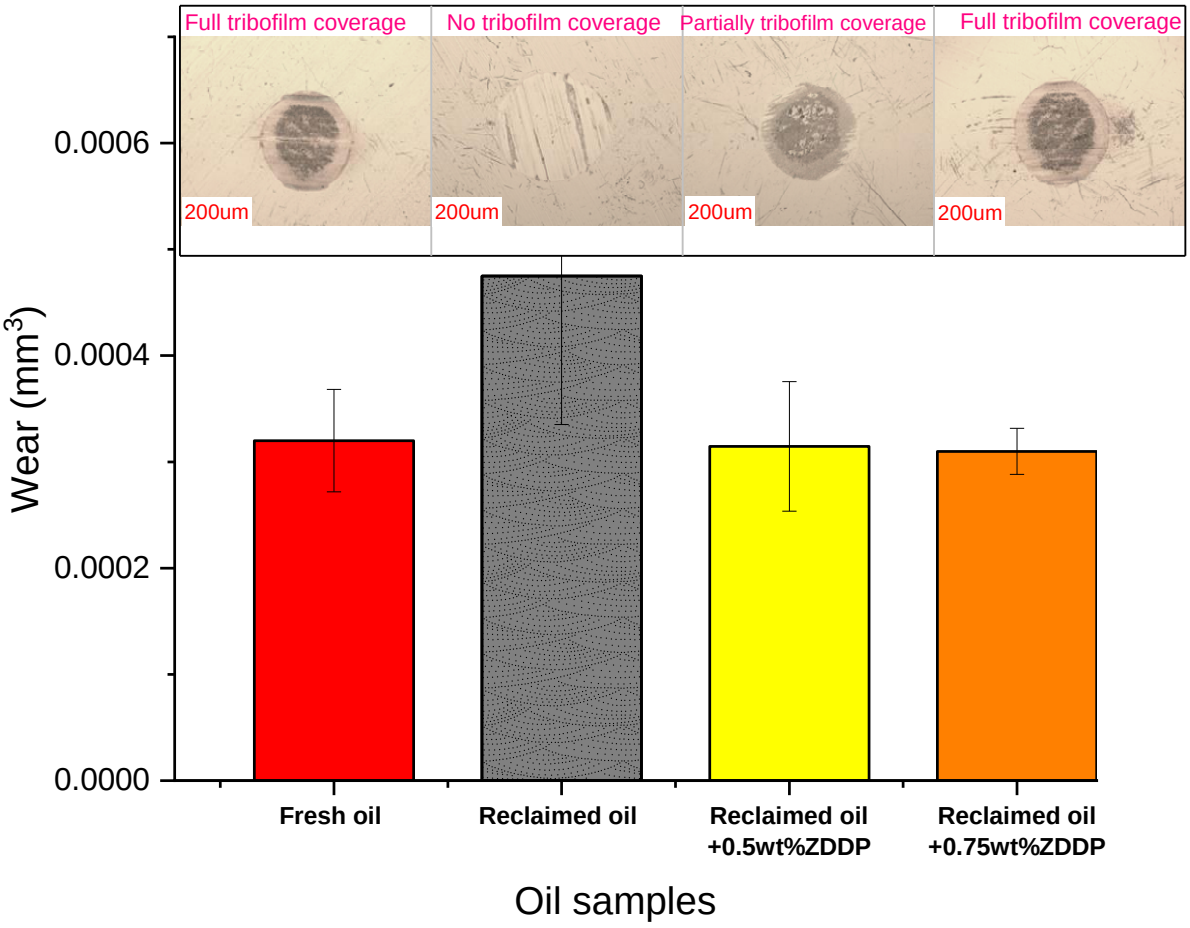

Figure 9.12: The effect of replenishing the reclaimed oil (after removing soot) with a small percentage of ZDDP on the oil performance.

The results can be summarized that used oil contained 0.62 wt% soot required at least 3 wt% ZDDP to perform similar to the fresh oil. However, removing the soot to the level of 0. 26 wt% reclaimed the used oil function and reduced the wear value significantly. The reclaimed oil did not perform such as fresh oil due to additive depletion and additive adsorption on soot. To re-gain the reclaimed oil performance to be similar to the fresh oil with full coverage of tribofilm on the surfaces, the reclaimed oil requires at least adding 0.75 wt% ZDDP.

9.4.2 Effect of water on ZDDP replenishment

The effect of water contamination on the ZDDP replenishment in used oil is presented in Chapter 8. It is good to observe that water in fresh engine oil contaminated with CB showed an increase in wear with the increase in water level (discussed in Section 9.3.2). In this study, the presence of 1 wt% water in used oil during the replenishment process causes an increase in wear compared to the replenishment process in the absence of water (Figure 8.16). The results depict that it is possible to reach a similar performance of the fresh oil after adding 3 wt% ZDDP to the used oil. However, the ZDDP replenishment in the presence of 1 wt% water did not perform similar to the fresh oil, even after adding 5 %wt ZDDP to the same oil. The results are in line with other studies [149]–[151], [275], [280] stating that water contamination had a significant effect on wear and tribofilm formation. Water in the oil affects the formation and growth of tribofilm producing higher wear [249], [275], [280]. Fitch and Jaggernauth [26] showed that antiwear additive can be destroyed even by a slight amount of water in oil. All the aforementioned studies confirm that water contamination influences the generated tribofilm regardless of the water level in the oil.

Smiechowski et al. [171] revealed the high polarity of water molecules in the oil impede the function of dispersants/detergents as a result of the formation of reverse micelles [171]. The formation of reverse micelles affects the efficiency of dispersants/detergents causing agglomeration of soot hence the starvation phenomenon. Water molecules due to high polarity attach to rubbing surfaces influencing the formation and adhesion of tribofilm on surfaces [26],

[168], [169]. Thus, the contact surfaces face more abrasive wear caused by soot without the primary protection which comes from the formation of tribofilm on the contact surfaces.

Reclaiming the used oil contaminated with 1 wt%water and 0.62 wt%soot by centrifugation improved the oil performance (Figure 8.20). However, there was a decrease in additives concentration, after centrifugation of both soot and free water, caused by additive adsorption on soot and additive depletion by water (Figure 8.19). Additive depletion by water and the remaining dissolved water in the oil influence the reclaimed oil performance producing higher wear (Figure 8.20). The results in Section 9.3.3 were discussed the effect of additive depletion by water and dissolved water on the oil performance. Besides, additive adsorption on real soot is in a parallel line with several studies [10]–[13] and discussed in Section 9.2.2.

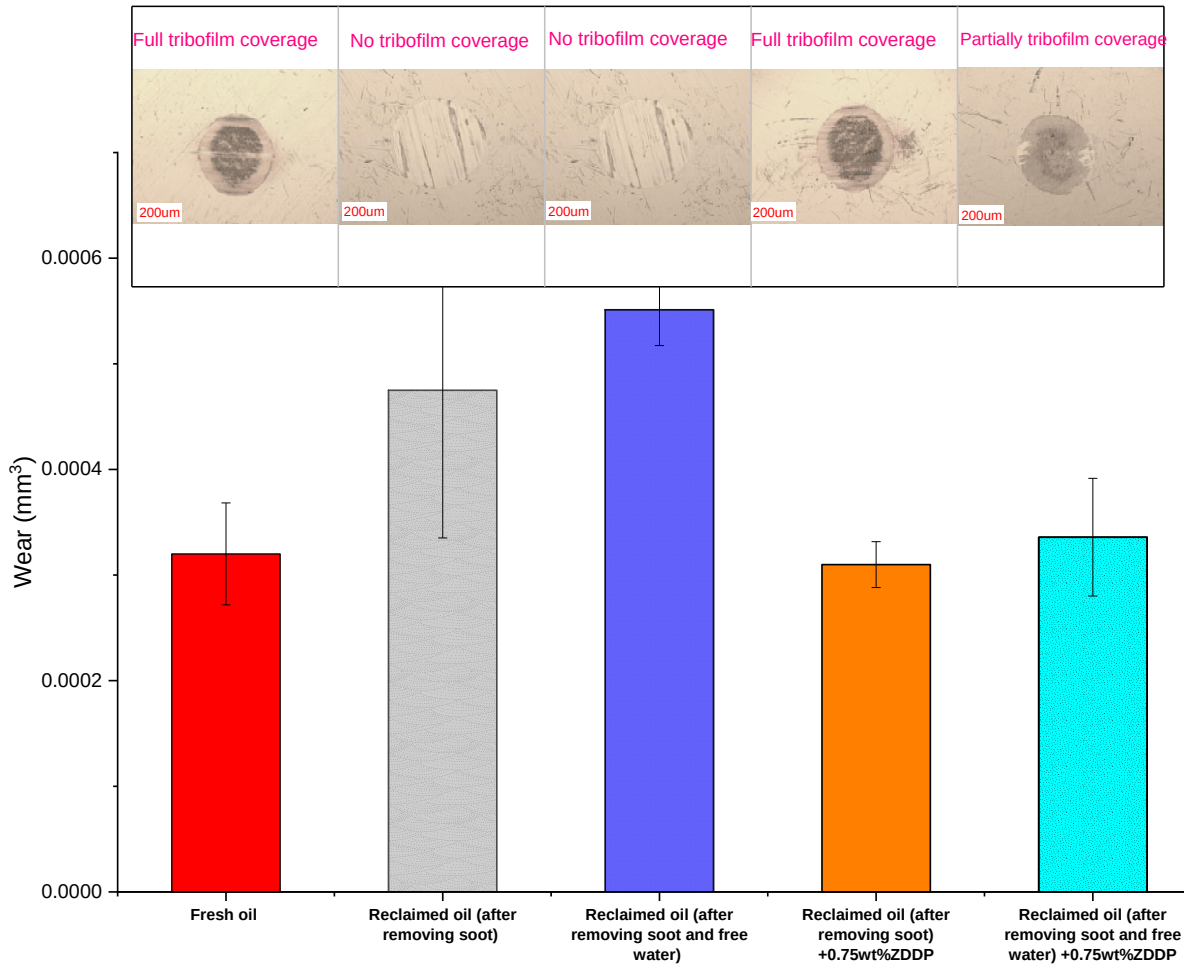

Figure 9.13: The effect of water on the ZDDP replenishment process.

ZDDP replenishment with level ≥0.75 wt% added to the reclaimed oils, either after removing soot from used oil or after removal of both soot and free water from used oil, shows a decrease in wear with an increase in ZDDP percentage in the oil. However, both reclaimed oils almost performed similarly to the fresh oil after adding 0.75 wt% ZDDP (Figure 8.18). Further surface investigation and tribofilm formation, the results indicate no full tribofilm coverage on the surface and the existence of abrasive wear in some regions (Figure 8.21c and Figure 8.22). It can be summarised that additive depletion by water and remaining dissolved water influence the ZDDP replenishment and a higher level of ZDDP is required to regain the oil performance similar to fresh oil (Figure 9.13).

10 Chapter (10) Conclusions and future work

This chapter lists the conclusions that derive from this thesis. At the end of this chapter, the novelty of work, a few suggestions about future work and recommendations to industry in this research area are also presented.

10.1 Conclusions

10.1.1 CBP effects on engine oil

The effect of CBP contamination at varying levels on engine oil has been investigated. The main conclusions are:

10.1.1.1 Effects of CBP on chemical and physical properties of engine oil

- Oil additives were seen to adsorb on CBP.
- Chemical analysis of aged oils revealed the formation of degradation products in the oil.
- At both ageing and no-ageing conditions, the results demonstrated an increase in viscosity with increasing the level of CBP in oils.

10.1.1.2 Effects of CBP on tribological performance

- At a low CB level (≤0.75 wt%), the particles acted as a friction modifier producing low friction during the test.
- A high level of CBP in the oil caused oil starvation increasing the friction.
- The oil containing the same level of CB under ageing conditions performed higher wear compared to non-aged oil.

10.1.1.3 Effects of degradation products and additive adsorption on tribological performance

- After removing CB, the aged oils performed higher wear compared to fresh oil due to additive adsorption on CB and oil degradation.

10.1.1.4 Effects of oil ageing on the physical structure and mechanical properties of CBP

- The crystal structure of CBP after ageing in the oil was changed.
- Nano-compression experiments revealed that the deformation load applied to break the CB particle after ageing was approximately double compared to the deformation load of fresh CBP.

10.1.2 Effects of soot size distribution on the efficiency of depth filters

- The media filter with an increase in depth filter improved the filter efficiency to remove the soot from used oil compared to the media filter with less depth.
- Soot size distribution in used oil influenced the efficiency of the depth filter.

10.1.3 Effects of removing soot on reclaimed oil performance

- Removing the soot from used oil caused a decrease in additive concentration due to additive adsorption on soot.
- At the lower level of soot (<0.26 wt%) in used oil, there was no significant effect came from soot level on wear.
- The reclaimed oil after removing soot did not perform similar to the fresh oil due to the additive adsorption on soot and antiwear decomposition.

10.1.4 Effects of water contamination on engine oils

The effect of water contamination at varying levels on the oil has been investigated. The main conclusions are divided into the following sections.

10.1.4.1 Water effects on wear

- The results showed the ability of the oil to hold more dissolved water at a higher temperature.
- Wear increased with an increase in water level in the fresh oil and the oil-contaminated by CB.

10.1.4.2 Effects of additive depletion and dissolved water on reclaimed oil performance

- Removal of free water from the oil resulted in additive depletion.
- Wear was increased after removing free water from the oils due to additive depletion.

10.1.5 Effects of oil contamination on ZDDP replenishment

ZDDP replenishment at varying levels has been investigated for used oil containing soot or/and water. The main conclusions are summarised in the following sections.

10.1.5.1 Effects of soot on ZDDP replenishment

- Heavy-duty used oil re-gain the performance similar to fresh oil after adding 3 wt% ZDDP.
- ZDDP replenishment after removing the soot from used oil to a certain level displayed less amount of ZDDP (0.75 wt%) to perform similar to the fresh oil.

10.1.5.2 Effects of water on ZDDP replenishment in used oil

- Adding 1 wt% water to used oil influences the replenishment process caused an increase in wear.
- A higher level of ZDDP (>0.75 wt%) was required to regain the oil performance.

10.2 Novelty of work

The novelty of this research as demonstrated in Chapter 1 is highlighting the importance of considering the effect of soot and water not only on tribological performance but also on additives depletion in heavy-duty diesel engines. Otherwise, the performance of diesel engine oil can be influenced due to additive depletion and oil contamination (soot and water) accelerating the oil change. This work reported that depleted additives can be replenished by adding ZDDP antiwear additives to regain the fresh oil performance. But this requires removing the soot and water from used oil to a certain level.

This work could also contribute to a better understanding of the differences between using artificial standard ageing producers in the lab compared to examining used oil from trucks. It observed a harsh ageing process in the labs compared to used oil drained from trucks' engines.

10.3 Future work

This project studied the effect of oil contamination, including soot and water, additive depletion, additive adsorption, oil degradation and filtration techniques on the reclamation process of engine oil and ZDDP replenishment. Due to time constraints, there are still different aspects of oil contamination, oil reclamation and additives replenishment that were not explored in this current research. Based on these research findings, possible recommendations for future work are:

- Investigate additive adsorption on soot, oil degradation at different ageing conditions using base oil and CBP mixed with antiwear additive or dispersants/detergents separately. This will determine the interactions between different additives and CBP under ageing conditions.
- Calculate the hardness of soot or CB using the modelling method to measure the deformation area of CB particles after nanoindentation experiments. Further

investigations of the effect of different additives on the hardness of soot particles can help to understand the change of soot hardness on the abrasive behaviour of soot.

- Study the effect of different additives such as dispersants on soot size distribution in engine oils to investigate its effects on the efficiency of depth filters.
- Study the efficiency of depth filters when the cycled oil is heated up during the filtration process. While increasing the filtration period and depth filter thickness will need further investigation to find out its effect on the filtration efficiency.
- Find the relationship between soot size distribution and its effect on the tribological performance of engine oils.
- Investigate the effect of different oil contaminates, additives, oil types and ageing time on the water saturation level at different temperatures. This will help to understand the effect of water saturation level on the additive depletion by water and tribofilm formation.
- Study the effect of water on the oil contaminated with different levels of CB at different ageing conditions. This provides a depth understanding of the effect of water on soot agglomeration and starvation in the inlet of rubbing surfaces causing higher wear and friction.
- Study the effect of fuel contamination in oils on the additive depletion by fuel and its effects on friction and wear.
- Investigate the replenishment process by adding fresh FFO and different additives to used and reclaimed oils to extend the service life of engine oil.

10.4 Recommendations to industry

Based on the project findings, the recommendations to the industry are summarised as follows:

- Ageing the oil in the lab uses harsh conditions compared to the conditions in real engines. Therefore, the author suggests using real used oil for further investigations.

- Additives are adsorbed on soot and hence influence the oil performance.
- Removal of free water from the oil results in additives depletion.
- The reclaimed oil after removing the soot or water does not perform similar to the fresh oil due to additives depletion by water or soot.
- ZDDP replenishment process can regain the oil performance after adding 0.75 wt% ZDDP and removing the soot to a certain level.
- If both soot and water contamination exist in the oil, a higher level of ZDDP (>0.75%wt) is required to regain the oil performance.

11 Chapter (11) References

[1] P. Examiner and W. D. Griffin, “(12) United States Patent,” 2010.

[2] J. Semjonovs, G. Springis, and A. Leitans, “Increasing of engine oil change interval by using additional oil filter in diesel engines,” Eng. Rural Dev., vol. 29, no. 13/2014, pp. 247–252, 2014.

[3] A. Rammohan, “Engine’s lubrication oil degradation reasons and detection methods : A review,” Chem. Pharm. Sci., vol. 9, no. 4, pp. 3363–3366, 2016.

[4] L. Guan, X. L. Feng, G. Xiong, and J. A. Xie, “Application of dielectric spectroscopy for engine lubricating oil degradation monitoring,” Sensors Actuators, A Phys., vol. 168, no. 1, pp. 22–29, 2011.

[5] R. M. Mortier, M. F. Fox, and S. T. Orszulik, “Chemistry and Technology of Lubricants,” Dordr. Springer, vol. 107115, pp. 56–75, 2010.

[6] Z. Zhang, D. Simionesie, and C. Schaschke, “Graphite and Hybrid Nanomaterials as Lubricant Additives,” Lubricants, vol. 2, no. 2, pp. 44–65, 2014.

[7] H. Cen, A. Morina, and A. Neville, “Effect of lubricant ageing on lubricants physical and chemical properties and tribological performance; Part I: effect of lubricant chemistry,” Ind. Lubr. Tribol., vol. 70, no. 2, pp. 385–392, 2018.

[8] R. Nguele, H. S. Salim, and K. Sasaki, “Oil Condition Monitoring Degradation Mechanisms and Additive Depletion,” J. Multidiscip. Eng. Sci. Technol., vol. 2, no. 3, pp. 355–360, 2015.

[9] R. Penchaliah, T. J. Harvey, R. J. K. Wood, K. Nelson, and H. E. G. Powrie, “The effects of diesel contaminants on tribological performance on sliding steel on steel contacts,” vol. 225, pp. 779–797, 2011.

[10] F. Motamen Salehi, A. Morina, and A. Neville, “Zinc Dialkyldithiophosphate Additive Adsorption on Carbon Black Particles,” Tribol. Lett., vol. 66, no. 3, p. 0, 2018.

[11] R. Nguele, H. S. Al-salim, and K. Mohammad, “Modeling and Forecasting of Depletion of Additives in Car Engine Oils Using Attenuated Total Reflectance Fast Transform Infrared Spectroscopy,” pp. 206–222, 2014.

[12] D. J. Patty and R. R. Lokollo, “FTIR Spectrum Interpretation of Lubricants with Treatment of Variation Mileage,” vol. 52, pp. 13–20, 2016.

[13] N. Dörr, A. Agocs, C. Besser, A. Ristić, and M. Frauscher, “Engine Oils in the Field : A Comprehensive Chemical Assessment of Engine Oil Degradation in a Passenger Car,” Tribol. Lett., 2019.

[14] K. M. Jefferd, J. S. Rogerson, D. E. Copp, R. L. Brundle, and M. A. Huntly, “The impact of lubricants on heavy duty diesel engine fuel economy and exhaust emissions,” 2000.

[15] R. I. Taylor, “Heavy duty diesel engine fuel economy: Lubricant sensitivities,” SAE Tech. Pap., 2000.

[16] W. Van Dam, T. Miller, G. M. Parsons, and Y. Takeuchi, “The impact of lubricant viscosity and additive chemistry on fuel economy in heavy duty diesel engines,” SAE Int. J. Fuels Lubr., vol. 5, no. 1, pp. 459–469, 2012.

[17] K. Holmberg and A. Erdemir, “Influence of tribology on global energy consumption, costs and emissions,” Friction, vol. 5, no. 3, pp. 263–284, 2017.

[18] B. A. A. L. van Setten, M. Makkee, and J. A. Moulijn, “Science and technology of catalytic diesel particulate filters,” Catal. Rev., vol. 43, no. 4, pp. 489–564, 2001.

[19] K. Vyavhare, S. Bagi, M. Patel, and P. B. Aswath, “Impact of Diesel Engine Oil Additives-Soot Interactions on Physiochemical, Oxidation, and Wear Characteristics of Soot,” Energy and Fuels, vol. 33, no. 5, pp. 4515–4530, 2019.

[20] D. A. Green and R. Lewis, “Effect of soot on oil properties and wear of engine components,” J. Phys. D. Appl. Phys., vol. 40, no. 18, pp. 5488–5501, 2007.

[21] C. C. Kuo, C. A. Passut, T.-C. Jao, A. A. Csontos, and J. M. Howe, “Wear mechanism in Cummins M-11 high soot diesel test engines,” SAE, vol. 107, pp. 499–511, 1998.

[22] E. Hu, X. Hu, T. Liu, L. Fang, K. D. Dearn, and H. Xu, “The role of soot particles in the tribological behavior of engine lubricating oils,” Wear, vol. 304, no. 1–2, pp. 152–161, 2013.

[23] M. Ratoi, R. C. Castle, C. H. Bovington, and H. A. Spikes, “The influence of soot and dispersant on ZDDP film thickness and friction,” Lubr. Sci., vol. 17, no. 1, pp. 25–43, 2004.

[24] H. Sato, N. Tokuoka, H. Yamamoto, and M. Sasaki, “Study on wear mechanism by soot contaminated in engine oil (first report: relation between characteristics of used oil and wear),” SAE Tech. Pap., no. 0148–7191, p. 9, 1999.

[25] S. George, S. Balla, V. Gautam, and M. Gautam, “Effect of diesel soot on lubricant oil viscosity,” Tribol. Int., vol. 40, no. 5, pp. 809–818, 2007.

[26] J. C. Fitch and S. Jaggernauth, “Moisture - The Second Most Destructive Lubricant Contaminate , and its Effects on Bearing Life,” P/PM Technol., vol. 12, no. 5, pp. 1–4, 1994.

[27] G. Ray and G. Fogel, “Estimating Water Content In Oils: Moisture In Solution, Emulsified Water, And Free Water,” 1996.

[28] E. Harika, J. Bouyer, and M. Fillon, “Impact of lubricant contamination with water on hydrodynamic thrust bearing performance,” no. October, 2010.

[29] M. D. Pall and M. Vesala, “Setting Control Limits for Water Contamination In Hydraulic and Lube Systems,” in In The 10th Scandinavian International Conference on Fluid Powe, 2009, pp. 1–7.

[30] J. Floria, “Phosphate Ester Hydrolysis in Aqueous Solution : Associative versus Dissociative Mechanisms,” vol. 5647, no. 97, pp. 719–734, 1998.

[31] B. Bhushan, Introduction to tribology. John Wiley & Sons, 2013.

[32] I. Hutchings and P. Shipway, “Learn more about Friction,” 2017.

[33] K. C. Ludema, “Friction, wear, lubrication: a textbook in tribology,” CRC Press, 1996.

[34] A. Comfort, “An Introduction to Heavy-Duty Diesel Engine Frictional Losses And Lubricant Properties Affecting Fuel Economy – Part I,” SAE Tech. Pap., 2003.

[35] G. Stachowiak and A. W. Batchelor, “Engineering tribology.” Butterworth-Heinemann, Oxford, 2001.

[36] G. W. Stachowiak, Wear: materials, mechanisms and practice. John Wiley & Sons, 2006.

[37] K. Kato and K. Adachi, Wear Mechanisms. Modern Tribology Handbook, 2001.

[38] G. E. Totten, D. K. Wills, and D. G. Feldmann, “Hydraulic Failure Analysis: Fluids,

Components, and System Effects," 2001.

[39] K. Kato, "Classification of Wear Mechanisms / models," vol. 216, no. October 2001, pp. 349–355, 2002.

[40] F. Di Puccio and L. Mattei, "Biotribology of artificial hip joints," vol. 6, no. 1, pp. 77–94, 2015.

[41] C. Lipson and L. V Colwell, Handbook of mechanical wear. University of Michigan Press, 1961.

[42] V. K. Dodiya, "A Study of Various Wear Mechanism and its Reduction Method," vol. 2, no. 09, pp. 242–248, 2016.

[43] F. K. Geitner and H. P. Bloch, "Laser surface engineering of titanium and its alloys for improved wear, corrosion and high-temperature oxidation resistance," pp. 483–521, 2013.

[44] S. Henry, B. Sanders, N. Hrivnak, and D. Kathy, Introduction to Surface Engineering for Corrosion and Wear. ASM Interational, 2001.

[45] J. Halme and P. Andersson, "Rolling contact fatigue and wear fundamentals for rolling bearing diagnostics – state of the art," vol. 224, pp. 377–393, 2009.

[46] H. C. Meng and K. C. Ludema, "Wear models and predictive," vol. 183, pp. 443–457, 1995.

[47] I. Minami, "Applied Sciences Molecular Science of Lubricant Additives," p. 445, 2017.

[48] S. R. Schmid, B. J. Hamrock, and B. O. Jacobson, Fundamentals of machine elements. CRC Press, 2013.

[49] C. Sahay and S. Ghosh, "Understanding Surface Quality : Beyond Average Roughness (Ra) Understanding Surface Quality : Beyond Average Roughness (R a)," 2018.

[50] A. A. Lubrecht, C. H. Venner, and F. Colin, "Film thickness calculation in elasto-hydrodynamic lubricated line and elliptical contacts," Proc. Inst. Mech. Eng. Part J J. Eng. Tribol., vol. 223, no. 3, pp. 511–515, 2009.

[51] G. Stachowiak and A. W. Batchelor, Engineering tribology. Butterworth-Heinemann, 2013.

[52] L. Burstein, “Lubrication and roughness,” in Tribology for Engineers, Woodhead Publishing Limited, 2011, pp. 65–120.

[53] A. C. Redlich, D. Bartel, H. Schorr, and L. Deters, “A Deterministic EHL Model for Point Contacts in Mixed Lubrication Regime,” in Tribology Series, 2000, pp. 85–93.

[54] Q. Xin, “Friction and lubrication in diesel engine system design,” in Diesel Engine System Design, 2013, pp. 651–758.

[55] S. Affatato, “Tribological interactions of modern biomaterials used in total hip arthroplasty (THA),” in Perspectives in Toral Hip Arthroplasty, 2014, pp. 99–110.

[56] M. Kamal, A. Ali, M. A. A. Abdelkareem, A. Elagouz, and F. Essa, “Mini Review on the Significance Nano-Lubricants in Boundary Lubrication Regime,” no. April, 2017.

[57] K. Carnes, “The ten greatest events in tribology history,” Tribol. Lubr. Technol., vol. 61, no. 6, p. 38, 2005.

[58] B. L. Papke, “Mineral Oil Base Fluids,” Encycl. Tribol., pp. 2257–2261, 2013.

[59] S. F. Brown and J. Rosenbaum, “Base Oil Groups : Manufacture , Properties and Performance,” no. April, 2015.

[60] L. J. Gschwender, D. C. Kramer, and B. K. Lok, “Liquid Lubricants and Lubrication,” 2001.

[61] W. Bock, “Hydraulic fluids with new , modern base oils – structure and composition , difference to conventional hydraulic fluids ; experience in the field,” pp. 171–180.

[62] G. Pereira et al., “Chemical and mechanical analysis of tribofilms from fully formulated oils Part 1 – Films on 52100 steel,” Tribol. - Mater. Surfaces Interfaces, vol. 1, no. 1, pp. 48–61, 2007.

[63] A. Morina, A. Neville, M. Priest, and J. H. Green, “ZDDP and MoDTC interactions and their effect on tribological performance–tribofilm characteristics and its evolution,” Tribol. Lett., vol. 24, no. 3, pp. 243–256, 2006.

[64] R. Unnikrishnan, M. C. Jain, A. K. Harinarayan, and A. K. Mehta, “Additive–additive interaction: an XPS study of the effect of ZDDP on the AW/EP characteristics of molybdenum based additives,” Wear, vol. 252, no. 3–4, pp. 240–249, 2002.

[65] J. Martin, C. Grossiord, K. Varlot, B. Vacher, and J. Igarashi, “Synergistic effects in binary systems of lubricant additives: a chemical hardness approach,” Tribol. Lett., vol. 8, no. 4, pp. 193–201, 2000.

[66] C. Espejo, C. Wang, B. Thiébaut, C. Charrin, A. Neville, and A. Morina, “The role of MoDTC tribochemistry in engine tribology performance. A Raman microscopy investigation,” Tribol. Int., vol. 150, p. 106366, 2020.

[67] W. Li et al., “Ultralow Boundary Lubrication Friction by Three-Way Synergistic Interactions among Ionic Liquid, Friction Modifier, and Dispersant,” ACS Appl. Mater. Interfaces, vol. 12, no. 14, pp. 17077–17090, 2020.

[68] H. Okubo, C. Tadokoro, and S. Sasaki, “In Situ Raman-SLIM Monitoring for the Formation Processes of MoDTC and ZDDP Tribofilms at Steel/Steel Contacts under Boundary Lubrication,” Tribol. Online, vol. 15, no. 3, pp. 105–116, 2020.

[69] X. Zhang, L. Yang, Y. Li, H. Li, W. Wang, and B. Ye, “Impacts of lead/zinc mining and smelting on the environment and human health in China,” Environ. Monit. Assess., vol. 184, no. 4, pp. 2261–2273, 2012.

[70] Q. Zeng, “Superlow friction of high mileage used oil with CuDTC in presence of MoDTC,” Ind. Lubr. Tribol., vol. 69, no. 2, pp. 190–198, Jan. 2017.

[71] M. Gautam, K. Chitoor, M. Durbha, and J. C. Summers, “Effect of diesel soot contaminated oil on engine wear investigation of novel oil formulations,” Tribol. Int., vol. 32, no. 12, pp. 687–699, 1999.

[72] P. Willermet, “Some engine oil additives and their effects on antiwear film formation,” Tribol. Lett., vol. 5, no. 1, pp. 41–47, 1998.

[73] D. A. Green and R. Lewis, “The effects of soot-contaminated engine oil on wear and friction: A review,” Proc. Inst. Mech. Eng. Part D J. Automob. Eng., vol. 222, no. 9, pp. 1669–1689, 2008.

[74] Y. Gallo, “Late Cycle Soot Oxidation in Diesel Engines,” Lund University, 2016.

[75] R. Penchaliah, T. J. Harvey, R. J. K. Wood, K. Nelson, and H. E. G. Powrie, “The effects of diesel contaminants on tribological performance on sliding steel on steel contacts,” Proc. Inst. Mech. Eng. Part J J. Eng. Tribol., vol. 225, no. 8, pp. 779–797, 2011.

[76] C. Liu, S. Nemoto, and S. Ogano, “Effect of soot properties in diesel engine oils on

frictional characteristics," Tribol. Trans., vol. 46, no. 1, pp. 12–18, 2003.

[77] P. Ramkumar, L. Wang, T. J. Harvey, R. J. K. Wood, K. Nelson, and E. S. Yamaguchi, "The effect of diesel engine oil contamination on friction and wear," Word Tribol. Congr., vol. 42010, pp. 537–538, 2005.

[78] F. Chinas-Castillo and H. A. Spikes, "The behavior of diluted sooted oils in lubricated contacts," Tribol. Lett., vol. 16, no. 4, pp. 317–322, 2004.

[79] L. Joly-Pottuz et al., "Diamond-derived carbon onions as lubricant additives," Tribol. Int., vol. 41, no. 2, pp. 69–78, 2008.

[80] P. Colacicco and D. Mazuyer, "The role of soot aggregation on the lubrication of diesel engines," Tribol. Trans., vol. 38, no. 4, pp. 959–965, 1995.

[81] I. Berbezier, J. M. Martin, and P. Kapsa, "The role of carbon in lubricated mild wear," Tribol. Int., vol. 19, no. 3, pp. 115–122, 1986.

[82] S. Corso and R. Adamo, "The effect of diesel soot on reactivity of oil additives and valve train materials," 1984.

[83] S. George, S. Balla, and M. Gautam, "Effect of diesel soot contaminated oil on engine wear," vol. 262, no. September 2006, pp. 1113–1122, 2007.

[84] D. A. Green, R. Lewis, and R. S. Dwyer-Joyce, "The Wear Effects and Mechanisms of Soot Contaminated Automotive Lubricants," vol. 1996, no. May 2006.

[85] D. A. Green, R. Lewis, and R. S. Dwyer-Joyce, "Wear effects and mechanisms of soot contaminated automotive lubricants," Proc. Inst. Mech. Eng. Part J J. Eng. Tribol., vol. 220, no. 3, pp. 159–169, 2006.

[86] R. Mainwaring, "Soot and wear in heavy duty diesel engines," SAE Int., vol. 106, pp. 1721–1738, 1997.

[87] S. Li, A. A. Csontos, B. M. Gable, C. A. Passut, and T.-C. Jao, "Wear in cummins M-11/EGR test engines," SAE Trans., pp. 2258–2271, 2002.

[88] P. R. Ryason and T. P. Hansen, "Voluminosity of soot aggregates: a means of characterizing soot-laden oils," SAE Trans., pp. 897–903, 1991.

[89] J. Zirker and F. Larry, "Oil Bypass Filter Technology Performance Evaluation," no.

January, 2003.

[90] M. Kawamura, T. Ishiguro, K. Fujita, and H. Morimoto, “Deterioration of antiwear properties of diesel engine oils during use,” Wear, vol. 123, no. 3, pp. 269–280, 1988.

[91] D. Green, “The tribological effects of soot contaminated lubricants on engine components,” University of Sheffield, 2007.

[92] F. Metrics, “Oil Degradation Mechanisms,” 2012. [Online]. Available: http://www.fluidmetrics.com/degradation.html.

[93] L. S. Khuong et al., “A review on the effect of bioethanol dilution on the properties and performance of automotive lubricants in gasoline engines,” RSC Adv., vol. 6, no. 71, pp. 66847–66869, 2016.

[94] ASTM Standards, “Standard Practice for Condition Monitoring of In-Service Lubricants by Trend Analysis Using Fourier Transform Infrared (FT-IR),” vol. i, 2010.

[95] N. Robinson and B. S. Hons, “Monitoring Oil Degradation with Infrared Spectroscopy,” Set Point Technol., pp. 1–8, 2000.

[96] A. N. Hui Cen, Ardian Morina, “Effect of lubricant ageing on lubricant physical and chemical properties and tribological performance. Part I: effect of lubricant chemistry,” 2018.

[97] D. Uy et al., “Characterization of gasoline soot and comparison to diesel soot: Morphology, chemistry, and wear,” Tribol. Int., vol. 80, pp. 198–209, 2014.

[98] V. Sharma et al., “Structure and chemistry of crankcase and exhaust soot extracted from diesel engines,” Carbon N. Y., vol. 103, pp. 327–338, 2016.

[99] H. Bhowmick and S. K. Biswas, “Relationship between physical structure and tribology of single soot particles generated by burning ethylene,” Tribol. Lett., vol. 44, no. 2, pp. 139–149, 2011.

[100] F. Chinas-Castillo and H. A. Spikes, “The behavior of diluted sooted oils in lubricated contacts,” Tribol. Lett., vol. 16, no. 4, pp. 317–322, 2004.

[101] V. Sharma, S. Bagi, M. Patel, O. Aderniran, and P. B. Aswath, “Influence of Engine Age on Morphology and Chemistry of Diesel Soot Extracted from Crankcase Oil,” Energy and Fuels, vol. 30, no. 3, pp. 2276–2284, 2016.

[102] X. Han, K. Zheng, Y. Zhang, X. Zhang, Z. Zhang, and Z. L. Wang, “Low-temperature in situ large-strain plasticity of silicon nanowires,” Adv. Mater., vol. 19, no. 16, pp. 2112–2118, 2007.

[103] J. Deneen, W. M. Mook, A. Minor, W. W. Gerberich, and C. B. Carter, “In situ deformation of silicon nanospheres,” J. Mater. Sci., vol. 41, no. 14, pp. 4477–4483, 2006.

[104] I. Lahouij, F. Dassenoy, B. Vacher, and J. M. Martin, “Real time TEM imaging of compression and shear of single fullerene-like MoS2nanoparticle,” Tribol. Lett., vol. 45, no. 1, pp. 131–141, 2012.

[105] A. Asthana, K. Momeni, A. Prasad, Y. K. Yap, and R. S. Yassar, “In situ observation of size-scale effects on the mechanical properties of ZnO nanowires,” Nanotechnology, vol. 22, no. 26, 2011.

[106] Z. L. Wang, P. Poncharal, and W. A. De Heer, “Measuring physical and mechanical properties of individual carbon nanotubes by in situ TEM,” vol. 61, pp. 1025–1030, 2000.

[107] I. Lahouij, F. Dassenoy, B. Vacher, K. Sinha, D. A. Brass, and M. Devine, “Understanding the deformation of soot particles/agglomerates in a dynamic contact: Tem in situ compression and shear experiments,” Tribol. Lett., vol. 53, no. 1, pp. 91–99, 2014.

[108] I. Z. Jenei et al., “Mechanical characterization of diesel soot nanoparticles: in situ compression in a transmission electron microscope and simulations,” Nanotechnology, vol. 29, no. 8, p. 085703, 2018.

[109] H. Bhowmick, S. K. Majumdar, and S. K. Biswas, “Influence of physical structure and chemistry of diesel soot suspended in hexadecane on lubrication of steel-on-steel contact,” Wear, vol. 300, no. 1–2, pp. 180–188, 2013.

[110] A. La Rocca, G. Di Liberto, P. J. Shayler, and M. W. Fay, “Tribology International The nanostructure of soot-in-oil particles and agglomerates from an automotive diesel engine,” Tribiology Int., vol. 61, pp. 80–87, 2013.

[111] S. Kook, R. Zhang, K. Szeto, L. M. Pickett, and T. Aizawa, “In-Flame Soot Sampling and Particle Analysis in a Diesel Engine,” SAE Int. J. Fuels Lubr., vol. 6, no. 1, pp. 80–97, 2013.

[112] S. Li, A. A. Csontos, B. M. Gable, C. A. Passut, and E. P. Additives, “Wear in Cummins M-1 1 / EGR Test Engin,” vol. 111, no. May, pp. 2258–2271, 2020.

[113] Z. R. Yue, W. Jiang, L. Wang, S. D. Gardner, and C. U. Pittman, “Surface characterization of electrochemically oxidized carbon fibers,” Carbon N. Y., vol. 37, no. 11, pp. 1785–1796, 1999.

[114] A. La Rocca, G. Di Liberto, P. J. Shayler, C. D. J. Parmenter, and M. W. Fay, “Application of nanoparticle tracking analysis platform for the measurement of soot-in-oil agglomerates from automotive engines,” Tribol. Int., vol. 70, pp. 142–147, 2014.

[115] S. Kook et al., “Automated Detection of Primary Particles from Transmission Electron Microscope (TEM) Images of Soot Aggregates in Diesel Engine Environments,” SAE Int. J. Engines, vol. 9, no. 1, pp. 279–296, 2015.

[116] A. La Rocca, G. Di Liberto, P. J. Shayler, C. D. J. Parmenter, and M. W. Fay, “Application of nanoparticle tracking analysis platform for the measurement of soot-in-oil agglomerates from automotive engines,” Tribol. Int., vol. 70, no. February, pp. 142–147, 2014.

[117] A. Kontou, M. Southby, N. Morgan, and H. A. Spikes, “Influence of Dispersant and ZDDP on Soot Wear,” Tribol. Lett., vol. 66, no. 4, pp. 1–15, 2018.

[118] T. S. Loftis and M. B. Lanius, “A new method for combination full-flow and bypass filtration: Venturi Combo,” SAE Tech. Pap., 1997.

[119] B. D. Morgan, F. Consultant, and A. M. S. Filtration, “What is Oil Filtration Full Flow versus Depth Filtration,” 2008.

[120] A. L. Samways, “Centrifugal cleaning of fluid power oils,” SAE Tech. Pap., vol. 108, no. May, pp. 267–278, 1999.

[121] Pall Food and Beverage, “Understanding Particle Filtration in Liquids in Food and Beverage Industry Applications Overview,” no. Figure 2, pp. 1–8, 2016.

[122] C. Akduman, “Nanofibers in filtration,” no. August, 2019.

[123] “TREATMENT OF THE SYSTEM OIL IN MEDIUM SPEED AND CROSSHEAD DIESEL ENGINE INSTALLATIONS The International Council on Combustion Engines Conseil International des,” no. 24, 2005.

[124] C. A. Eachus, “The Trouble with Water,” Tribol. Lubr. Technol., no. October, pp. 32–38, 2005.

[125] J. Sander, “Water Contamination : Management of Water During the Lubricant Life Cycle,” Fort Worth Lubr. Eng. Inc., pp. 1–9, 2009.

[126] U. . E. P. Agency, “Quailty Criteria for Water,” no. 2, pp. 46–49, 1976.

[127] C. Leigh-Jones, “Water contamination in oil,” Mot. Sh., vol. 85, no. 1005, pp. 34–35, 2004.

[128] J. Peter Clark, “Emulsion: When Oil and Water Do Mix,” Food Technol., vol. 67, no. 8, pp. 1–8, 2013.

[129] G. Ray and G. Fogel, “Estimating Water Content In Oils: Moisture In Solution, Emulsified Water, And Free Water,” in Proceedings of a Joint Conference, 1996, pp. 1–14.

[130] W. Needelman and G. LaVallee, “Forms of water in oil and their control,” in Noria Lubrication Excellence Conference, Columbus Ohio, 2006.

[131] R. E. Cantley, “The effect of water in lubricating oil on bearing fatigue life,” ASLE Trans., vol. 20, no. 3, pp. 244–248, 1977.

[132] A. Neugebauer, “Going Green: What About Water ?,” no. August, pp. 2–3, 2009.

[133] Y. Itoh, “Used Engine Oil Analysis User Interpretation Guide,” Int. Counc. Combust. Engines, no. 30, 2011.

[134] F. Higgins and J. Seelenbinder, “Low Level Quantitative FTIR Analysis of Water in Oil Using a Novel Water Stabilization Technique,” 2013.

[135] B. B. Rahimi, A. Semnani, A. N. Ejhieh, S. Langeroodi, and M. H. Davood, “Application of ICP-OES in the Comparative Analysis of a Used and Fresh Gasoline Motor Oil,” vol. 12, no. 2, 2012.

[136] J. Evans, “How Do Oils Degrade ?,” Wear Check, no. 52, pp. 1–6, 2011.

[137] J. Evans, “How Do Oils Degrade ?,” Wear Check, vol. 52, pp. 1–6, 2011.

[138] L. Raymond, Hydrogen Embrittlement: Prevention and Control, vol. 962. ASTM International, 1988.

[139] W. Zhang, “Evaluation of Susceptibility to Hydrogen Embrittlement — A Rising Step Load Testing Method,” no. August, pp. 389–395, 2016.

[140] D. Brondel, R. Edwards, A. Hayman, D. Hill, and T. Semerad, “Corrosion in the Oil Industry,” Oilf. Rev., pp. 4–69, 1994.

[141] Z. Chen, X. He, C. Xiao, and S. H. Kim, “Effect of Humidity on Friction and Wear — A Critical Review,” pp. 1–26, 2018.

[142] J. K. Lancaster, “A review of the influence of environmental humidity and water on friction, lubrication and wear,” Tribol. Int., vol. 23, no. 6, pp. 371–389, 1990.

[143] S. Ross and Y. Suzin, “Lubricant Foaming abd Aeration,” 1982.

[144] B. Ave and F. Worth, “Water Contamination : Management of Water During The Lubricant Life Cycle,” 2009.

[145] D. W. Johnson, Turbine Engine Lubricant and Additive Degradation Mechanisms. In Aerospace Engineering. IntechOpen 2018.

[146] L. C. Ancho, “Oxidation in lubricant base oils,” The filter, vol. 4, pp. 6–7, 2006.

[147] L. R. Rudnick, Lubricant additives: chemistry and applications. CRC press, 2017.

[148] A. L. Clayden, “Water in Crankcase Oil S1,” in SAE Technical Paper, 1924.

[149] H. Cen, A. Morina, A. Neville, R. Pasaribu, and I. Nedelcu, “Effect of water on ZDDP anti-wear performance and related tribochemistry in lubricated steel/steel pure sliding contacts,” Tribol. Int., vol. 56, pp. 47–57, 2012.

[150] P. Parsaeian, M. C. P. Van Eijk, I. Nedelcu, A. Neville, and A. Morina, “Study of the interfacial mechanism of ZDDP tribofilm in humid environment and its effect on tribochemical wear; Part I: Experimental,” Tribol. Int., vol. 107, no. October 2016, pp. 135–143, 2017.

[151] P. Parsaeian et al., “An experimental and analytical study of the effect of water and its tribochemistry on the tribocorrosive wear of boundary lubricated systems with ZDDP-containing oil,” Wear, vol. 358–359, pp. 23–31, 2016.

[152] H. L. Costa and H. A. Spikes, “Impact of ethanol on the formation of antiwear tribofilms from engine lubricants,” Tribol. Int., vol. 93, pp. 364–376, 2016.

[153] W. H. Van Glabbeek, T. K. Sheiretov, and C. Cusano, “The Effect of Dissolved Water on the Tribological Properties of Polyalkylene Glycol and Polyolester Oils,” vol. 61801, no. 217, 1994.

[154] F. M. Salehi, “The Effect of Oil Properties on Engine Oil Pump Failure Mechanisms,” p. 235, 2016.

[155] N. Canter, “Lubricant additives: What degree are they removed by filtration systems?,” Tribol. Lubr. Technol., vol. 69, no. 12, pp. 26-28,30-34, 2013.

[156] H. Spikes, “The history and mechanisms of ZDDP,” Tribol. Lett., vol. 17, no. 3, pp. 469–489, 2004.

[157] S. Kumar, N. M. Mishra, and P. S. Mukherjee, “Additives depletion and engine oil condition - A case study,” Ind. Lubr. Tribol., vol. 57, no. 2, pp. 69–72, 2005.

[158] K. Hosonuma, K. Yoshida, and A. Matsunaga, “The decomposition products of zinc dialkyldithiophosphate in an engine and their interaction with diesel soot,” Wear, vol. 103, no. 4, pp. 297–309, 1985.

[159] Y. Olomolehin, R. Kapadia, and H. Spikes, “Antagonistic interaction of antiwear additives and carbon black,” Tribol. Lett., vol. 37, no. 1, pp. 49–58, 2010.

[160] S. Antusch, M. Dienwiebel, E. Nold, P. Albers, U. Spicher, and M. Scherge, “On the tribochemical action of engine soot,” Wear, vol. 269, no. 1–2, pp. 1–12, 2010.

[161] M. Patel, C. L. Azanza Ricardo, P. Scardi, and P. B. Aswath, “Morphology, structure and chemistry of extracted diesel soot—Part I: Transmission electron microscopy, Raman spectroscopy, X-ray photoelectron spectroscopy and synchrotron X-ray diffraction study,” Tribol. Int., vol. 52, pp. 29–39, 2012.

[162] V. Sharma, S. Bagi, M. Patel, O. Aderniran, and P. B. Aswath, “Influence of Engine Age on Morphology and Chemistry of Diesel Soot Extracted from Crankcase Oil,” Energy and Fuels, vol. 30, no. 3, pp. 2276–2284, 2016.

[163] M. Patel and P. B. Aswath, “Structure and chemistry of crankcase and cylinder soot and tribofilms on piston rings from a Mack T-12 dynamometer engine test,” Tribol. Int., vol. 77, pp. 111–121, 2014.

[164] S. Bagi, V. Sharma, M. Patel, and P. B. Aswath, “Effects of Diesel Soot Composition and Accumulated Vehicle Mileage on Soot Oxidation Characteristics,” Energy and

Fuels, vol. 30, no. 10, pp. 8479–8490, 2016.

[165] H. Spedding and R. C. Watkins, “The antiwear mechanism of zddp ’ s Part I,” no. 1, pp. 9–12, 1982.

[166] F. G. Rounds, “Some factors affecting the decomposition of three commercial zinc organodithiophosphates,” ASLE Trans., vol. 18, no. 2, pp. 79–89, 1975.

[167] M. L. S. Fuller, M. Kasrai, G. M. Bancroft, K. Fyfe, and K. H. Tan, “Solution decomposition of zinc dialkyl dithiophosphate and its effect on antiwear and thermal film formation studied by X-ray absorption spectroscopy,” vol. 31, no. 10, pp. 627–644, 1999.

[168] R. Garvey and G. Fogel, “Estimating water content in oils: moisture in solution, emulsified water, and free water,” 1996.

[169] A. Zingaro, “Sources and effects of contaminants; roles of lubrication ‘and component sensitivity; and the dynamic nature of contamination in hydraulic systems - all as related to control strategies,” pp. 37–40, 1994.

[170] B. Acharya, K. S. Avva, B. Thapa, T. N. Pardue, and J. Krim, “Synergistic Effect of Nanodiamond and Phosphate Ester Anti-Wear Additive Blends,” 2018.

[171] M. F. Smiechowski and H. B. Martin, “Electrochemical Characterization Of Lubricants For Microfabricated Sensor Applications,” PhD Thesis, 2005.

[172] N. Soda, Y. Kimura, and A. Tanaka, “Wear of some fcc metals during unlubricated sliding Part I. Effects of load, velocity and atmospheric pressure on wear,” Wear, vol. 33, no. 1, pp. 1–16, 1975.

[173] P. P. Data, “United States Patent (45) Date of Patent :,” vol. 2, no. 12, pp. 1–4, 2008.

[174] S. Kumar, N. M. Mishra, and P. S. Mukherjee, “Additives depletion and engine oil condition - A case study,” Ind. Lubr. Tribol., vol. 57, no. 2, pp. 69–72, 2005.

[175] B. W. Schwandt, B. M. Verdegan, C. E. Holm, S. L. Fallon, and M. M. Khosropour, “Cleanable heavy duty oil filters for trucks and buses,” SAE Tech. Pap., vol. 105, no. May, pp. 2439–2447, 1996.

[176] R. Thom, K. Kollmann, W. Warnecke, and M. Frend, “Extended Oil Drain Intervals: Conservation of Resources or Reduction of Engine Life,” SAE Trans., vol. 104, pp. 706–

718, Jul. 1995.

[177] S. E. Schwartz, “(12) United States Patent,” vol. 1, no. 12, 2001.

[178] D. Sniderman, “The chemistry and function of lubricant additives,” Tribol. Lubr. Technol., vol. 73, no. 11, pp. 18–28, 2017.

[179] D. F. McCready, “Engine Oil Additive Dry Lubricant Powder,” no. 19, 1983.

[180] O. Raymond Rohde, Bartlesville, “Engine Oil Additive Dry Lubricant Powder,” no. 19, 1973.

[181] B. Township, M. I. Us, E. J. Adams, M. I. Us, and C. Thomas, “Oil Make-Up and Replenishment Oil Filter and Method of Use,” vol. 1, no. 19, 2011.

[182] E. Schneider and St. Motors Corporation, “Automatic Additive Replenishment System for IC Engine Lubricating Oil,” vol. 2, no. 12, 2005.

[183] O. Raymond Rohde, Bartlesville, “United States Patent (19),” no. 19, 1978.

[184] F. Lefebvre, Byron, Ft. Lauderdale, “Engine Oil Additive Dry Lubricant Powder,” no. 19, 1997.

[185] I. DeJovine, James M. Homewood, “United States Patent (19),” no. 19, 1979.

[186] Y. C. Lin and H. So, “Limitations on use of ZDDP as an antiwear additive in boundary lubrication,” Tribol. Int., vol. 37, no. 1, pp. 25–33, 2004.

[187] L. J. Taylor and H. A. Spikes, “Friction-enhancing properties of zddp antiwear additive: Part i—friction and morphology of zddp reaction films,” Tribol. Trans., vol. 46, no. 3, pp. 303–309, 2003.

[188] Z. Yin, M. Kasrai, M. Fuller, G. M. Bancroft, K. Fyfe, and K. H. Tan, “Application of soft X-ray absorption spectroscopy in chemical characterization of antiwear films generated by ZDDP Part I: the effects of physical parameters,” Wear, vol. 202, no. 2, pp. 172–191, 1997.

[189] A. Tomala, A. Naveira-Suarez, I. C. Gebeshuber, and R. Pasaribu, “Effect of base oil polarity on micro and nanofriction behaviour of base oil + ZDDP solutions,” Tribol. - Mater. Surfaces Interfaces, vol. 3, no. 4, pp. 182–188, 2009.

[190] A. Ghanbarzadeh et al., “A Semi-deterministic Wear Model Considering the Effect of

Zinc Dialkyl Dithiophosphate Tribofilm," Tribol. Lett., vol. 61, no. 1, pp. 1–15, 2016.

[191] M. Kano, Y. Yasuda, and J. P. Ye, "The effect of ZDDP and MoDTC additives in engine oil on the friction properties of DLC-coated and steel cam followers," Lubr. Sci., vol. 17, no. 1, pp. 95–103, 2004.

[192] L. J. Taylor and H. A. Spikes, "Friction-enhancing properties of zddp antiwear additive: Part i—friction and morphology of zddp reaction films," Tribol. Trans., vol. 46, no. 3, pp. 303–309, 2003.

[193] J. Umer, N. J. Morris, R. Rahmani, H. Rahnejat, S. Howell-Smith, and S. Balakrishnan, "Effect of dispersant concentration with friction modifiers and anti-wear additives on the tribofilm composition and boundary friction," J. Tribol., vol. 143, no. 11, p. 111901, 2021.

[194] ASTM D 4636-17, "Standard Test Method for Corrosiveness and Oxidation Stability of Hydraulic Oils , Aircraft Turbine Engine Lubricants , and Other Highly," vol. 99, no. Reapproved, 1999.

[195] C. Besser, C. Schneidhofer, N. Dörr, F. Novotny-Farkas, and G. Allmaier, "Investigation of long-term engine oil performance using lab-based artificial ageing illustrated by the impact of ethanol as fuel component," Tribol. Int., vol. 46, no. 1, pp. 174–182, 2012.

[196] Z. Siwei, "Leaf Coppin," vol. 00, no. February, pp. 167–180, 2001.

[197] A. Turbine and E. Lubricants, "Standard Test Method for Corrosiveness and Oxidation Stability of Hydraulic Oils , Aircraft Turbine Engine Lubricants , and Other Highly," Order A J. Theory Ordered Sets Its Appl., pp. 1–10, 2004.

[198] F. Motamen Salehi, A. Morina, and A. Neville, "The effect of soot and diesel contamination on wear and friction of engine oil pump," Tribol. Int., vol. 115, no. August 2018, pp. 285–296, 2017.

[199] I. R. Superseding et al., "VEHICLE RECOMMENDED," 2018.

[200] ASTM D7844-20, "Standard Test Method for Condition Monitoring of Soot in In-Service Lubricants by Trend Analysis using Fourier Transform Infrared (FT-IR) Spectrometry," ASTM Int. West Conshohocken, PA, 2020.

[201] H. Bordg, G. Desserprix, A. Royet, and M. Stewart, "Soot contamination in engine oil."

[202] S. Glassford, B. Byrne, and S. G. Kazarian, "Recent applications of ATR FTIR

spectroscopy and imaging to proteins Stefanie E. Glassford," Biochim. Biophys. acta-Proteins proteomics, vol. 1834, no. 12, pp. 2849–2858, 2013.

[203] P. Kewat, "Investigation of growth of oxides , amines and halogen compounds in engine oil using FT-IR spectroscopy," 2018.

[204] A. Ausili, M. Sánchez, and J. C. Gómez-Fernández, "Attenuated total reflectance infrared spectroscopy: A powerful method for the simultaneous study of structure and spatial orientation of lipids and membrane proteins," Biomed. Spectrosc. Imaging, vol. 4, no. 2, pp. 159–170, 2015.

[205] S. Ghosh, V. L. Prasanna, B. Sowjanya, P. Srivani, and M. Alagaraja, "Inductively coupled plasma - Optical emission spectroscopy : A review Inductively Coupled Plasma – Optical Emission Spectroscopy : A Review .," no. January 2013, 2016.

[206] ASTM Standards, "Standard Practice for Calculating Viscosity Index from Kinematic Viscosity at 40," Br. Stand. 4459, vol. 93, no. Reapproved, pp. 1–6, 1991.

[207] M. Johnson, "'White light' interferometry," Fibre Opt. '90, vol. 1314, no. 2002, p. 307, 1990.

[208] A. K. Y. A. Dorgham, "Reaction kinetics and rheological characteristics of ultra-thin P-based triboreactive films," no. December, 2017.

[209] JPK Instruments AG, "The NanoWizard ® AFM Handbook," p. 40, 2005.

[210] E. Casero, L. Vázquez, A. M. Parra-Alfambra, and E. Lorenzo, "AFM, SECM and QCM as useful analytical tools in the characterization of enzyme-based bioanalytical platforms," Analyst, vol. 135, no. 8, pp. 1878–1903, 2010.

[211] V. Vaiano, D. Sannino, and O. Sacco, "Transmission Electron Microscopy," in Nanomaterials for the Detection and Removal of Wastewater Pollutants, B. Bonelli, F. S. Freyria, I. Rossetti, and R. Sethi, Eds. Elsevier, 2020, pp. 285–301.

[212] W. Ndugire and M. Yan, "X-Ray Photoelectron Spectroscopy Carbohydrate-Presenting Metal Nanoparticles : Synthesis , Characteriza- tion and Applications Matrices for natural-fibre reinforced composites," 2020.

[213] S. N. Crobu M, Rossi A, Mangolini F, "Chain-length-identification strategy in zinc polyphosphate glasses by means of XPS and ToF-SIMS," Anal. Bioanal. Chem., vol. 403(5), pp. 1415–32., 2012.

[214] M. Crobu, A. Rossi, F. Mangolini, and N. D. Spencer, “Tribochemistry of bulk zinc metaphosphate glasses,” Tribol. Lett., vol. 39, no. 2, pp. 121–134, 2010.

[215] J. Zhang, M. Ueda, S. Campen, and H. Spikes, “Boundary Friction of ZDDP Tribofilms,” Tribol. Lett., vol. 69, no. 1, pp. 1–17, 2021.

[216] H. Cen, A. Morina, A. Neville, R. Pasaribu, and I. Nedelcu, “Effect of water on ZDDP anti-wear performance and related tribochemistry in lubricated steel/steel pure sliding contacts,” Tribol. Int., vol. 56, pp. 47–57, 2012.

[217] P. H. Nedelcu I, Piras E, Rossi A, “XPS analysis on the influence of water on the evolution of zinc dialkyldithiophosphate–derived reaction layer in lubricated rolling contacts,” Surf. Interface Anal., vol. 44(8), pp. 1219–24, 2012.

[218] V. Vishwakarma and S. Uthaman, “X-Ray Diffraction Environmental impact of sustainable green concrete Methods for Assessing Surface Cleanli- ness Zinc-substituted hydroxyapatite,” 2020.

[219] K. Jurkiewicz, M. Pawlyta, and A. Burian, “Structure of Carbon Materials Explored by Local Transmission Electron Microscopy and Global Powder Diffraction Probes,” C, vol. 4, no. 4, p. 68, 2018.

[220] S. International, SAE Oil Filter Test Procedure HS-806/2009. USA, 2009.

[221] B. W. Schwandt et al., “Systems for Diesel Engines,” vol. 102, no. May, pp. 1–11, 2020.

[222] J. J. Truhan, J. Qu, and P. J. Blau, “A rig test to measure friction and wear of heavy duty diesel engine piston rings and cylinder liners using realistic lubricants,” Tribol. Int., vol. 38, no. 3, pp. 211–218, 2005.

[223] ASTMD6304-07, “Standard Test Method for Determination of Water in Petroleum Products , Lubricating Oils , and Additives by Coulometric Karl Fischer Titration 1,” pp. 7–12.

[224] I. Berbezier, J. M. Martin, and P. Kapsa, “The role of carbon in lubricated mild wear,” Tribol. Int., vol. 19, no. 3, pp. 115–122, 1986.

[225] L. D. Aguilera-camacho, B. Eduardo, J. S. Garc, and K. J. Moreno, “Thermal Stability and Lubrication Properties of Biodegradable Castor Oil on AISI 4140 Steel,” pp. 1–15, 2018.

[226] M. Aktary, M. T. McDermott, and J. Torkelson, “Morphological evolution of films formed from thermooxidative decomposition of ZDDP,” Wear, vol. 247, no. 2, pp. 172–179, 2001.

[227] L. I. Farfan-Cabrera, E. A. Gallardo-Hernández, J. Pérez-González, B. M. Marín-Santibáñez, and R. Lewis, “Effects of Jatropha lubricant thermo-oxidation on the tribological behaviour of engine cylinder liners as measured by a reciprocating friction test,” Wear, vol. 426–427, 2019.

[228] J. K. Mannekote and S. V. Kailas, “The effect of oxidation on the tribological performance of few vegetable oils,” J. Mater. Res. Technol., vol. 1, no. 2, pp. 91–95, 2012.

[229] A. Y. El-Naggar et al., “Oxidation stability of lubricating base oils,” Pet. Sci. Technol., vol. 36, no. 3, pp. 179–185, 2018.

[230] F. M. Salehi, A. Morina, and A. Neville, “Tribology International The effect of soot and diesel contamination on wear and friction of engine oil pump,” vol. 115, no. May, pp. 285–296, 2017.

[231] R. J. K. Wood et al., Electrostatic monitoring of the effects of carbon black on lubricated steel / steel sliding contacts, vol. 48. Elsevier Masson SAS, 2005.

[232] P. R. Ryason, I. Y. Chan, and J. T. Gilmore, “Polishing wear by soot,” vol. 137, pp. 15–24, 1990.

[233] J. J. Truhan, J. Qu, and P. J. Blau, “The effect of lubricating oil condition on the friction and wear of piston ring and cylinder liner materials in a reciprocating bench test,” vol. 259, no. 2005, pp. 1048–1055, 2008.

[234] H. Ghiassi, P. Toth, I. C. Jaramillo, and J. A. S. Lighty, “Soot oxidation-induced fragmentation: Part 1: The relationship between soot nanostructure and oxidation-induced fragmentation,” Combust. Flame, vol. 163, pp. 179–187, 2016.

[235] A. D. Sediako, A. Bennett, W. L. Roberts, and M. J. Thomson, “In Situ Imaging Studies of Combustor Pressure Effects on Soot Oxidation,” Energy and Fuels, vol. 33, no. 2, pp. 1582–1589, 2019.

[236] K. Kamegawa, K. Nishikubo, and H. Yoshida, “Oxidative degradation of carbon blacks with nitric acid (I) - Changes in pore and crystallographic structures,” Carbon N. Y., vol.

36, no. 4, pp. 433–441, 1998.

[237] S. Zhang et al., “Control of graphitization degree and defects of carbon blacks through ball-milling,” RSC Adv., vol. 4, no. 1, pp. 505–509, 2014.

[238] B. Gupta, N. Kumar, K. Panda, V. Kanan, S. Joshi, and I. Visoly-Fisher, “Role of oxygen functional groups in reduced graphene oxide for lubrication,” Sci. Rep., vol. 7, pp. 1–14, 2017.

[239] V. Sharma et al., “Structure and chemistry of crankcase and exhaust soot extracted from diesel engines,” Carbon N. Y., vol. 103, pp. 327–338, 2016.

[240] I. Z. Jenei et al., “Mechanical characterization of diesel soot nanoparticles: In situ compression in a transmission electron microscope and simulations,” Nanotechnology, vol. 29, no. 8, 2018.

[241] A. Martini, U. S. Ramasamy, and M. Len, “Review of Viscosity Modifier Lubricant Additives,” Tribol. Lett., vol. 66, no. 2, pp. 1–34, 2018.

[242] M. Lapuerta, F. Martos, and J. Herreros, “Effect of engine operating conditions on the size of primary particles composing diesel soot agglomerates,” J. Aerosol Sci. - J AEROSOL SCI, vol. 38, pp. 455–466, 2007.

[243] D. Su, R. Jentoft, J. Mueller, D. Rothe, E. Jacob, and C. D. Simpson, “Microstructure and oxidation behaviour of Euro IV diesel engine soot: a comparative study with synthetic model soot substances.”

[244] J. Xi and B.-J. Zhong, “Soot in Diesel Combustion Systems,” Chem. Eng. Technol., vol. 29, pp. 665–673, 2006.

[245] M. S. El-Shobokshy, “The effect of diesel engine load on particulate carbon emission,” Atmos. Environ., vol. 18, no. 11, pp. 2305–2311, 1984.

[246] O. H. Phillips, P. D. Lane, and M. C. Shadday, “Diesel engine wear with spin-on by-pass lube oil filters,” SAE Tech. Pap., 1979.

[247] F. Motamen Salehi, A. Morina, and A. Neville, “Zinc Dialkyldithiophosphate Additive Adsorption on Carbon Black Particles,” Tribol. Lett., vol. 66, no. 3, p. 0, 2018.

[248] A. B. Fialkovskii, R V; Korbut, L F; Lisovskaya, M A; Vipper, “Magnesium sulfonate additives,” Chem. Technol. Fuels Oils (Engl. Transl.); (United States), vol. 19:3, no. 3,

pp. 31–32, 1983.

[249] P. Parsaeian, M. C. P. Van Eijk, I. Nedelcu, A. Neville, and A. Morina, “Tribology International Study of the interfacial mechanism of ZDDP tribo fi lm in humid environment and its e ff ect on tribochemical wear ; Part I : Experimental,” Tribiology Int., vol. 107, no. September 2016, pp. 135–143, 2017.

[250] E. Liu and S. D. Kouame, “An XPS study on the composition of zinc dialkyl dithiophosphate tribofilms and their effect on camshaft lobe wear,” Tribol. Trans., vol. 57, no. 1, pp. 18–27, 2013.

[251] M. Crobu, A. Rossi, F. Mangolini, and N. D. Spencer, “Chain-length-identification strategy in zinc polyphosphate glasses by means of XPS and ToF-SIMS,” Anal. Bioanal. Chem., vol. 403, no. 5, pp. 1415–1432, 2012.

[252] M. S. Fuller, M. Kasrai, G. Bancroft, K. Fyfe, and K. H. Tan, “Solution decomposition of zinc dialkyl dithiophosphate and its effect on antiwear and thermal film formation studied by X-ray absorption spectroscopy,” Tribol. Int., vol. 31, pp. 627–644, 1998.

[253] M. Nicholls, T. Do, P. Norton, M. Kasrai, and G. Bancroft, “Review of the lubrication of metallic surfaces by zinc dialkyl-dithiophosphates,” Tribol. Int., vol. 38, pp. 15–39, 2005.

[254] F. M. Salehi and D. N. K. A. Morina, “Corrosive – Abrasive Wear Induced by Soot in Boundary Lubrication Regime,” Tribol. Lett., vol. 63, no. 2, pp. 1–11, 2016.

[255] F. W. Yang et al., “Tribological properties and action mechanism of a highly hydrolytically stable N-containing heterocyclic borate ester,” Ind. Lubr. Tribol., vol. 68, no. 5, pp. 569–576, 2016.

[256] J. A. Heredia-Cancino, M. Ramezani, and M. E. Álvarez-Ramos, “Effect of degradation on tribological performance of engine lubricants at elevated temperatures,” Tribol. Int., vol. 124, pp. 230–237, 2018.

[257] S. Q. A. Rizvi, “A Comprehensive Review of Lubricant Chemistry, Technology, Selection, and Design,” A Compr. Rev. Lubr. Chem. Technol. Sel. Des., 2009.

[258] F. G. Rounds, “Soots from used diesel-engine oils: their effects on wear as measured in 4-ball wear tests.”

[259] N. Dörr et al., “Correlation Between Engine Oil Degradation, Tribochemistry, and Tribological Behavior with Focus on ZDDP Deterioration,” Tribol. Lett., vol. 67, no. 2,

pp. 1–17, 2019.

[260] P. Ramkumar et al., “The effect of diesel engine oil contamination on friction and wear,” Proc. World Tribol. Congr. III - WTC 2005, no. September 2005, 2005.

[261] E. Hu, X. Hu, T. Liu, L. Fang, K. D. Dearn, and H. Xu, “The role of soot particles in the tribological behavior of engine lubricating oils,” Wear, vol. 304, no. 1–2, pp. 152–161, 2013.

[262] D. A. Green and R. Lewis, “The effects of soot-contaminated engine oil on wear and friction: A review,” Proc. Inst. Mech. Eng. Part D J. Automob. Eng., vol. 222, no. 9, pp. 1669–1689, 2008.

[263] C. Liu, S. Nemoto, and S. Ogano, “Effect of soot properties in diesel engine oils on frictional characteristics,” Tribol. Trans., vol. 46, no. 1, pp. 12–18, 2003.

[264] D. Uy, A. O’Neill, S. Simko, and A. Gangopadhyay, “Soot_additive interactions in engine oils,” Lubr. Sci., vol. 22, pp. 19–36, 2009.

[265] R. H. Hurt, A. F. Sarofim, and J. P. Longwell, “Gasification-induced densification of carbons: From soot to form coke,” Combust. Flame, vol. 95, no. 4, pp. 430–432, 1993.

[266] F. A. Heckman, “Microstructure of carbon black,” Rubber Chem. Technol., vol. 37, no. 5, pp. 1245–1298, 1964.

[267] J. B. Donnet, J. Schultz, and A. Eckhardt, “Etude de la microstructure d’un noir de carbone thermique,” Carbon N. Y., vol. 6, no. 6, pp. 781–788, 1968.

[268] K. Kamegawa, K. Nishikubo, and H. Yoshida, “Oxidative degradation of carbon blacks with nitric acid (I)—Changes in pore and crystallographic structures,” Carbon N. Y., vol. 36, no. 4, pp. 433–441, 1998.

[269] G. Faraji, H. S. Kim, and H. T. Kashi, “Chapter 7 - Mechanical Properties of Ultrafine-Grained and Nanostructured Metals,” in Severe Plastic Deformation, G. Faraji, H. S. Kim, and H. T. Kashi, Eds. Elsevier, 2018, pp. 223–257.

[270] J. L. Butler, J. P. Stewart, and R. E. Teasley, “Lube oil filtration effect on diesel engine wear,” SAE Tech. Pap., 1971.

[271] I. M. Hutten, “Testing of Nonwoven Filter Media,” Handb. Nonwoven Filter Media, pp. 245–290, 2007.

[272] Anonymous, “Scientific Technical Report,” vol. ISSN 1610-, no. December, pp. 1–101, 2000.

[273] R. D. Whitby, Lubricant Analysis and Condition Monitoring. CRC Press, 2021.

[274] Y. Qin, Y. Wu, P. Liu, F. Zhao, and Z. Yuan, “Experimental studies on effects of temperature on oil and water relative permeability in heavy-oil reservoirs,” Sci. Rep., vol. 8, no. 1, pp. 1–9, 2018.

[275] A. Dorgham, A. Azam, P. Parsaeian, C. Wang, A. Morina, and A. Neville, “An Assessment of the Effect of Relative Humidity on the Decomposition of the ZDDP Antiwear Additive,” Tribol. Lett., vol. 69, no. 2, pp. 1–12, 2021.

[276] P. Parsaeian, A. Ghanbarzadeh, M. C. P. Van Eijk, I. Nedelcu, A. Neville, and A. Morina, “A new insight into the interfacial mechanisms of the tribofilm formed by zinc dialkyl dithiophosphate,” Appl. Surf. Sci., vol. 403, pp. 472–486, 2017.

[277] P. Parsaeian et al., “An experimental and analytical study of the effect of water and its tribochemistry on the tribocorrosive wear of boundary lubricated systems with ZDDP-containing oil,” Wear, vol. 358–359, pp. 23–31, 2016.

[278] J. Galsworthy, S. Hammond, and D. Hone, “Oil-soluble colloidal additives,” Curr. Opin. Colloid Interface Sci., vol. 5, no. 5–6, pp. 274–279, 2000.

[279] P. Carden et al., “The effect of low viscosity oil on the wear, friction and fuel consumption of a heavy duty truck engine,” SAE Tech. Pap., vol. 2, no. 2, 2013.

[280] P. Parsaeian, M. C. P. Van Eijk, I. Nedelcu, A. Neville, and A. Morina, “Study of the interfacial mechanism of ZDDP tribofilm in humid environment and its effect on tribochemical wear; Part I: Experimental,” Tribol. Int., vol. 107, pp. 135–143, 2017.